

Novel Reactivity and Applications of Transition Metal-Catalyzed Nucleophilic Substitution Reactions

Thesis by
Xiaoyu (Dan) Tong

In Partial Fulfillment of the Requirements for the Degree of
Doctor of Philosophy

The logo for the California Institute of Technology (Caltech), consisting of the word "Caltech" in a bold, orange, sans-serif font.

*Division of Chemistry and Chemical Engineering
California Institute of Technology
Pasadena, California*

2024
(Defended May 15, 2024)

©2024

Xiaoyu Tong

ORCID: 0000-0002-1343-6335

To my family

Acknowledgments

I remember reading about some research saying that human connections are one of the most important aspects to mental and physical well-being, ranking above success or prestige. Looking back at my five years at Caltech, I have come to realize that this is profoundly accurate. Compared to the time I spent trudging towards a PhD, forming meaningful bonds with the individuals I'll mention below took relatively little time. Yet, I firmly believe the accomplishment of a PhD is only made meaningful because of these people who stood by me. I also believe that years later, I will mostly forget about what I will describe in this thesis, but I will remember the people I acknowledge in this small section.

I would first like to thank my research advisor, Prof. Greg Fu. He was the main reason I chose to come to Caltech, and the decision to join his group was the second-best decision I made during my time as a graduate student. Greg's scientific rigor, wisdom, and positivity will continue to inspire me for many years to come. I feel fortunate and privileged that he entrusted me with challenging projects right from the start, allowed me to take on research in various directions, and gave me the freedom to pursue projects that I was most interested in. I thank him for showing me the way of science. I thank him for his boost to my professional development. I thank him for what he has taught me, and for what he has enabled me to do.

I extend heartfelt thanks to my committee members—Prof. Jonas Peters, Prof. Brian Stoltz, and Prof. Sarah Reisman. Their constructive feedback and encouragement provided an environment conducive to both my professional growth and scientific exploration. I am grateful for their mentorship during pivotal moments like the candidacy and proposal exams, where I never felt examined but supported.

The Fu lab has been an overall very positive environment for me. I enjoyed working with all the past and present Fu lab members with whom I overlapped, and I thank all of them! I want to acknowledge a few of them who have been the most impactful. I met Robert Anderson during a graduate school visiting weekend in February 2019, and from then on, he has been one of my closest friends. I thank him for, among numerous other things, officiating my wedding, helping me with my proposals (but not the most important one), and for his invaluable trivia and life advice. I wish him good luck in the future, at Caltech and beyond. I want to thank Dr. Wendy Zhang for bringing people together in the Fu lab and around Caltech. She continues to be the strongest person I know. I wish her happiness and success. I want to acknowledge Dr. Dylan Freas because of his contagious optimism and kindness. I hope one day I will be able to give a presentation as good as one of his. Wendy and Dylan were also most helpful in my initial period at Caltech and in the Fu lab. I want to thank Hyungdo Cho for his friendship, scientific support, and for bringing me onboard his fantastic project. I look up to him as a graduate student and an excellent scientist.

I was fortunate to have collaborated with a large number of colleagues at Caltech, perhaps more than a Fu lab student typically would. I thoroughly enjoyed all of these experiences. Through my five years here, I worked closely, at one time or another, with Dr. Felix Schneck, Dr. Zepeng Yang, Dr. Hyungdo Cho, Robert Anderson, Dr. Giuseppe Zuccarello, Christian Johansen, Matt Wong, and Dr. Shaoqian Yang. Each one of them is a great scientist and team player. I started working with Felix when I was literally floundering in the mechanistic quagmire of my first project, and he immediately turned things around. I cannot thank him enough. I also appreciate the efforts of Matt and Shaoqian on the projects that I started. Overall, I am grateful to all my collaborators and for these collaborative experiences that made my research life at Caltech that much more diverse. I want to thank Arianna Ayonon for her work on the project which I continued to work on,

and for taking the time and walking me through the initial data. I also want to thank Dr. Haohua Huo and Dr. Zhaobin Wang for providing me with initial data for my first project. Although we have barely met or not at all, their notebooks serve as a strong inspiration to me.

Additionally, many Fu lab members who I have not closely worked with have given me inspiration, help, and encouragement. I am lucky to have known them and to call them my dear friends—Dr. Caiyou Chen, Dr. Asik Hossain, Dr. Feng Zhong, Dr. Renhe Li, Zhuoyan Wang, Dr. Robynne Neff, Dr. Suzanne Batiste, and Dr. Jason Rygus: thank you all for making the Fu lab a wonderful place to work.

I want to acknowledge all who have helped me during my time at Vanderbilt University. My undergraduate research advisor, Dr. Nathan Schley, was the original motivation for me to attend Caltech. He might just be the most knowledgeable chemist I have ever met. Thank you for your guidance through the formative years of my academic career. Additionally, I want to express my gratitude to Dr. Steven Townsend for delivering an amazing semester of freshman organic chemistry and inspiring my passion for organic chemistry. Another professor who has had an extraordinary influence on my scientific journey is Dr. Christina White. I am honored to have been part of her lab, where I learned invaluable lessons in organic chemistry—much more than my short time there would indicate.

Looking further back, I am grateful for my many friends with whom I have shared years, and in some cases, more than a decade, of memories: Tianyi He, Wentao Yu, Wenyu Du, Yunsheng Tian, Jingyi Gao, Ruihang Du, Xinyu Luo, Xiaoqian Huang, Haotian Sun, Tianlun Sun, Anyi Chen, Charlotte Yutong Wang, and many others. Also, I want to acknowledge Xiaojia “XJ” Xu for encouraging me to do science not for the money or prestige, but for the enjoyment of learning and

discovering. I want to extend my gratitude to each one of you for the precious moments, and I wish you were all here.

I also want to thank my family, to whom this thesis is dedicated. To my mom and dad, Suwen Zhang and Yibin Tong, I want you to know I feel privileged to have parents like you. You are the reason I chose to and can become a scientist. My entire extended family also has been very supportive during my time at Caltech, and I thank you all, especially Zongjian Tong, my grandfather, and Xiaoxiang Tong, my cousin.

Choosing the Fu lab was only the second-best decision I made in graduate school, because of you, Jessie Jiang. Life can be hard sometimes, yet you possess the remarkable ability to make the heaviest burdens feel as light as feathers, lifting the weight of the world with ease. Thank you for your love and your unwavering support. Thank you for everything.

Abstract

For more than 20 years, the Fu lab has explored the use of transition metal catalysts to enable novel nucleophilic substitution reactions. However, deficiencies in both fundamental reactivity and useful applications persist in this area. The research detailed in this thesis focuses on the development of reactivity and applications of transition metal-catalyzed nucleophilic substitution reactions.

Chapter 2 recounts the development of the nickel-catalyzed enantioconvergent alkylation reaction of racemic α -zincated amides with unactivated alkyl electrophile. This method constitutes a new example of the use of racemic nucleophiles in asymmetric cross-coupling reaction. It also addresses the long-standing challenge of controlling the absolute stereochemistry in the alkylation reaction between enolates and unactivated electrophiles. The reaction takes place under mild conditions. The products of this reaction are conveniently transformed into a range of chiral organic compounds. Taking advantage of a wide array of techniques, we have studied the mechanism of the reaction. Specifically, we determined and structurally characterized the predominant nickel-containing species during the reaction. Strong experimental support was obtained for the mechanism by which the electrophile is engaged in the reaction.

Chapter 3 describes the conception, discovery, optimization, and application of a nickel-catalyzed enantioconvergent arylation of racemic cyclic electrophiles—namely, 3-halo-pyrrolidines. We tackled the difficulties associated with the use of this highly challenging class of substrates via extensive ligand optimization and the application of design of experiments. After the reaction scope was explored, we applied it towards the expedient synthesis of an array of bioactive pyrrolidines that previously involved long and inefficient routes.

Chapter 4 includes the development of the first iron-catalyzed cross-coupling reaction in the Fu lab—the reductive cross-coupling reaction of readily available olefins with unactivated 1° alkyl electrophiles, including the discovery of the surprising effect of a magnesium salt, substrate scope, and preliminary mechanistic study. Additionally, at the end of this chapter, efforts towards the optimization of an iron-catalyzed reductive cross-coupling reaction of olefins with 2° alkyl electrophiles are reported. The effects of ligands are examined in detail.

Chapter 5 outlines the discovery and optimization of a novel copper-catalyzed asymmetric alkylation reaction of a variety of nucleophiles.

Published Content and Contributions

This dissertation contains materials adapted with permission from the following publications:

1. Tong, X.; Schneck, F.; Fu, G. C. Catalytic Enantioselective α -Alkylation of Amides by Unactivated Alkyl Electrophiles. *J. Am. Chem. Soc.* **2022**, *144*, 14856–14863, DOI: 10.1021/jacs.2c06154.

X.T. developed the reaction and explored the substrate scope. X.T. participated in the mechanistic study. X.T. participated in the writing of the manuscript.

2. Tong, X.; Yang, Z.; Del Angel Aguillar, C. E.; Fu, G. C. Iron-Catalyzed Reductive Cross-Coupling of Alkyl Electrophiles with Olefins. *Angew. Chem. Int. Ed.* **2023**, *62*, e202306663, DOI: 10.1002/anie.202306663.

X.T. developed the reaction, explored the substrate scope, and conducted the mechanistic study. X.T. participated in the writing of the manuscript.

Table of Contents

Acknowledgments	iv
Abstract	viii
Published Content and Contributions	x
Table of Contents	xi
List of Abbreviations	xiv
Chapter 1: Introduction	1
1.1. Nucleophilic Substitution Reactions	1
1.2. Nickel-Catalyzed Enantioselective Nucleophilic Substitution Reactions.....	4
1.3. Iron-Catalyzed Cross-Coupling Reactions.....	8
1.4. Copper-Catalyzed Substitution Reactions of Heteroatom Nucleophiles	9
1.5. References	10
Chapter 2: Catalytic Enantioselective α-Alkylation of Amides by Unactivated	
Alkyl Electrophiles	14
2.1. Introduction	14
2.2. Results and Discussion.....	17
2.2.1. Synthesis	17
2.2.1. Mechanism.....	21
2.3. Conclusion.....	29
2.4. Experimental Section	31
2.4.1. General Information.....	31
2.4.2. Preparation of L*	32
2.4.3. Preparation of Amides.....	33
2.4.4. Enantioselective α -Alkylations.....	48
2.4.5. Effect of Reaction Parameters.....	79
2.4.6. Functional-Group Compatibility.....	82

2.4.7. Derivatization of the Coupling Products.....	83
2.4.8. Assignment of Absolute Configuration.....	91
2.4.9. Mechanistic Studies	95
2.5. References	155
Chapter 3: Synthesis of Chiral Pyrrolidines via Nickel-Catalyzed Enantioconvergent Arylation: Control of Isolated Cyclic Stereocenter	160
3.1. Introduction	160
3.2. Results and Discussion.....	163
3.3. Conclusion.....	170
3.4. Experimental Section	171
3.4.1. General Information.....	171
3.4.2. Synthesis of Chiral Ligands	172
3.4.3. Nickel-Catalyzed Asymmetric Arylation Reaction.....	183
3.4.4. Design of Experiments.....	186
3.4.5. Effect of Reaction Parameters.....	192
3.4.6. Functional-Group Compatibility.....	193
3.5. References	194
Chapter 4: Iron-Catalyzed Reductive Cross-Coupling of Alkyl Electrophiles with Olefins	197
4.1. Introduction	197
4.2. Results and Discussion.....	199
4.3. Conclusion.....	206
4.4. Development of a Variant for Unactivated Secondary Alkyl Electrophiles	207
4.5. Experimental Section	210
4.5.1. General Information.....	210
4.5.2. Iron-Catalyzed Reductive Cross-Couplings and Hydroborations	212
4.5.3. Observations during Reaction Development	229

4.5.4. Effect of Reaction Parameters.....	234
4.5.5. Mechanistic Studies	236
4.5.6. Studies of Functional-Group Compatibility.....	247
4.5.7. Reaction Development for Secondary Alkyl Electrophiles	249
4.6. References	250
Chapter 5: Copper-Catalyzed Enantioconvergent Alkylation of Diverse Nitrogen and Oxygen Nucleophiles	254
5.1. Introduction	254
5.2. Results and Discussion.....	256
5.2.1. Asymmetric Alkylation with Diverse Nucleophiles	256
5.2.2. Application of the Asymmetric Alkylation Reaction	260
5.3. Conclusion.....	262
5.4. Experimental Section	263
5.4.1. General Information.....	263
5.4.2. Copper-Catalyzed Asymmetric Substitution Reaction	264
5.4.3. Design of Experiments.....	267
5.5. References	269

List of Abbreviations

*	indicates presence of chiral center
Å	Ångstrom
$[\alpha]_{25}$	specific rotation at wavelength of sodium D line
Ac	acetyl
Ad	1-adamantyl
Aq.	aqueous
Ar	aryl
Bn	benzyl
Boc	tert-butyloxycarbonyl
br	broad
<i>n</i> -Bu	butyl
<i>i</i> -Bu	<i>iso</i> -butyl
<i>t</i> -Bu	<i>tert</i> -butyl
<i>c</i>	concentration for specific rotation measurements
°C	degrees Celsius
Cbz	benzyloxycarbonyl
Cy	cyclohexyl
d	doublet
D	deuterium
DCM	dichloromethane
DMAP	4-dimethylaminopyridine
DMA	<i>N,N</i> -dimethylacetamide

DME	1,2-dimethoxyethane
DMF	<i>N,N</i> -dimethylformamide
DMSO	dimethyl sulfoxide
dr	diastereomeric ratio
ee	enantiomeric excess
e.g.	for example (Latin “ <i>exempli gratia</i> ”)
EPR	electron paramagnetic resonance
equiv.	equivalent
ESI	electrospray ionization
Et	ethyl
EWG	electron-withdrawing group
g	gram(s)
GC	gas chromatography
h	hour(s)
HPLC	high-performance liquid chromatography
HRMS	high-resolution mass spectroscopy
Hz	hertz
i.e.	that is (Latin “ <i>id est</i> ”)
IR	infrared (spectroscopy)
<i>J</i>	coupling constant
L	Liter or ligand
LDA	lithium diisopropylamide
m	multiplet; milli; meter

<i>m</i>	meta
m/z	mass to charge ratio
M	metal; molar; molecular ion
mCPBA	meta-chloroperbenzoic acid
Me	methyl
Mes	2,4,6-trimethylbenzenesulfonate
MHz	megahertz
mL	milliliter
μ	micro
min	minute(s)
Ms	methanesulfonate group
<i>n</i>	normal
NMR	nuclear magnetic resonance
Nu	nucleophile
<i>o</i>	ortho
<i>p</i>	para
Ph	phenyl
pin	pinacolato
Piv	pivalate
ppm	parts per million
PTFE	polytetrafluoroethylene
<i>n</i> -Pr	propyl
<i>i</i> -Pr	<i>iso</i> -propyl

q	quartet
R	alkyl group
rac	racemic
ref	reference
r.t.	room temperature
s	singlet
sat.	saturated
S _N 1	unimolecular nucleophilic substitution
S _N 2	bimolecular nucleophilic substitution
t	triplet
TBAF	tetrabutylammonium fluoride
TBS	<i>tert</i> -butyldimethylsilyl
TBDPS	<i>tert</i> -butyldiphenylsilyl
TEMPO	2,2,6,6-tetramethylpiperidin-1-yloxy
Tf	trifluoromethanesulfonyl
TFA	trifluoroacetic acid
THF	tetrahydrofuran
TLC	thin-layer chromatography
TMS	trimethylsilyl
TOF	time-of-flight
Ts	<i>p</i> -toluenesulfonyl
X	halogen atom, leaving group, or anionic ligand

Chapter 1: Introduction

1.1. Nucleophilic Substitution Reactions

Nucleophilic substitutions are among the most useful reactions available to practitioners of organic chemistry and are widely applied in the synthesis of modern small-molecule drugs.¹ However, traditional S_N1 and S_N2 reactions suffer from significant drawbacks. In particular, S_N1 reactions are limited to tertiary electrophiles and some activated (benzylic or allylic) electrophiles that can lead to stable carbocation intermediates. Additionally, the Brønsted/Lewis acidic conditions that promote S_N1 reactions can deactivate a broad array of nucleophiles, including basic amines. S_N2 reactions are similarly constrained, limited to only unhindered primary and a subset of (often activated) secondary electrophiles. Furthermore, the basic environments typically required for S_N2 reactions can promote undesired elimination reactions, which can compete with the desired substitution process (**Figure 1.1**).²

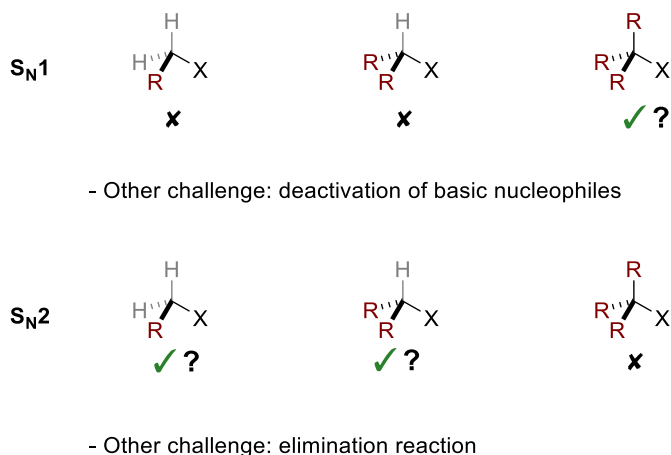


Figure 1.1. Traditional nucleophilic substitution reactions, limit in scope, and challenges.

Another important drawback of these traditional transformations is the difficulty in controlling the stereochemistry of the product: when the carbon atom undergoing substitution is a

stereogenic center, the use of racemic starting materials will lead to the formation of racemic substitution products. Specifically, because of the involvement of carbocation intermediates, S_N1 reactions produce a racemic mixture when stereochemistry is relevant, although a few recent studies have shown that certain specialized substrates can participate in enantioconvergent S_N1 reactions.^{3,4} S_N2 reactions, on the other hand, are inherently stereospecific: in order to obtain enantioenriched product, enantioenriched starting material must be used. These limitations of S_N1 and S_N2 reactions are direct consequences of their mechanisms, which would be difficult to overcome without taking advantage of alternative reaction pathways.

Transition metal catalysis has emerged as one of the most important strategies to complement these traditional substitution reactions. Cross-coupling reactions are essentially identical to traditional nucleophilic substitution reactions in terms of retrosynthetic logic—disconnecting a bond to reveal an electrophile and a nucleophile. Over the past three decades, transition metal-catalyzed cross-couplings have revolutionized the way small-molecule drugs are synthesized.¹ However, as recently as early 2000s, the use of alkyl electrophiles in transition metal-catalyzed substitution reactions was considered challenging.⁵ This traditional wisdom can be justified by considering the mechanism of a typical palladium-catalyzed cross-coupling reaction, which includes three steps: oxidative addition, transmetalation, and reductive elimination (**Figure 1.2**). In this two-electron mechanistic regime, oxidative addition is often sluggish in the case of alkyl electrophiles, especially unactivated secondary/tertiary electrophiles. In many cases, the oxidative additions of alkyl electrophiles to low-valent transition metal catalysts proceed through S_N2 mechanism,⁶ and thus would suffer from the same limitations as a classic S_N2 reaction. Further complicating the reaction, β-hydride elimination from metal-alkyl intermediates can outpace reductive elimination when a β-hydrogen atom is available, giving rise to olefin by-products rather

than the desired coupling product. As a result, before 2004, almost all of the synthetically practical cross-coupling reactions involve sp^2 - and sp -hybridized substrates.⁷

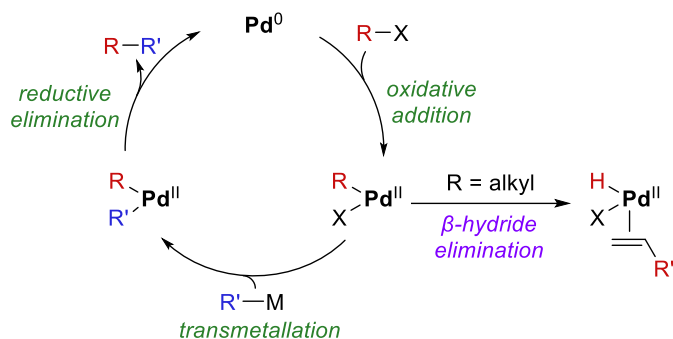


Figure 1.2. Representative mechanism of palladium-catalyzed cross-coupling reaction.

Because of these limitations, the Fu lab focuses on the development of transition metal-catalyzed nucleophilic substitution reactions to broaden the scope of classic nucleophilic substitutions and cross-coupling reactions. The Fu lab also seeks to control the absolute stereochemistry of the products in catalytic reactions with racemic starting materials. In this direction, we have reported the development of many transition metal-catalyzed nucleophilic substitution reactions with alkyl electrophiles (**Figure 1.3A**).^{2,7} These reactions typically involve the oxidative addition of alkyl electrophiles via the intermediacy of alkyl radicals, which lead to broader reaction generality, as well as the ability to control the stereochemistry of the product via the interaction between chiral catalysts and prochiral radicals (**Figure 1.3B**). Furthermore, the Fu lab is interested in leveraging the unique properties of earth-abundant metal catalysts in facilitating these reactions (**Figure 1.3C**).

Although significant progress has been made, transition metal-catalyzed nucleophilic substitution reactions remain an exciting area of research due to the prospects of novel reactivity and broader applications. The research described in this thesis focuses on the investigation of

reactivity and applications of catalytic nucleophilic substitutions mediated by nickel, iron, and copper.

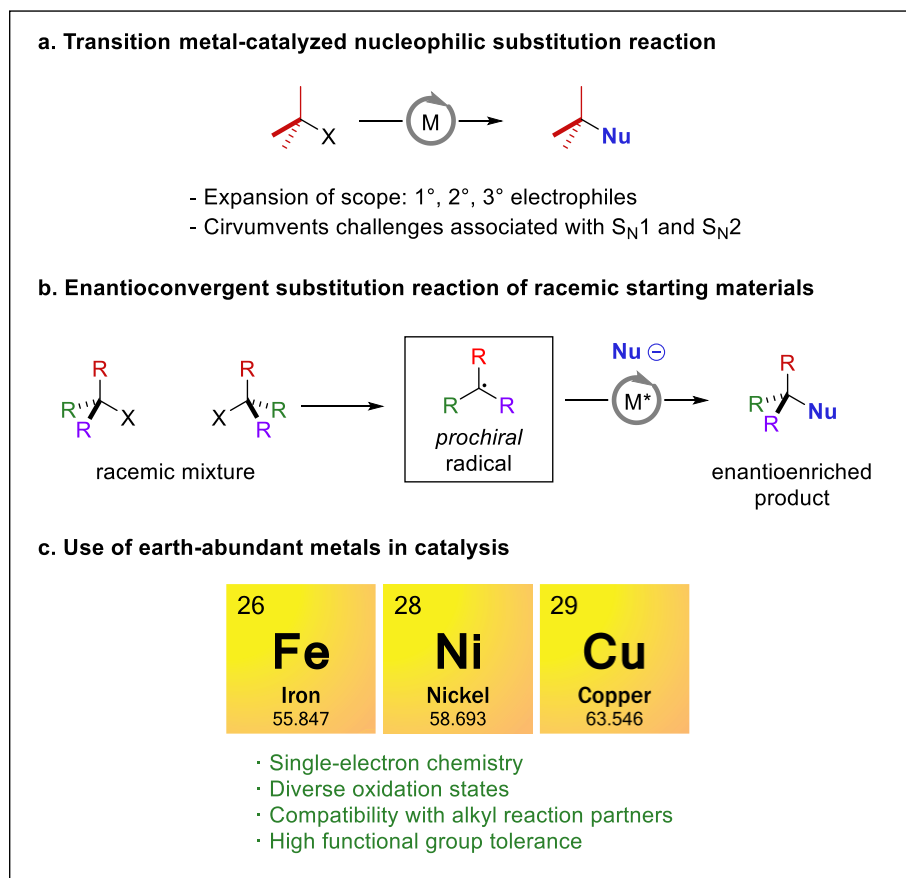


Figure 1.3. *a. Transition metal-catalyzed nucleophilic substitution reaction; b. Enantioconvergent substitution reaction of racemic starting materials; c. Use of earth-abundant metals in catalysis.*

1.2. Nickel-Catalyzed Enantioselective Nucleophilic Substitution Reactions

Compared to palladium, nickel is more abundant and less expensive. The less basic nickel also disfavors β -hydride elimination^{8,9} and readily undergoes single-electron chemistry with access to a range of oxidation states, most importantly, Ni(I), Ni(II), and Ni(III).⁸ Leveraging these characteristics, since 2003, the Fu lab has utilized nickel complexes to catalyze cross-coupling

reactions between diverse organometallic nucleophiles and a broad range of alkyl electrophiles. In general, these reactions proceed through the pathway outlined in **Figure 1.4**.^{10,11} In the beginning, a small amount of metalloradical nickel(I) complex converts the alkyl electrophile into an alkyl radical via halogen atom abstraction. The alkyl radical then reacts with an organonickel(II) complex (often the resting state), which is generated through the transmetalation reaction between nickel(II)-halide and the organometallic nucleophile. The resulting nickel(III) complex leads to the product via reductive elimination. Notably, the radical-chain single-electron oxidative addition of the alkyl electrophile is an important departure from the conventional two-electron mechanism observed with palladium catalysis. It allows for facile oxidative addition of the alkyl electrophile and affords an opportunity for a chiral nickel catalyst to convert both enantiomers of the racemic electrophile to a single enantiomer of the product. Indeed, a significant number of nickel-catalyzed enantioconvergent substitution reactions have been reported.¹²

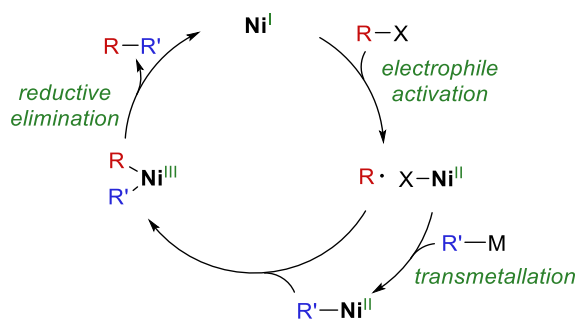


Figure 1.4. Typical mechanism of a nickel-catalyzed cross-coupling reaction of alkyl electrophile.

Despite the well-documented use of racemic alkyl electrophiles,¹² the use of racemic nucleophiles has been seldom explored in enantioconvergent substitution reactions.^{13–15} Therefore, **Chapter 2** describes the development of a nickel-catalyzed asymmetric substitution reaction of racemic α -zincated amides with unactivated alkyl electrophiles (**Figure 1.5**). From a conceptual point of view, the reaction 1) is a new example of the use of racemic nucleophiles in substitution

reactions and 2) addresses the long-standing synthetic challenge of asymmetric enolate alkylation reaction with generic unactivated electrophiles. We also demonstrated that the product can be transformed in one step to a variety of chiral organic molecules. Employing a range of techniques, we investigated the mechanism of this novel transformation. We gained significant insight into many of the elemental steps and important intermediates of the reaction, including a crystallographically characterized alkylnickel(II) resting state complex.

Continuing the research in nickel catalysis and turning our focus towards the synthesis of useful chiral products, we recognize that isolated stereocenters located within cyclic structures are prevalent in bioactive compounds and drugs.¹⁶ However, the development of enantioselective cross-coupling reactions has overwhelmingly favored the construction of acyclic stereocenters or those adjacent to functional groups.^{12,17} Thus, **Chapter 3** details the development of a nickel-catalyzed asymmetric arylation reaction of racemic 3-iodopyrrolidines, providing facile access to chiral 3-arylpyrrolidines and addressing the previously unmet challenge of controlling isolated cyclic stereocenters in enantioconvergent substitution reactions. Iterative ligand optimization led to the discovery of a novel chiral ligand that facilitates the reaction. Taking place under mild conditions, the reaction tolerates a wide range of substrates. We further showcased the utility of the method by applying it to streamline the synthesis of a variety of molecules with direct application in medicinal chemistry.

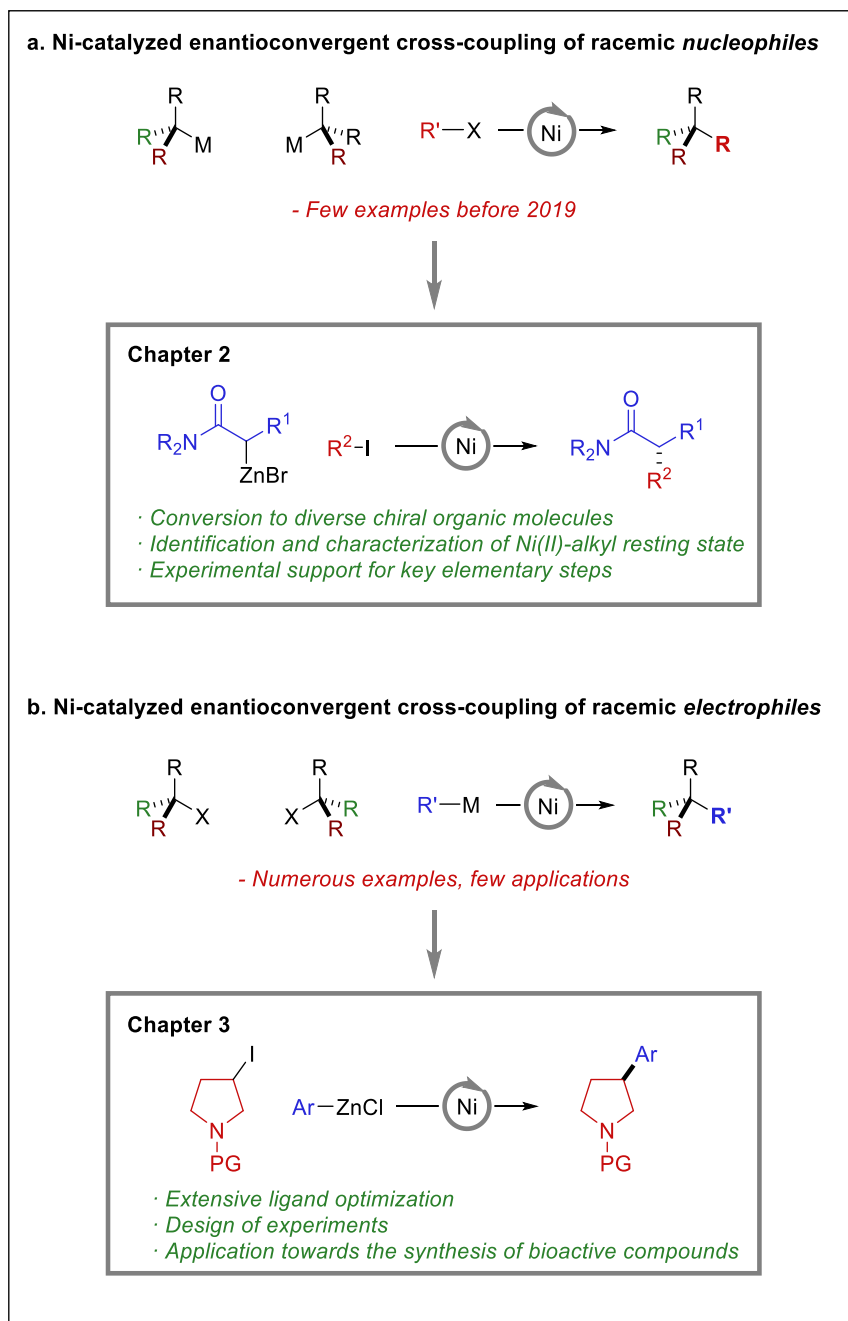


Figure 1.5. Nickel-catalyzed enantioconvergent cross-coupling reactions: a. Nickel-catalyzed enantioconvergent cross-coupling of racemic nucleophiles; b. Nickel-catalyzed enantioconvergent cross-coupling of racemic electrophiles.

1.3. Iron-Catalyzed Cross-Coupling Reactions

Iron is the most abundant transition metal on earth, accounting for more than 5% of the mass of earth's crust. It is also generally considered non-toxic.¹⁸ Therefore, the broader incorporation of iron in place of other expensive or toxic metals in chemical processes can confer significant economic and environmental benefits. Although substantial progress has been made in the development of nickel-catalyzed alkyl-alkyl bond formation, examples using catalysts based on iron have been lacking. Despite the limited examples, it is well known that the unique electronic structure of iron allows for activation of a range of alkyl electrophiles, often via radical intermediates.¹⁹ More encouragingly, recent years have seen explosive growth in iron-catalyzed reactions in organic chemistry, including many examples of iron-catalyzed cross-coupling reactions. However, a persistent shortcoming in both historical and novel iron-catalyzed cross-coupling reactions is the need for highly reactive nucleophiles, especially Grignard reagents.²⁰

At the same time, for a number of transition metal-catalyzed cross-coupling reactions, many laboratories have shown that, in the presence of hydride reagents (such as silanes and boranes), reactive organometallic nucleophiles can be replaced by olefins—a class of accessible and stable feedstock chemicals.²¹⁻²³ However, such a process is not known for iron. Furthering the Fu lab's research into base metal-catalyzed cross-coupling reactions, in **Chapter 4** we report the iron-catalyzed reductive coupling reaction, whereby unactivated primary alkyl electrophiles are coupled with olefins. The reaction employs commercially available components and proceeds under mild conditions. Preliminary mechanistic studies support the involvement of the alkyl radical generated from the electrophile. Without significant modification of the reaction conditions, we can apply the same catalytic system towards another type of hydrofunctionalization—hydroboration of olefins. We further report the development and the ongoing optimization of an

analogous iron-catalyzed reaction in which unactivated secondary alkyl electrophiles are used as reaction partner (**Figure 1.6**).

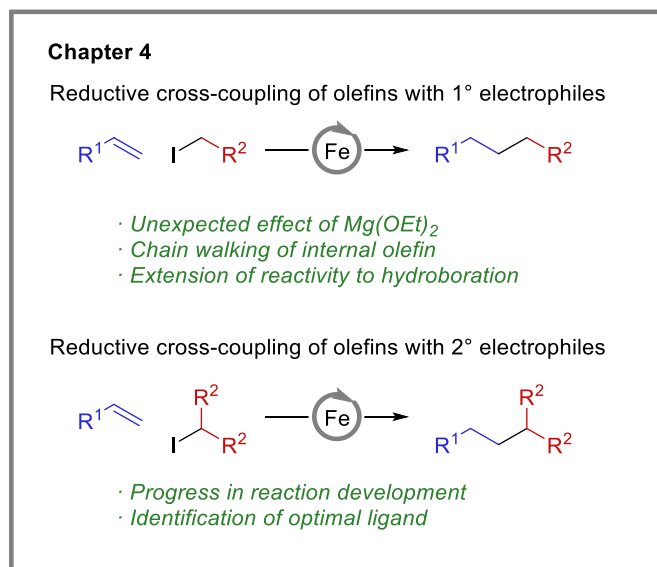


Figure 1.6. Iron-catalyzed reductive cross-coupling reactions with olefins.

1.4. Copper-Catalyzed Substitution Reactions of Heteroatom Nucleophiles

While nickel catalysis is extensively studied in the Fu lab for the construction of carbon–carbon bonds, copper catalysis for the construction of carbon-heteroatom bonds has emerged as another important research area over the past decade. In collaboration with the Peters lab, the Fu lab has reported a number of copper-catalyzed cross-couplings between various heteroatom nucleophiles and alkyl (and some aryl) electrophiles.^{24–28} Many enantioconvergent reactions have been reported as well.^{29–32}

However, many combinations of nucleophiles and electrophiles remain underexplored. Thus, in **Chapter 5**, we briefly discuss the discovery and development of a copper-catalyzed

enantioconvergent alkylation of an array of *N*- and *O*-nucleophiles, paving the way towards the synthesis of biologically important molecules.

1.5. References

- (1) Brown, D. G.; Boström, J. Analysis of Past and Present Synthetic Methodologies on Medicinal Chemistry: Where Have All the New Reactions Gone? *J. Med. Chem.* **2016**, *59*, 4443–4458.
- (2) Fu, G. C. Transition-Metal Catalysis of Nucleophilic Substitution Reactions: A Radical Alternative to S_N1 and S_N2 Processes. *ACS Cent. Sci.* **2017**, *3*, 692–700.
- (3) Singh, V. K.; Zhu, C.; De, C. K.; Leutzsch, M.; Baldinelli, L.; Mitra, R.; Bistoni, G.; List, B. Taming Secondary Benzylic Cations in Catalytic Asymmetric S_N1 Reactions. *Science* **2023**, *382*, 325–329.
- (4) Wendlandt, A. E.; Vangal, P.; Jacobsen, E. N. Quaternary Stereocentres via an Enantioconvergent Catalytic S_N1 Reaction. *Nature* **2018**, *556*, 447–451.
- (5) Denmark, S. E.; Sweis, R. F. Organosilicon Compounds in Cross-Coupling Reactions. In *Metal-Catalyzed Cross-Coupling Reactions*; John Wiley & Sons, Ltd, 2004; pp 163–216.
- (6) Rio, J.; Liang, H.; Perrin, M.-E. L.; Perego, L. A.; Grimaud, L.; Payard, P.-A. We Already Know Everything about Oxidative Addition to Pd(0): Do We? *ACS Catal.* **2023**, *13*, 11399–11421.
- (7) Choi, J.; Fu, G. C. Transition Metal-Catalyzed Alkyl–Alkyl Bond Formation: Another Dimension in Cross-Coupling Chemistry. *Science* **2017**, *356*, eaaf7230.
- (8) Diccianni, J.; Lin, Q.; Diao, T. Mechanisms of Nickel-Catalyzed Coupling Reactions and Applications in Alkene Functionalization. *Acc. Chem. Res.* **2020**, *53*, 906–919.

- (9) Leatherman, M. D.; Svejda, S. A.; Johnson, L. K.; Brookhart, M. Mechanistic Studies of Nickel(II) Alkyl Agostic Cations and Alkyl Ethylene Complexes: Investigations of Chain Propagation and Isomerization in (α -Diimine)Ni(II)-Catalyzed Ethylene Polymerization. *J. Am. Chem. Soc.* **2003**, *125*, 3068–3081.
- (10) Schley, N. D.; Fu, G. C. Nickel-Catalyzed Negishi Arylations of Propargylic Bromides: A Mechanistic Investigation. *J. Am. Chem. Soc.* **2014**, *136*, 16588–16593.
- (11) Yin, H.; Fu, G. C. Mechanistic Investigation of Enantioconvergent Kumada Reactions of Racemic α -Bromoketones Catalyzed by a Nickel/Bis(oxazoline) Complex. *J. Am. Chem. Soc.* **2019**, *141*, 15433–15440.
- (12) Yus, M.; Nájera, C.; Foubelo, F.; Sansano, J. M. Metal-Catalyzed Enantioconvergent Transformations. *Chem. Rev.* **2023**, *123*, 11817–11893.
- (13) Huo, H.; Gorsline, B. J.; Fu, G. C. Catalyst-Controlled Doubly Enantioconvergent Coupling of Racemic Alkyl Nucleophiles and Electrophiles. *Science* **2020**, *367*, 559–564.
- (14) Cordier, C. J.; Lundgren, R. J.; Fu, G. C. Enantioconvergent Cross-Couplings of Racemic Alkylmetal Reagents with Unactivated Secondary Alkyl Electrophiles: Catalytic Asymmetric Negishi α -Alkylations of *N*-Boc-Pyrrolidine. *J. Am. Chem. Soc.* **2013**, *135*, 10946–10949.
- (15) Mu, X.; Shibata, Y.; Makida, Y.; Fu, G. C. Control of Vicinal Stereocenters through Nickel-Catalyzed Alkyl–Alkyl Cross-Coupling. *Angew. Chem. Int. Ed.* **2017**, *56*, 5821–5824.
- (16) McGrath, N. A.; Brichacek, M.; Njardarson, J. T. A Graphical Journey of Innovative Organic Architectures That Have Improved Our Lives. *J. Chem. Educ.* **2010**, *87*, 1348–1349.

- (17) Cherney, A. H.; Kadunce, N. T.; Reisman, S. E. Enantioselective and Enantiospecific Transition-Metal-Catalyzed Cross-Coupling Reactions of Organometallic Reagents to Construct C–C Bonds. *Chem. Rev.* **2015**, *115*, 9587–9652.
- (18) Frey, P. A.; Reed, G. H. The Ubiquity of Iron. *ACS Chem. Biol.* **2012**, *7*, 1477–1481.
- (19) Sears, J. D.; Neate, P. G. N.; Neidig, M. L. Intermediates and Mechanism in Iron-Catalyzed Cross-Coupling. *J. Am. Chem. Soc.* **2018**, *140*, 11872–11883.
- (20) *Ni- and Fe-Based Cross-Coupling Reactions*; Correa, A., Ed.; Topics in Current Chemistry Collections; Springer: Cham, 2017.
- (21) Li, Y.; Nie, W.; Chang, Z.; Wang, J.-W.; Lu, X.; Fu, Y. Cobalt-Catalysed Enantioselective C(sp³)–C(sp³) Coupling. *Nat. Catal.* **2021**, *4*, 901–911.
- (22) Wang, Y.-M.; Bruno, N. C.; Placeres, Á. L.; Zhu, S.; Buchwald, S. L. Enantioselective Synthesis of Carbo- and Heterocycles through a CuH-Catalyzed Hydroalkylation Approach. *J. Am. Chem. Soc.* **2015**, *137*, 10524–10527.
- (23) Lu, X.; Xiao, B.; Zhang, Z.; Gong, T.; Su, W.; Yi, J.; Fu, Y.; Liu, L. Practical Carbon–Carbon Bond Formation from Olefins through Nickel-Catalyzed Reductive Olefin Hydrocarbonation. *Nat. Commun.* **2016**, *7*, 11129.
- (24) Creutz, S. E.; Lotito, K. J.; Fu, G. C.; Peters, J. C. Photoinduced Ullmann C–N Coupling: Demonstrating the Viability of a Radical Pathway. *Science* **2012**, *338*, 647–651.
- (25) Do, H.-Q.; Bachman, S.; Bissember, A. C.; Peters, J. C.; Fu, G. C. Photoinduced, Copper-Catalyzed Alkylation of Amides with Unactivated Secondary Alkyl Halides at Room Temperature. *J. Am. Chem. Soc.* **2014**, *136*, 2162–2167.
- (26) Uyeda, C.; Tan, Y.; Fu, G. C.; Peters, J. C. A New Family of Nucleophiles for Photoinduced, Copper-Catalyzed Cross-Couplings via Single-Electron Transfer: Reactions

- of Thiols with Aryl Halides Under Mild Conditions (0 °C). *J. Am. Chem. Soc.* **2013**, *135*, 9548–9552.
- (27) Tan, Y.; Muñoz-Molina, J. M.; Fu, G. C.; Peters, J. C. Oxygen Nucleophiles as Reaction Partners in Photoinduced, Copper-Catalyzed Cross-Couplings: O-Arylations of Phenols at Room Temperature. *Chem. Sci.* **2014**, *5*, 2831–2835.
- (28) Ahn, J. M.; Peters, J. C.; Fu, G. C. Design of a Photoredox Catalyst That Enables the Direct Synthesis of Carbamate-Protected Primary Amines via Photoinduced, Copper-Catalyzed N-Alkylation Reactions of Unactivated Secondary Halides. *J. Am. Chem. Soc.* **2017**, *139*, 18101–18106.
- (29) Kainz, Q. M.; Matier, C. D.; Bartoszewicz, A.; Zultanski, S. L.; Peters, J. C.; Fu, G. C. Asymmetric Copper-Catalyzed C-N Cross-Couplings Induced by Visible Light. *Science* **2016**, *351*, 681–684.
- (30) Bartoszewicz, A.; Matier, C. D.; Fu, G. C. Enantioconvergent Alkylations of Amines by Alkyl Electrophiles: Copper-Catalyzed Nucleophilic Substitutions of Racemic α -Halolactams by Indoles. *J. Am. Chem. Soc.* **2019**, *141*, 14864–14869.
- (31) Chen, C.; Fu, G. C. Copper-Catalysed Enantioconvergent Alkylation of Oxygen Nucleophiles. *Nature* **2023**, *618*, 301–307.
- (32) Chen, C.; Peters, J. C.; Fu, G. C. Photoinduced Copper-Catalysed Asymmetric Amidation via Ligand Cooperativity. *Nature* **2021**, *596*, 250–256.

Chapter 2: Catalytic Enantioselective α -Alkylation of Amides

by Unactivated Alkyl Electrophiles

Adapted in part with permission from:

Tong, X.; Schneck, F.; Fu, G. C. Catalytic Enantioselective α -Alkylation of Amides by Unactivated Alkyl Electrophiles. *J. Am. Chem. Soc.* **2022**, *144*, 14856–14863.

© 2022 American Chemical Society

2.1. Introduction

Because carbonyl groups that bear an α stereocenter are a common motif in biologically active molecules,¹ the development of efficient methods for generating this subunit has been a long-standing objective in organic synthesis (**Figure 2.1A**).^{2–4} One straightforward approach to accessing such structures is through the α -alkylation of enolates, a process that accounted for 11% of all carbon–carbon bond-forming reactions run in bulk in a Pfizer research facility between 1985 and 2002.⁵ The development of methods by Evans, Myers, and others that achieve the *stereoselective* α -alkylation of carbonyl derivatives through the use of a covalently bound chiral auxiliary represents one of the landmark advances in the field of asymmetric synthesis (**Figure 2.1B**);^{6–8} such methods have been widely applied throughout academia and industry,⁹ including syntheses on a metric-ton scale.¹⁰

Controlling the stereochemistry of the α carbon with a chiral catalyst, rather than a stoichiometric chiral auxiliary, is a logical next step in the development of this strategic carbon–carbon bond-forming process. However, to our knowledge, asymmetric catalysis of the fundamental transformation illustrated in **Figure 2.1A** has not yet been described, although some

progress has been reported for certain specialized substrates.^{11–15} For example, in the case of generic/unactivated electrophiles (versus a specialized/activated electrophile, such as an allyl electrophile¹⁵), only phase-transfer catalysis has provided good enantioselectivity, but the carbonyl coupling partner must include an activating, generally an α -imino, substituent.^{11,14} In the case of specialized electrophiles, progress has been described with phase-transfer reagents, transition metals, Brønsted acids, and amines.^{11–15}

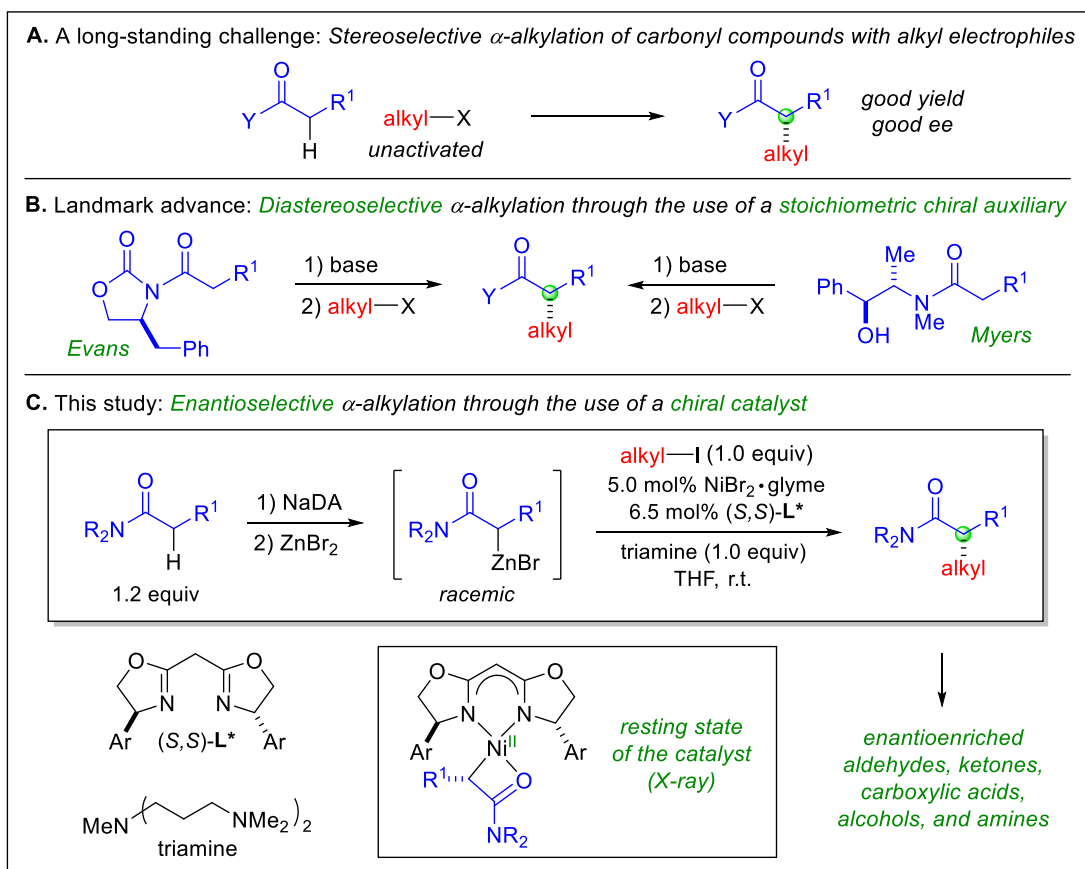


Figure 2.1. Catalytic enantioselective intermolecular α -alkylation of carbonyl compounds with unactivated alkyl electrophiles. (A) A long-standing challenge in organic synthesis: stereoselective α -alkylation of carbonyl compounds with unactivated alkyl electrophiles. (B) Landmark advance: diastereoselective α -alkylation through the use of a stoichiometric chiral auxiliary. (C) This study:

enantioselective α -alkylation through the use of a chiral catalyst. Ar = 3,5-di-tert-butylphenyl; NaDA = sodium diisopropylamide; R = carbon substituent; X = leaving group (e.g., halide); Y = H, carbon, nitrogen, or oxygen.

Catalyzing the α -alkylation of alkali-metal (e.g., lithium) enolates is challenging, due to their high nucleophilicity and Brønsted basicity, which can lead to undesired processes such as direct, uncatalyzed α -alkylation (to furnish racemic product) and acid–base reactions (including loss of HX from the electrophile and enolization/racemization of the product). Due to their attenuated nucleophilicity and Brønsted basicity, readily available Reformatsky reagents (broadly defined as α -zincated carbonyl compounds) are an attractive alternative to alkali-metal enolates for use in catalyzed reactions.¹⁶

Although metal-catalyzed couplings of Reformatsky reagents with alkyl electrophiles have not been described,¹⁷ progress has been reported in the development of metal-catalyzed couplings of other alkyl nucleophiles with alkyl electrophiles, including asymmetric processes.^{18,19} To achieve the goal of catalytic enantioselective α -alkylation of carbonyl compounds with unactivated alkyl electrophiles, we sought to develop a method that would solve the two key challenges: catalysis of a new carbon–carbon bond-forming process (the coupling of a Reformatsky reagent with an unactivated alkyl electrophile) and effective control of stereochemistry.

Herein we describe the realization of our objective, establishing that a chiral catalyst based on nickel, an earth-abundant metal, can achieve this strategic carbon–carbon bond-forming process with good yield and ee (**Figure 2.1C**). The α -alkylated products of the coupling can be transformed in one step, without racemization, into a broad spectrum of useful classes of chiral molecules. Our mechanistic studies provide significant insight into the reaction pathway; of particular note is our

structural characterization of the predominant resting state of nickel during catalysis, specifically, an alkylnickel(II) complex in which nickel is bound to the stereogenic α -carbon of the carbonyl group, the stereochemistry of which corresponds to that observed in the major enantiomer of the coupling product.

2.2. Results and Discussion

2.2.1. Synthesis

In our initial studies, we employed as the nucleophile a racemic Reformatsky reagent generated through the reaction of an α -bromoamide with zinc metal, and we determined that a chiral nickel catalyst can provide good yield and enantioselectivity in an α -alkylation with an unactivated alkyl iodide (**Figure 2.2**, Method A) (for an overview of the impact of changes in various reaction parameters on the yield and the enantioselectivity, see **2.4. Experimental Section**).²⁰ We subsequently established that the corresponding Reformatsky reagent generated via deprotonation of the amide,^{21,22} followed by in situ nickel-catalyzed asymmetric α -alkylation, affords similar yield and ee in a one-pot process (**Figure 2.2**, Method B). No detectable racemization of the potentially labile α stereocenter of the product is observed with either method.

A variety of Reformatsky reagents and unactivated alkyl electrophiles serve as suitable coupling partners in these catalytic asymmetric intermolecular α -alkylations, generally leading to carbon–carbon bond formation with similar yield and enantioselectivity for the two methods (**Figure 2.2**). With respect to the nucleophile, the α -alkyl substituent may vary in size from methyl to isopropyl, and various functional groups may be present (products **1–9**; for additional information on functional-group compatibility, see **2.4. Experimental Section**). Although

azetidines have been employed as effective stoichiometric chiral auxiliaries in diastereoselective α -alkylations of enolates,²³ the stereochemistry of the nickel catalyst, not that of the azetidine, predominantly controls the stereochemistry of the product in the case of an azetidine that bears a stereocenter (products **8** and **9**). Furthermore, when employing a different chiral ligand **L7**, tertiary amide nucleophiles derived from morpholine and dimethylamine, rather than the more specialized azetidine, can undergo enantioselective alkylation with high enantioselectivity (products **S1**, **S2**). The high yield and the high enantioselectivity for couplings to form products such as **2**, taken together, establish that the chiral nickel catalyst is achieving a stereoconvergent reaction that utilizes both enantiomers of the racemic nucleophile, not merely carrying out a simple kinetic resolution.

With respect to the electrophile, an array of unactivated alkyl iodides are suitable coupling partners in these nickel-catalyzed enantioconvergent α -alkylations. Primary alkyl electrophiles that vary in steric demand, including a β -branched substrate, engage in carbon–carbon bond formation with good enantioselectivity (products **10–12** in **Figure 2.3**; however, unactivated secondary alkyl electrophiles are not useful coupling partners under these conditions). A variety of functional groups can be present in the electrophile, including a silyl ether, aryl ether, primary alkyl fluoride, primary alkyl chloride, trifluoromethyl group, ester, carbamate, alkylboronate ester, or acetal (products **13–23**). On a gram scale in the presence of 3.0 mol % nickel, catalytic enantioselective α -alkylation proceeds with similar yield and ee as for a reaction conducted on a 0.6 mmol scale (product **10**).

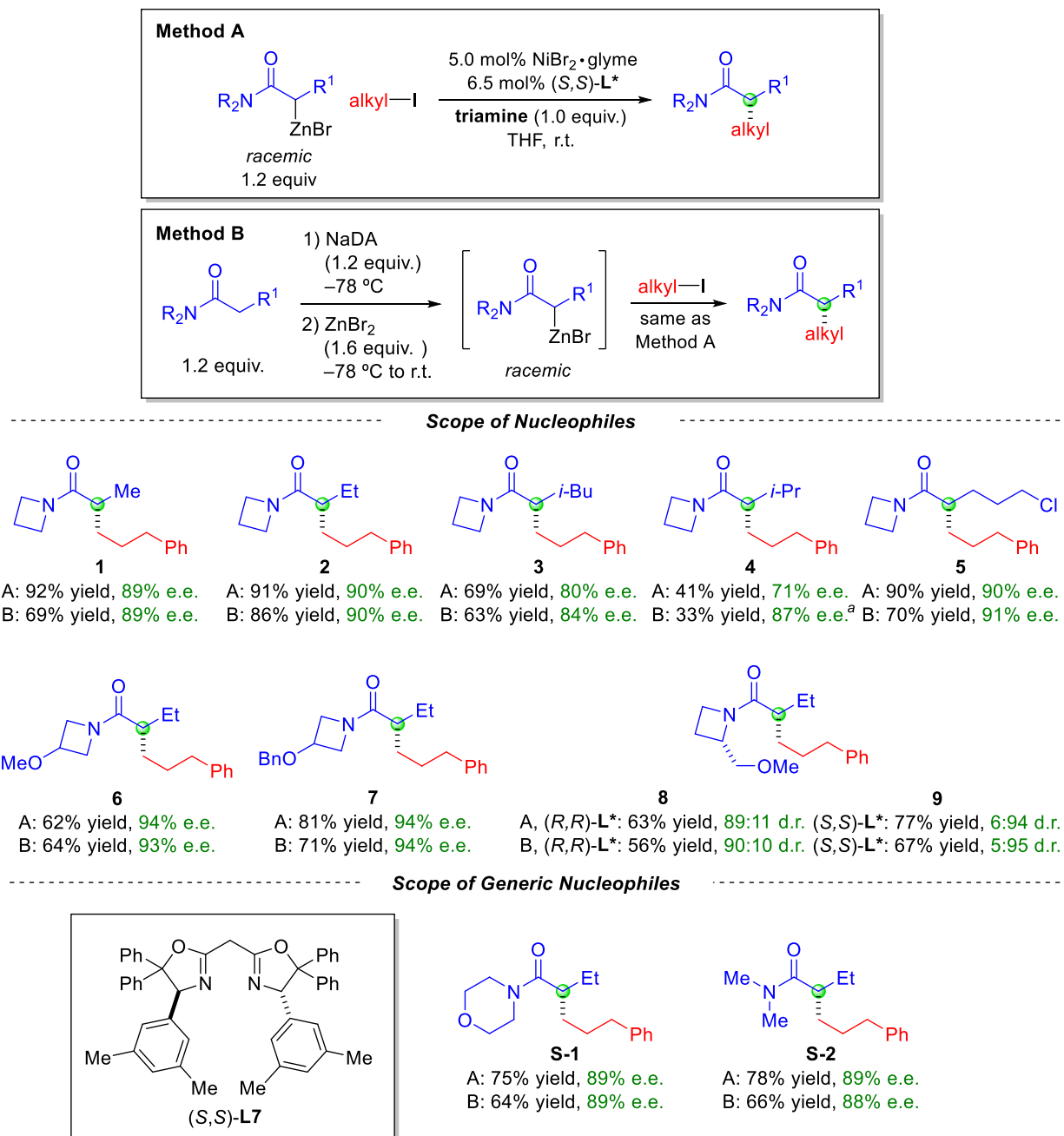


Figure 2.2. Nickel-catalyzed asymmetric α -alkylation of carbonyl compounds: scope of nucleophiles, including two examples of generic nucleophiles. All data represent the average of two experiments, and the percent yield represents purified product. (A) Scope (0.6 mmol scale, unless otherwise noted). ^aReaction performed with 10 mol % NiBr₂·glyme and 13 mol % L*.

Scope of Electrophiles

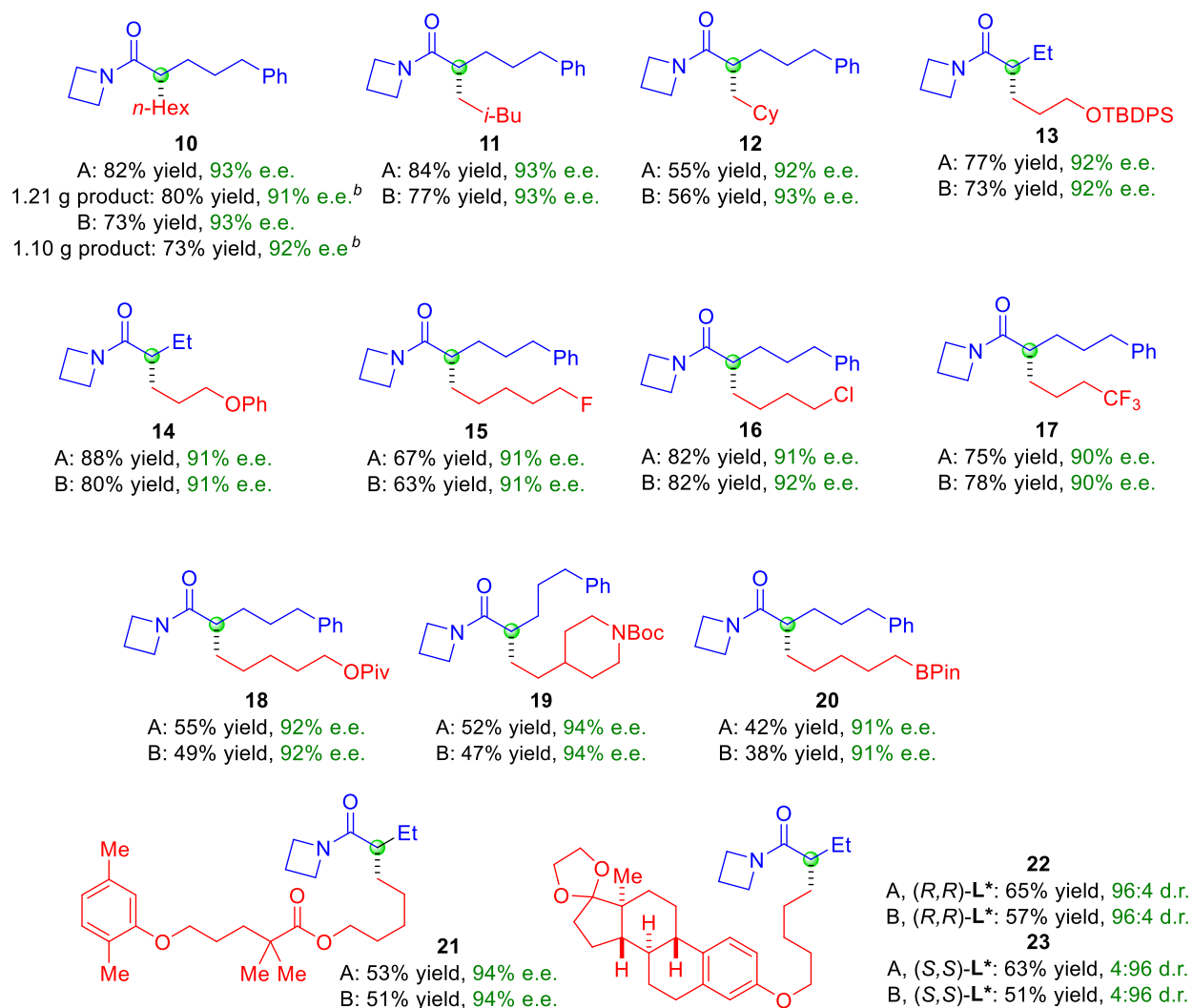


Figure 2.3. Nickel-catalyzed asymmetric α -alkylation of carbonyl compounds: scope of electrophiles. All data represent the average of two experiments, and the percent yield represents purified product. (A) Scope (0.6 mmol scale, unless otherwise noted). ^bReaction performed with 3.0 mol % NiBr₂-glyme and 3.8 mol % L*.

The enantioenriched *N*-acylazetidines that are generated in these nickel-catalyzed asymmetric α -alkylations are particularly attractive due to their ready transformation into an array of useful families of compounds (**Figure 2.4**). In addition to the previously described conversion

of *N*-acylazetidines to ketones,²⁴ the enantioenriched *N*-acylazetidine can be converted into other carbonyl compounds (an aldehyde and a carboxylic acid), and it can be reduced to an alcohol or an amine. All of these transformations proceed with essentially no racemization ($\leq 1\%$) of the potentially labile α stereocenter.

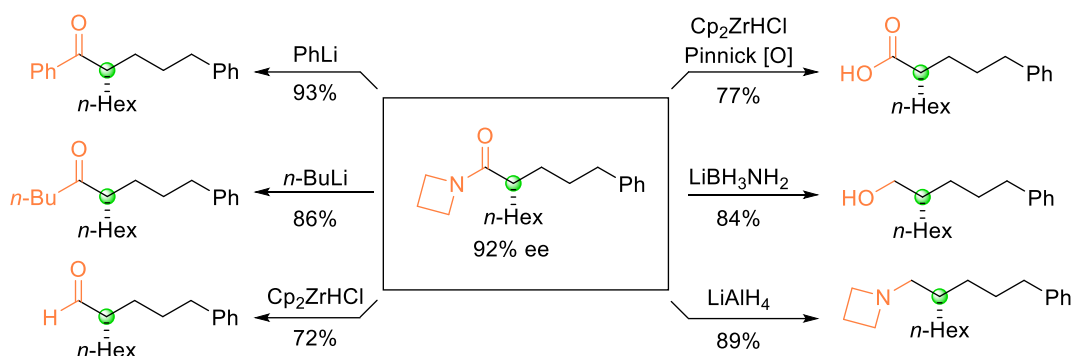


Figure 2.4. Transformation of alkylation product to other useful families of enantioenriched compounds (all proceed with essentially no racemization ($\leq 1\%$)).

2.2.2. Mechanism

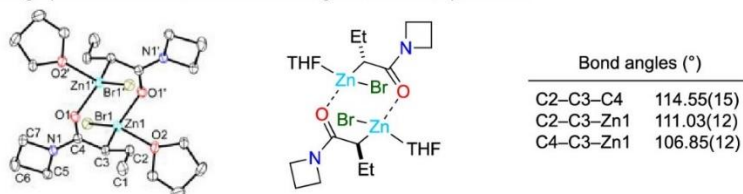
Only two types of racemic alkyl nucleophiles, both somewhat specialized in comparison with Reformatsky reagents, have previously been shown to serve as useful partners in enantioconvergent couplings with unactivated alkyl electrophiles;^{25,26} there have been no detailed experiment-based mechanistic studies of such coupling processes. This deficiency provided a strong impetus for us to investigate the mechanism of our new method for the catalytic asymmetric α -alkylation of carbonyl compounds, with a particular interest in the structure and reactivity of the nucleophile (the Reformatsky reagent), as well as any alkylnickel intermediate derived from the nucleophile.

Our mechanistic studies began with an investigation of the Reformatsky reagent. A number of crystal structures of zincated carbonyl derivatives have been reported, including compounds that are oxygen-bound only (e.g., zinc enolates of ketones^{27,28}) as well as carbon-bound (~tetrahedral carbon; amide derivatives^{28,29}). Although we originally hypothesized that our nucleophile, derived from an amide, likely involved a carbon-bound zinc, we also considered the possibility that the ring strain of the azetidine might impede electron donation by the nitrogen lone pair to the carbonyl group,²⁴ leading to an oxygen-bound zinc enolate, as observed for ketone derivatives. To resolve this question, we pursued the structural characterization of a representative nucleophile.

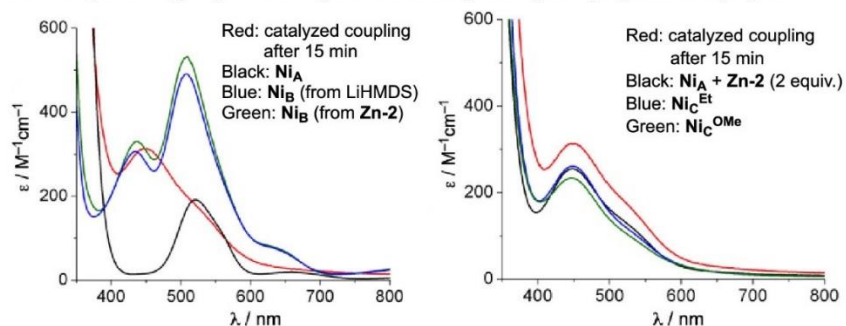
X-ray crystallographic analysis of **Zn-2** revealed a dimeric carbonyl-bridged C-metalated structure in the solid state (**Figure 2.5A**), consistent with prior studies of Reformatsky reagents derived from amides.^{28,29} The dimeric Reformatsky reagents are heterochiral, and the C2–C3–C4, C2–C3–Zn1, and C4–C3–Zn1 bond angles of the stereogenic carbon range from 106° to 115°.

Recognizing that the structure of the nucleophile in solution is more relevant to catalysis than its structure in the solid state, we investigated the Reformatsky reagent via NMR spectroscopy, and we determined that the α -CH group of **Zn-2** appears at δ 1.79 in the ¹H NMR spectrum and at δ 37.6 in the ¹³C NMR spectrum (THF-*d*₈, rt), which are consistent with a C-metalated structure and inconsistent with an O-bound zinc enolate. Furthermore, **Zn-2** exhibits an absorption in its infrared spectrum at 1597 cm⁻¹, which we assign to the C=O stretching of a carbonyl group.

A. Crystallographic characterization of racemic organozinc nucleophile **Zn-2**



B. UV-vis spectroscopy: **Ni_C** is the resting state of the catalyst during a coupling reaction in progress



C. Synthesis of nickel(II) complexes, including the resting state during catalysis (**Ni_C**)

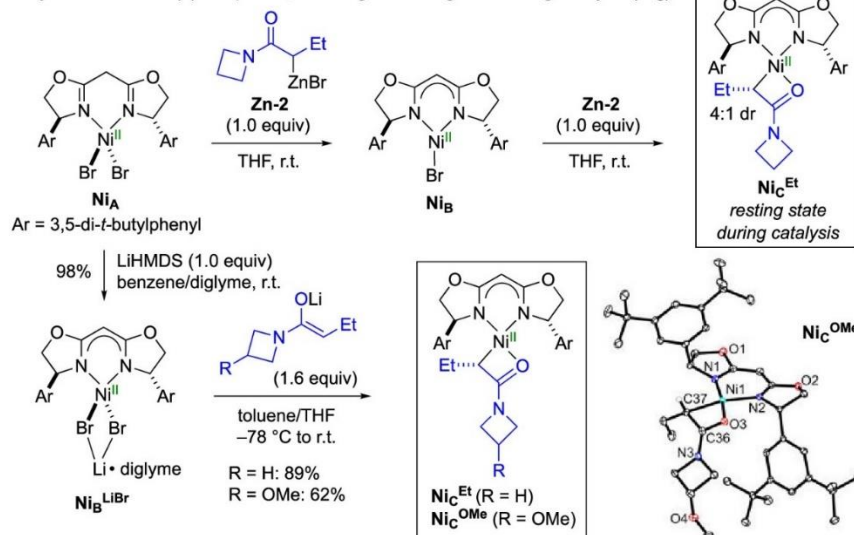


Figure 2.5. Mechanistic studies. (A) Crystallographic characterization of racemic organozinc nucleophile **Zn-2** (thermal ellipsoids at 50% probability; hydrogen atoms have been omitted for clarity). (B) UV-vis spectroscopy: **Ni_C** is the resting state of the catalyst during a coupling reaction in progress (THF, rt). (C) Synthesis of nickel(II) complexes, including the resting state during catalysis (**Ni_C**) (thermal ellipsoids at 50% probability; most hydrogen atoms have been omitted for clarity).

Understanding the dynamics of the Reformatsky reagent, specifically, the rate of racemization of the α stereocenter, could help to frame our consideration of the origin of stereoselectivity in our nickel-catalyzed enantioconvergent alkylations; to the best of our knowledge, the barrier for this interconversion has not previously been measured for Reformatsky reagents. We have determined that the diastereotopic methylene protons in the β position of Reformatsky reagent **Zn-2** can be distinguished in THF- d_8 at room temperature, indicating that the α stereocenter is configurationally stable on the NMR time scale under these conditions, corresponding to a barrier for interconversion of at least 14 kcal/mol.

With useful information in hand about the Reformatsky reagent, we sought to identify the nickel-containing species that are present during catalysis. When monitoring through electron paramagnetic resonance (EPR) spectroscopy the coupling that provides product **2** (**Figure 2.2A**), we observe no signal, consistent with the absence of detectable amounts of nickel(I) and nickel(III) species during the reaction. On the other hand, the UV-vis spectrum of this coupling reveals an absorbance with $\lambda_{\text{max}} = 449$ nm (red trace on the left side of **Figure 2.5B**). On the basis of our previous mechanistic studies of other nickel-catalyzed enantioconvergent couplings,^{30,31} we speculated that a nickel(II) complex might be responsible for this absorbance.

Treatment of NiBr₂·glyme with bisoxazoline ligand **L*** in THF at room temperature provides a 94% yield of NiBr₂L* (**Ni_A**), which exhibits a UV-vis spectrum that is distinct from a catalyzed coupling in progress (red versus black traces on the left side of **Figure 2.5B**). Because bisoxazoline **L*** bears a potentially labile methylene proton between the two oxazolines, we sought to determine whether the ligand may be deprotonated under the reaction conditions. Treatment of **Ni_A** with LiHMDS, a strong, non-nucleophilic Brønsted base, generates a 98% yield of **Ni_B** (**Figure 2.5C**; isolated as a LiBr/diglyme adduct, **Ni_B^{LiBr}**; for the crystallographic

characterization of NiB^{LiBr} , see **2.4 Experimental Section**), which also displays a UV-vis spectrum different from a catalyzed coupling (red versus blue traces on the left side of **Figure 2.5B**) but essentially identical to the spectrum produced upon treatment of NiA with one equivalent of Reformatsky reagent **Zn-2** (blue versus green traces on the left side of **Figure 2.5B**), indicating that NiB may be formed via deprotonation of NiA by **Zn-2** at the outset of catalysis (**Figure 2.5C**).³²

Treatment of NiB with an additional equivalent of Reformatsky reagent **Zn-2** leads to a UV-vis spectrum that is very similar to that of a coupling in progress (red versus black traces on the right side of **Figure 2.5B**). Hypothesizing that an organonickel(II) complex might be responsible for these UV-vis spectra, we independently synthesized and characterized two such complexes through the reaction of NiB^{LiBr} with the lithium enolates of two amides (NiC^{Et} and NiC^{OMe} ; **Figure 2.5C**). The UV-vis spectra of both of these alkylnickel(II) complexes are very similar to the spectrum of a catalyzed coupling (red, blue, and green traces on the right side of **Figure 2.5B**), consistent with such a complex being the resting state of the catalyst during a reaction.

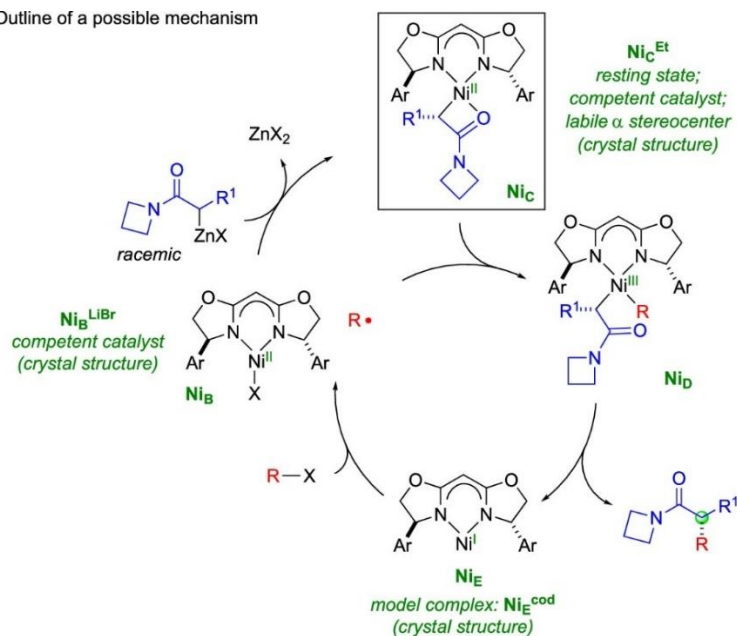
Next, we determined the structure of NiC^{OMe} via X-ray crystallography (**Figure 2.5C**). The metalated amide is bound to an approximately square-planar nickel through the α carbon ((*S*) stereochemistry with (*S,S*)-**L***) and the carbonyl group (C36–O3, 1.291(2) Å and C36–C37, 1.451(2) Å, which are similar to the corresponding bonds in **Zn-2**: C4–O1, 1.275(2) Å and C3–C4, 1.459(2) Å). The configuration of the coupling product generated by (*S,S*)-**L*** corresponds to alkylation of the carbon–nickel bond of NiC^{OMe} with retention of stereochemistry.

Analysis of NiC^{Et} via ^1H NMR spectroscopy reveals the presence of both epimers at the α carbon in THF-*d*₈ at room temperature (4:1 ratio). NOESY experiments establish that the major

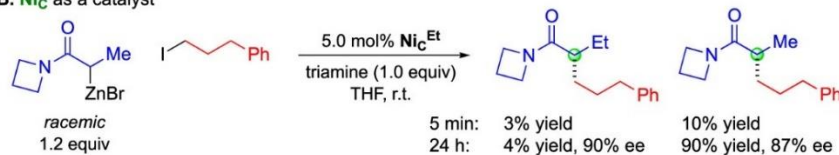
diastereomer has (*S*) stereochemistry at the α carbon, which is presumably favored because the α -H, rather than the α -Et, is proximal to the bulky aryl substituent of the chiral ligand (see C37 in the crystal structure of **NiC**^{OMe} in **Figure 2.5C**). We have determined that the diastereomers interconvert with $\Delta G^\ddagger(S \rightarrow R) = 19.5 \text{ kcal}\cdot\text{mol}^{-1}$ and $\Delta G^\ddagger(R \rightarrow S) = 18.5 \text{ kcal}\cdot\text{mol}^{-1}$ (see **2.4. Experimental Section**). This interconversion provides a mechanism by which the 4:1 mixture of epimers can furnish the α -alkylation product with high ee.

Building on our previous mechanistic studies,^{30,31} we provide in **Figure 2.6A** a possible pathway for these nickel-catalyzed enantioconvergent α -alkylations. At the outset, $\text{NiBr}_2\cdot\text{glyme}$, **L***, and the Reformatsky reagent react to generate **NiC**, which is the resting state of nickel during a catalyzed coupling (**Figure 2.5B, C**) and is formed within 5 min of mixing the reaction components (see **2.4. Experimental Section**). A nickel(I) metalloradical, **NiE** (vide infra), abstracts a halogen atom from the electrophile (R-X) to afford an alkyl radical (R^\bullet) and **NiB** (which reacts with the Reformatsky reagent to produce **NiC**). Alkyl radical R^\bullet couples with the resting state of nickel, **NiC**, to furnish a dialkylnickel(III) complex, **NiD**, which reductively eliminates to provide the desired enantioenriched α -alkylation product and to regenerate nickel(I) complex **NiE**.

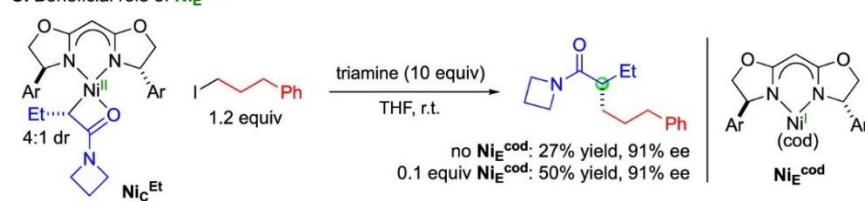
A. Outline of a possible mechanism



B. Ni_C as a catalyst



C. Beneficial role of Ni_E^{cod}



D. Support for the intermediacy of an organic radical, R•

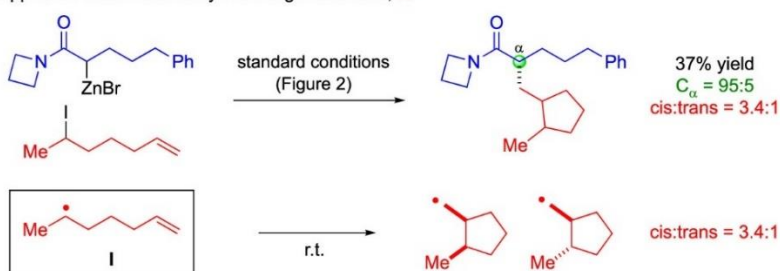


Figure 2.6. Mechanistic studies (continued). (A) Outline of a possible mechanism. For the sake of simplicity, all steps are drawn as irreversible, and the full coordination sphere around nickel is not always provided. (B) **Ni_C** as a catalyst. (C) Beneficial role of **Ni_E^{cod}**. (D) Support for the intermediacy of an organic radical, R•.

Consistent with the proposed mechanism (**Figure 2.6A**), NiC^{Et} and NiB^{LiBr} serve as suitable catalysts for enantioconvergent α -alkylation, affording product **2** (**Figure 2.2A**) with a similar rate and enantioselectivity as $\text{NiBr}_2 \cdot \text{glyme}/\text{L}^*$ under the standard reaction conditions (see **2.4. Experimental Section**). To gain insight into the reactivity profile of postulated intermediate NiC , we carried out a crossover experiment wherein we employed NiC^{Et} , which bears an amide with an α -ethyl substituent, as a catalyst in the cross-coupling of an α -methyl-substituted Reformatsky reagent (**Figure 2.6B**). Our observation that most of the α -ethyl-substituted product is generated at the outset of the reaction suggests that exchange of the organic groups between NiC^{Et} and the Reformatsky reagent is not occurring extremely rapidly relative to the rate of carbon–carbon bond formation from NiC^{Et} .

We have also investigated stoichiometric couplings of NiC^{Et} with an alkyl electrophile. A modest yield and good enantioselectivity (27% yield, 91% ee) are observed upon treating NiC^{Et} with a primary alkyl iodide (**Figure 2.6C**). As outlined in **Figure 2.6A**, we hypothesize that a nickel(I) metalloradical, NiE , serves as a chain-carrying radical in the catalytic cycle; under our standard coupling conditions, such species may be generated, for example, by a comproportionation reaction or by bond homolysis from a nickel(II) complex. To provide support for the beneficial impact of a nickel(I) complex on carbon–carbon bond formation, we independently synthesized nickel(I)/ L^* derivative NiE^{cod} (for the crystal structure, see **2.4. Experimental Section**), and we determined that the presence of a small amount of this complex (0.1 equiv) does indeed enhance the yield of the coupling reaction (50% yield, 91% ee; **Figure 2.6C**).

As our proposed catalytic cycle suggests that the R group of the alkyl electrophile (R–X) binds to nickel via a radical pathway (**Figure 2.6A**), we sought evidence that R^{\bullet} is formed under

our coupling conditions. Using 6-iodo-1-heptene as a mechanistic probe, we observe coupling products wherein the electrophile has cyclized to generate a 3.4:1 mixture of cis and trans isomers of cyclopentanes, the same ratio of isomers that has been reported for the cyclization of radical **I** (**Figure 2.6D**).³³ Furthermore, since **I** cyclizes with a rate constant of $\sim 1 \times 10^5 \text{ s}^{-1}$ at 25 °C,³³ much slower than the rate of diffusion (generally $\sim 10^8\text{--}10^9 \text{ s}^{-1}$ at 25 °C),³⁴ our observation of cyclized product is consistent with out-of-cage coupling of R[•], as required by the mechanism illustrated in **Figure 2.6A**. Taken together, our various studies are fully congruent with the catalytic enantioselective radical-based pathway outlined in **Figure 2.6A**, which complements classic approaches to stereoselective α -alkylation that have relied on polar reactions and stoichiometric chiral auxiliaries.⁶⁻⁸

2.3. Conclusion

The catalytic enantioselective α -alkylation of carbonyl compounds with unactivated alkyl electrophiles is a classic, long-standing challenge in asymmetric synthesis. A recent review of transition-metal-catalyzed reactions of enolates¹² concluded that a “methodology for building stereogenic centers with nonfunctionalized sp^3 -hybridized electrophiles...is...missing at this point”. In this study, we address this deficiency, demonstrating that a chiral nickel catalyst can achieve enantioconvergent couplings of racemic Reformatsky reagents with unactivated alkyl electrophiles; the method displays good functional-group tolerance, and the products of the coupling can be transformed without racemization into a wide range of other families of useful enantioenriched compounds. Exploiting an array of mechanistic tools, we have gained insight into key intermediates and elementary steps of this enantioconvergent α -alkylation, including crystallographic characterization of an alkylnickel(II) complex that contains a nickel-bound

stereogenic carbon and serves as the resting state of the catalyst under the reaction conditions. This work demonstrates the ability of nickel catalysis to address a long-sought objective in asymmetric synthesis, via a novel mechanism.

2.4. Experimental Section

2.4.1. General Information

Unless otherwise noted, reagents received from commercial suppliers were used as received. All reactions were performed under an atmosphere of dry nitrogen. Glassware was oven-dried at 150 °C for a minimum of 12 h, or flame-dried utilizing a gas flame under high vacuum. All solvents were purified by passage through activated aluminum oxide in a solvent-purification system.

NMR spectra were collected on a Bruker 400 MHz, Varian 500 MHz, or Varian 600 MHz spectrometer at ambient temperature (unless otherwise indicated); chemical shifts (δ) are reported in ppm downfield from tetramethylsilane, using the solvent resonance as an internal standard. SFC analyses were carried out on an Agilent 1260 Infinity II system with Daicel CHIRALPAK® or Daicel CHIRALCEL® columns (4.6 \times 250 mm, particle size 5 μ m). FT-IR measurements were carried out on a Thermo Scientific Nicolet iS5 FT-IR spectrometer equipped with an iD5 ATR accessory. HRMS were acquired on an Agilent 1260 Infinity II HPLC, Agilent 6230 LC-TOF system in electrospray ionization (ESI+) mode, a Waters LCT Premier XE Time-of-Flight mass spectrometer in electrospray ionization (ESI+) mode, or a JEOL AccuTOF GC-Alpha (JMS-T2000GC) that was fitted with a LIFDI ionization source from Linden CMS. Optical rotation data were obtained with a Jasco P-2000 polarimeter at 589 nm, using a 100 mm pathlength cell in the solvent and at the concentration indicated. GC analyses were carried out on an Agilent 6890N GC. Flash column chromatography was performed using silica gel (SiliaFlash® P60, particle size 40–63 μ m, Silicycle). X-ray crystallographic analyses were carried out by the Caltech X-Ray Crystallography Facility. X-band continuous-wave EPR measurements were carried out on a Bruker EMX spectrometer with the sample in frozen solvent at 77 K. Electronic absorption spectra were collected on a Cary 50 UV-vis spectrometer using a 10 mm path length quartz cuvette

(solution) or on a Cary 5000 UV-vis spectrometer with integration sphere (solid state). Elemental analyses were carried out with a PerkinElmer 2400 Series II CHN Elemental Analyzer.

2.4.2. Preparation of L*

In a glovebox, (*S*)-2-amino-2-(3,5-di-*tert*-butylphenyl)ethan-1-ol (35) (6.13 g, 24.6 mmol, >99% ee), diethyl malonimidate dihydrochloride (2.84 g, 12.3 mmol), and THF (49 mL) were added to a 100 mL round-bottom flask equipped with a stir bar. The flask was capped with a septum, the joint was wrapped with electrical tape, and the flask was removed from the glovebox. The mixture was stirred at 50 °C for 60 h, and then it was cooled to r.t. and partitioned between DCM (100 mL) and water (50 mL). The phases were separated, and the aqueous phase was extracted with DCM (30 mL × 2). The combined organic phase was washed with brine (50 mL), dried with Na₂SO₄, and concentrated. The residue was then purified by column chromatography on silica gel (10% → 40% Etowah/hexanes) to afford the desired product. 3.06 g (5.76 mmol, 49% yield). White solid.

(*R,R*)-L* was prepared following the same route, starting from (*R*)-2-amino-2-(3,5-di-*tert*-butylphenyl)ethan-1-ol (>99% ee).

¹H NMR (400 MHz, CDCl₃) δ 7.33 (t, *J* = 1.8 Hz, 2H), 7.11 (d, *J* = 1.9 Hz, 4H), 5.26 – 5.17 (m, 2H), 4.68 (dd, *J* = 10.2, 8.4 Hz, 2H), 4.26 (dd, *J* = 8.4, 7.5 Hz, 2H), 3.61 (t, *J* = 1.2 Hz, 2H), 1.30 (s, 36H).

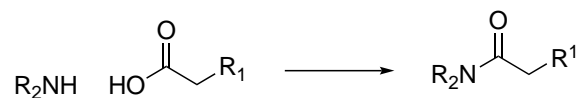
¹³C NMR (101 MHz, CDCl₃) δ 162.5, 151.1, 141.2, 121.8, 120.9, 75.5, 70.4, 34.9, 31.5, 28.6.

FT-IR (film): 2960, 2902, 2868, 1668, 1598, 1476, 1168, 978 cm⁻¹.

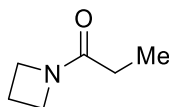
HRMS (ESI+) *m/z* [M+H]⁺ calcd for C₃₅H₅₁N₂O₂: 531.3946, found: 531.3947.

$[\alpha]_D^{22} = -124$ (c 1.0, CHCl_3), from (*S,S*)-**L***.

2.4.3. Preparation of Amides



General Procedure 1 (GP-1). A 250 mL round-bottom flask was charged with a stir bar, the amine (or amine·HCl) (1.2 equiv), the carboxylic acid (1.0 equiv), hydroxybenzotriazole hydrate (1.3 equiv), DCM (volume to generate [carboxylic acid] = ~0.2 M), diisopropylethylamine (3.0 equiv), and *N*-(3-dimethylaminopropyl)-*N*'-ethylcarbodiimide hydrochloride (1.2 equiv; in one portion). The resulting mixture was stirred at r.t. overnight, and then it was partitioned between equal volumes (~ the same volume as the reaction mixture) of DCM and 1 N HCl. The phases were separated, and the aqueous phase was extracted twice with DCM. The combined organic phase was washed with brine, dried with Na_2SO_4 , and concentrated. The residue was purified by column chromatography on silica gel to afford the desired product.



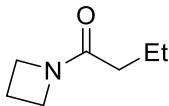
1-(Azetidin-1-yl)propan-1-one. The title compound was synthesized according to **GP-1** from azetidine-HCl and propionic acid (7.00 mmol). The product was purified by column chromatography on silica gel (100% EtOAc). 570 mg (5.04 mmol, 72% yield). Colorless oil.

^1H NMR (500 MHz, CDCl_3) δ 4.12 (t, $J = 7.6$ Hz, 2H), 4.01 (t, $J = 7.6$ Hz, 2H), 2.26 (p, $J = 7.7$ Hz, 2H), 2.08 (q, $J = 7.6$ Hz, 2H), 1.12 (t, $J = 7.6$, 3H).

^{13}C NMR (101 MHz, CDCl_3) δ 173.9, 50.0, 47.8, 24.4, 15.1, 9.0.

FT-IR (film): 2952, 2881, 1646, 1456, 1436, 1168 cm^{-1} .

HRMS (ESI-MS) m/z $[\text{M}+\text{H}]^+$ calcd for $\text{C}_6\text{H}_{12}\text{NO}$: 114.0914, found: 114.0912.



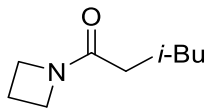
1-(Azetidin-1-yl)butan-1-one. The title compound was synthesized according to **GP-1** from azetidine-HCl and butyric acid (20.0 mmol). The product was purified by column chromatography on silica gel (100% EtOAc). 1.94 g (15.3 mmol, 76% yield). Colorless oil.

^1H NMR (400 MHz, CDCl_3) δ 4.15 – 4.07 (m, 2H), 4.04 – 3.95 (m, 2H), 2.30 – 2.17 (m, 2H), 2.06 – 1.98 (m, 2H), 1.70 – 1.55 (m, 2H), 0.93 (t, $J = 7.4$ Hz, 3H).

^{13}C NMR (101 MHz, CDCl_3) δ 173.2, 50.1, 47.7, 33.1, 30.9, 18.4, 15.0, 14.0.

FT-IR (film): 2960, 2934, 2877, 1654, 1457, 1437, 1168 cm^{-1} .

HRMS (ESI-MS) m/z $[\text{M}+\text{H}]^+$ calcd for $\text{C}_7\text{H}_{14}\text{NO}$: 128.1070, found: 128.1065.



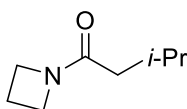
1-(Azetidin-1-yl)-4-methylpentan-1-one. The title compound was synthesized according to **GP-1** from azetidine-HCl and 4-methylvaleric acid (10.0 mmol). The product was purified by column chromatography on silica gel (100% EtOAc). 1.10 g (7.09 mmol, 71% yield). Colorless oil.

^1H NMR (400 MHz, CDCl_3) δ 4.17 – 4.04 (m, 2H), 4.00 (t, $J = 7.7$ Hz, 2H), 2.32 – 2.17 (m, 2H), 2.09 – 2.00 (m, 2H), 1.61 – 1.53 (m, 1H), 1.53 – 1.43 (m, 2H), 0.89 (d, $J = 6.4$ Hz, 6H).

^{13}C NMR (101 MHz, CDCl_3) δ 173.5, 50.1, 47.8, 33.7, 29.3, 27.9, 22.3, 15.0.

FT-IR (film): 2954, 2876, 1654, 1458, 1429, 1168, 966, 732 cm^{-1} .

HRMS (ESI-MS) m/z $[\text{M}+\text{H}]^+$ calcd for $\text{C}_9\text{H}_{18}\text{NO}$: 156.1383, found: 156.1379.



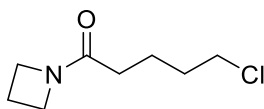
1-(Azetidin-1-yl)-3-methylbutan-1-one. The title compound was synthesized according to **GP-1** from azetidine-HCl and isovaleric acid (5.00 mmol). The product was purified by column chromatography on silica gel (100% EtOAc). 540 mg (3.82 mmol, 76% yield). Colorless oil.

^1H NMR (400 MHz, CDCl_3) δ 4.20 – 4.07 (m, 2H), 4.02 (t, $J = 7.7$ Hz, 2H), 2.31 – 2.22 (m, 2H), 2.22 – 2.04 (m, 1H), 1.93 (d, $J = 7.2$ Hz, 2H), 0.95 (d, $J = 6.6$ Hz, 6H).

^{13}C NMR (101 MHz, CDCl_3) δ 172.8, 50.2, 47.6, 40.2, 25.7, 22.6, 14.9.

FT-IR (film): 2956, 2882, 1648, 1438, 1384, 1169, 828, 690 cm^{-1} .

HRMS (ESI-MS) m/z $[\text{M}+\text{H}]^+$ calcd for $\text{C}_8\text{H}_{16}\text{NO}$: 142.1227, found: 142.1224.



1-(Azetidin-1-yl)-5-chloropentan-1-one. The title compound was synthesized according to **GP-1** from azetidine-HCl and 5-chlorovaleric acid (5.00 mmol). The product was purified by

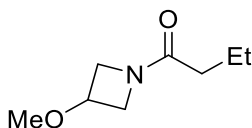
column chromatography on silica gel (100% EtOAc). 850 mg (4.84 mmol, 76% yield). Colorless oil.

^1H NMR (400 MHz, CDCl_3) δ 4.17 – 4.08 (m, 2H), 4.01 (t, $J = 7.7$ Hz, 2H), 3.54 (t, $J = 6.4$ Hz, 2H), 2.32 – 2.20 (m, 2H), 2.09 (t, $J = 7.0$ Hz, 2H), 1.87 – 1.69 (m, 4H).

^{13}C NMR (101 MHz, CDCl_3) δ 172.4, 50.1, 47.8, 44.7, 32.2, 30.2, 22.1, 15.1.

FT-IR (film): 2952, 2881, 1646, 1456, 1436, 1168 cm^{-1} .

HRMS (ESI-MS) m/z $[\text{M}+\text{H}]^+$ calcd for $\text{C}_8\text{H}_{15}\text{ClNO}$: 176.0837, found: 176.0835.



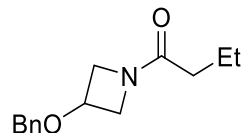
1-(3-Methoxyazetidin-1-yl)butan-1-one. The title compound was synthesized according to **GP-1** from 3-methoxy-azetidine-HCl and butyric acid (8.49 mmol). The product was purified by column chromatography on silica gel (100% EtOAc). 1.18 g (7.51 mmol, 88% yield). Colorless oil.

^1H NMR (400 MHz, CDCl_3) δ 4.28 – 4.21 (m, 1H), 4.21 – 4.08 (m, 2H), 4.00 – 3.92 (m, 1H), 3.91 – 3.81 (m, 1H), 3.29 (s, 3H), 2.11 – 1.99 (m, 2H), 1.71 – 1.55 (m, 2H), 0.93 (t, $J = 7.4$ Hz, 3H).

^{13}C NMR (101 MHz, CDCl_3) δ 173.4, 68.7, 57.0, 56.2, 54.7, 33.5, 18.3, 13.9.

FT-IR (film): 2934, 2874, 2833, 1652, 1453, 1130, 882 cm^{-1} .

HRMS (ESI-MS) m/z $[\text{M}+\text{H}]^+$ calcd for $\text{C}_8\text{H}_{16}\text{NO}_2$: 158.1176, found: 158.1172.



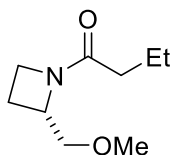
1-(3-Benzyloxyazetidin-1-yl)butan-1-one. The title compound was synthesized according to **GP-1** from 3-benzyloxy-azetidine-HCl and butyric acid (7.78 mmol). The product was purified by column chromatography on silica gel (100% EtOAc). 1.28 g (5.50 mmol, 71% yield). Colorless oil.

^1H NMR (500 MHz, CDCl_3) δ 7.40 – 7.29 (m, 5H), 4.53 – 4.43 (m, 2H), 4.37 (tt, $J = 6.8, 4.3$ Hz, 1H), 4.23 (ddd, $J = 9.2, 6.6, 1.4$ Hz, 1H), 4.14 (dd, $J = 10.6, 6.5$ Hz, 1H), 4.01 (dd, $J = 9.1, 4.2$ Hz, 1H), 3.91 (dd, $J = 10.6, 4.3$ Hz, 1H), 2.12 – 2.01 (m, 2H), 1.63 (dt, $J = 15.9, 7.9$ Hz, 2H), 0.94 (t, $J = 7.4$ Hz, 3H).

^{13}C NMR (101 MHz, CDCl_3) δ 173.4, 137.0, 128.6, 128.2, 128.0, 71.3, 67.0, 57.4, 55.1, 33.6, 18.4, 13.9.

FT-IR (film): 3058, 3029, 2960, 2936, 2872, 1648, 1450, 1132, 1021, 744, 734, 698 cm^{-1} .

HRMS (ESI-MS) m/z $[\text{M}+\text{H}]^+$ calcd for $\text{C}_{14}\text{H}_{20}\text{NO}_2$: 234.1489, found: 234.1495.



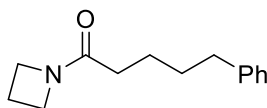
(S)-1-(2-(Methoxymethyl)azetidin-1-yl)butan-1-one. The title compound was synthesized according to **GP-1** from (*S*)-2-(methoxymethyl)azetidine-HCl and butyric acid (1.58 mmol). The product was purified by column chromatography on silica gel (100% EtOAc). 260 mg (1.51 mmol, 96% yield). Colorless oil.

^1H NMR (400 MHz, CDCl_3) δ 4.46 (dt, $J = 9.1, 4.7$ Hz, 1H), 4.13 – 3.50 (m, 4H), 3.39 (d, $J = 2.6$ Hz, 3H), 2.43 – 1.92 (m, 4H), 1.76 – 1.56 (m, 2H), 0.94 (t, $J = 7.4$ Hz, 3H). Rotamers detected.

^{13}C NMR (101 MHz, CDCl_3) δ 174.1, 173.7, 75.2, 72.1, 61.6, 60.1, 59.30, 59.25, 48.3, 45.6, 33.8, 33.6, 19.1, 18.7, 18.5, 18.2, 14.0, 13.9. Rotamers detected.

FT-IR (film): 2962, 2878, 1647, 1423, 1324, 1108, 669, 592 cm^{-1} .

HRMS (ESI-MS) m/z $[\text{M}+\text{H}]^+$ calcd for $\text{C}_9\text{H}_{18}\text{NO}_2$: 172.1333, found: 172.1331.



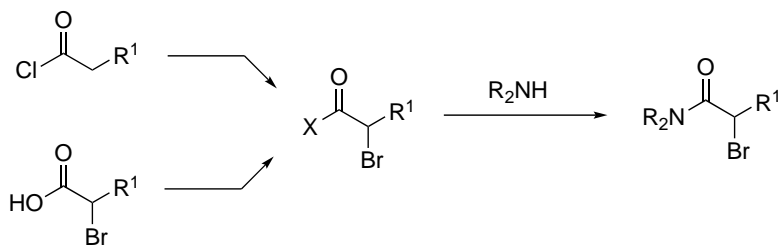
1-(Azetidin-1-yl)-5-phenylpentan-1-one. The title compound was synthesized according to **GP-1** from azetidine-HCl and 5-phenylvaleric acid (20.0 mmol). The product was purified by column chromatography on silica gel (100% EtOAc). 3.70 g (17.05 mmol, 85% yield). Colorless oil.

^1H NMR (500 MHz, CDCl_3) δ 7.29 – 7.23 (m, 2H), 7.19 – 7.14 (m, 3H), 4.09 (t, $J = 7.6$ Hz, 2H), 4.00 (t, $J = 7.8$ Hz, 2H), 2.62 (t, $J = 6.9$ Hz, 2H), 2.24 (tt, $J = 8.3, 7.7$ Hz, 2H), 2.10 – 2.04 (m, 2H), 1.70 – 1.60 (m, 4H).

^{13}C NMR (101 MHz, CDCl_3) δ 173.1, 142.3, 128.4, 128.3, 125.7, 50.1, 47.7, 35.8, 31.3, 31.1, 24.6, 15.0.

FT-IR (film): 3059, 3023, 3002, 2934, 2879, 1648, 1432, 1120, 1030, 770, 701, 690 cm^{-1} .

HRMS (ESI-MS) m/z $[\text{M}+\text{H}]^+$ calcd for $\text{C}_{14}\text{H}_{20}\text{NO}$: 218.1540, found: 218.1548.



General Procedure 2 (GP-2).

GP-2A: A 100 mL round-bottom flask was charged with a stir bar, the acyl chloride (1.0 equiv), and bromine (1.2 equiv). A reflux condenser (cooled at 0 °C) was attached, and the mixture was heated at 70 °C for 1 h. Then, the mixture was cooled to r.t., and most of the excess bromine and the HBr was removed with the aid of a strong flow of nitrogen over 5 min. The α-bromo acyl halide was used in the next step without further purification.

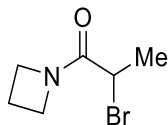
GP-2B: A 250 mL round-bottom flask was charged with a stir bar, the α-bromo acid (1.0 equiv), and DMF (1 drop). DCM (volume to generate [α-bromo acid] = ~0.4 M) was added, and the mixture was stirred and cooled to 0 °C. Then, oxalyl chloride (1.1 equiv) was added dropwise. The mixture was warmed to r.t. and stirred for 2 h. The volatiles were then removed using a rotary evaporator in a fume hood (water bath <25 °C) to afford the α-bromo acyl chloride, which was used in the next step without further purification.

Acylation. A 250 mL round-bottom flask was charged with a stir bar, the dialkylamine (or amine·HCl) (1.2 equiv), and triethylamine (2.2 equiv). DCM (volume to generate [acyl halide] = ~0.4 M) was added, and the mixture was stirred and cooled to 0 °C. The α-bromo acyl halide (1.0 equiv) was added dropwise as a solution (~1.2 M) in DCM. Then, the reaction mixture was warmed to r.t. and stirred for 1 h. Next, the mixture was partitioned between equal volumes (~ the same volume as the reaction mixture) of DCM and 2 N HCl. The phases were separated, the aqueous phase was extracted with DCM, and the combined organic phase was washed with brine, dried

with Na₂SO₄, and concentrated. The residue was then purified by column chromatography on silica gel to afford the desired product.



General Procedure 3 (GP-3). This procedure is a modification of a previous report. (36) A 250 mL round-bottom flask was charged with a stir bar, the amide (1.0 equiv), and DCM (volume to generate [amide] = ~0.1 M). The mixture was stirred and cooled to 0 °C. Then, triflic anhydride (1.1 equiv) was added dropwise, and the mixture was stirred at 0 °C for 15 min. Next, 2,6-lutidine-*N*-oxide (1.0 equiv) was added dropwise, and the mixture was stirred at 0 °C for 5 min. NaBr (5.0 equiv) and tetrabutylammonium bromide (0.01 equiv) were then added together to the reaction mixture, which was warmed to r.t. and stirred for 20 h. Next, the mixture was washed with saturated aqueous NH₄Cl and brine, and the organic phase was dried with Na₂SO₄ and concentrated. The residue was purified by column chromatography on silica gel to afford the desired product.



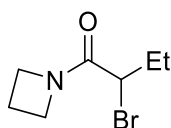
1-(Azetidin-1-yl)-2-bromopropan-1-one. The title compound was synthesized according to **GP-2** from azetidine-HCl and 2-bromopropionyl bromide (19.2 mmol). The product was purified by column chromatography on silica gel (40 → 60% EtOAc/hexanes). 3.35 g (17.5 mmol, 91% yield). Pale yellow oil.

^1H NMR (400 MHz, CDCl_3) δ 4.41 – 4.28 (m, 1H), 4.28 – 4.15 (m, 2H), 4.15 – 3.95 (m, 2H), 2.40 – 2.25 (m, 2H), 1.77 (dd, $J = 6.7, 1.2$ Hz, 3H).

^{13}C NMR (101 MHz, CDCl_3) δ 168.6, 50.8, 48.5, 37.3, 20.9, 15.4.

FT-IR (film): 2958, 2882, 1655, 1457, 1447, 1435, 1304, 1012, 829, 690 cm^{-1} .

HRMS (ESI-MS) m/z $[\text{M}+\text{H}]^+$ calcd for $\text{C}_6\text{H}_{11}\text{BrNO}$: 192.0019, found: 192.0017.



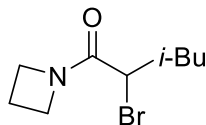
1-(Azetidin-1-yl)-2-bromobutan-1-one. The title compound was synthesized according to **GP-2B** from azetidine-HCl and 2-bromobutyric acid (30.0 mmol). The product was purified by column chromatography on silica gel (40 → 60% EtOAc/hexanes). 5.11 g (24.8 mmol, 83% yield). Yellow oil.

^1H NMR (400 MHz, CDCl_3) δ 4.34 – 4.23 (m, 1H), 4.23 – 4.15 (m, 1H), 4.15 – 4.04 (m, 1H), 4.04 – 3.94 (m, 2H), 2.31 (ttd, $J = 8.6, 6.9, 1.4$ Hz, 2H), 2.16 – 1.88 (m, 2H), 0.99 (t, $J = 7.3$ Hz, 3H).

^{13}C NMR (101 MHz, CDCl_3) δ 168.2, 50.8, 48.5, 44.7, 27.6, 15.3, 12.1.

FT-IR (film): 2970, 2881, 1654, 1456, 1437, 1118, 730 cm^{-1} .

HRMS (ESI-MS) m/z $[\text{M}+\text{H}]^+$ calcd for $\text{C}_7\text{H}_{13}\text{BrNO}$: 206.0176, found: 206.0175.



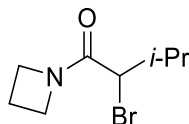
1-(Azetidin-1-yl)-2-bromo-4-methylpentan-1-one. The title compound was synthesized according to **GP-2A** from azetidine-HCl and 4-methylvaleryl chloride (27.3 mmol). The product was purified by column chromatography on silica gel (40 → 60% EtOAc/hexanes). 3.11 g (13.3 mmol, 49% yield). Pale yellow oil.

^1H NMR (400 MHz, CDCl_3) δ 4.37 – 4.24 (m, 1H), 4.24 – 3.96 (m, 4H), 2.39 – 2.24 (m, 2H), 1.97 – 1.80 (m, 2H), 1.81 – 1.67 (m, 1H), 0.93 (d, $J = 6.6$ Hz, 3H), 0.89 (d, $J = 6.6$ Hz, 3H).

^{13}C NMR (101 MHz, CDCl_3) δ 168.3, 50.8, 48.5, 42.7, 41.5, 26.2, 22.5, 21.9, 15.3.

FT-IR (film): 2956, 2882, 1663, 1438, 1368, 1239, 1120, 828 cm^{-1} .

HRMS (ESI-MS) m/z $[\text{M}+\text{H}]^+$ calcd for $\text{C}_9\text{H}_{17}\text{BrNO}$: 234.0489, found: 234.0493.



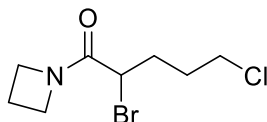
1-(Azetidin-1-yl)-2-bromo-3-methylbutan-1-one. The title compound was synthesized according to **GP-2A** from azetidine-HCl and isovaleryl chloride (10.0 mmol). The product was purified by column chromatography on silica gel (30% → 50% EtOAc/hexanes) to give a dark oil, which was recrystallized from hexanes and EtOAc to give a white solid. 1.04 g (4.71 mmol, 47% yield).

^1H NMR (400 MHz, CDCl_3) δ 4.32 – 4.15 (m, 2H), 4.15 – 3.97 (m, 2H), 3.79 (d, $J = 9.4$ Hz, 1H), 2.41 – 2.19 (m, 3H), 1.13 (d, $J = 6.6$ Hz, 3H), 0.99 (d, $J = 6.6$ Hz, 3H).

^{13}C NMR (101 MHz, CDCl_3) δ 168.3, 51.1, 50.9, 48.4, 31.6, 20.8, 19.9, 15.3.

FT-IR (film): 2962, 2934, 2877, 1658, 1437, 1169, 1121, 855, 632 cm^{-1} .

HRMS (ESI-MS) m/z $[\text{M}+\text{H}]^+$ calcd for $\text{C}_8\text{H}_{15}\text{BrNO}$: 220.0332, found: 220.0331.



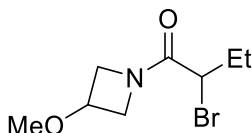
1-(Azetidin-1-yl)-2-bromo-5-chloropentan-1-one. The title compound was synthesized according to **GP-2A** from azetidine-HCl and 5-chlorovaleryl chloride (20.0 mmol). The product was purified by column chromatography on silica gel (40 \rightarrow 60% EtOAc/hexanes). 1.51 g (5.93 mmol, 30% yield). Pale yellow oil.

^1H NMR (500 MHz, CDCl_3) δ 4.38 – 4.26 (m, 1H), 4.25 – 4.16 (m, 1H), 4.16 – 4.08 (m, 2H), 4.04 (td, $J = 9.5, 7.1$ Hz, 1H), 3.57 (t, $J = 6.4$ Hz, 2H), 2.43 – 2.29 (m, 2H), 2.28 – 2.09 (m, 2H), 2.02 – 1.79 (m, 2H).

^{13}C NMR (101 MHz, CDCl_3) δ 167.7, 50.8, 48.6, 44.1, 41.9, 31.4, 30.3, 15.4.

FT-IR (film): 2958, 2883, 1654, 1456, 1439, 1275, 1168, 1078, 828 cm^{-1} .

HRMS (ESI-MS) m/z $[\text{M}+\text{H}]^+$ calcd for $\text{C}_8\text{H}_{14}\text{BrClNO}$: 253.9942, found: 253.9940.



2-Bromo-1-(3-methoxyazetidin-1-yl)butan-1-one. The title compound was synthesized according to **GP-2B** from 3-methoxy-azetidine-HCl and 2-bromobutyric acid (18.3 mmol). The

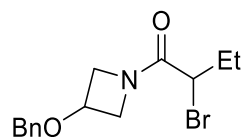
product was purified by column chromatography on silica gel (40 → 60% EtOAc/hexanes). 2.95 g (12.5 mmol, 68% yield). Pale yellow oil.

^1H NMR (400 MHz, CDCl_3) δ 4.47 – 4.29 (m, 1H), 4.28 – 3.93 (m, 5H), 3.31 (s, 3H), 2.19 – 1.92 (m, 2H), 0.99 (t, $J = 7.3$ Hz, 3H). Rotamers detected.

^{13}C NMR (101 MHz, CDCl_3) δ 168.5, 168.4, 68.9, 68.7, 57.81, 57.75, 56.3, 56.2, 55.54, 55.52, 45.1, 44.8, 27.6, 12.1. Rotamers detected.

FT-IR (film): 2969, 2932, 2875, 1662, 1454, 1438, 1128, 1031, 717 cm^{-1} .

HRMS (ESI-MS) m/z $[\text{M}+\text{H}]^+$ calcd for $\text{C}_8\text{H}_{15}\text{BrNO}_2$: 158.1176, found: 158.1172.



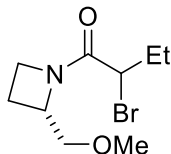
1-(3-(Benzyloxy)azetidin-1-yl)-2-bromobutan-1-one. The title compound was synthesized according to **GP-2B** from 3-benzyloxy-azetidine-HCl and 2-bromobutyric acid (7.78 mmol). The product was purified by column chromatography on silica gel (40 → 60% EtOAc/hexanes). 1.28 g (5.50 mmol, 71% yield). Yellow oil.

^1H NMR (500 MHz, CDCl_3) δ 7.40 – 7.30 (m, 5H), 4.55 – 4.44 (m, 2H), 4.44 – 3.86 (m, 6H), 2.09 (tdd, $J = 14.3, 7.1, 4.2$ Hz, 1H), 1.99 (dp, $J = 14.8, 7.4$ Hz, 1H), 1.00 (t, $J = 7.3$ Hz, 3H). Rotamers detected.

^{13}C NMR (101 MHz, CDCl_3) δ 168.3, 136.82, 136.79, 128.68, 128.66, 128.31, 128.27, 128.1, 128.0, 71.5, 71.4, 67.2, 66.9, 58.13, 58.06, 55.9, 45.1, 44.9, 27.7, 27.6, 12.1. Rotamers detected.

FT-IR (film): 3028, 2969, 2934, 2875, 1662, 1448, 1128, 1084, 1072, 739, 684 cm^{-1} .

HRMS (ESI-MS) m/z $[M+H]^+$ calcd for $C_{14}H_{19}BrNO_2$: 312.0594, found: 312.0591.



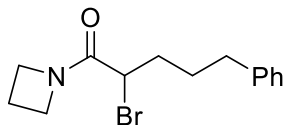
2-Bromo-1-((S)-2-(methoxymethyl)azetidin-1-yl)butan-1-one (mixture of 2 diastereomers) The title compound was synthesized according to **GP-2B** from (S)-2-(methoxymethyl)azetidine-HCl and 2-bromobutyric acid (7.31 mmol). The product was purified by column chromatography on silica gel (20 → 60% EtOAc/hexanes). The two diastereomers were not separated and were used directly for the synthesis of the organozinc reagent. 1.24 g (4.96 mmol, 68% yield). Yellow oil.

1H NMR (400 MHz, $CDCl_3$) δ 4.74 – 3.47 (m, 6H), 3.46 – 3.34 (m, 3H), 2.53 – 1.79 (m, 4H), 1.03 – 0.92 (m, 3H). Diastereomers and rotamers detected.

^{13}C NMR (101 MHz, $CDCl_3$) δ 169.8, 168.6, 168.5, 76.1, 74.9, 71.6, 71.1, 62.6, 62.5, 61.1, 61.0, 59.5, 59.4, 59.3, 59.1, 49.0, 48.9, 46.5, 45.9, 45.5, 45.4, 45.2, 45.1, 28.4, 27.8, 27.6, 27.5, 18.8, 18.7, 18.5, 12.2, 12.1, 12.01, 11.98. Diastereomers and rotamers detected.

FT-IR (film): 2968, 2886, 1658, 1433, 1349, 1246, 1103, 656 cm^{-1} .

HRMS (ESI-MS) m/z $[M+H]^+$ calcd for $C_9H_{18}NO_2$: 250.0438, found: 250.0441.



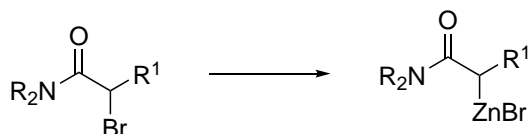
1-(Azetidin-1-yl)-2-bromo-5-phenylpentan-1-one. The title compound was synthesized according to **GP-3** from 1-(azetidin-1-yl)-5-phenylpentan-1-one (11.5 mmol). The product was purified by column chromatography on silica gel (10% → 40% EtOAc/hexanes). 2.27 g (7.66 mmol, 67% yield). Yellow oil.

^1H NMR (400 MHz, CDCl_3) δ 7.34 – 7.26 (m, 2H), 7.24 – 7.13 (m, 3H), 4.31 – 4.19 (m, 1H), 4.10 (tt, $J = 9.7, 7.0$ Hz, 2H), 4.06 – 3.95 (m, 2H), 2.75 – 2.55 (m, 2H), 2.39 – 2.21 (m, 2H), 2.19 – 1.93 (m, 2H), 1.84 – 1.58 (m, 2H).

^{13}C NMR (101 MHz, CDCl_3) δ 168.1, 141.6, 128.4, 126.0, 50.7, 48.5, 42.7, 35.3, 33.8, 29.2, 15.3.

FT-IR (film): 3059, 3023, 2933, 2879, 1648, 1454, 1432, 1120, 1030, 779, 701, 690 cm^{-1} .

HRMS (ESI-MS) m/z $[\text{M}+\text{H}]^+$ calcd for $\text{C}_{14}\text{H}_{19}\text{BrNO}$: 218.1540, found: 218.1548.

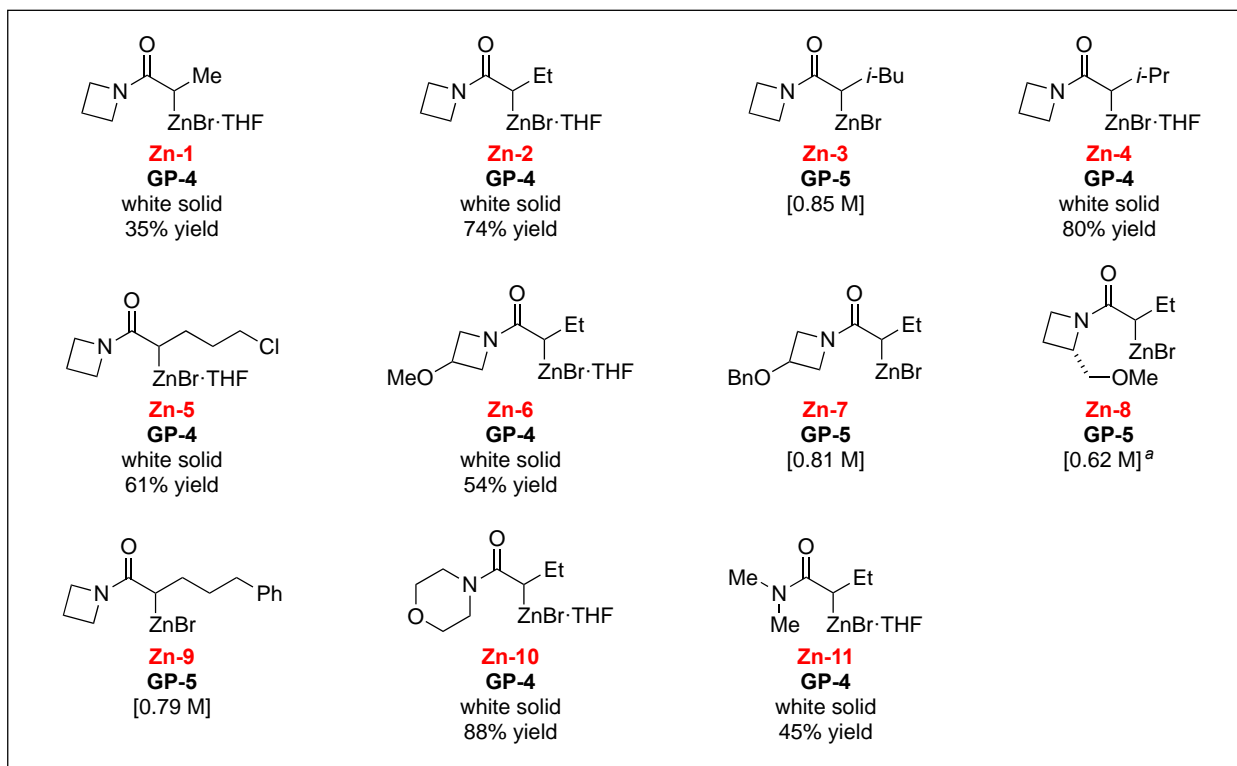


General Procedure 4 (GP-4). The α -bromoamide was azeotropically dried with toluene three times and dried under high vacuum at 40 °C for 1 h prior to use. In a glovebox, a 40 mL vial was charged with a cross-shaped stir bar, zinc powder (0.99 equiv, ~100 mesh, Alfa, 99.9%), iodine (0.05 equiv), and THF (0.3 mL/mmol of the α -bromoamide). The mixture was stirred vigorously until the brown color of iodine faded. Then, the α -bromoamide in THF (0.3 mL/mmol of α -bromoamide) was added dropwise. The vial was capped tightly with a septum cap, and the joint

was wrapped with electrical tape. Next, the vial was removed from the glovebox and heated at 80 °C for 12 h. Then, it was taken into the glovebox and stored at –40 °C for 2 days. The resulting mixture was filtered through a frit, and the white solid was washed with an ample quantity of cold THF. The collected solid was dried under high vacuum for 5 min (excessive drying (>1 h) can lead to Reformatsky reagent that performs poorly in catalysis) to give the Reformatsky reagent as a white solid. The Reformatsky reagent can be stored under nitrogen at –40 °C for up to 6 months without detectable deterioration.

General Procedure 5 (GP-5). The α -bromoamide was azeotropically dried with toluene three times and then dried under high vacuum at 40 °C for 1 h prior to use. In the air, a 100 mL Schlenk tube was charged with a stir bar and zinc powder (1.5 equiv, ~100 mesh, Alfa, 99.9%). The Schlenk tube containing the zinc powder was dried under high vacuum (~500 mtorr) with a torch for 1 min, and then it was cooled under vacuum and then backfilled with nitrogen. Next, THF (0.3 mL/mmol of α -bromoamide) was added via syringe under a strong positive flow of nitrogen to the un-capped (open) Schlenk tube. Iodine (0.05 equiv) was added in one portion, and then the mixture was stirred vigorously until the brown color of iodine faded. A solution of the α -bromoamide (1.0 equiv) in THF (0.3 mL/mmol of α -bromoamide), prepared in a 20 mL vial equipped with a nitrogen balloon, was added via syringe in one portion to the gray suspension of zinc powder. The vial that contained residual α -bromoamide was rinsed with THF (0.2 mL/mmol of α -bromoamide), and the solution was transferred via syringe to the Schlenk tube. Then, the Schlenk tube was capped tightly under a nitrogen atmosphere and transferred to an oil bath. The reaction mixture was stirred vigorously at 80 °C for 12 h. Then the mixture was cooled to r.t. and filtered through a syringe filter (PTFE, 0.45 μ M) to afford a yellow or pale yellow solution (routinely 0.7 – 0.85 M, determined through

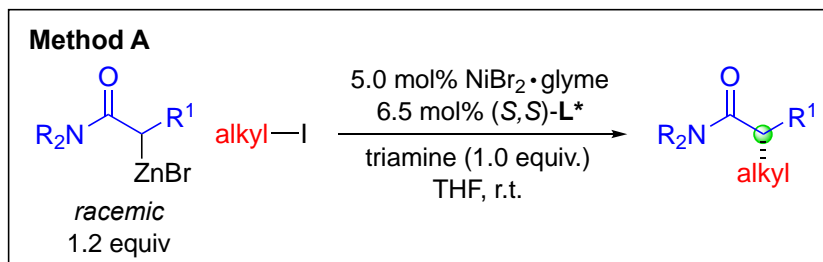
titration using iodine in THF), which can be stored under nitrogen in a freezer at $-40\text{ }^{\circ}\text{C}$ for up to 1 month without detectable deterioration.



^aA total of 1.37 mL THF per mmol of α -bromoamide was used, resulting in an expected concentration of $\sim 0.65\text{ M}$.

2.4.4. Enantioselective α -Alkylations

The procedures below have been developed to minimize the use of a glovebox. However, because the reaction is sensitive to air and to moisture, we recommend that a glovebox, if available, be used. Syringes were evacuated and backfilled with nitrogen on a Schlenk line (3 cycles) immediately prior to use. Commercially available 2,6,10-trimethyl-2,6,10-triazaundecane ("triamine") was distilled under reduced pressure and stored under nitrogen.



General Procedure 6 (GP-6) – Method A. α -Alkylations using the Reformatsky reagent as a solid: In the air, $\text{NiBr}_2 \cdot \text{glyme}$ (9.3 mg, 0.030 mmol, 5.0 mol%, slightly hygroscopic, stored under a dry nitrogen atmosphere) and chiral ligand L^* (21 mg, 0.039 mmol, 6.5 mol%) were added to a 20 mL vial that contained a stir bar. The vial was sealed with a septum cap, and the joint was wrapped with electrical tape. The vial was purged with a strong flow of nitrogen on a Schlenk line for 30 min. Then, THF (3.0 mL if the electrophile is a liquid, 2.0 mL if the electrophile is a solid) was added, and the outlet needle was removed. After covering the puncture holes with grease, the mixture was stirred at r.t. for 45 min, leading to a magenta solution.

[If the electrophile is a solid, the electrophile was added to a separate 4 mL vial, which was capped with a septum cap and then evacuated and backfilled with nitrogen (3 cycles). THF (volume to produce a 0.6 M solution of electrophile) was added to dissolve the electrophile.]

In a glovebox, the nucleophile (0.72 mmol, 1.2 equiv) was added to a 20 mL vial equipped with a stir bar. The vial was capped with a septum cap, wrapped with electrical tape, brought out of the glovebox, and then placed under a positive pressure of nitrogen on a Schlenk line. The solution of the catalyst was transferred via syringe into the vial that contained the nucleophile. The resulting mixture was stirred vigorously for 3 min, leading to a yellow or brown mixture. The triamine (0.14 mL, 0.60 mmol, 1.0 equiv) was added via syringe, followed immediately by the electrophile (neat or 1.0 mL of the solution prepared in the previous paragraph, 0.60 mmol, 1.00 equiv). The vial was then detached from the Schlenk line, and all puncture holes were covered

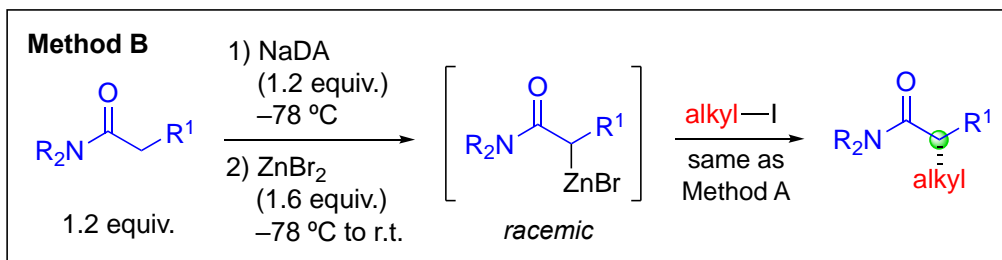
with grease. The reaction mixture was stirred at r.t. for 24 h, and then the reaction was quenched by the addition of EtOH (0.5 mL). The mixture was diluted with Et₂O (10 mL), stirred for 10 s, and then filtered through a plug of silica (flushing with Et₂O (40 mL)). The resulting solution was concentrated, and the product was purified by column chromatography on silica gel.

General Procedure 7 (GP-7) – Method A. α -Alkylations using the Reformatsky reagent as a solution: In the air, NiBr₂·glyme (9.3 mg, 0.030 mmol, 5.0 mol%, slightly hygroscopic, stored under a dry nitrogen atmosphere) and chiral ligand **L*** (21 mg, 0.039 mmol, 6.5 mol%) were added to a 20 mL vial that contained a stir bar. The vial was sealed with a septum cap, and the joint was wrapped with electrical tape. The vial was purged with a strong flow of nitrogen on a Schlenk line for 30 min. Then, THF (1.0 mL if the electrophile is solid, 2.0 mL if the electrophile is liquid) was added, and the outlet needle was removed. After covering the puncture holes with grease, the mixture was stirred at r.t. for 45 min, leading to a magenta solution.

[If the electrophile is a solid, the electrophile was added to a separate 4 mL vial, which was capped with a septum cap and then evacuated and backfilled with nitrogen (3 cycles). THF (volume to produce a 0.6 M solution of electrophile) was added to dissolve the electrophile.]

The solution of the nucleophile (0.72 mmol) was added via syringe in a continuous stream to the vial containing the solution of the catalyst. The mixture was then stirred vigorously for 3 min, leading to a yellow or brown solution. The triamine (0.14 mL, 0.60 mmol, 1.0 equiv) was added via syringe, followed immediately by the electrophile (neat or 1.0 mL of the solution prepared in the previous paragraph, 0.60 mmol, 1.0 equiv). The vial was then detached from the Schlenk line, and all puncture holes were covered with grease. The reaction mixture was stirred at r.t. for 24 h, and then the reaction was quenched by the addition of EtOH (0.5 mL). The mixture was diluted with Et₂O (10 mL), stirred for 10 s, and then filtered through a plug of silica (flushing with Et₂O

(40 mL). The resulting solution was concentrated, and the product was purified by column chromatography on silica gel.



General Procedure 8 (GP-8) – Method B. Preparation of the solution of NaDA: (21) In the air, Na (~300 mg, ~2 × 2 × 2 mm blocks) was added to a 20 mL vial equipped with a large stir bar. The vial was capped with a septum cap, and the joint was wrapped with electrical tape. The vial was evacuated and backfilled with nitrogen on a Schlenk line (3 cycles). The Na was washed with THF (2.0 mL) to remove the oil, and this solution was removed via syringe. Fresh THF (1.7 mL) was added, the vial was detached from the Schlenk line, and a nitrogen-filled balloon was attached. The mixture was cooled to 0 °C, and then diisopropylamine (1.0 mL) was added, followed immediately by isoprene (0.33 mL). The resulting mixture was stirred at 0 °C for 45 min, and the resulting yellow solution of NaDA was maintained at this temperature until use (within 1 h). The concentration of the solution (routinely ~1.9–2.0 M) can be determined by titration using benzoic acid in THF with specks of 4-(phenylazo)diphenylamine as an indicator (a change of color from yellow to magenta signals the end of titration).

Preparation of the solution of ZnBr₂: In the air, ZnBr₂ (252 mg, 1.12 mmol, hygroscopic, stored under a dry atmosphere) was quickly added to an oven-dried 4 mL vial. The vial was sealed with a septum cap and evacuated on a Schlenk line. The vial containing ZnBr₂ was flame-dried for ~1

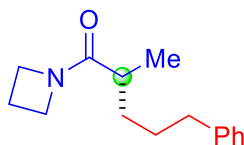
min and then allowed to cool to r.t. under vacuum. Next, the vial was refilled with nitrogen, and THF (1.2 mL) was added via syringe. The vial can be shaken to accelerate the dissolution of ZnBr₂.

Preparation of the solution of catalyst: In the air, NiBr₂·glyme (14 mg, 0.045 mmol, 7.5 mol%, slightly hygroscopic, stored under a dry nitrogen atmosphere) and chiral ligand **L*** (32 mg, 0.059 mmol, 9.8 mol%) were added to a 20 mL vial that contained a stir bar. The vial was sealed with a septum cap, and the joint was wrapped with electrical tape. The vial was purged with a strong flow of nitrogen on a Schlenk line for 30 min. Then, THF (1.5 mL) was added, and the outlet needle was removed. After covering the puncture holes with grease, the mixture was stirred at r.t. for 45 min, leading to a magenta solution.

Generation of the Reformatsky reagent: In the air, the amide (0.72 mmol, 1.2 equiv) was added to a 20 mL vial equipped with a stir bar. The vial was evacuated and backfilled with nitrogen on a Schlenk line (3 cycles), and then THF (0.8 mL) was added. The solution of the amide was cooled to -78 °C, and then the solution of NaDA (0.72 mmol, ~0.36 mL, 1.2 equiv) was added dropwise via syringe. The mixture was stirred at -78 °C for 25 min, and then a solution of ZnBr₂ (0.94 mmol, 1.0 mL, 1.6 equiv) was added dropwise. The resulting mixture was allowed to warm to r.t. and stirred for 30 min, resulting in an opaque, white solution.

α-Alkylation: A solution of the catalyst (1.0 mL) was added via syringe to the vial containing the nucleophile. The mixture was stirred at r.t. for 3 min, and then the triamine (0.14 mL, 0.60 mmol, 1.0 equiv) was added via syringe, followed immediately by the addition of the electrophile (0.60 mmol, 1.0 equiv) via syringe (if the electrophile is a solid, it was dissolved in THF (0.5 mL) under nitrogen). The vial was detached from the Schlenk line, and all puncture holes were covered with grease. The reaction mixture was stirred at r.t. for 24 h, and then the reaction was quenched by the addition of EtOH (0.5 mL). The mixture was diluted with Et₂O (10 mL), stirred for 1 min,

and then filtered through a plug of silica (flushing with Et₂O (40 mL)). The resulting solution was concentrated, and the product was purified by column chromatography on silica gel.



1-(Azetidin-1-yl)-2-methyl-5-phenylpentan-1-one (1). The title compound was synthesized according to **GP-6** from (3-iodopropyl)benzene and **Zn-1**. The title compound was also synthesized according to **GP-8** from (3-iodopropyl)benzene and 1-(azetidin-1-yl)propan-1-one. The product was purified by column chromatography on silica gel (30% → 60% EtOAc/hexanes). Mixed fractions were purified by preparative TLC (11:7 EtOAc/hexanes). Pale yellow oil.

GP-6 (*R,R*)-**L***: 128 mg, 92% yield, 89% ee; (*S,S*)-**L***: 127 mg, 92% yield, 89% ee.

GP-8 (*R,R*)-**L***: 96 mg, 69% yield, 89% ee; (*S,S*)-**L***: 96 mg, 69% yield, 88% ee.

SFC analysis: The ee was determined via SFC on a CHIRALPAK IG-3 column (15% *i*-PrOH in supercritical CO₂, 2.5 mL/min); retention times for compound obtained using (*S,S*)-**L***: 7.7 min (minor), 10.3 min (major).

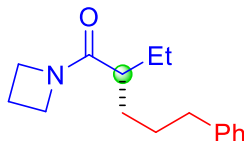
¹H NMR (400 MHz, CDCl₃) δ 7.32 – 7.23 (m, 2H), 7.22 – 7.13 (m, 3H), 4.10 (t, *J* = 7.6 Hz, 2H), 4.04 – 3.93 (m, 2H), 2.59 (qdd, *J* = 13.8, 8.7, 6.5 Hz, 2H), 2.37 – 2.17 (m, 3H), 1.79 – 1.50 (m, 3H), 1.45 – 1.32 (m, 1H), 1.07 (d, *J* = 6.9 Hz, 3H).

¹³C NMR (101 MHz, CDCl₃) δ 176.3, 142.4, 128.4, 128.3, 125.7, 50.0, 47.6, 36.0, 34.9, 33.5, 29.6, 17.2, 15.0.

FT-IR (film): 2932, 2879, 1647, 1436, 1168, 1014, 756, 699 cm⁻¹.

HRMS (ESI-MS) *m/z* [M+H]⁺ calcd for C₁₅H₂₂NO: 232.1696, found: 232.1700.

$[\alpha]_{\text{D}}^{22} = -27$ (c 1.0, CHCl_3); 89% ee, from (*S,S*)-**L***



1-(Azetidin-1-yl)-2-ethyl-5-phenylpentan-1-one (2). The title compound was synthesized according to **GP-6** from (3-iodopropyl)benzene and **Zn-2**. The title compound was also synthesized according to **GP-8** from (3-iodopropyl)benzene and 1-(azetidin-1-yl)butan-1-one. The product was purified by column chromatography on silica gel (30% → 60% EtOAc/hexanes). Mixed fractions were purified by preparative TLC (11:7 EtOAc/hexanes). Pale yellow oil.

GP-6 (*R,R*)-**L***: 133 mg, 90% yield, 90% ee; (*S,S*)-**L***: 136 mg, 92% yield, 89% ee.

GP-8 (*R,R*)-**L***: 125 mg, 85% yield, 90% ee; (*S,S*)-**L***: 127 mg, 86% yield, 89% ee.

SFC analysis: The ee was determined via SFC on a CHIRALPAK IG-3 column (25% *i*-PrOH in supercritical CO_2 , 2.5 mL/min); retention times for compound obtained using (*S,S*)-**L***: 4.2 min (minor), 5.7 min (major).

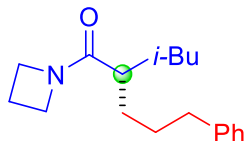
^1H NMR (400 MHz, CDCl_3) δ 7.32 – 7.23 (m, 2H), 7.22 – 7.14 (m, 3H), 4.22 – 3.91 (m, 4H), 2.67 – 2.50 (m, 2H), 2.23 (p, $J = 7.7$ Hz, 2H), 2.12 (tt, $J = 9.2, 5.0$ Hz, 1H), 1.75 – 1.35 (m, 6H), 0.87 (t, $J = 7.4$ Hz, 3H).

^{13}C NMR (101 MHz, CDCl_3) δ 175.8, 142.4, 128.4, 128.3, 125.7, 50.0, 47.4, 42.6, 36.2, 32.2, 29.8, 25.8, 14.9, 12.2.

FT-IR (film): 2956, 2935, 2875, 1644, 1434, 1168, 1119, 723 cm^{-1} .

HRMS (ESI-MS) m/z $[\text{M}+\text{H}]^+$ calcd for $\text{C}_{16}\text{H}_{24}\text{NO}$: 246.1853, found: 246.1849.

$[\alpha]_D^{22} = -15$ (c 1.0, CHCl_3); 89% ee, from (*S,S*)-**L***.



1-(Azetidin-1-yl)-2-isobutyl-5-phenylpentan-1-one (3). The title compound was synthesized according to **GP-7** from (3-iodopropyl)benzene and **Zn-3**. The title compound was also synthesized according to **GP-8** from (3-iodopropyl)benzene and 1-(azetidin-1-yl)-2-bromo-4-methylpentan-1-one. The product was purified by column chromatography on silica gel (20% → 60% EtOAc/hexanes). Mixed fractions were purified by preparative TLC (11:7 EtOAc/hexanes). Pale yellow oil.

GP-7 (*R,R*)-**L***: 110 mg, 67% yield, 80% ee; (*S,S*)-**L***: 116 mg, 71% yield, 80% ee.

GP-8 (*R,R*)-**L***: 103 mg, 63% yield, 84% ee; (*S,S*)-**L***: 101 mg, 62% yield, 83% ee.

SFC analysis: The ee was determined via SFC on a CHIRALPAK IC-3 column (15% *i*-PrOH in supercritical CO_2 , 2.5 mL/min); retention times for compound obtained using (*S,S*)-**L***: 13.8 min (minor), 14.9 min (major).

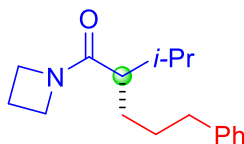
^1H NMR (400 MHz, CDCl_3) δ 7.32 – 7.23 (m, 2H), 7.22 – 7.13 (m, 3H), 4.18 – 4.06 (m, 2H), 4.00 (t, $J = 7.8$ Hz, 2H), 2.67 – 2.50 (m, 2H), 2.32 – 2.15 (m, 3H), 1.72 – 1.48 (m, 5H), 1.48 – 1.35 (m, 1H), 1.18 (ddd, $J = 13.0, 7.8, 5.2$ Hz, 1H), 0.87 (dd, $J = 6.5, 3.7$ Hz, 6H).

^{13}C NMR (101 MHz, CDCl_3) δ 176.0, 142.4, 128.5, 128.3, 125.8, 50.0, 47.5, 41.8, 38.7, 36.2, 32.8, 29.8, 26.0, 23.2, 22.6, 14.9.

FT-IR (film): 2946, 2932, 2876, 1646, 1456, 1436, 1169, 827, 691 cm^{-1} .

HRMS (ESI-MS) m/z $[M+H]^+$ calcd for $C_{18}H_{28}NO$: 274.2166, found: 274.2160.

$[\alpha]_D^{22} = -2.0$ (c 1.0, $CHCl_3$); 83% ee, from (*S,S*)-**L***.



1-(Azetidin-1-yl)-2-isopropyl-5-phenylpentan-1-one (4). The title compound was synthesized according to **GP-6** from (3-iodopropyl)benzene and **Zn-4**. The title compound was also synthesized according to **GP-8** from (3-iodopropyl)benzene and 1-(azetidin-1-yl)-2-bromo-3-methylbutan-1-one. The product was purified by column chromatography on silica gel (20% → 40% EtOAc/hexanes). Mixed fractions were purified by preparative TLC (11:7 EtOAc/hexanes). Pale yellow oil.

GP-6 (*R,R*)-**L***: 66 mg, 42% yield, 70% ee; (*S,S*)-**L***: 60 mg, 39% yield, 71% ee.

GP-8 (*R,R*)-**L***: 52 mg, 33% yield, 86% ee; (*S,S*)-**L***: 52 mg, 33% yield, 88% ee.

SFC analysis: The ee was determined via SFC on a CHIRALPAK IG-3 column (15% *i*-PrOH in supercritical CO_2 , 2.5 mL/min); retention times for compound obtained using (*S,S*)-**L***: 8.6 min (minor), 12.9 min (major).

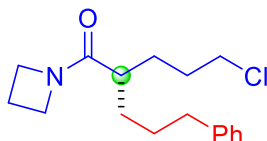
1H NMR (400 MHz, $CDCl_3$) δ 7.32 – 7.26 (m, 2H), 7.24 – 7.10 (m, 3H), 4.19 – 4.05 (m, 2H), 4.01 (ddd, $J = 10.2, 6.9, 2.2$ Hz, 2H), 2.67 – 2.51 (m, 2H), 2.21 (p, $J = 7.7$ Hz, 2H), 1.98 – 1.75 (m, 2H), 1.75 – 1.48 (m, 3H), 1.48 – 1.37 (m, 1H), 0.92 (dd, $J = 8.4, 6.5$ Hz, 6H).

^{13}C NMR (101 MHz, $CDCl_3$) δ 175.5, 142.5, 128.5, 128.3, 125.7, 50.0, 47.8, 47.2, 36.4, 30.8, 30.1, 29.9, 21.1, 20.3, 14.8.

FT-IR (film): 2952, 2876, 1644, 1436, 1170, 828, 731 cm^{-1} .

HRMS (ESI-MS) m/z $[\text{M}+\text{H}]^+$ calcd for $\text{C}_{17}\text{H}_{26}\text{NO}$: 260.2009, found: 260.2004.

$[\alpha]_{\text{D}}^{22} = -5.1$ (c 1.0, CHCl_3); 88% ee, from (*S,S*)-**L***.



1-(Azetidin-1-yl)-5-chloro-2-(3-phenylpropyl)pentan-1-one (5). The title compound was synthesized according to **GP-6** from (3-iodopropyl)benzene and **Zn-5**. The title compound was also synthesized according to **GP-8** from (3-iodopropyl)benzene and 1-(azetidin-1-yl)-5-chloropentan-1-one. The product was purified by column chromatography on silica gel (30% → 60% EtOAc/hexanes). Mixed fractions were purified by preparative TLC (11:7 EtOAc/hexanes). Pale yellow oil.

GP-6 (*R,R*)-**L***: 158 mg, 90% yield, 90% ee; (*S,S*)-**L***: 159 mg, 90% yield, 90% ee.

GP-8 (*R,R*)-**L***: 121 mg, 69% yield, 90% ee; (*S,S*)-**L***: 125 mg, 71% yield, 91% ee.

SFC analysis: The ee was determined via SFC on a CHIRALPAK IG-3 column (20% *i*-PrOH in supercritical CO_2 , 2.5 mL/min); retention times for compound obtained using (*S,S*)-**L***: 7.6 min (minor), 9.1 min (major).

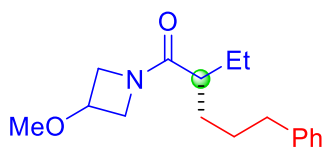
^1H NMR (400 MHz, CDCl_3) δ 7.32 – 7.24 (m, 2H), 7.22 – 7.13 (m, 3H), 4.06 (dt, $J = 37.7$, 7.8 Hz, 4H), 3.49 (qt, $J = 10.8$, 6.4 Hz, 2H), 2.68 – 2.50 (m, 2H), 2.23 (tdd, $J = 10.2$, 5.7, 2.7 Hz, 3H), 1.86 – 1.50 (m, 7H), 1.45 (ddt, $J = 10.3$, 7.0, 5.0 Hz, 1H).

^{13}C NMR (101 MHz, CDCl_3) δ 175.1, 142.2, 128.44, 128.35, 125.8, 50.0, 47.5, 44.9, 40.2, 36.1, 32.3, 30.6, 29.8, 29.6, 15.0.

FT-IR (film): 3022, 3001, 2943, 2882, 1646, 1455, 1436, 1238, 1153, 700 cm^{-1} .

HRMS (ESI-MS) m/z $[\text{M}+\text{H}]^+$ calcd for $\text{C}_{17}\text{H}_{25}\text{ClNO}$: 294.1620, found: 294.1621.

$[\alpha]_{\text{D}}^{22} = -7.5$ (c 1.0, CHCl_3); 91% ee, from (*S,S*)-**L***.



2-Ethyl-1-(3-methoxyazetidin-1-yl)-5-phenylpentan-1-one (6). The title compound was synthesized according to **GP-6** from (3-iodopropyl)benzene and **Zn-6**. The title compound was also synthesized according to **GP-8** from (3-iodopropyl)benzene and 1-(3-methoxyazetidin-1-yl)butan-1-one. The product was purified by column chromatography on silica gel (20% \rightarrow 60% EtOAc/hexanes). Mixed fractions were purified by preparative TLC (11:7 EtOAc/hexanes). Pale yellow oil.

GP-6 (*R,R*)-**L***: 100 mg, 61% yield, 94% ee; (*S,S*)-**L***: 103 mg, 62% yield, 93% ee.

GP-8 (*R,R*)-**L***: 102 mg, 62% yield, 93% ee; (*S,S*)-**L***: 108 mg, 65% yield, 93% ee.

SFC analysis: The ee was determined via SFC on a CHIRALPAK IG-3 column (20% *i*-PrOH in supercritical CO_2 , 2.5 mL/min); retention times for compound obtained using (*S,S*)-**L***: 5.1 min (minor), 6.4 min (major).

^1H NMR (400 MHz, CDCl_3) δ 7.32 – 7.23 (m, 2H), 7.17 (tq, $J = 8.1, 1.4$ Hz, 3H), 4.30 – 4.19 (m, 1H), 4.17 (td, $J = 5.1, 2.7$ Hz, 1H), 4.16 – 4.08 (m, 1H), 4.03 – 3.92 (m, 1H), 3.88 (ttd, $J = 5.2,$

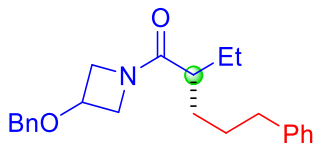
3.4, 1.7 Hz, 1H), 3.29 (d, $J = 0.6$ Hz, 3H), 2.68 – 2.49 (m, 2H), 2.13 (tt, $J = 9.1, 5.0$ Hz, 1H), 1.75 – 1.50 (m, 4H), 1.50 – 1.37 (m, 2H), 0.87 (q, $J = 7.6$ Hz, 3H). Rotamers detected.

^{13}C NMR (101 MHz, CDCl_3) δ 176.03, 176.00, 142.4, 142.3, 128.4, 128.3, 125.8, 125.7, 68.62, 68.59, 56.9, 56.2, 54.43, 54.40, 43.12, 43.09, 36.2, 36.1, 32.2, 32.1, 29.8, 29.5, 25.8, 25.7, 12.2, 12.1. Rotamers detected.

FT-IR (film): 3016, 2932, 2870, 1648, 1452, 1124, 1002, 732 cm^{-1} .

HRMS (ESI-MS) m/z $[\text{M}+\text{H}]^+$ calcd for $\text{C}_{17}\text{H}_{26}\text{NO}_2$: 276.1959, found: 276.1961.

$[\alpha]_{\text{D}}^{22} = -11$ (c 1.0, CHCl_3); 93% ee, from (*S,S*)-**L***.



1-(3-(Benzyloxy)azetidin-1-yl)-2-ethyl-5-phenylpentan-1-one (7). The title compound was synthesized according to **GP-7** from (3-iodopropyl)benzene and **Zn-7**. The title compound was also synthesized according to **GP-8** from (3-iodopropyl)benzene and 1-(3-benzyloxyazetidin-1-yl)butan-1-one. The product was purified by column chromatography on silica gel (20% → 40% EtOAc/hexanes). Pale yellow oil.

GP-7 (*R,R*)-**L***: 172 mg, 82% yield, 94% ee; (*S,S*)-**L***: 166 mg, 79% yield, 94% ee.

GP-8 (*R,R*)-**L***: 151 mg, 72% yield, 94% ee; (*S,S*)-**L***: 148 mg, 70% yield, 94% ee.

SFC analysis: The ee was determined via SFC on a CHIRALPAK IG-3 column (20% *i*-PrOH in supercritical CO_2 , 2.5 mL/min); retention times for compound obtained using (*S,S*)-**L***: 9.9 min (minor), 12.7 min (major).

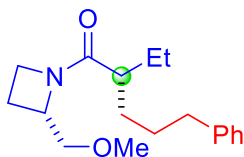
^1H NMR (400 MHz, CDCl_3) δ 7.41 – 7.22 (m, 7H), 7.22 – 7.12 (m, 3H), 4.53 – 4.41 (m, 2H), 4.41 – 4.29 (m, 1H), 4.28 – 4.08 (m, 2H), 4.03 – 3.95 (m, 1H), 3.94 – 3.87 (m, 1H), 2.68 – 2.48 (m, 2H), 2.17 – 2.05 (m, 1H), 1.73 – 1.35 (m, 6H), 0.92 – 0.79 (m, 3H). Rotamers detected.

^{13}C NMR (101 MHz, CDCl_3) δ 176.0, 175.9, 142.4, 142.3, 137.0, 128.6, 128.4, 128.3, 128.20, 128.19, 128.0, 125.8, 125.7, 71.33, 71.31, 66.9, 66.8, 57.2, 54.84, 54.81, 43.13, 43.08, 36.2, 36.1, 32.2, 32.1, 29.8, 29.6, 25.8, 25.7, 12.2, 12.1. Rotamers detected.

FT-IR (film): 3001, 2934, 2874, 1650, 1454, 1169, 1127, 1022, 737 cm^{-1} .

HRMS (ESI-MS) m/z $[\text{M}+\text{H}]^+$ calcd for $\text{C}_{23}\text{H}_{30}\text{NO}_2$: 352.2272, found: 352.2269.

$[\alpha]_{\text{D}}^{22} = -5.3$ (c 1.0, CHCl_3); 94% ee, from (*S,S*)-**L***.



2-Ethyl-1-((*S*)-2-(methoxymethyl)azetidin-1-yl)-5-phenylpentan-1-one (8, 9). The title compound was synthesized according to **GP-7** from (3-iodopropyl)benzene and **Zn-8**. The title compound was also synthesized according to **GP-8** from (3-iodopropyl)benzene and (*S*)-1-(2-(methoxymethyl)azetidin-1-yl)butan-1-one. The product was purified by column chromatography on silica gel (20% → 60% EtOAc/hexanes). Mixed fractions were purified by preparative TLC (11:7 EtOAc/hexanes). Yellow oil.

GP-6 (*R,R*)-**L***: 110 mg, 63% yield, 89:11 dr; (*S,S*)-**L***: 133 mg, 77% yield, 6:94 dr.

GP-8 (*R,R*)-**L***: 97 mg, 56% yield, 90:10 dr; (*S,S*)-**L***: 116 mg, 67% yield, 5:95 dr.

SFC analysis: The dr was determined via SFC on a CHIRALPAK ID-3 column (15% *i*-PrOH in supercritical CO₂, 2.5 mL/min); retention times for compound obtained using (*S,S*)-**L***: 6.9 min (minor), 7.4 min (major).

NMR data for the product from (*R,R*)-**L***:

¹H NMR (400 MHz, CDCl₃) δ 7.30 – 7.23 (m, 2H), 7.22 – 7.10 (m, 3H), 4.48 (ddd, *J* = 14.0, 8.8, 5.7 Hz, 1H), 4.09 – 3.49 (m, 4H), 3.39 – 3.28 (m, 3H), 2.73 – 2.49 (m, 2H), 2.41 – 2.14 (m, 2H), 2.14 – 1.89 (m, 1H), 1.75 – 1.39 (m, 6H), 0.91 – 0.84 (m, 3H).

¹³C NMR (101 MHz, CDCl₃) δ 177.0, 176.0, 142.5, 142.4, 128.5, 128.4, 128.31, 128.25, 125.74, 125.67, 75.6, 71.7, 61.4, 59.9, 59.2, 59.1, 48.3, 45.4, 43.0, 42.9, 36.3, 36.2, 36.1, 32.5, 32.3, 32.1, 31.5, 29.93, 29.86, 29.4, 26.03, 25.99, 25.7, 19.0, 18.3, 12.2, 11.9. Rotamers detected.

NMR data for the product from (*S,S*)-**L***:

¹H NMR (400 MHz, CDCl₃) δ 7.30 – 7.24 (m, 2H), 7.22 – 7.12 (m, 3H), 4.56 – 4.39 (m, 1H), 4.07 – 3.48 (m, 4H), 3.39 – 3.28 (m, 3H), 2.68 – 2.48 (m, 2H), 2.43 – 2.13 (m, 2H), 2.13 – 1.88 (m, 1H), 1.72 – 1.37 (m, 6H), 0.88 (t, *J* = 7.4 Hz, 3H).

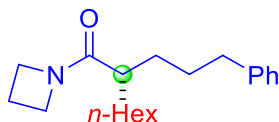
¹³C NMR (101 MHz, CDCl₃) δ 176.9, 176.0, 142.6, 142.5, 128.44, 128.41, 128.3, 128.2, 125.7, 125.6, 75.5, 71.7, 61.4, 60.0, 59.2, 59.1, 48.3, 45.5, 43.1, 36.2, 32.5, 32.1, 29.9, 29.5, 26.0, 25.9, 25.7, 19.1, 18.3, 12.3, 11.9. Rotamers detected.

FT-IR (film): 2932, 1644, 1452, 1430, 1335, 1247, 1124, 750, 699, 511 cm⁻¹.

HRMS (ESI-MS) *m/z* [M+H]⁺ calcd for C₁₈H₂₈NO₂: 290.2115, found:290.2118.

[α]_D²² = –30 (*c* 1.0, CHCl₃); 90:10 dr, from (*R,R*)-**L***.

[α]_D²² = –88 (*c* 1.0, CHCl₃); 5:95 dr, from (*S,S*)-**L***.



1-(Azetidin-1-yl)-2-(3-phenylpropyl)octan-1-one (10). The title compound was synthesized according to **GP-7** from 1-iodohexane and **Zn-9**. The title compound was also synthesized according to **GP-8** from 1-iodohexane and 1-(azetidin-1-yl)-5-phenylpentan-1-one. The product was purified by column chromatography on silica gel (2% → 5% acetone/DCM). Mixed fractions were purified by preparative TLC (5:4 EtOAc/hexanes). Pale yellow oil.

GP-7 (*R,R*)-**L***: 152 mg, 84% yield, 92% ee; (*S,S*)-**L***: 145 mg, 80% yield, 93% ee.

GP-8 (*R,R*)-**L***: 130 mg, 72% yield, 92% ee; (*S,S*)-**L***: 132 mg, 73% yield, 93% ee.

SFC analysis: The ee was determined via SFC on a CHIRALPAK ID-3 column (15% *i*-PrOH in supercritical CO₂, 2.5 mL/min); retention times for compound obtained using (*S,S*)-**L***: 15.8 min (major), 17.5 min (minor).

¹H NMR (400 MHz, CDCl₃) δ 7.32 – 7.23 (m, 2H), 7.18 (td, *J* = 7.1, 1.0 Hz, 3H), 4.18 – 4.06 (m, 2H), 4.05 – 3.97 (m, 2H), 2.67 – 2.49 (m, 2H), 2.33 – 2.08 (m, 3H), 1.74 – 1.48 (m, 4H), 1.48 – 1.13 (m, 10H), 0.92 – 0.83 (m, 3H).

¹³C NMR (101 MHz, CDCl₃) δ 175.9, 142.4, 128.5, 128.3, 125.7, 50.0, 47.4, 40.9, 36.2, 32.8, 32.5, 31.8, 29.8, 29.5, 27.7, 22.7, 14.9, 14.1.

FT-IR (film): 3022, 3003, 2927, 2854, 1648, 1456, 1436, 1169, 744 cm⁻¹.

HRMS (ESI-MS) *m/z* [M+H]⁺ calcd for C₂₀H₃₂NO: 302.2479, found: 302.2481.

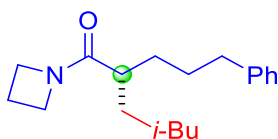
[α]_D²² = -4.2 (*c* 1.0, CHCl₃); 92% ee, from (*R,R*)-**L***.

Gram-scale reactions: The general procedures were followed and scaled up (5.0 mmol of electrophile), except for the following changes: 3 mol% NiBr₂·glyme and 3.8 mol% **L*** were used,

the reactions were set up in 100 mL flasks, and the reaction time was 48 h (for **GP-8**: the transfer and addition of the solution of NaDA should be carried out in portions up to 0.4 mL, since NaDA can decompose after ~1 min at r.t. and then clog the syringe needle). At the end of the reaction, the mixture was directly partitioned between Et₂O (50 mL) and half-saturated NH₄Cl (50 mL, 1:1 water:saturated NH₄Cl). The phases were separated, and the aqueous phase was extracted with Et₂O (50 mL × 2). The combined organic phase was washed with brine, dried with Na₂SO₄, and concentrated. The resulting residue was purified by column chromatography on silica gel.

GP-7 (*R,R*)-**L***: 1.21 g, 80% yield, 91% ee.

GP-8 (*S,S*)-**L***: 1.10 g, 73% yield, 92% ee.



1-(Azetidin-1-yl)-5-methyl-2-(3-phenylpropyl)hexan-1-one (11). The title compound was synthesized according to **GP-7** from 1-iodo-3-methylbutane and **Zn-9**. The title compound was also synthesized according to **GP-8** from 1-iodo-3-methylbutane and 1-(azetidin-1-yl)-5-phenylpentan-1-one. The product was purified by column chromatography on silica gel (2% → 5% acetone/DCM). Mixed fractions were purified by preparative TLC (5:4 EtOAc/hexanes). Pale yellow oil.

GP-7 (*R,R*)-**L***: 141 mg, 82% yield, 93% ee; (*S,S*)-**L***: 147 mg, 85% yield, 93% ee.

GP-8 (*R,R*)-**L***: 133 mg, 77% yield, 94% ee; (*S,S*)-**L***: 133 mg, 77% yield, 92% ee.

SFC analysis: The ee was determined via SFC on a CHIRALPAK IG-3 column (15% *i*-PrOH in supercritical CO₂, 2.5 mL/min); retention times for compound obtained using (*S,S*)-**L***: 9.7 min (major), 12.5 min (minor).

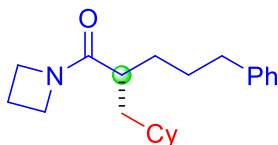
¹H NMR (400 MHz, CDCl₃) δ 7.32 – 7.23 (m, 2H), 7.18 (td, *J* = 6.7, 1.6 Hz, 3H), 4.17 – 4.05 (m, 2H), 4.05 – 3.95 (m, 2H), 2.67 – 2.50 (m, 2H), 2.29 – 2.08 (m, 3H), 1.75 – 1.31 (m, 7H), 1.22 – 1.00 (m, 2H), 0.86 (dd, *J* = 6.6, 0.8 Hz, 6H).

¹³C NMR (101 MHz, CDCl₃) δ 175.9, 142.4, 128.5, 128.3, 125.7, 50.0, 47.4, 41.2, 36.8, 36.2, 32.5, 30.7, 29.8, 28.2, 22.61, 22.56, 14.9.

FT-IR (film): 3022, 3002, 2945, 1647, 1456, 1436, 1168, 730, 716 cm⁻¹.

HRMS (ESI-MS) *m/z* [M+H]⁺ calcd for C₁₉H₃₀NO: 288.2322, found: 288.2323.

[α]_D²² = +1.9 (*c* 1.0, CHCl₃); 93% ee, from (*S,S*)-**L***.



1-(Azetidin-1-yl)-2-(cyclohexylmethyl)-5-phenylpentan-1-one (12). The title compound was synthesized according to **GP-7** from 1-iodo-3-methylbutane and **Zn-9**. The title compound was also synthesized according to **GP-8** from 1-iodo-3-methylbutane and 1-(azetidin-1-yl)-5-phenylpentan-1-one. The product was purified by column chromatography on silica gel (2% → 4% acetone/DCM). Mixed fractions were purified by preparative TLC (5:4 EtOAc/hexanes). Pale yellow oil.

GP-7 (*R,R*)-**L***: 104 mg, 55% yield, 92% ee; (*S,S*)-**L***: 101 mg, 54% yield, 91% ee.

GP-8 (*R,R*)-**L***: 108 mg, 57% yield, 92% ee; (*S,S*)-**L***: 102 mg, 54% yield, 93% ee.

SFC analysis: The ee was determined via SFC on a CHIRALPAK IG-3 column (20% *i*-PrOH in supercritical CO₂, 2.5 mL/min); retention times for compound obtained using (*S,S*)-**L***: 12.4 min (major), 13.8 min (minor).

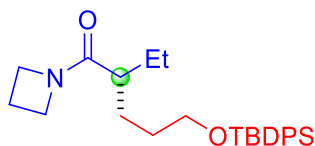
¹H NMR (400 MHz, CDCl₃) δ 7.37 – 7.25 (m, 2H), 7.25 – 7.09 (m, 3H), 4.10 (t, *J* = 7.6 Hz, 2H), 4.01 (t, *J* = 7.8 Hz, 2H), 2.67 – 2.50 (m, 2H), 2.41 – 2.11 (m, 3H), 1.76 – 1.45 (m, 9H), 1.40 (tdd, *J* = 10.8, 7.7, 4.1 Hz, 1H), 1.29 – 1.10 (m, 5H), 0.93 – 0.78 (m, 2H).

¹³C NMR (101 MHz, CDCl₃) δ 176.1, 142.4, 128.5, 128.3, 125.7, 50.0, 47.5, 40.3, 37.9, 36.2, 35.5, 33.8, 33.5, 32.7, 29.8, 26.6, 26.3, 26.2, 15.0.

FT-IR (film): 3022, 2922, 2850, 1650, 1455, 1433, 1168, 736 cm⁻¹.

HRMS (ESI-MS) *m/z* [M+H]⁺ calcd for C₂₁H₃₂NO: 314.2479, found: 314.2478.

[α]_D²² = -5.5 (*c* 1.0, CHCl₃); 91% ee, from (*S,S*)-**L***.



1-(Azetidin-1-yl)-5-((*tert*-butyldiphenylsilyl)oxy)-2-(3-phenylpropyl)pentan-1-one (13).

The title compound was synthesized according to **GP-6** from *tert*-butyl(3-iodopropoxy)diphenylsilane and **Zn-2**. The title compound was also synthesized according to **GP-8** from *tert*-butyl(3-iodopropoxy)diphenylsilane and 1-(azetidin-1-yl)butan-1-one. The product was purified by column chromatography on silica gel (2% → 6% acetone/DCM). Colorless oil.

GP-6 (*R,R*)-**L***: 189 mg, 75% yield, 91% ee; (*S,S*)-**L***: 198 mg, 78% yield, 92% ee.

GP-8 (*R,R*)-**L***: 182 mg, 72% yield, 91% ee; (*S,S*)-**L***: 185 mg, 73% yield, 92% ee.

SFC analysis: The ee was determined via SFC on a CHIRALPAK IE-3 column (10% *i*-PrOH in supercritical CO₂, 2.5 mL/min); retention times for compound obtained using (*S,S*)-**L***: 12.3 min (major), 14.2 min (minor).

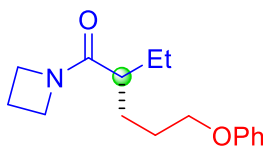
¹H NMR (400 MHz, CDCl₃) δ 7.70 – 7.62 (m, 4H), 7.47 – 7.33 (m, 6H), 4.15 – 3.96 (m, 4H), 3.63 (td, *J* = 6.1, 1.8 Hz, 2H), 2.27 – 2.13 (m, 2H), 2.12 – 2.02 (m, 1H), 1.67 – 1.35 (m, 6H), 1.04 (s, 9H), 0.87 (t, *J* = 7.4 Hz, 3H).

¹³C NMR (101 MHz, CDCl₃) δ 175.7, 135.6, 134.03, 133.98, 129.6, 127.6, 63.8, 49.9, 47.4, 42.2, 30.5, 28.4, 26.9, 25.7, 19.2, 15.0, 12.1.

FT-IR (film): 3069, 2994, 2957, 2874, 1648, 1429, 1111, 704 cm⁻¹.

HRMS (ESI-MS) *m/z* [M+H]⁺ calcd for C₂₆H₃₈NO₂Si: 424.2667, found: 424.2688.

[α]_D²² = -7.2 (*c* 1.0, CHCl₃); 92% ee, from (*S,S*)-**L***.



1-(Azetidin-1-yl)-2-ethyl-5-phenoxypropan-1-one (14). The title compound was synthesized according to **GP-6** from (3-iodopropoxy)benzene and **Zn-2**. The title compound was also synthesized according to **GP-8** from (3-iodopropoxy)benzene and 1-(azetidin-1-yl)butan-1-one. The product was purified by column chromatography on silica gel (30% → 60% EtOAc/hexanes). Mixed fractions were purified by preparative TLC (5:4 EtOAc/hexanes). Pale yellow oil.

GP-6 (*R,R*)-**L***: 137 mg, 87% yield, 91% ee; (*S,S*)-**L***: 140 mg, 89% yield, 91% ee.

GP-8 (*R,R*)-**L***: 125 mg, 80% yield, 90% ee; (*S,S*)-**L***: 126 mg, 80% yield, 91% ee.

SFC analysis: The ee was determined via SFC on a CHIRALPAK IF-3 column (10% *i*-PrOH in supercritical CO₂, 2.5 mL/min); retention times for compound obtained using (*S,S*)-**L***: 12.9 min (minor), 14.1 min (major).

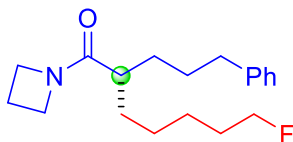
¹H NMR (400 MHz, CDCl₃) δ 7.32 – 7.22 (m, 2H), 6.97 – 6.88 (m, 1H), 6.92 – 6.85 (m, 2H), 4.17 (t, *J* = 7.6 Hz, 2H), 4.08 – 4.00 (m, 2H), 4.00 – 3.85 (m, 2H), 2.31 – 2.15 (m, 3H), 1.85 – 1.68 (m, 3H), 1.72 – 1.54 (m, 2H), 1.54 – 1.40 (m, 1H), 0.90 (t, *J* = 7.4 Hz, 3H).

¹³C NMR (101 MHz, CDCl₃) δ 175.5, 159.0, 129.5, 120.6, 114.5, 67.8, 50.0, 47.5, 42.3, 28.8, 27.4, 25.8, 15.0, 12.1.

FT-IR (film): 2958, 2934, 1645, 1601, 1498, 1470, 1436, 1244, 1170, 758 cm⁻¹.

HRMS (ESI-MS) *m/z* [M+H]⁺ calcd for C₁₆H₂₄NO₂: 262.1802, found: 262.1804.

[α]_D²² = -4.5 (*c* 1.0, CHCl₃); 91% ee, from (*S,S*)-**L***.



1-(Azetidin-1-yl)-7-fluoro-2-(3-phenylpropyl)heptan-1-one (15). The title compound was synthesized according to **GP-7** from 1-fluoro-5-iodopentane and **Zn-9**. The title compound was also synthesized according to **GP-8** from 1-fluoro-5-iodopentane and 1-(azetidin-1-yl)-5-phenylpentan-1-one. The product was purified by column chromatography on silica gel (2% → 6% acetone/DCM). Mixed fractions were purified by preparative TLC (5:4 EtOAc/hexanes). Colorless oil.

GP-7 (*R,R*)-**L***: 126 mg, 69% yield, 91% ee; (*S,S*)-**L***: 117 mg, 64% yield, 91% ee.

GP-8 (*R,R*)-**L***: 119 mg, 65% yield, 91% ee; (*S,S*)-**L***: 112 mg, 61% yield, 91% ee.

SFC analysis: The ee was determined via SFC on a CHIRALPAK IG-3 column (20% *i*-PrOH in supercritical CO₂, 2.5 mL/min); retention times for compound obtained using (*S,S*)-**L***: 6.9 min (major), 8.2 min (minor).

¹H NMR (400 MHz, CDCl₃) δ 7.32 – 7.23 (m, 2H), 7.22 – 7.13 (m, 3H), 4.48 (t, *J* = 6.1 Hz, 1H), 4.36 (t, *J* = 6.1 Hz, 1H), 4.17 – 4.04 (m, 2H), 4.01 (t, *J* = 7.8 Hz, 2H), 2.67 – 2.50 (m, 2H), 2.33 – 2.11 (m, 3H), 1.79 – 1.19 (m, 12H).

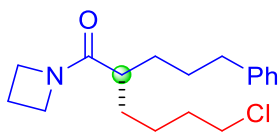
¹³C NMR (101 MHz, CDCl₃) δ 175.7, 142.4, 128.4, 128.3, 125.8, 84.1 (d, *J* = 164 Hz), 50.0, 47.5, 40.8, 36.1, 32.6, 32.5, 30.3 (d, *J* = 19.5 Hz), 29.7, 27.2, 25.3 (d, *J* = 5.3 Hz), 14.9.

¹⁹F NMR (282 MHz, CDCl₃) δ –218.3 (tt, *J* = 47.3, 25.3 Hz).

FT-IR (film): 2934, 2882, 2856, 1645, 1458, 1436, 1168, 732 cm⁻¹.

HRMS (ESI-MS) *m/z* [M+H]⁺ calcd for C₁₉H₂₉FNO: 306.2228, found: 306.2238.

[α]_D²² = +3.9 (*c* 1.0, CHCl₃); 91% ee, from (*S,S*)-**L***.



1-(Azetidin-1-yl)-6-chloro-2-(3-phenylpropyl)hexan-1-one (16). The title compound was synthesized according to **GP-7** from 1-chloro-4-iodobutane and **Zn-9**. The title compound was also synthesized according to **GP-8** from 1-chloro-4-iodobutane and 1-(azetidin-1-yl)-5-

phenylpentan-1-one. The product was purified by column chromatography on silica gel (3% → 4% acetone/DCM). Pale yellow oil.

GP-7 (*R,R*)-**L***: 153 mg, 83% yield, 91% ee; (*S,S*)-**L***: 150 mg, 81% yield, 91% ee.

GP-8 (*R,R*)-**L***: 152 mg, 82% yield, 92% ee; (*S,S*)-**L***: 149 mg, 81% yield, 92% ee.

SFC analysis: The ee was determined via SFC on a CHIRALPAK IE-3 column (12% *i*-PrOH in supercritical CO₂, 2.5 mL/min); retention times for compound obtained using (*S,S*)-**L***: 15.8 min (major), 17.5 min (minor).

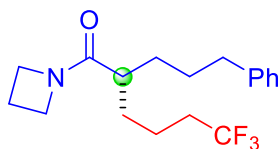
¹H NMR (400 MHz, CDCl₃) δ 7.32 – 7.23 (m, 2H), 7.21 – 7.14 (m, 3H), 4.12 (q, *J* = 6.2, 4.8 Hz, 2H), 4.01 (t, *J* = 7.8 Hz, 2H), 3.58 – 3.46 (m, 2H), 2.60 (tdd, *J* = 12.2, 9.5, 4.8 Hz, 2H), 2.32 – 2.10 (m, 3H), 1.82 – 1.50 (m, 6H), 1.50 – 1.32 (m, 4H).

¹³C NMR (101 MHz, CDCl₃) δ 175.5, 142.3, 128.4, 128.3, 125.8, 50.0, 47.5, 44.9, 40.8, 36.1, 32.7, 32.5, 31.9, 29.7, 25.0, 14.9.

FT-IR (film): 2934, 2883, 2854, 1647, 1459, 1438, 1168, 731, 619 cm⁻¹.

HRMS (ESI-MS) *m/z* [M+H]⁺ calcd for C₁₈H₂₇ClNO: 308.1776, found: 308.1783.

[α]_D²² = -0.7 (*c* 1.0, CHCl₃); 91% ee, from (*S,S*)-**L***.



1-(Azetidin-1-yl)-6,6,6-trifluoro-2-(3-phenylpropyl)hexan-1-one (17). The title compound was synthesized according to **GP-7** from 1,1,1-trifluoro-4-iodobutane and **Zn-9**. The title compound was also synthesized according to **GP-8** from 1,1,1-trifluoro-4-iodobutane and 1-

(azetidin-1-yl)-5-phenylpentan-1-one. The product was purified by column chromatography on silica gel (2% → 4% acetone/DCM). Pale yellow oil.

GP-7 (*R,R*)-**L***: 148 mg, 75% yield, 91% ee; (*S,S*)-**L***: 146 mg, 74% yield, 89% ee.

GP-8 (*R,R*)-**L***: 156 mg, 79% yield, 90% ee; (*S,S*)-**L***: 150 mg, 76% yield, 90% ee.

SFC analysis: The ee was determined via SFC on a CHIRALPAK IE-3 column (10% *i*-PrOH in supercritical CO₂, 2.5 mL/min); retention times for compound obtained using (*S,S*)-**L***: 5.2 min (major), 5.8 min (minor).

¹H NMR (400 MHz, CDCl₃) δ 7.39 – 7.25 (m, 2H), 7.25 – 7.08 (m, 3H), 4.15 – 4.07 (m, 2H), 4.02 (t, *J* = 7.8 Hz, 2H), 2.68 – 2.50 (m, 2H), 2.35 – 2.13 (m, 3H), 2.13 – 1.92 (m, 2H), 1.75 – 1.36 (m, 8H).

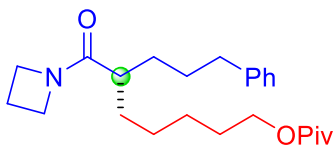
¹³C NMR (101 MHz, CDCl₃) δ 175.0, 142.2, 128.43, 128.36, 125.8, 125.6, 50.0, 47.5, 40.7, 36.1, 33.9 (q, *J* = 28.6 Hz), 32.4, 31.6, 29.5, 20.1, 14.9.

¹⁹F NMR (282 MHz, CDCl₃) δ –66.4 (t, *J* = 10.9 Hz).

FT-IR (film): 2934, 2884, 1646, 1458, 1438, 1255, 1134, 1037, 705 cm⁻¹.

HRMS (ESI-MS) *m/z* [M+H]⁺ calcd for C₁₈H₂₅F₃NO: 328.1883, found: 328.1885.

[α]_D²² = +6.8 (*c* 1.0, CHCl₃); 89% ee, from (*S,S*)-**L***.



6-(Azetidine-1-carbonyl)-9-phenylnonyl pivalate (18). The title compound was synthesized according to **GP-7** from 5-iodopentyl pivalate and **Zn-9**. The title compound was also synthesized according to **GP-8** from 5-iodopentyl pivalate and 1-(azetidin-1-yl)-5-phenylpentan-1-one. The product was purified by column chromatography on silica gel (5% → 8% acetone/DCM). Mixed fractions were purified by preparative TLC (5:4 EtOAc/hexanes). Colorless oil.

GP-7 (*R,R*)-**L***: 130 mg, 56% yield, 91% ee; (*S,S*)-**L***: 126 mg, 54% yield, 92% ee.

GP-8 (*R,R*)-**L***: 106 mg, 46% yield, 91% ee; (*S,S*)-**L***: 119 mg, 51% yield, 92% ee.

SFC analysis: The ee was determined via SFC on a CHIRALPAK IE-3 column (20% *i*-PrOH in supercritical CO₂, 2.5 mL/min); retention times for compound obtained using (*S,S*)-**L***: 6.6 min (major), 7.4 min (minor).

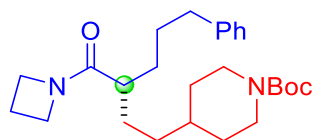
¹H NMR (400 MHz, CDCl₃) δ 7.31 – 7.25 (m, 2H), 7.23 – 7.11 (m, 3H), 4.17 – 3.92 (m, 6H), 2.67 – 2.49 (m, 2H), 2.29 – 2.11 (m, 3H), 1.71 – 1.26 (m, 11H), 1.19 (s, 9H).

¹³C NMR (101 MHz, CDCl₃) δ 178.7, 175.7, 142.4, 128.4, 128.3, 125.8, 64.4, 50.0, 47.4, 40.9, 38.7, 36.2, 32.7, 32.5, 29.7, 28.6, 27.4, 27.2, 26.2, 14.9.

FT-IR (film): 2932, 2883, 2857, 1726, 1647, 1456, 1436, 1168, 1155, 1030, 729 cm⁻¹.

HRMS (ESI-MS) *m/z* [M+H]⁺ calcd for C₂₄H₃₇NO₃: 388.2847, found: 388.2842.

[α]²²_D = +1.9 (*c* 1.0, CHCl₃); 92% ee, from (*S,S*)-**L***.



tert-Butyl 4-(3-(azetidine-1-carbonyl)-6-phenylhexyl)piperidine-1-carboxylate (19). The title compound was synthesized according to **GP-7** *tert*-butyl 4-(2-iodoethyl)piperidine-1-carboxylate and **Zn-9**. The title compound was also synthesized according to **GP-8** from *tert*-butyl 4-(2-iodoethyl)piperidine-1-carboxylate and 1-(azetidin-1-yl)-5-phenylpentan-1-one. The product was purified by preparative TLC (11:7 EtOAc/hexanes). Colorless oil.

GP-7 (*R,R*)-**L***: 137 mg, 53% yield, 94% ee; (*S,S*)-**L***: 132 mg, 51% yield, 94% ee.

GP-8 (*R,R*)-**L***: 118 mg, 46% yield, 94% ee; (*S,S*)-**L***: 120 mg, 47% yield, 94% ee.

SFC analysis: The ee was determined via SFC on a CHIRALCEL OJ-3 column (5% *i*-PrOH in supercritical CO₂, 2.5 mL/min); retention times for compound obtained using (*S,S*)-**L***: 11.0 min (major), 13.2 min (minor).

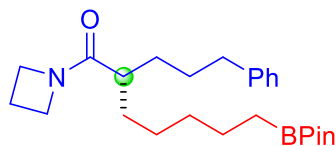
¹H NMR (400 MHz, CDCl₃) δ 7.32 – 7.25 (m, 2H), 7.22 – 7.09 (m, 3H), 4.26 – 3.85 (m, 6H), 2.75 – 2.42 (m, 4H), 2.29 – 2.18 (m, 2H), 2.13 (tt, *J* = 9.4, 5.0 Hz, 1H), 1.73 – 1.49 (m, 6H), 1.45 (s, 9H), 1.42 – 0.94 (m, 7H).

¹³C NMR (101 MHz, CDCl₃) δ 175.6, 154.9, 142.3, 128.4, 128.3, 125.8, 79.2, 50.0, 47.4, 41.1, 36.3, 36.2, 34.4, 32.5, 32.2, 32.1, 29.8, 29.7, 28.5, 14.9.

FT-IR (film): 2933, 2881, 2853, 1691, 1647, 1456, 1424, 1168, 1085, 707 cm⁻¹.

HRMS (ESI-MS) *m/z* [M+H]⁺ calcd for C₂₆H₄₁N₂O₃: 429.3112, found: 429.3107.

[α]_D²² = +2.2 (*c* 1.0, CHCl₃); 94% ee, from (*S,S*)-**L***.



1-(Azetidin-1-yl)-2-(3-phenylpropyl)-7-(4,4,5,5-tetramethyl-1,3,2-dioxaborolan-2-yl)heptan-1-one (20). The title compound was synthesized according to **GP-7** from 2-(5-iodopentyl)-4,4,5,5-tetramethyl-1,3,2-dioxaborolane and **Zn-9**. The title compound was also synthesized according to **GP-8** from 2-(5-iodopentyl)-4,4,5,5-tetramethyl-1,3,2-dioxaborolane and 1-(azetidin-1-yl)-5-phenylpentan-1-one. The product was purified by column chromatography on silica gel (5% → 8% acetone/DCM), purified again by preparative TLC (11:7 EtOAc/hexanes), and again by preparative TLC (9% acetone/DCM). Colorless oil.

GP-7 (*R,R*)-**L***: 107 mg, 43% yield, 91% ee; (*S,S*)-**L***: 102 mg, 41% yield, 91% ee.

GP-8 (*R,R*)-**L***: 99 mg, 40% yield, 91% ee; (*S,S*)-**L***: 90 mg, 36% yield, 91% ee.

SFC analysis: The ee was determined via SFC on a CHIRALPAK ID-3 column (30% *i*-PrOH in supercritical CO₂, 2.5 mL/min); retention times for compound obtained using (*S,S*)-**L***: 5.0 min (major), 5.7 min (minor).

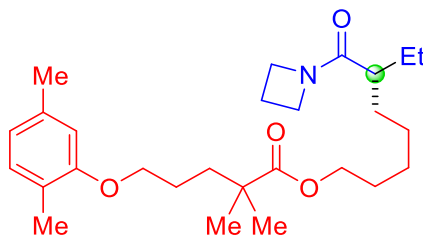
¹H NMR (500 MHz, CDCl₃) δ 7.28 (d, *J* = 7.7 Hz, 2H), 7.21 – 7.14 (m, 3H), 4.11 (p, *J* = 7.8 Hz, 2H), 4.04 – 3.97 (m, 2H), 2.58 (qdd, *J* = 13.9, 9.0, 6.2 Hz, 2H), 2.27 – 2.13 (m, 3H), 1.71 – 1.61 (m, 2H), 1.59 – 1.48 (m, 2H), 1.25 (s, 20H), 0.76 (t, *J* = 7.8 Hz, 2H).

¹³C NMR (101 MHz, CDCl₃) δ 175.9, 142.5, 128.5, 128.3, 125.7, 82.9, 49.9, 47.4, 40.9, 36.2, 32.8, 32.6, 31.5, 29.8, 27.6, 24.8, 24.0, 14.9 (α-B carbon not observed).

FT-IR (film): 2975, 2932, 2858, 1646, 1435, 1359, 1316, 1168, 840, 744 cm⁻¹.

HRMS (ESI-MS) *m/z* [M+H]⁺ calcd for C₂₅H₄₁BNO₃: 414.3174, found: 414.3180.

[α]_D²² = -1.0 (*c* 1.0, CHCl₃); 91% ee, from (*S,S*)-**L***.



6-(Azetidine-1-carbonyl)octyl 5-(2,5-dimethylphenoxy)-2,2-dimethylpentanoate (21). The title compound was synthesized according to **GP-7** from 5-iodopentyl 5-(2,5-dimethylphenoxy)-2,2-dimethylpentanoate and **Zn-2**. The title compound was also synthesized according to **GP-8** from 5-iodopentyl 5-(2,5-dimethylphenoxy)-2,2-dimethylpentanoate and 1-(azetidin-1-yl)butan-1-one. The product was purified by column chromatography on silica gel (20% → 60% EtOAc/hexanes). Mixed fractions were purified by preparative TLC (11:7 EtOAc/hexanes). Pale yellow oil.

GP-7 (*R,R*)-**L***: 143 mg, 54% yield, 94% ee; (*S,S*)-**L***: 140 mg, 52% yield, 94% ee.

GP-8 (*R,R*)-**L***: 133 mg, 50% yield, 94% ee; (*S,S*)-**L***: 137 mg, 51% yield, 94% ee.

SFC analysis: The ee was determined via SFC on a CHIRALPAK IG-3 column (20% *i*-PrOH in supercritical CO₂, 2.5 mL/min); retention times for compound obtained using (*S,S*)-**L***: 8.7 min (major), 9.6 min (minor).

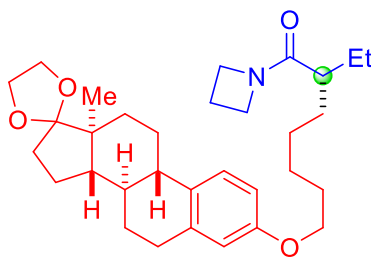
¹H NMR (400 MHz, CDCl₃) δ 7.00 (dd, *J* = 7.4, 0.9 Hz, 1H), 6.65 (ddd, *J* = 7.4, 1.7, 0.8 Hz, 1H), 6.61 (d, *J* = 1.6 Hz, 1H), 4.14 (td, *J* = 7.6, 3.3 Hz, 2H), 4.07 – 3.98 (m, 4H), 3.97 – 3.85 (m, 2H), 2.30 (d, *J* = 0.8 Hz, 3H), 2.29 – 2.18 (m, 2H), 2.17 (s, 3H), 2.09 (tt, *J* = 9.5, 4.8 Hz, 1H), 1.78 – 1.69 (m, 4H), 1.66 – 1.57 (m, 4H), 1.47 – 1.26 (m, 5H), 1.21 (s, 6H), 0.87 (t, *J* = 7.4 Hz, 3H).

¹³C NMR (101 MHz, CDCl₃) δ 177.9, 175.8, 156.9, 136.5, 130.3, 123.5, 120.7, 111.9, 67.9, 64.4, 49.9, 47.4, 42.6, 42.1, 37.1, 32.3, 28.6, 27.4, 26.2, 25.7, 25.2 (3C: overlapping signal), 21.4, 15.8, 14.9, 12.1.

FT-IR (film): 2932, 2883, 1725, 1649, 1436, 1255, 1168, 1129, 1044, 828, 717 cm^{-1} .

HRMS (ESI-MS) m/z $[\text{M}+\text{H}]^+$ calcd for $\text{C}_{27}\text{H}_{43}\text{NO}_4$: 446.3265, found: 446.3274.

$[\alpha]_{\text{D}}^{22} = -3.5$ (c 1.0, CHCl_3); 94% ee, from (*S,S*)-**L***.



1-(Azetidin-1-yl)-2-ethyl-7-(((8*R*,9*S*,13*S*,14*S*)-13-methyl-6,7,8,9,11,12,13,14,15,16-decahydrospiro[cyclopenta[a]phenanthrene-17,2'-[1,3]dioxolan]-3-yl)oxy)heptan-1-one (22, 23). The title compound was synthesized according to **GP-6** from (*8R,9S,13S,14S*)-3-((5-iodopentyl)oxy)-13-methyl-6,7,8,9,11,12,13,14,15,16-decahydrospiro[cyclopenta[a]phenanthrene-17,2'-[1,3]dioxolane] and Zn-2. The title compound was also synthesized according to **GP-8** from (*8R,9S,13S,14S*)-3-((5-iodopentyl)oxy)-13-methyl-6,7,8,9,11,12,13,14,15,16-decahydrospiro[cyclopenta[a]phenanthrene-17,2'-[1,3]dioxolane] and 1-(azetidin-1-yl)butan-1-one. The product was purified by column chromatography on silica gel (30% → 60% EtOAc/hexanes). Mixed fractions were purified by preparative TLC (11:7 EtOAc/hexanes). Yellow oil.

GP-6 (*R,R*)-**L***: 200 mg, 65% yield, 96:4 dr; (*S,S*)-**L***: 193 mg, 63% yield, 4:96 dr.

GP-8 (*R,R*)-**L***: 175 mg, 57% yield, 96:4 dr; (*S,S*)-**L***: 158 mg, 51% yield, 4:96 dr.

SFC analysis: The dr was determined via SFC on a CHIRALPAK IG-3 column (35% *i*-PrOH in supercritical CO_2 , 2.5 mL/min); retention times for compound obtained using (*S,S*)-**L***: 11.6 min (minor), 14.3 min (major).

NMR data for the product from (*R,R*)-**L***:

^1H NMR (500 MHz, CDCl_3) δ 7.18 (d, $J = 8.6$ Hz, 1H), 6.67 (dd, $J = 8.6, 2.7$ Hz, 1H), 6.60 (d, $J = 2.7$ Hz, 1H), 4.21 – 4.08 (m, 2H), 4.02 (td, $J = 7.8, 1.8$ Hz, 2H), 3.98 – 3.84 (m, 6H), 2.99 – 2.72 (m, 2H), 2.37 – 2.16 (m, 4H), 2.11 (tt, $J = 9.5, 5.0$ Hz, 1H), 2.02 (ddd, $J = 14.1, 11.6, 2.8$ Hz, 1H), 1.95 – 1.68 (m, 6H), 1.66 – 1.27 (m, 14H), 0.92 – 0.85 (m, 6H).

^{13}C NMR (101 MHz, CDCl_3) δ 175.9, 156.9, 138.0, 132.6, 126.3, 119.5, 114.4, 112.0, 67.7, 65.3, 64.6, 50.0, 49.4, 47.4, 46.2, 43.6, 42.5, 39.1, 34.3, 32.3, 30.8, 29.8, 29.2, 27.5, 27.0, 26.21, 26.16, 25.7, 22.4, 15.0, 14.4, 12.2.

NMR data for the product from (*S,S*)-**L***:

^1H NMR (400 MHz, CDCl_3) δ 7.23 – 7.15 (m, 1H), 6.68 (dd, $J = 8.6, 2.8$ Hz, 1H), 6.61 (d, $J = 2.7$ Hz, 1H), 4.19 – 4.10 (m, 2H), 4.07 – 3.98 (m, 2H), 3.98 – 3.83 (m, 6H), 2.92 – 2.76 (m, 2H), 2.36 – 2.17 (m, 4H), 2.11 (ddt, $J = 14.7, 10.3, 5.1$ Hz, 1H), 2.06 – 1.97 (m, 1H), 1.95 – 1.69 (m, 6H), 1.66 – 1.27 (m, 14H), 0.97 – 0.79 (m, 6H).

^{13}C NMR (101 MHz, CDCl_3) δ 175.9, 156.9, 138.0, 132.6, 126.3, 119.5, 114.4, 112.0, 67.7, 65.3, 64.6, 50.0, 49.4, 47.4, 46.2, 43.6, 42.5, 39.1, 34.3, 32.3, 30.8, 29.8, 29.2, 27.5, 27.0, 26.21, 26.16, 25.8, 22.4, 15.0, 14.4, 12.2.

FT-IR (film): 2932, 2874, 2816, 1645, 1474, 1450, 1256, 1169, 1041, 780, 716 cm^{-1} .

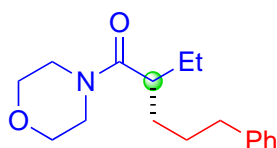
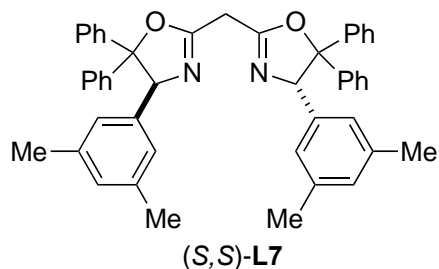
HRMS (ESI-MS) m/z $[\text{M}+\text{H}]^+$ calcd for $\text{C}_{32}\text{H}_{48}\text{NO}_4$: 510.3578, found: 510.3576.

$[\alpha]_{\text{D}}^{22} = +21$ (c 1.0, CHCl_3); 96:4 dr, from (*R,R*)-**L***.

$[\alpha]_{\text{D}}^{22} = +9.2$ (c 1.0, CHCl_3); 4:96 dr, from (*S,S*)-**L***.

Application of the method to other amides: In addition to the *N*-acylazetidine substrates reported in Fig. 2, we have established that the catalytic enantioselective α -Alkylation of an *N*-acylmorpholine and an *N,N*-dimethylamide can be achieved with good yield and

enantioselectivity, using ligand **L7**. These examples point to the generality of the reactivity described in the present study.



2-Methyl-1-morpholino-5-phenylpentan-1-one (S-1). The title compound was synthesized according to **GP-6** from (3-iodopropyl)benzene and **Zn-10**, using 10 mol% NiBr₂·glyme and 13 mol% **L7**, instead of **L***. The title compound was also synthesized according to **GP-8** from (3-iodopropyl)benzene and 1-morpholinopropan-1-one, using 10 mol% NiBr₂·glyme and 13 mol% **L7**, instead of **L***. The product was purified by column chromatography on silica gel (10% → 50% EtOAc/hexanes). Mixed fractions were purified by preparative TLC (1:1 EtOAc/hexanes). Pale yellow oil.

GP-6 (*R,R*)-**L***: 126 mg, 76% yield, 88% ee; (*S,S*)-**L***: 122 mg, 74% yield, 89% ee.

GP-8 (*R,R*)-**L***: 108 mg, 65% yield, 88% ee; (*S,S*)-**L***: 104 mg, 63% yield, 89% ee.

SFC analysis: The ee was determined via SFC on a CHIRALPAK IG-3 column (15% *i*-PrOH in supercritical CO₂, 2.5 mL/min); retention times for compound obtained using (*S,S*)-**L7**: 6.2 min (minor), 6.7 min (major).

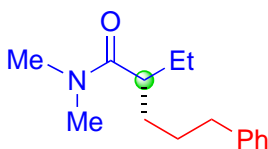
^1H NMR (400 MHz, CDCl_3) δ 7.31 – 7.23 (m, 2H), 7.23 – 7.07 (m, 3H), 3.76 – 3.38 (m, 8H), 2.70 – 2.47 (m, 3H), 1.78 – 1.44 (m, 6H), 0.86 (t, $J = 7.4$ Hz, 3H).

^{13}C NMR (101 MHz, CDCl_3) δ 174.5, 142.2, 128.4, 128.3, 125.8, 67.2, 66.9, 46.2, 42.22, 42.15, 36.0, 32.2, 29.4, 25.8, 12.0.

FT-IR (film): 3022, 2959, 2927, 2854, 2335, 1637, 1454, 1227, 1116, 1032, 702, 690 cm^{-1} .

HRMS (ESI-MS) m/z $[\text{M}+\text{H}]^+$ calcd for $\text{C}_{17}\text{H}_{26}\text{NO}_2$: 276.1959, found: 276.1963.

$[\alpha]_{\text{D}}^{22} = -10$ (c 1.0, CHCl_3); 89% ee, from (*S,S*)-**L7**.



2-Methyl-1-morpholino-5-phenylpentan-1-one (S-2). The title compound was synthesized according to **GP-6** from (3-iodopropyl)benzene and **Zn-11**, using **L7** instead of **L***. The title compound was also synthesized according to **GP-8** from (3-iodopropyl)benzene and *N,N*-dimethylpropionamide, using **L7** instead of **L***. The product was purified by column chromatography on silica gel (20% → 40% EtOAc/hexanes). Pale yellow oil.

GP-6 (*R,R*)-**L***: 110 mg, 79% yield, 89% ee; (*S,S*)-**L***: 106 mg, 76% yield, 89% ee.

GP-8 (*R,R*)-**L***: 90 mg, 64% yield, 88% ee; (*S,S*)-**L***: 95 mg, 67% yield, 88% ee.

SFC analysis: The ee was determined via SFC on a CHIRALPAK OJ-3 column (5% *i*-PrOH in supercritical CO_2 , 2.5 mL/min); retention times for compound obtained using (*S,S*)-**L7**: 3.8 min (minor), 4.3 min (major).

^1H NMR (400 MHz, CDCl_3) δ 7.30 – 7.25 (m, 2H), 7.22 – 7.08 (m, 3H), 3.02 (s, 3H), 2.96 (s, 3H), 2.67 – 2.51 (m, 3H), 1.79 – 1.39 (m, 6H), 0.86 (t, $J = 7.4$ Hz, 3H).

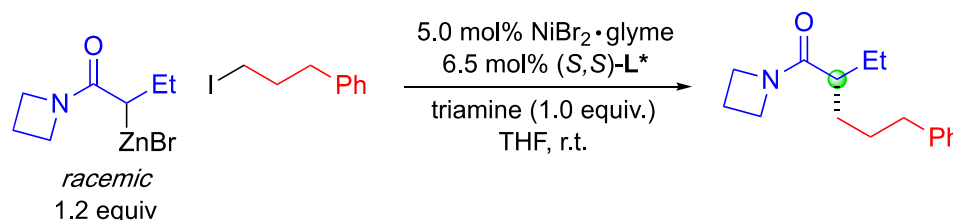
^{13}C NMR (101 MHz, CDCl_3) δ 176.1, 142.5, 128.4, 128.3, 125.7, 42.8, 37.4, 36.2, 35.6, 32.5, 29.7, 26.1, 12.0.

FT-IR (film): 2931, 2358, 1642, 1453, 1259, 1135, 699 cm^{-1} .

HRMS (ESI-MS) m/z $[\text{M}+\text{H}]^+$ calcd for $\text{C}_{15}\text{H}_{24}\text{NO}$: 234.1854, found: 234.1850.

$[\alpha]_{\text{D}}^{22} = -22$ (c 1.0, CHCl_3); 88% ee, from (*R,R*)-**L7**.

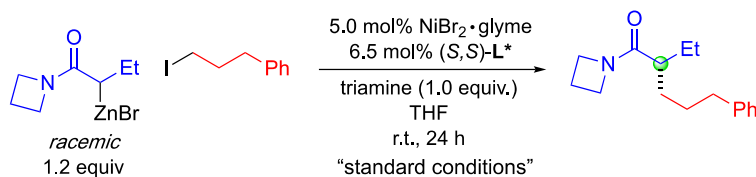
2.4.5. Effect of Reaction Parameters



General Procedure 9 (GP-9). In a glovebox, NiBr₂·glyme (15.4 mg, 0.050 mmol) and **L**^{*} (35 mg, 0.065 mmol) were added to a 20 mL vial that contained a stir bar. Then, THF (5 mL) was added, and the mixture was stirred at r.t. for 45 min, leading to a magenta solution. To a 4 mL vial that contained a stir bar was added **Zn-2** (42 mg, 0.12 mmol, 1.2 equiv) and 0.5 mL of the solution of the catalyst (5.0 mol% Ni). The mixture was stirred for ~3 min, and then the triamine (24 mL, 0.10 mmol, 1.0 equiv) and the electrophile (3-iodopropyl)benzene (16 mL, 0.10 mmol, 1.0 equiv) were added via syringe. The vial was capped, wrapped with electrical tape, and removed from the glovebox. The reaction mixture was stirred at r.t. for 24 h, and then the reaction was quenched by the addition of EtOH (0.1 mL). Dodecane (23 mL, 0.10 mmol, 1.0 equiv, internal standard) was

added via syringe, and then the reaction mixture was diluted with Et₂O (2 mL), stirred for 10 s, and then filtered through a plug of silica (flushing with Et₂O (8 mL)). Part of the solution (~1 mL) was removed for GC analysis of the yield. The rest of the mixture was concentrated, the product was isolated by preparative TLC (3:2 EtOAc:hexanes), and the ee was determined via SFC analysis.

GP-9 was followed, with changes as described in the table. All data represent the average of two experiments.



Entry	Variation from the "standard conditions"	Yield (%)	ee (%)
1	None	93	90
2	L1 , instead of L*	7	0
3	L2 , instead of L*	9	2
4	L3 , instead of L*	24	-17
5	L4 , instead of L*	76	-83
6	L5 , instead of L*	36	-27
7	L6 , instead of L*	32	20
8	No triamine	8	86
9	TMEDA (1.5 equiv), instead of triamine	39	57
10	Alkyl bromide as the electrophile	59	90
11	1.0 equiv of the nucleophile	86	89
12	2-MeTHF, instead of THF	91	90
13	MTBE, instead of THF	50	88
14	2.5 mol% NiBr ₂ ·glyme, 3.3 mol% L*	87	89
15	1.0 mol% NiBr ₂ ·glyme, 1.3 mol% L*	76	86
16	12 h, instead of 24 h	77	90
17	0.1 equiv H ₂ O added	64	90
18	0.5 mL air added to the headspace	51	83

L1

L2

L3

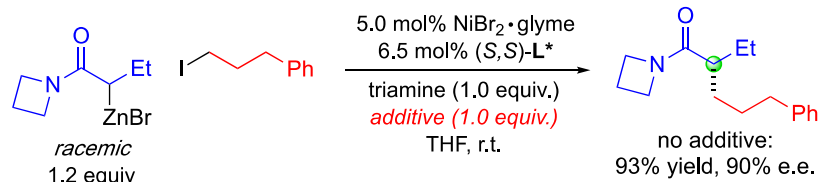
L4

L5

L6

2.4.6. Functional-Group Compatibility

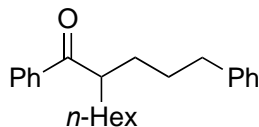
GP-9 was followed, with the addition of 1.0 equiv of each additive. All data represent the average of two experiments.



recovery of additive				
yield of product	90%	>95%	>95%	91%
e.e. of product	74%	80%	83%	64%
	90%	89%	89%	81%
recovery of additive				
yield of product	91%	93%	91%	95%
e.e. of product	85%	85%	79%	85%
	90%	90%	90%	90%
recovery of additive				
yield of product	90%	95%	>95%	>95%
e.e. of product	62%	75%	83%	86%
	87%	89%	90%	90%
recovery of additive				
yield of product	>95%	>95%	>95%	>95%
e.e. of product	89%	56%	85%	80%
	90%	89%	90%	90%
recovery of additive				
yield of product	92%	>95%	73%	95%
e.e. of product	77%	93%	62%	30%
	90%	90%	90%	81%
recovery of additive				
yield of product	90%	>95%	58%	
e.e. of product	40%	9%	30%	
	5%	44%	44%	

2.4.7. Derivatization of the Coupling Products

All reactions were carried out using 1-(azetidin-1-yl)-2-(3-phenylpropyl)octan-1-one (**10**), synthesized with (*S,S*)-**L*** (92% ee) and (*R,R*)-**L*** (91% ee).



1-Phenyl-2-(3-phenylpropyl)octan-1-one. 1-(Azetidin-1-yl)-2-(3-phenylpropyl)octan-1-one (**10**) (60 mg, 0.20 mmol, 1.0 equiv) was added to a 8 mL vial that contained a stir bar. The vial was evacuated and backfilled with nitrogen on a Schlenk line. Then, THF (2 mL) was added, and the mixture was stirred and cooled to -78 °C. PhLi (1.7 M solution in *n*-Bu₂O, 0.36 mL, 0.60 mmol) was added dropwise, and then the mixture was stirred at -78 °C for 15 min. Next, saturated aqueous NH₄Cl (0.5 mL) was added to the mixture at -78 °C, and it was stirred and warmed to r.t. The mixture was partitioned between Et₂O and H₂O (20 mL each). The phases were separated, and the aqueous phase was extracted with Et₂O (20 mL \times 2). The combined organic phase was washed with brine, dried with Na₂SO₄, and concentrated. The residue was purified by column chromatography on silica gel (3% \rightarrow 5% Et₂O /hexanes). Colorless oil.

(*R,R*)-**L***: 60 mg, 93% yield, 90% ee; (*S,S*)-**L***: 59 mg, 92% yield, 91% ee.

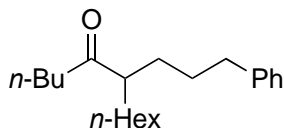
SFC analysis: The ee was determined via SFC on a CHIRALCEL OJ-3 column (2% *i*-PrOH in supercritical CO₂, 2.5 mL/min); retention times for compound obtained using (*S,S*)-**L***: 10.6 min (minor), 11.4 min (major).

^1H NMR (400 MHz, CDCl_3) δ 7.97 – 7.90 (m, 2H), 7.60 – 7.51 (m, 1H), 7.50 – 7.41 (m, 2H), 7.25 – 7.21 (m, 2H), 7.19 – 7.07 (m, 3H), 3.48 – 3.37 (m, 1H), 2.58 (td, $J = 7.6, 3.9$ Hz, 2H), 1.88 – 1.70 (m, 2H), 1.65 – 1.42 (m, 4H), 1.28 – 1.14 (m, 8H), 0.89 – 0.80 (m, 3H).

^{13}C NMR (101 MHz, CDCl_3) δ 204.7, 142.2, 137.7, 132.9, 128.6, 128.4, 128.3, 128.2, 125.7, 46.0, 36.1, 32.6, 32.1, 31.6, 29.5, 29.4, 27.5, 22.6, 14.1.

FT-IR (film): 3059, 3028, 2928, 2855, 1678, 1448, 1218, 978, 704 cm^{-1} .

$[\alpha]_{\text{D}}^{22} = -4.8$ (c 1.0, CHCl_3); 91% ee, from (*S,S*)-**L***.



6-(3-Phenylpropyl)dodecan-5-one. 1-(Azetidin-1-yl)-2-(3-phenylpropyl)octan-1-one (**10**) (60 mg, 0.20 mmol, 1.0 equiv) was added to a 8 mL vial that contained a stir bar. The vial was evacuated and backfilled with nitrogen on a Schlenk line. Then, THF (2 mL) was added, and the mixture was stirred and cooled to -78 °C. *n*-BuLi (1.6 M solution in hexanes, 0.38 mL, 0.60 mmol) was added dropwise, and the resulting mixture was stirred at -78 °C for 15 min. Next, saturated aqueous NH_4Cl (0.5 mL) was added to the mixture at -78 °C, and it was stirred and warmed to r.t. The mixture was partitioned between Et_2O and H_2O (20 mL each). The phases were separated, and the aqueous phase was extracted with Et_2O (20 mL \times 2). The combined organic phase was washed with brine, dried with Na_2SO_4 , and concentrated. The residue was purified by column chromatography on silica gel (0% \rightarrow 3% Et_2O /hexanes). Colorless oil.

(*R,R*)-**L***: 50 mg, 83% yield, 90% ee; (*S,S*)-**L***: 54 mg, 89% yield, 92% ee.

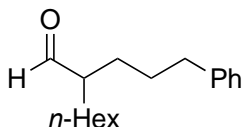
SFC analysis: The ee was determined via SFC on a CHIRALPAK IC-3 column (1% *i*-PrOH in supercritical CO₂, 2.5 mL/min); retention times for compound obtained using (*S,S*)-**L***: 14.8 min (major), 16.0 min (minor).

¹H NMR (400 MHz, CDCl₃) δ 7.31 – 7.24 (m, 2H), 7.22 – 7.11 (m, 3H), 2.58 (p, *J* = 6.8 Hz, 2H), 2.45 (tt, *J* = 8.0, 5.4 Hz, 1H), 2.40 – 2.32 (m, 2H), 1.71 – 1.40 (m, 7H), 1.40 – 1.12 (m, 11H), 0.95 – 0.81 (m, 6H).

¹³C NMR (101 MHz, CDCl₃) δ 215.0, 142.2, 128.4, 128.3, 125.8, 52.3, 42.0, 36.0, 31.8, 31.7, 31.3, 29.4, 29.3, 27.5, 25.6, 22.6, 22.4, 14.1, 13.9.

FT-IR (film): 2955, 2930, 2856, 1709, 1456, 1377, 1076, 699 cm⁻¹.

[α]_D²² = +1.7 (*c* 1.0, CHCl₃); 92% ee, from (*S,S*)-**L***.



2-(3-Phenylpropyl)octanal. In a glovebox, 1-(azetidin-1-yl)-2-(3-phenylpropyl)octan-1-one (**10**) (60 mg, 0.20 mmol, 1.0 equiv), Schwartz's reagent (54 mg, 0.21 mmol, 1.05 equiv), and then THF (2 mL) were added to a 8 mL vial that contained a stir bar. The vial was sealed with a cap and removed from the glovebox. The reaction mixture was stirred at r.t. for 30 min, and then it was diluted with Et₂O, passed through a pad of silica, and concentrated. The residue was purified by column chromatography on silica gel (0% → 5% Et₂O /hexanes). Colorless oil.

(*R,R*)-**L***: 35 mg, 70% yield, 90% ee; (*S,S*)-**L***: 37 mg, 74% yield, 92% ee.

To determine the ee of the product, a small amount of the aldehyde (~15 mg) was dissolved in 9:1 Et₂O/MeOH (1 mL) in the air in a 4 mL vial that contained a stir bar. The mixture was cooled

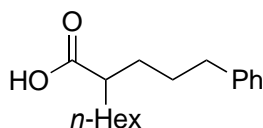
to 0 °C, and then NaBH₄ (~10 mg, excess) was added. The mixture was stirred at 0 °C with venting for 2 h, and then the reaction was quenched by the addition of 2 N HCl. The reaction mixture was diluted with Et₂O (10 mL) and washed with H₂O (5 mL). The organic phase was concentrated, passed through a short plug of silica (flushing with Et₂O), and then concentrated. The residue was directly analyzed by SFC analysis, as described below for the alcohol.

¹H NMR (400 MHz, CDCl₃) δ 9.55 (d, *J* = 3.1 Hz, 1H), 7.30 – 7.26 (m, 2H), 7.22 – 7.11 (m, 3H), 2.62 (t, *J* = 7.3 Hz, 2H), 2.31 – 2.19 (m, 1H), 1.72 – 1.56 (m, 4H), 1.51 – 1.37 (m, 2H), 1.34 – 1.19 (m, 8H), 0.96 – 0.80 (m, 3H).

¹³C NMR (101 MHz, CDCl₃) δ 205.5, 141.9, 128.38, 128.36, 125.9, 51.9, 35.9, 31.6, 29.4, 28.9, 28.8, 28.4, 27.0, 22.6, 14.1.

FT-IR (film): 2927, 2854, 2360, 1725, 1456, 1168, 828, 745 cm⁻¹.

[α]_D²² = -1.2 (*c* 1.0, CHCl₃); 90% ee, from (*R,R*)-**L***.



2-(3-Phenylpropyl)octanoic acid. In a glovebox, 1-(azetidin-1-yl)-2-(3-phenylpropyl)octan-1-one (**10**) (60 mg, 0.20 mmol, 1.0 equiv), Schwartz's reagent (54 mg, 0.21 mmol, 1.05 equiv), and then THF (2 mL) were added to a 20 mL vial that contained a stir bar. The vial was sealed with a cap and removed from the glovebox. The mixture was stirred at r.t. for 30 min, and then the cap was removed, the mixture was cooled to 0 °C, and H₂O (2 mL), *t*-BuOH (2 mL), and 2-methyl-2-butene (1.1 mL, 10.0 mmol, 50 equiv) were added in turn. The resulting mixture was stirred at 0 °C for 10 min, and then NaH₂PO₄·H₂O (552 mg, 4.0 mmol, 20 equiv) was added, followed by

NaClO₂ (181 mg, 2.0 mmol, 10 equiv). The mixture was stirred at r.t. for 2 h, and then it was partitioned between Et₂O and H₂O. The aqueous phase was extracted twice with Et₂O, and the combined organic phase was concentrated and purified by column chromatography on silica gel (10% → 20% EtOAc/hexanes). Colorless oil.

(*R,R*)-**L***: 39 mg, 76% yield, 91% ee; (*S,S*)-**L***: 41 mg, 78% yield, 92% ee.

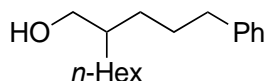
To determine the ee of the product, a small amount of the carboxylic acid (~15 mg) was dissolved in THF (1 mL) in a 4 mL vial that contained a stir bar (under nitrogen). The mixture was cooled to 0 °C, and then LAH (~10 mg, excess) was added. The resulting mixture was stirred at r.t. overnight, and then the reaction was quenched by the addition of 2 N HCl. The reaction mixture was diluted with Et₂O (20 mL) and washed with H₂O (10 mL × 2). The organic phase was concentrated, passed through a short plug of silica (flushing with Et₂O), and then concentrated. The residue was directly analyzed by SFC analysis, as described below for the alcohol.

¹H NMR (500 MHz, CDCl₃) δ 11.41 (br, 1H), 7.26 (t, *J* = 7.4 Hz, 2H), 7.19 – 7.12 (m, 3H), 2.61 (t, *J* = 7.3 Hz, 2H), 2.36 (td, *J* = 8.5, 5.2 Hz, 1H), 1.78 – 1.57 (m, 4H), 1.57 – 1.37 (m, 2H), 1.37 – 1.14 (m, 8H), 0.87 (t, *J* = 6.7 Hz, 3H).

¹³C NMR (126 MHz, CDCl₃) δ 182.6, 142.1, 128.4, 128.3, 125.8, 45.4, 35.8, 32.2, 31.74, 31.66, 29.21, 29.15, 27.3, 22.6, 14.1.

FT-IR (film): 3022, 2928, 2858, 1702, 1453, 1168, 834, 726 cm⁻¹.

[α]_D²² = +4.0 (*c* 1.0, CHCl₃); 92% ee, from (*S,S*)-**L***.



2-(3-Phenylpropyl)octan-1-ol. Under nitrogen, a solution of *n*-BuLi (2.5 M solution in hexanes, 0.93 mL, 2.3 mmol) was added dropwise to a stirred solution of *i*-Pr₂NH (0.35 mL, 2.5 mmol) in THF (2.5 mL) at -78 °C. This solution was stirred at -78 °C for 10 min, and then it was warmed to 0 °C and stirred for another 10 min. Next, BH₃NH₃ (76 mg, 2.5 mmol) was added in one portion, and the resulting suspension was stirred at 0 °C for 15 min. The mixture was then warmed to r.t. and stirred for 15 min.

Part of this suspension of LiBH₃NH₂ (1.8 mL) was transferred via syringe to another 8 mL vial that contained a stir bar (under nitrogen), which was then cooled to 0 °C. A solution of 1-(azetidin-1-yl)-2-(3-phenylpropyl)octan-1-one (**10**) (60 mg, 0.20 mmol, 1.0 equiv) in THF (2 mL) in a culture tube was added dropwise to the vial that contained LiBH₃NH₂. The culture tube was then rinsed with THF (0.5 mL), and this rinse was added to the reaction vial. The reaction mixture was warmed to r.t. and stirred for 3 h. Next, 2 N HCl was added dropwise at 0 °C, and the resulting mixture was stirred at 0 °C for 30 min. The mixture was then partitioned between Et₂O and H₂O, and the aqueous phase was extracted twice with Et₂O. The combined organic phase was concentrated and purified by column chromatography on silica gel (10% → 20% EtOAc/hexanes). Colorless oil.

(*R,R*)-**L***: 40 mg, 81% yield, 90% ee; (*S,S*)-**L***: 43 mg, 87% yield, 92% ee.

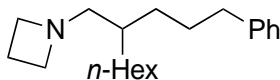
SFC analysis: The ee was determined via SFC on a CHIRALPAK IE-3 column (2% *i*-PrOH in supercritical CO₂, 2.5 mL/min); retention times for compound obtained using (*S,S*)-**L***: 13.9 min (minor), 14.9 min (major).

^1H NMR (400 MHz, CDCl_3) δ 7.31 – 7.26 (m, 2H), 7.23 – 7.12 (m, 3H), 3.54 (dd, $J = 5.5, 1.5$ Hz, 2H), 2.61 (dd, $J = 8.8, 6.7$ Hz, 2H), 1.64 (dt, $J = 15.6, 7.8$ Hz, 2H), 1.54 – 1.19 (m, 14H), 0.97 – 0.82 (m, 3H).

^{13}C NMR (101 MHz, CDCl_3) δ 142.7, 128.4, 128.3, 125.7, 65.6, 40.5, 36.3, 31.9, 30.9, 30.6, 29.7, 28.8, 26.9, 22.7, 14.1.

FT-IR (film): 3339, 2925, 2854, 1169, 1032, 1031, 711 cm^{-1} .

$[\alpha]_{\text{D}}^{22} = -1.1$ (c 1.0, CHCl_3); 92% ee, from (*S,S*)-**L***.



1-(2-(3-Phenylpropyl)octyl)azetidine. 1-(Azetidin-1-yl)-2-(3-phenylpropyl)octan-1-one (**10**) (60 mg, 0.20 mmol, 1.0 equiv), THF (2 mL), and then LAH (1.0 M in THF, 0.80 mL, 0.80 mmol, 4.0 equiv) were added to a 20 mL vial that contained a stir bar. The vial was sealed with a cap, and the mixture was heated at 70 °C for 12 h. Next, the mixture was cooled to 0 °C, and the reaction was quenched by the addition of H_2O . The mixture was diluted with Et_2O (20 mL) and washed with H_2O (10 mL). The organic phase was concentrated and purified by column chromatography on silica gel (10% \rightarrow 90% EtOAc /hexanes). White low-melting solid.

(*R,R*)-**L***: 51 mg, 89% yield; (*S,S*)-**L***: 51 mg, 89% yield.

The ee of this product was determined by derivatization to the methyl carbamate (see below).

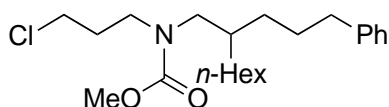
^1H NMR (500 MHz, CDCl_3) δ 7.30 – 7.26 (m, 2H), 7.24 – 7.07 (m, 3H), 3.13 (t, $J = 7.0$ Hz, 4H), 2.58 (t, $J = 7.8$ Hz, 2H), 2.26 (d, $J = 5.9$ Hz, 2H), 2.04 (p, $J = 7.0$ Hz, 2H), 1.69 – 1.50 (m, 2H), 1.37 – 1.19 (m, 13H), 0.88 (t, $J = 6.8$ Hz, 3H).

^{13}C NMR (101 MHz, CDCl_3) δ 142.9, 128.4, 128.2, 125.6, 64.9, 55.9, 36.5, 36.4, 32.2, 32.0, 31.9, 29.7, 28.8, 26.7, 22.7, 17.8, 14.1.

FT-IR (film): 2993, 2955, 2925, 2812, 1454, 1168, 1120, 746 cm^{-1} .

HRMS (ESI-MS) m/z $[\text{M}+\text{H}]^+$ calcd for $\text{C}_{20}\text{H}_{34}\text{N}$: 288.2686, found: 288.2699.

$[\alpha]_{\text{D}}^{22} = -1.3$ (c 1.0, CHCl_3); from (*S,S*)-**L***.



Methyl (3-chloropropyl)(2-(3-phenylpropyl)octyl)carbamate. (37) Following a literature procedure, 1-(2-(3-phenylpropyl)octyl)azetidone (15 mg, 0.052 mmol) was dissolved in DCM (0.4 mL) in a 4-mL vial equipped with a stir bar. The vial was briefly purged with nitrogen and capped with a septum cap. Then, methyl chloroformate (10 mL, 0.13 mmol) was added through the cap, and the mixture was stirred at r.t. for 16 h. Next, methanol (a few drops) and Et_2O (2 mL) were added to the mixture, which was then passed through a plug of silica gel. The residue was purified by preparative TLC (15% EtOAc /hexanes). Colorless oil.

(*R,R*)-**L***: 14 mg, 70% yield, 91% ee; (*S,S*)-**L***: 12 mg, 60% yield, 91% ee.

SFC analysis: The ee was determined via SFC on a CHIRALPAK IG-3 column (7% *i*-PrOH in supercritical CO_2 , 2.5 mL/min); retention times for compound obtained using (*S,S*)-**L***: 5.3 min (minor), 5.8 min (major).

^1H NMR (400 MHz, CDCl_3) δ 7.35 – 7.26 (m, 2H), 7.18 (td, $J = 5.5, 2.9$ Hz, 3H), 3.68 (br, 3H), 3.54 (br, 2H), 3.32 (br, 2H), 3.13 (br, 2H), 2.59 (t, $J = 7.7$ Hz, 2H), 2.00 (s, 2H), 1.75 – 1.52 (m, 3H), 1.39 – 1.11 (m, 12H), 0.88 (t, $J = 6.8$ Hz, 3H). Broadening presumably due to rotamers.

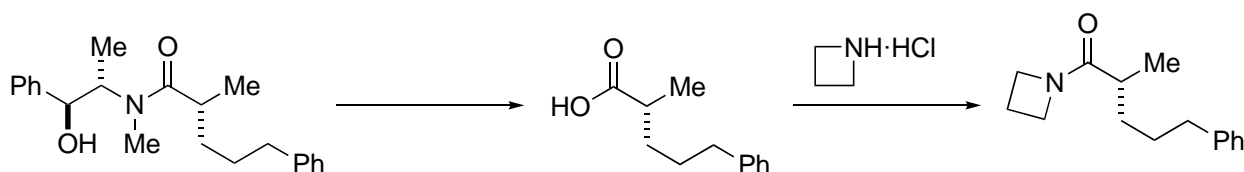
^{13}C NMR (101 MHz, CDCl_3) δ 157.1, 142.5, 128.4, 128.3, 125.7, 52.5, 51.7, 51.3, 45.4, 44.7, 42.6, 36.8, 36.5, 36.3, 31.9, 31.2, 30.9, 29.7, 28.3, 26.4, 22.7, 14.1. Rotamers detected.

FT-IR (film): 2926, 2854, 2539, 2360, 1704, 1458, 1218, 1106, 712 cm^{-1} .

HRMS (ESI-MS) m/z $[\text{M}+\text{H}]^+$ calcd for $\text{C}_{22}\text{H}_{37}\text{ClNO}_2$: 382.2508, found: 382.2509.

$[\alpha]_{\text{D}}^{22} = +3.6$ (c 1.0, CHCl_3); from (*R,R*)-**L***.

2.4.8. Assignment of Absolute Configuration

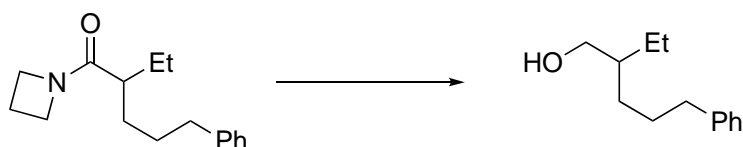


(*R*)-1-(Azetidin-1-yl)-2-methyl-5-phenylpentan-1-one ((*R*)-1). (*R*)-*N*-((1*S*,2*S*)-1-Hydroxy-1-phenylpropan-2-yl)-*N*,2-dimethyl-5-phenylpentanamide was prepared according to a literature procedure from (3-iodopropyl)benzene and *N*-((1*S*,2*S*)-1-hydroxy-1-phenylpropan-2-yl)-*N*-methylpropionamide. (8) Its conversion to the corresponding carboxylic acid, (*R*)-2-methyl-5-phenylpentanoic acid, was also accomplished via a literature procedure.^{Error! Bookmark not defined.} The title compound was synthesized according to **GP-1** from azetidine·HCl and (*R*)-2-methyl-5-phenylpentanoic acid (1.35 mmol). The product was purified by column chromatography on silica gel (30% → 60% EtOAc/hexanes). 242 mg (1.04 mmol, 77% yield, 96% ee). Pale yellow oil.

$[\alpha]_{\text{D}}^{22} = -37$ (c 1.0, CHCl_3); 96% ee, for (*R*) configuration.

Analytical data for this compound match **1** generated according to **GP-6** and **GP-7**.

This product has the same absolute configuration as **1** generated according to **GP-6** and **GP-7** from (*S,S*)-**L***, based on comparison of SFC data and optical rotation data, which are presented in Section IV.



2-Ethyl-5-phenylpentan-1-ol. The title compound was synthesized from 1-(azetidin-1-yl)-2-ethyl-5-phenylpentan-1-one (**2**) according to the following procedure.: Under nitrogen, a solution of *n*-BuLi (2.5 M solution in hexanes, 0.93 mL, 2.33 mmol) was added dropwise to a stirred solution of *i*-Pr₂NH (0.35 mL, 2.5 mmol) in THF (2.5 mL) at -78 °C. The resulting mixture was stirred at -78 °C for 10 min, and then it was warmed to 0 °C and stirred for 10 min. Next, BH₃NH₃ (76 mg, 2.5 mmol) was added in one portion, and the resulting suspension was stirred at 0 °C for 15 min, warmed to r.t., and stirred for 15 min.

Part of this suspension of LiBH₃NH₂ (1.8 mL) was transferred via syringe to another 8 mL vial (under nitrogen) that contained a stir bar. The vial was cooled to 0 °C, and then a solution of 1-(azetidin-1-yl)-2-ethyl-5-phenylpentan-1-one (**2**) (49 mg, 0.20 mmol, 1.0 equiv) in THF (2 mL) in a culture tube was added dropwise to the vial. The culture tube

was washed with THF (0.5 mL), and this wash was added to the reaction vial. The mixture was warmed to r.t. and stirred for 3 h. Then, 2 N HCl was added dropwise at 0 °C, and the resulting mixture was stirred at 0 °C for 30 min. Next, the mixture was partitioned between Et₂O and H₂O, and the aqueous phase was extracted twice with Et₂O. The combined organic phase was concentrated and purified by column chromatography on silica gel (10% → 20% EtOAc/hexanes). Colorless oil.

(*R,R*)-**L***: 32 mg, 83% yield, 89% ee; (*S,S*)-**L***: 32 mg, 83% yield, 89% ee.

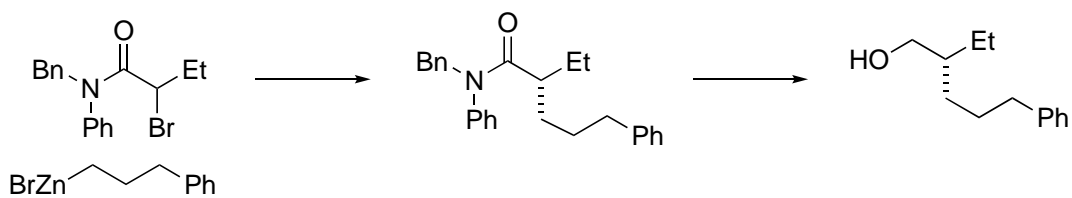
SFC analysis: The ee was determined via SFC on a CHIRALPAK ID-3 column (3% *i*-PrOH in supercritical CO₂, 2.5 mL/min); retention times for compound obtained using (*S,S*)-**L***: 10.3 min (major), 11.1 min (minor).

¹H NMR (400 MHz, CDCl₃) δ 7.33 – 7.26 (m, 2H), 7.22 – 7.13 (m, 3H), 3.55 (d, *J* = 5.1 Hz, 2H), 2.65 – 2.57 (m, 2H), 1.71 – 1.59 (m, 2H), 1.50 – 1.28 (m, 5H), 1.17 (s, 1H), 0.89 (t, *J* = 7.4 Hz, 3H).

¹³C NMR (101 MHz, CDCl₃) δ 142.6, 128.4, 128.3, 125.7, 65.2, 41.9, 36.3, 30.2, 28.8, 23.3, 11.1.

FT-IR (film): 3341, 3028, 2926, 1455, 1168, 1036, 757, 689 cm⁻¹.

[α]_D²² = -1.6 (*c* 1.0, CHCl₃); 89% ee, from (*S,S*)-**L***.



(R)-2-Ethyl-5-phenylpentan-1-ol (95% ee) was synthesized according to a literature procedure from *N*-benzyl-2-bromo-*N*-phenylbutanamide and (3-phenylpropyl)zinc(II) bromide, using (*S*)-*i*-Pr-PyBOX, followed by reduction with LiAlH₄.

$[\alpha]^{22}_{\text{D}} = -1.4$ (*c* 1.0, CHCl₃); 95% ee, (*R*)-configuration.

On the basis of comparison of SFC data and optical rotation data, this product has the same absolute configuration as 2-ethyl-5-phenylpentan-1-ol generated from the reduction of 1-(azetidin-1-yl)-2-ethyl-5-phenylpentan-1-one (**2**) synthesized using (*S,S*)-**L***.

The absolute configurations of the other α -alkylation products were assigned by analogy.

2.4.9. Mechanistic Studies

A. Spectroscopic Analysis of **Zn-2**

NMR spectroscopic analysis of **Zn-2** was performed, following recrystallization from THF at -35 °C.

^1H NMR (400 MHz, THF- d_8) δ 4.71 - 4.44 (m, 1H, $\text{H}_{\text{azetidone}}$), 4.44 - 4.18 (m, 1H, $\text{H}_{\text{azetidone}}$), 4.18 - 3.85 (m, 2H, $\text{H}_{\text{azetidone}}$), 2.32 - 1.87 (m, 3H, $\text{H}_{\text{azetidone}}$ + $\text{ZnCHCH}_2\text{CH}_3$), 1.79 (1H, $\text{ZnCHCH}_2\text{CH}_3$, detected by HSQC), 1.70 - 1.50 (m, 1H, $\text{ZnCHCH}_2\text{CH}_3$), 0.92 - 0.74 (m, 3H, $\text{ZnCHCH}_2\text{CH}_3$).

^{13}C NMR (100 MHz, THF- d_8): δ 184.3 ($\text{C}_{\text{carbonyl}}$), 68.0 (C_{THF}), 51.0 ($\text{C}_{\text{azetidone}}$), 49.4 ($\text{C}_{\text{azetidone}}$), 37.6 ($\text{ZnCHCH}_2\text{CH}_3$), 26.2 (C_{THF}), 22.2 ($\text{ZnCHCH}_2\text{CH}_3$) 17.1 ($\text{ZnCHCH}_2\text{CH}_3$), 15.4 ($\text{C}_{\text{azetidone}}$).

FT-IR (film): 1597 cm^{-1} .

Based on the separation of the diastereotopic protons of $\Delta\nu = 245$ Hz (based on HSQC) at r.t., $k < 544$ s^{-1} is estimated for the racemization of the nucleophile, corresponding to $\Delta G^\ddagger > 13.7$ kcal/mol.

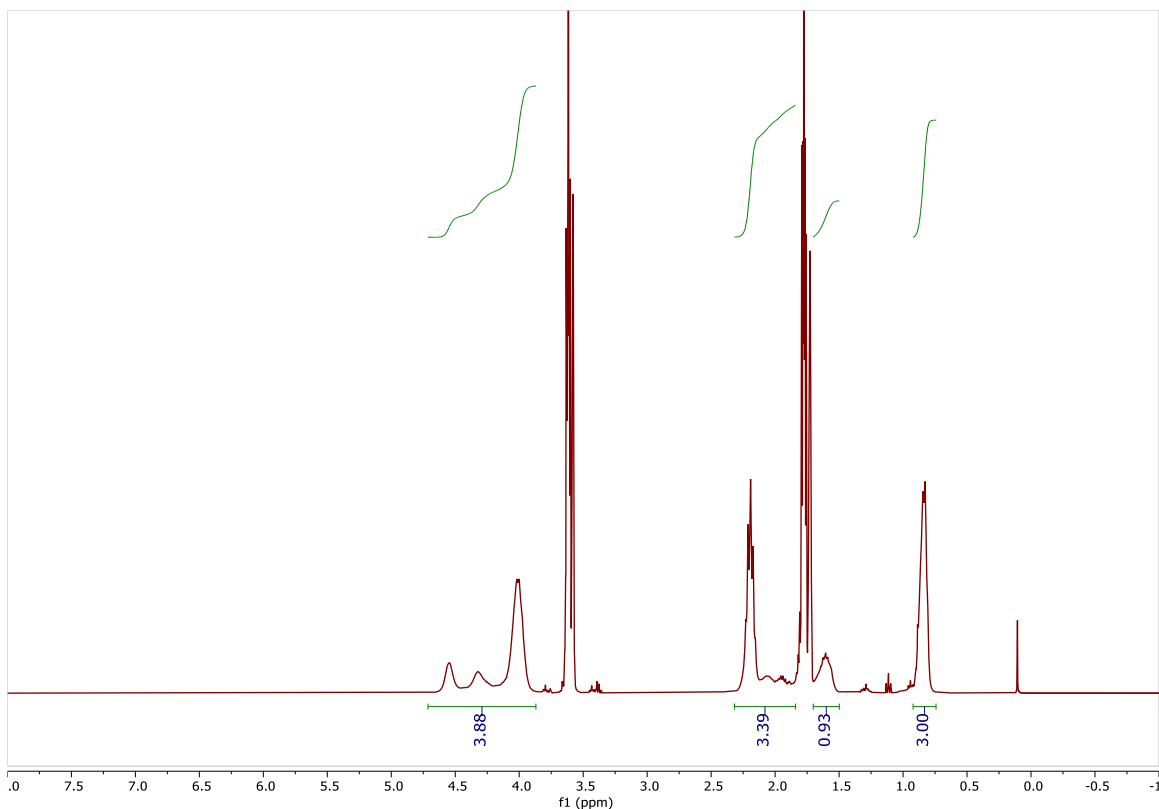


Figure S 1: ^1H NMR spectrum of **Zn-2** (400 MHz, THF- d_8 , r.t.).

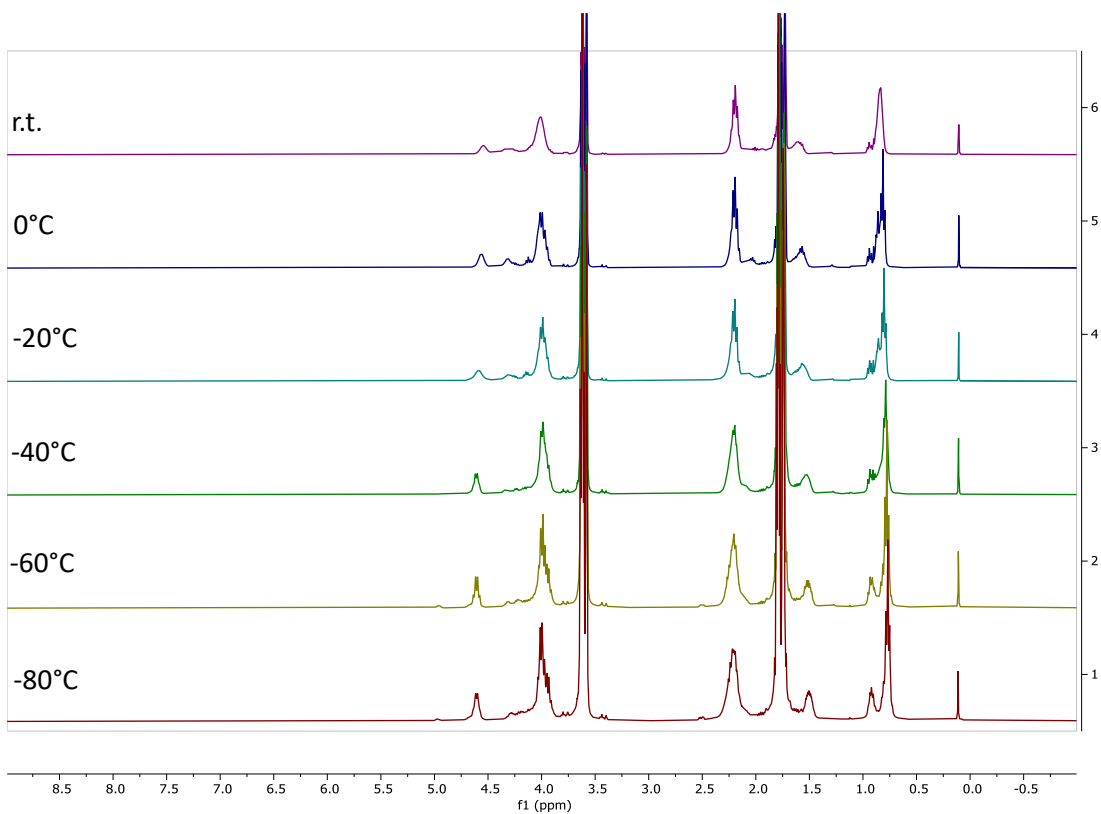


Figure S 2: Variable temperature ^1H NMR spectrum of **Zn-2** (400 MHz, THF-d_8).

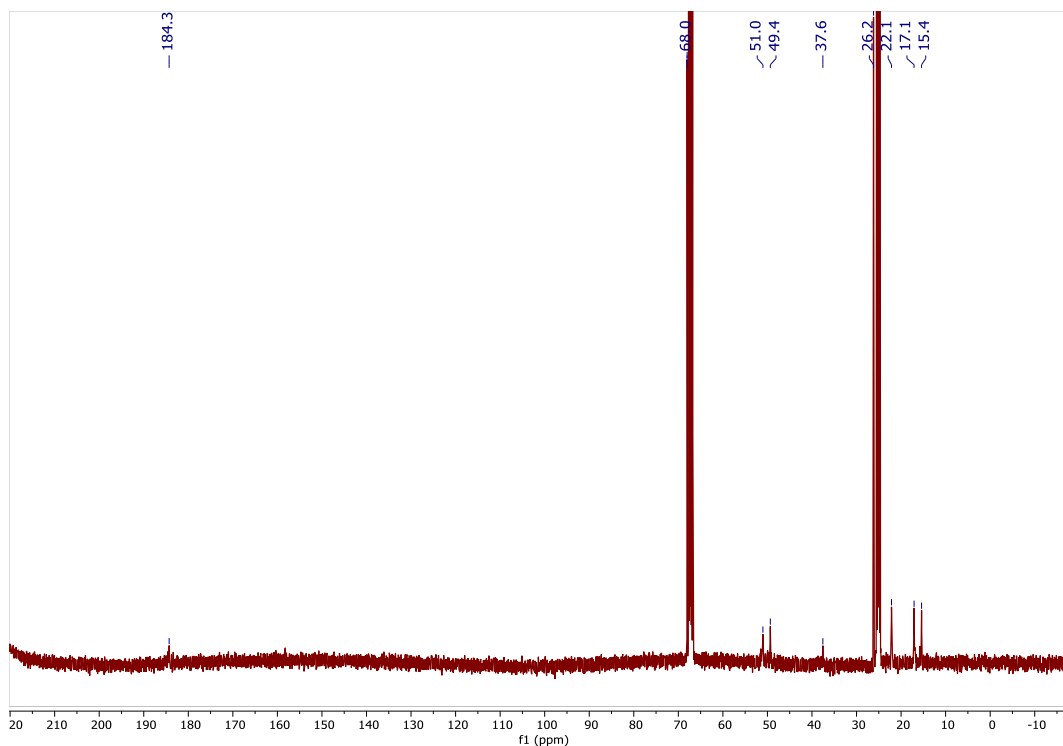


Figure S 3: ^{13}C NMR spectrum of **Zn-2** (100 MHz, THF-d_8 , r.t.).

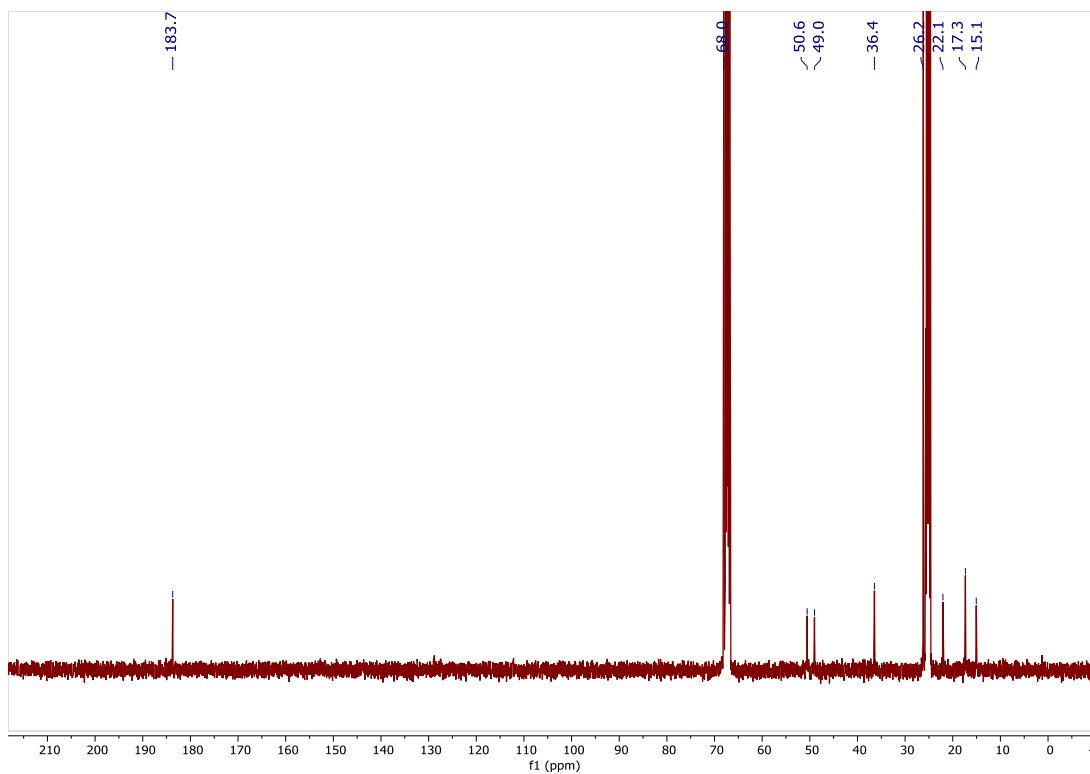


Figure S 4: ^{13}C NMR spectrum of Zn-2 (100 MHz, THF- d_8 , $-60\text{ }^\circ\text{C}$).

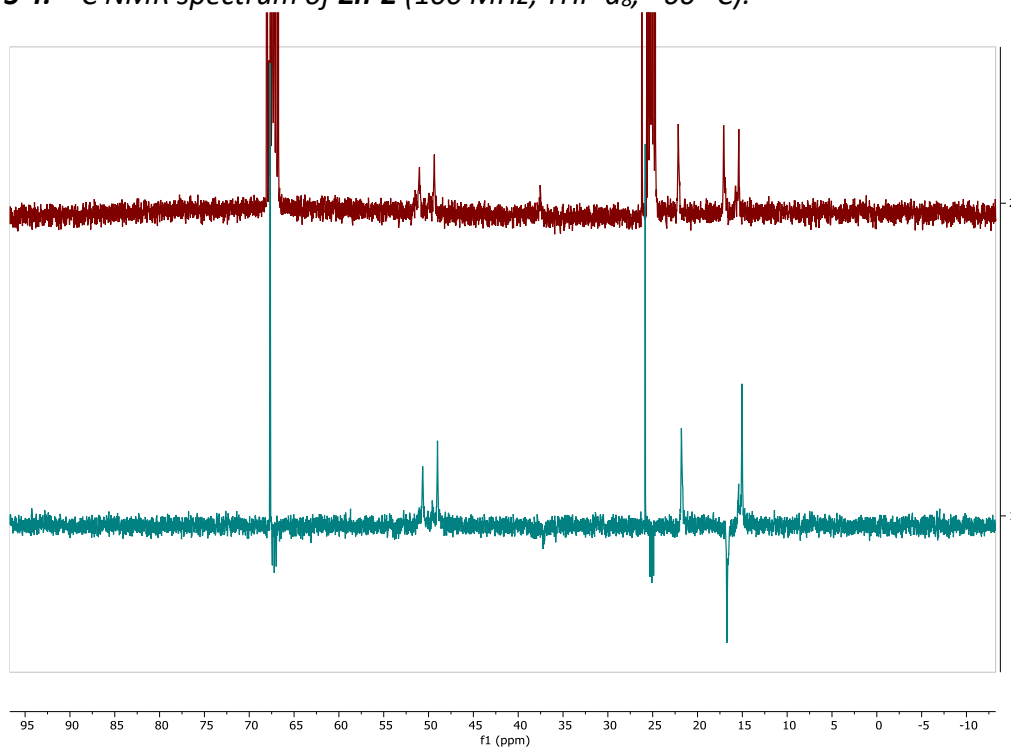


Figure S 5: ^{13}C NMR (top) and APT- ^{13}C NMR (bottom) spectra of Zn-2 (100 MHz, THF- d_8 , r.t.).

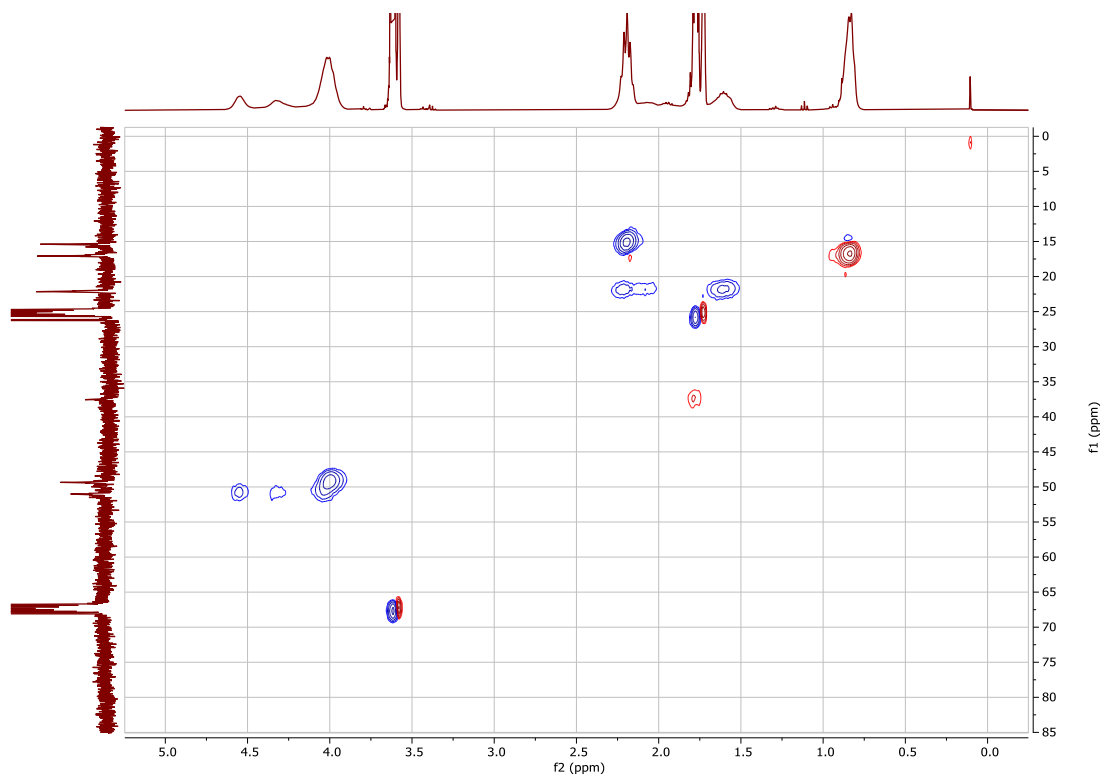


Figure S 6: HSQC NMR spectrum of **Zn-2** (THF- d_8 , r.t.).

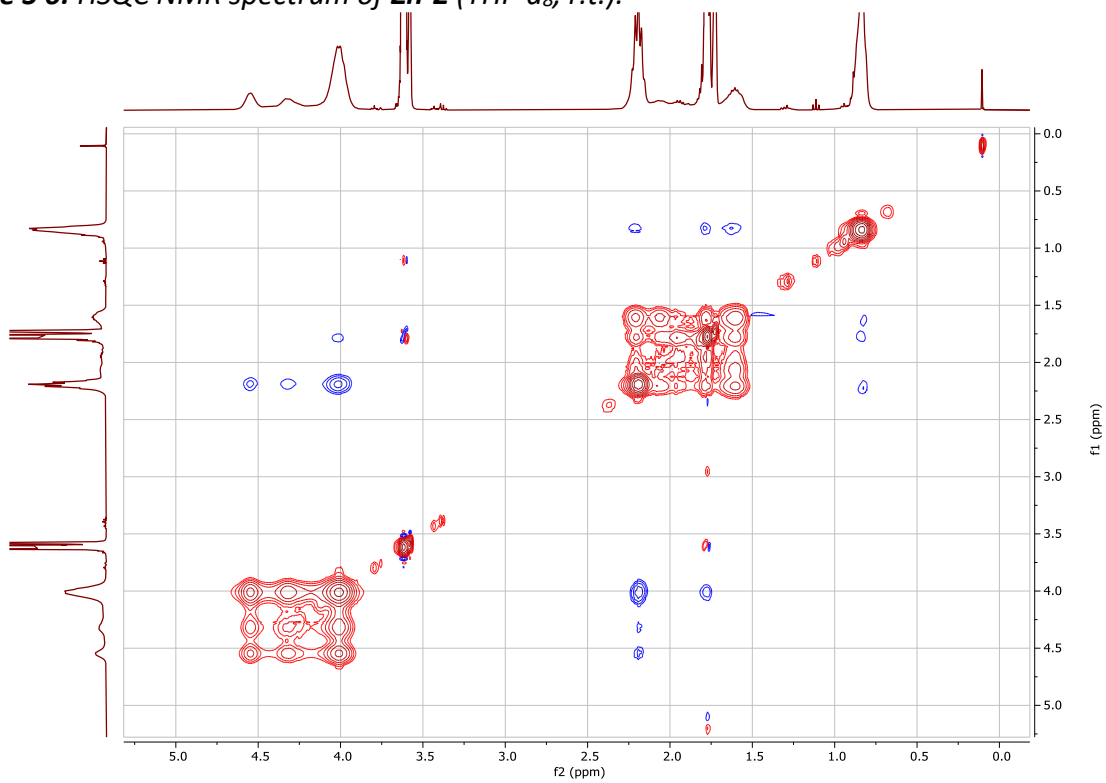
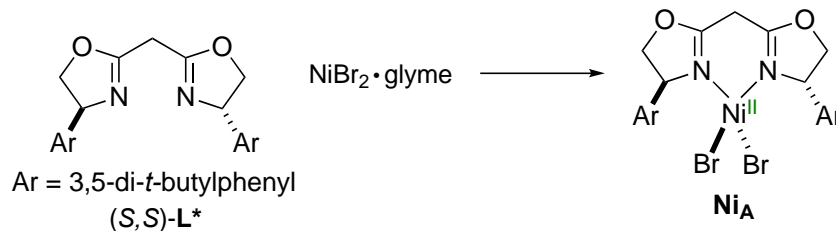


Figure S 7: NOESY NMR spectrum of **Zn-2** (THF- d_8 , r.t.).

B. Preparation of Nickel Complexes



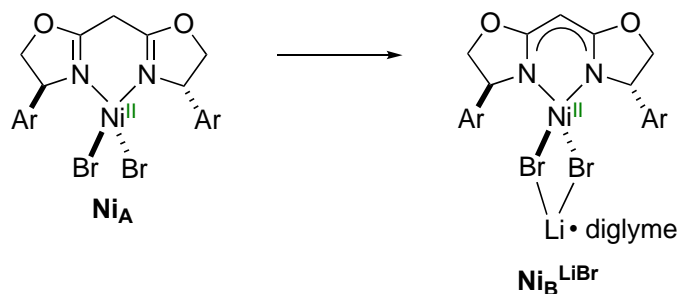
Ni_A. NiBr₂·glyme (58.0 mg, 0.188 mmol, 1.00 equiv) and (*S,S*)-L* (100 mg, 0.188 μmol, 1.00 equiv) were dissolved in THF (5 mL). The reaction mixture was stirred at r.t. overnight, and then the solvent was evaporated to give a magenta residue. The precipitate was suspended in pentane (5 mL) and then filtered. The yellow precipitate was repeatedly extracted with Et₂O to give a magenta solution. Evaporation of the solvent followed by drying under high vacuum provided 131 mg (176 μmol, 94%) of the product as a pale red solid.

¹H NMR (400 MHz, C₆D₆) δ 50.62 (br, 2H), 18.17 (br, 4H), 11.97 (br, 2H), 9.68 (br, 2H), 9.63 (br, 2H), 1.91 (br, 36H), -41.53 (br, 2H).

FT-IR (film): 2961, 2903, 2866, 1675, 1600, 1537, 1477, 1457, 1445, 1393, 1363, 1300, 1246, 1241, 1202, 1178, 1063, 1017, 899, 872, 710 cm⁻¹.

HRMS (TOF-MS) *m/z* [M+Na]⁺ calcd for C₃₅H₅₀Br₂N₂NaNiO₂: 769.1490, found: 769.1491.

Elemental analysis calcd for C₃₅H₅₀Br₂N₂NiO₂: C, 56.10; H, 6.73; N, 3.74. Found: C, 55.94; H, 6.48; N, 3.59.



$\text{Ni}_B^{\text{LiBr}}$ (100 mg, 0.133 mmol, 1.00 equiv) and diglyme (90 μL , 0.630 mmol, 4.74 equiv) were added to benzene (3 mL), and then a solution of LiHMDS (22.3 mg, 0.133 μmol , 1.00 equiv) in benzene (2 mL) was added dropwise. The mixture was stirred at r.t. for 1 h, and then the solvent was evaporated. The precipitate was triturated twice with pentane and washed with pentane (2 mL). Next, the solid was dissolved in Et_2O , providing a purple solution, which was then filtered. Evaporation of the solvent followed by drying under high vacuum provided 116 mg (0.130 mmol, 98%) of the desired product as a purple solid.

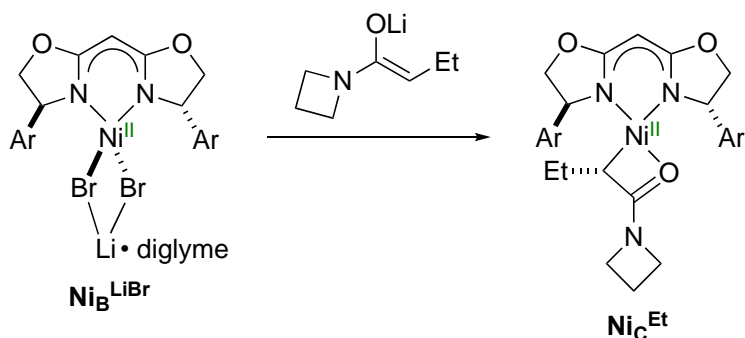
Single crystals suitable for X-ray diffraction were obtained by crystallization from Et_2O at $-35\text{ }^\circ\text{C}$.

^1H NMR (400 MHz, C_6D_6) δ 31.92 (br, 4H), 23.82 (br, 2H), 13.56 (br, 2H), 8.66 (br, 2H), 5.32 (br, 6H), 3.53 (br, 36H), -2.96 (br, 2H), -4.45 (br, 2H), -4.65 (br, 2H), -4.98 (br, 2H), -136.89 (br, 1H).

FT-IR (film): 2966, 2863, 1680, 1604, 1529, 1477, 1460, 1449, 1394, 1363, 1298, 1248, 1201, 1180, 1152, 1141, 1105, 1067, 1045, 908, 874, 740, 713, 660 cm^{-1} .

HRMS (LIFDI-MS) m/z $[\text{M}-\text{LiBr}-\text{diglyme}]^+$ calcd for $\text{C}_{35}\text{H}_{49}\text{BrN}_2\text{NiO}_2$: 666.2325, found: 666.2301.

Elemental analysis calcd for $\text{C}_{41}\text{H}_{63}\text{Br}_2\text{LiN}_2\text{NiO}_5$: C, 55.37; H, 7.14; N, 3.15. Found: C, 55.02; H, 7.05; N, 2.87.



NiC^{Et}. 1-(Azetidin-1-yl)butan-1-one (11 mg, 86 μmol , 1.5 equiv) was dissolved in THF (1 mL), and the resulting solution was cooled to $-78\text{ }^\circ\text{C}$. A solution of LDA (1.65 M in THF/heptene/ethylbenzene, 54 μL , 89 μmol , 1.6 equiv) was added dropwise, and the mixture was stirred at $-78\text{ }^\circ\text{C}$ for 30 min. **NiB^{LiBr}** (50 mg, 56 μmol , 1.0 equiv) was dissolved in toluene (3 mL) and cooled to $-78\text{ }^\circ\text{C}$, and then the solution of lithium enolate was added dropwise. After stirring at $-78\text{ }^\circ\text{C}$ for 30 min, vacuum was applied, and the solvent was evaporated while warming the mixture to r.t. After triturating twice with pentane, the resulting red solid was suspended in tetramethylsilane (4 mL) and stirred at $-78\text{ }^\circ\text{C}$ for 30 min. Filtration followed by evaporation of the solvent provided 36 mg (50 μmol , 89%) of the desired product as a brown solid.

^1H NMR (400 MHz, C_6D_6): (*S*)-**NiC**: δ 7.72 (d, $J = 1.8$ Hz, 2H, H_{Ar}), 7.53 (t, $J = 1.8$ Hz, 1H, H_{Ar}), 7.38 (t, $J = 1.8$ Hz, 1H, H_{Ar}), 7.33 (d, $J = 1.9$ Hz, 2H, H_{Ar}), 4.89 (s, 1H, H_{box}), 4.87 (t, $J = 5.7$ Hz, 1H, H_{box}), 4.15 (dd, $J = 8.7, 3.3$ Hz, 1H, H_{box}), 4.14 – 4.06 (m, 2H, H_{box}), 3.91 (dd, $J = 8.7, 7.9$ Hz, 1H, H_{box}), 3.71 (dd, $J = 7.9, 3.3$ Hz, 1H, H_{box}), 2.09 (ddq, $J = 14.6, 9.3, 7.3$ Hz, 1H, $\text{NiCHCH}_2\text{CH}_3$), 1.89 (dq, $J = 14.3, 7.2, 4.2$ Hz, 1H, $\text{NiCHCH}_2\text{CH}_3$), 1.42 (s, 18H, *t*-Bu), 1.31 (s, 18H, *t*-Bu), 1.28 (dd, $J = 9.8$ Hz, $J = 4.2$ Hz, 1H, $\text{NiCHCH}_2\text{CH}_3$), 0.95 (t, $J = 7.3$ Hz, 3H, $\text{NiCHCH}_2\text{CH}_3$) (not all resonances are identified, due to broadening).

(*R*)-**NiC**: δ 7.49 – 7.46 (m, 1H, H_{Ar}), 7.45 – 7.44 (m, 2H, H_{Ar}), 7.42 – 7.40 (m, 1H, H_{Ar}), 7.31 – 7.28 (m, 2H, H_{Ar}), 4.93 (s, 1H, H_{box}), 4.83 – 4.79 (m, 1H, H_{box}), 4.29 – 4.23 (m, 1H, H_{box}), 4.07

– 4.01 (m, 2H, H_{box}), 3.89 – 3.85 (m, 1H, H_{box}), 3.77 – 3.72 (m, 1H, H_{box}), 1.37 (s, 18H, *t*-Bu), 1.35 (s, 18H, *t*-Bu), 0.60 – 0.53 (m, 5H, NiCHCH₂CH₃+NiCHCH₂CH₃) (not all resonances are identified, due to overlap and broadening).

¹³C NMR (100 MHz, C₆D₆): (*S*)-**Nic**: δ 171.2 (C_{box}), 170.6 (C_{box}), 167.4 (C_{amid}), 151.4 (C_{aryl}), 150.7 (C_{aryl}), 146.7 (C_{aryl}), 146.1 (C_{aryl}), 121.1 (C_{aryl}), 121.0 (C_{aryl}), 120.9 (C_{aryl}), 120.8 (C_{aryl}), 75.0 (C_{box}), 73.9 (C_{box}), 69.7 (C_{box}), 66.6 (C_{box}), 55.9 (C_{box}), 48.1 (C_{azetidine}), 35.1 (C_{*t*-Bu}), 35.0 (C_{*t*-Bu}), 31.9 (C_{*t*-Bu}), 31.7 (C_{*t*-Bu}), 29.1 (NiCHCH₂CH₃), 23.7 (NiCHCH₂CH₃), 16.0 (NiCHCH₂CH₃), 15.6 (C_{azetidine}).

¹H NMR (400 MHz, THF-d₈, –50 °C): (*S*)-**Nic**: δ 7.49 (d, *J* = 1.8 Hz, 2H, H_{Ar}), 7.39 (t, *J* = 1.8 Hz, 1H, H_{Ar}), 7.32 (t, *J* = 1.8 Hz, 1H, H_{Ar}), 7.28 (d, *J* = 1.8 Hz, 2H, H_{Ar}), 4.57 (dd, *J* = 8.4, 2.7 Hz, 1H, H_{box}), 4.43 – 4.31 (m, 2H, H_{box}), 4.25 (t, *J* = 8.3 Hz, 1H, H_{box}), 4.07 (dd, *J* = 8.0, 2.7 Hz, 1H, H_{box}), 3.92 (s, 1H, H_{box}), 3.85 – 3.72 (m, 2H, H_{box}+H_{azetidine}), 3.40 – 3.28 (m, 2H, H_{azetidine}), 2.54 – 2.41 (m, 1H, H_{azetidine}), 2.15 – 2.01 (m, 1H, H_{azetidine}), 1.80 – 1.65 (m, 3H, NiCHCH₂CH₃+H_{azetidine}), 1.39 (s, 18H, *t*-Bu), 1.36 (s, 18H, *t*-Bu), 1.23 (t, *J* = 6.8 Hz, 1H, NiCHCH₂CH₃), 0.87 (t, *J* = 7.3 Hz, 3H, NiCHCH₂CH₃).

(*R*)-**Nic**: δ 7.36 (t, *J* = 1.8 Hz, 1H, H_{Ar}), 7.19 – 7.15 (m, 2H, H_{Ar}), 7.10 – 7.01 (m, 2H, H_{Ar}), 4.17 (t, *J* = 8.1 Hz, 1H, H_{Ar}), 3.97 (s, 1H, H_{box}), 3.89 (dd, *J* = 8.1, 1.9 Hz, 1H, H_{box}), 3.02 – 2.92 (m, 1H, H_{azetidine}), 2.39 – 2.29 (m, 1H, H_{azetidine}), 2.15 – 2.01 (m, 1H, H_{azetidine}), 1.35 (s, 18H, *t*-Bu), 0.26 (t, *J* = 7.1 Hz, 3H, NiCHCH₂CH₃), 0.06 – –0.06 (m, 1H, NiCHCH₂CH₃) (not all resonances are identified, due to overlap).

¹³C NMR (100 MHz, THF-d₈, –50 °C): (*S*)-**Nic**: δ 170.6 (C_{box}), 170.0 (C_{box}), 166.8 (C_{amid}), 151.2 (C_{aryl}), 150.2 (C_{aryl}), 146.9 (C_{aryl}), 146.1 (C_{aryl}), 121.2 (C_{aryl}), 121.1 (C_{aryl}), 121.0 (C_{aryl}), 120.7 (C_{aryl}), 75.3 (C_{box}), 74.0 (C_{box}), 69.6 (C_{box}), 65.9 (C_{box}), 55.0 (C_{box}), 48.5 (C_{azetidine}), 48.1 (C_{azetidine}),

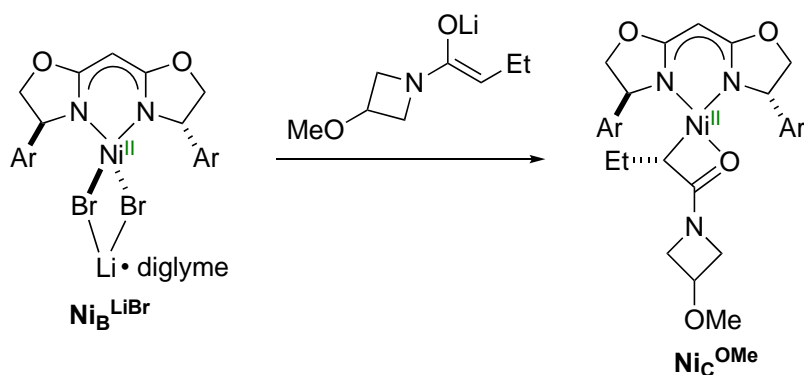
35.4 ($C_{t\text{-Bu}}$), 35.3 ($C_{t\text{-Bu}}$), 31.8 ($C_{t\text{-Bu}}$), 31.7 ($C_{t\text{-Bu}}$), 30.2 ($\text{NiCHCH}_2\text{CH}_3$), 23.7 ($\text{NiCHCH}_2\text{CH}_3$), 15.9 ($\text{NiCHCH}_2\text{CH}_3$), 15.8 ($C_{\text{azetidone}}$) (not all resonances are identified, due to overlap).

(*R*)-**Nic**: δ 170.8 (C_{box}), 170.4 (C_{box}), 167.4 (C_{amid}), 150.4 (C_{box}), 147.3 (C_{aryl}), 146.1 (C_{aryl}), 121.5 (C_{aryl}), 75.2 (C_{box}), 74.7 (C_{box}), 70.6 (C_{box}), 54.6 (C_{box}), 49.0 ($C_{\text{azetidone}}$), 47.0 ($C_{\text{azetidone}}$), 35.3 ($C_{t\text{-Bu}}$), 31.8 ($C_{t\text{-Bu}}$), 31.7 ($C_{t\text{-Bu}}$), 30.3 ($\text{NiCHCH}_2\text{CH}_3$), 23.4 ($\text{NiCHCH}_2\text{CH}_3$), 16.6 ($\text{NiCHCH}_2\text{CH}_3$), 15.7 ($C_{\text{azetidone}}$) (not all resonances are identified, due to overlap).

HRMS (TOF-MS) m/z [$M + H$] $^+$ calcd for $C_{42}H_{62}N_3NiO_3$: 714.4145, found: 714.4138.

Elemental analysis calcd for $C_{42}H_{61}N_3NiO_3$: C, 70.59; H, 8.60; N, 5.88. Found: C, 70.56; H, 8.43; N, 5.89.

FT-IR (film): 2963, 2863, 1653, 1613, 1598, 1534, 1477, 1460, 1448, 1393, 1381, 1362, 1332, 1302, 1248, 1221, 1213, 1151, 1142, 1068, 1045, 908, 876, 769, 762, 735, 713, 649 cm^{-1} .



Ni^C^{OMe}. 1-(3-Methoxyazetid-1-yl)butan-1-one (13.8 mg, 88 μmol , 1.6 equiv) was dissolved THF (1 mL), and the resulting solution was cooled to -78 $^{\circ}\text{C}$. A solution of LDA (1.65 M in THF/heptane/ethylbenzene, 53 μL , 88 μmol , 1.6 equiv) was added dropwise, and the resulting mixture was stirred at -78 $^{\circ}\text{C}$ for 30 min. **Ni^B^{LiBr}** (50 mg, 56 μmol , 1.0 equiv) was dissolved in toluene (3 mL) and cooled to -78 $^{\circ}\text{C}$, and then the solution of lithium enolate was added dropwise.

After stirring at $-78\text{ }^{\circ}\text{C}$ for 30 min, vacuum was applied, and the solvent was evaporated while warming the mixture to r.t. After triturating twice with pentane, the red solid was suspended in tetramethylsilane (4 mL) and stirred at $-78\text{ }^{\circ}\text{C}$ for 30 min. Filtration followed by evaporation of the solvent provided a brown solid, which was dissolved in pentane and crystallized at $-35\text{ }^{\circ}\text{C}$ to provide 26 mg (0.035 mmol, 62%) of the desired product as a red crystalline solid.

Single crystals suitable for X-ray diffraction were obtained by crystallization from pentane at $-78\text{ }^{\circ}\text{C}$.

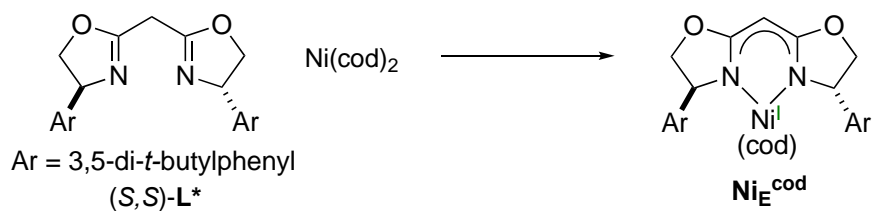
^1H NMR (400 MHz, C_6D_6): (*S*)-**NiC^{OMe}**: δ 7.73 (d, $J = 1.9$ Hz, 2H, H_{Ar}), 7.53 (t, $J = 1.8$ Hz, 1H, H_{Ar}), 7.42 (t, $J = 1.8$ Hz, 1H, H_{Ar}), 7.35 (d, $J = 1.9$ Hz, 2H, H_{Ar}), 4.90 (s, 1H, H_{box}), 4.86 (dd, $J = 7.9, 3.6$ Hz, 1H, H_{box}), 4.15 (dd, $J = 8.7, 3.3$ Hz, 1H, H_{box}), 4.10 (dd, $J = 8.0, 6.7$ Hz, 1H, H_{box}), 4.08 (d, $J = 2.5$ Hz, 1H, H_{box}), 3.91 (dd, $J = 8.7, 7.9$ Hz, 1H, H_{box}), 3.72 (dd, $J = 7.9, 3.3$ Hz, 1H, H_{box}), 3.53 (br, 2H, $\text{H}_{\text{azetidine}}$), 3.44 (br, 2H, $\text{H}_{\text{azetidine}}$), 2.72 (s, 3H, OMe), 2.13 – 1.99 (m, 1H, $\text{NiCHCH}_2\text{CH}_3$), 1.90 – 1.75 (m, 1H, $\text{NiCHCH}_2\text{CH}_3$), 1.42 (s, 18H, *t*-Bu), 1.35 (s, 18H, *t*-Bu), 0.94 (t, $J = 7.3$ Hz, 3H, $\text{NiCHCH}_2\text{CH}_3$) (not all resonances are identified, due to broadening and overlap).

(*R*)-**NiC^{OMe}**: δ 7.52 (t, $J = 1.8$ Hz, 1H, H_{Ar}), 7.47 (t, $J = 2.0$ Hz, 1H, H_{Ar}), 7.43 (br, 2H, H_{Ar}), 7.29 (br, 2H, H_{Ar}), 4.94 (s, 1H, H_{box}), 4.81 (dd, $J = 8.3, 2.3$ Hz, 1H, H_{box}), 4.22 (dd, $J = 7.9, 2.4$ Hz, 1H, H_{box}), 4.05 (dd, $J = 9.0, 8.0$ Hz, 1H, H_{box}), 3.92 – 3.85 (m, 2H, H_{box}), 3.76 – 3.70 (m, 1H, H_{box}), 2.81 (s, 3H, OMe), 1.42 (s, 18H, *t*-Bu), 1.37 (s, 18H, *t*-Bu), 0.58 – 0.50 (m, 5H, $\text{NiCHCH}_2\text{CH}_3 + \text{NiCHCH}_2\text{CH}_3$) (not all resonances are identified, due to broadening and overlap).

^{13}C NMR (100 MHz, C_6D_6): (*S*)-**NiC^{OMe}**: δ 171.2 (C_{box}), 170.7 (C_{box}), 167.6 (C_{amid}), 151.4 (C_{aryl}), 150.7 (C_{aryl}), 146.6 (C_{aryl}), 146.1 (C_{aryl}), 121.1 (C_{aryl}), 121.0 (C_{aryl}), 120.9 (C_{aryl}), 120.8 (C_{aryl}), 75.0 (C_{box}), 73.8 (C_{box}), 69.6 (C_{box}), 69.4 ($\text{C}_{\text{azetidine}}$), 66.6 (C_{box}), 55.9 (C_{box}), 55.5 (OMe),

55.1 ($C_{\text{azetidone}}$), 35.11 ($C_{t\text{-Bu}}$), 35.06 ($C_{t\text{-Bu}}$), 31.9 ($C_{t\text{-Bu}}$), 31.8 ($C_{t\text{-Bu}}$), 29.5 ($\text{NiCHCH}_2\text{CH}_3$), 23.4 ($\text{NiCHCH}_2\text{CH}_3$), 15.9 ($\text{NiCHCH}_2\text{CH}_3$) (not all resonances are identified, due to overlap).

HRMS (TOF-MS) m/z $[\text{M} + \text{H}]^+$ calcd for $\text{C}_{43}\text{H}_{64}\text{N}_3\text{NiO}_4$: 744.4250, found: 744.4236.



NiE^{cod}. Ni(cod)₂ (27.4 mg, 0.100 mmol, 1.0 equiv) and (S,S)-L* (53.0 mg, 0.100 mmol, 1.0 equiv) were dissolved in THF (4 mL) and cooled to $-35\text{ }^\circ\text{C}$. A precooled suspension of FcPF₆ (33.0 mg, 0.100 mmol, 1.0 equiv) in THF (3 mL) was added dropwise, and the resulting suspension was stirred at r.t. for 1 h. Next, the solvent was evaporated under high vacuum, and the residue was washed with pentane and extracted with THF. The resulting solution was filtered, the solvent was evaporated, and the residue was triturated with pentane, leaving a brown solid. The solid was dissolved in THF (4 mL), and the solution was cooled to $-35\text{ }^\circ\text{C}$. A precooled solution of LiHMDS (16.7 mg, 0.100 mmol, 1.0 equiv) in THF (3 mL) was added dropwise, and the resulting solution was stirred at r.t. for 1 h. After evaporation of the solvent, the residue was triturated and extracted with pentane. The yellow solution was filtered, and the solvent was evaporated. The yellow solid was re-dissolved in pentane (2 mL), the resulting solution was filtered, and the volume of the solution was reduced to $\sim 0.5\text{ mL}$ by evaporation under high vacuum. Crystallization at $-80\text{ }^\circ\text{C}$ provided 35 mg (0.046 mmol, 46%) of the desired product as a yellow crystalline solid.

Single crystals suitable for X-ray diffraction were obtained by crystallization from pentane at $-80\text{ }^{\circ}\text{C}$.

Elemental analysis calcd for $\text{C}_{43}\text{H}_{61}\text{N}_2\text{NiO}_2$: C, 74.13; H, 8.83; N, 4.02. Found: C, 74.59; H, 8.68; N, 3.82.

C. NMR and EPR Spectra of Nickel Complexes

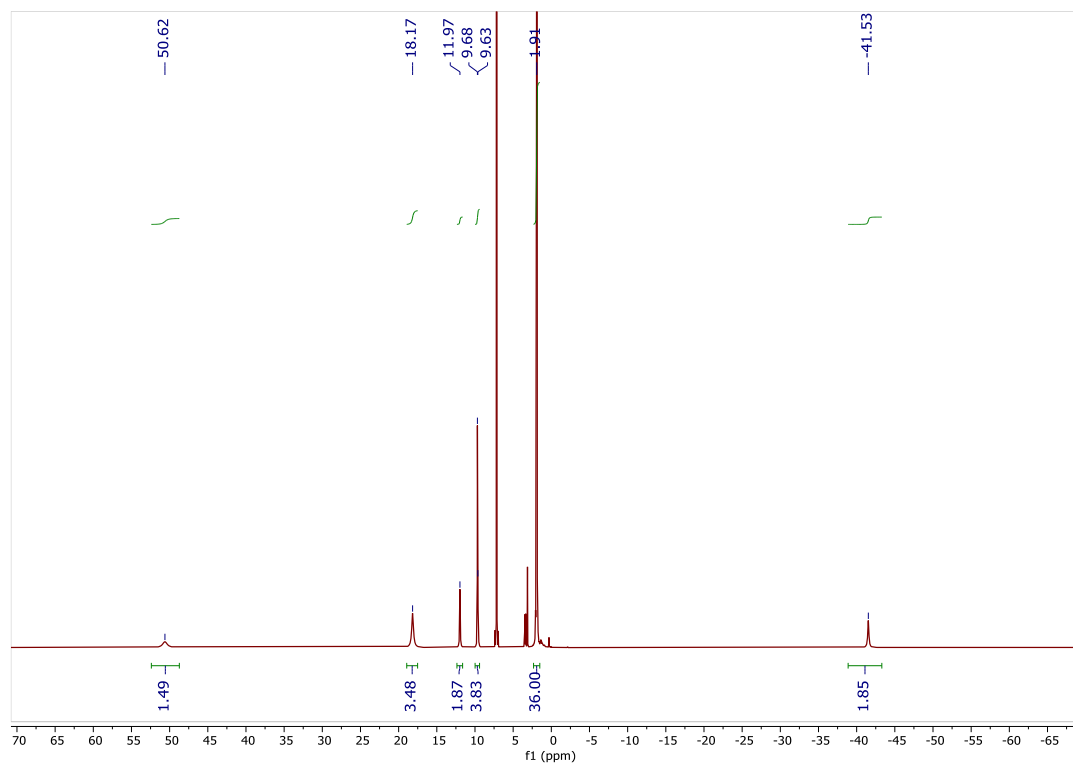


Figure S 8: ^1H NMR spectrum of Ni_A (400 MHz, C_6D_6 , r.t.).

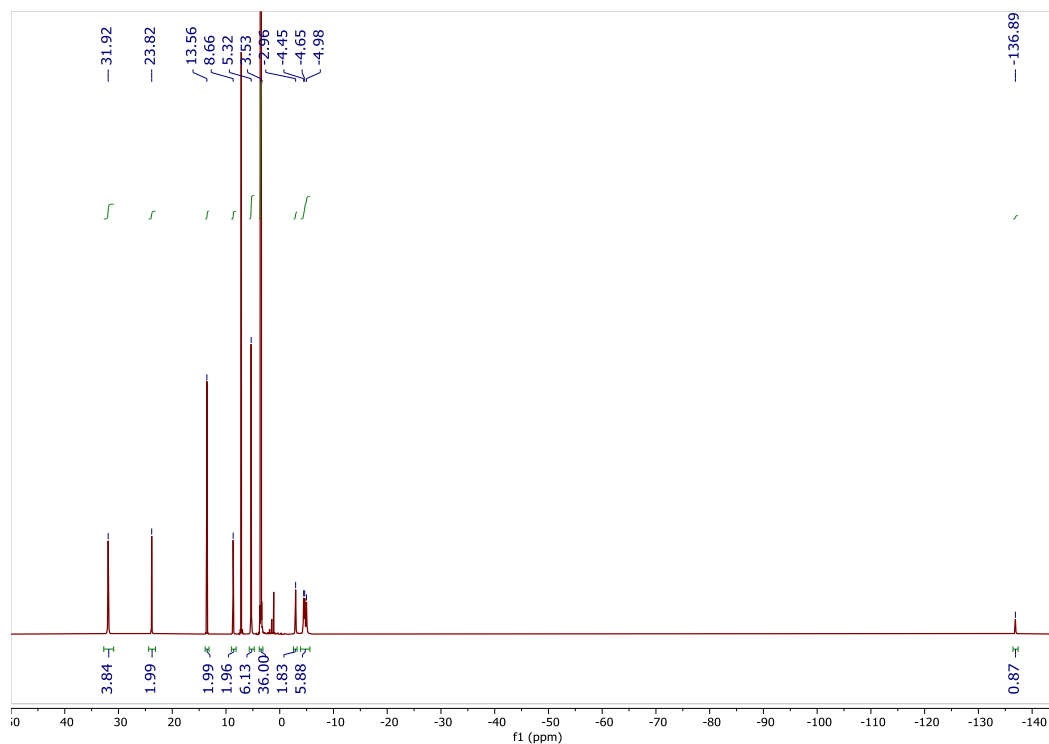


Figure S 9: ^1H NMR spectrum of $\text{Ni}_B^{\text{LiBr}}$ (400 MHz, C_6D_6 , r.t.).

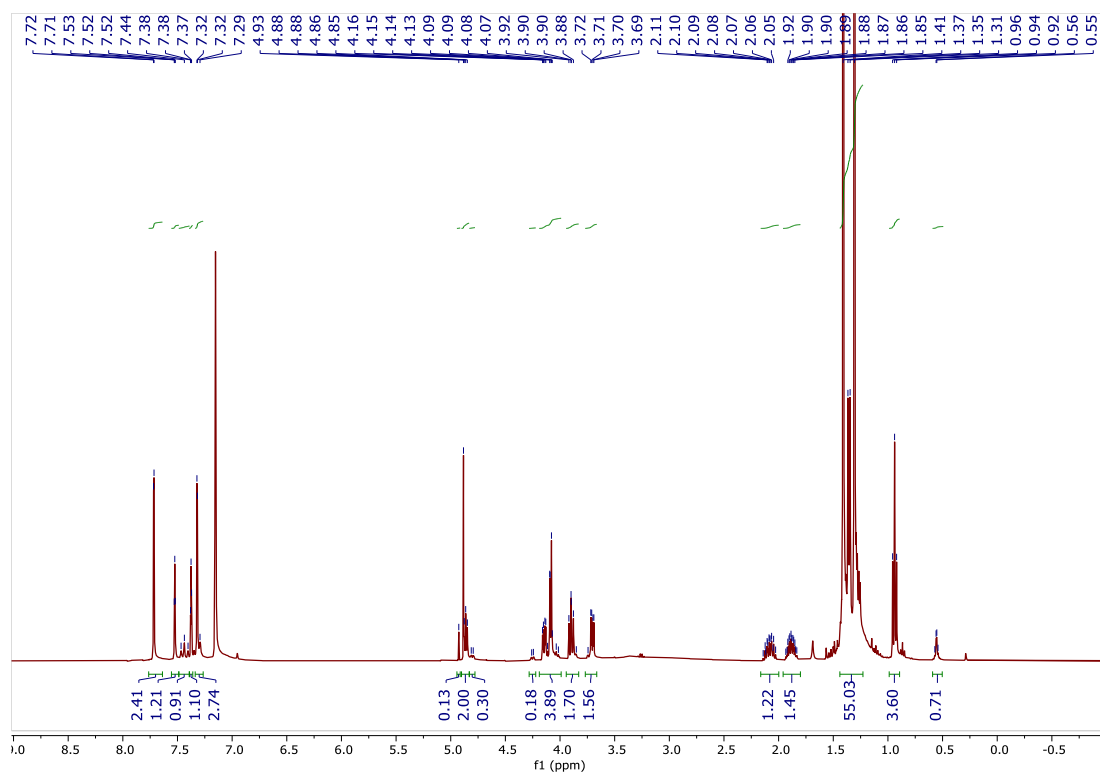


Figure S 10: ^1H NMR spectrum of Ni_C^{Et} (400 MHz, C_6D_6 , r.t.).

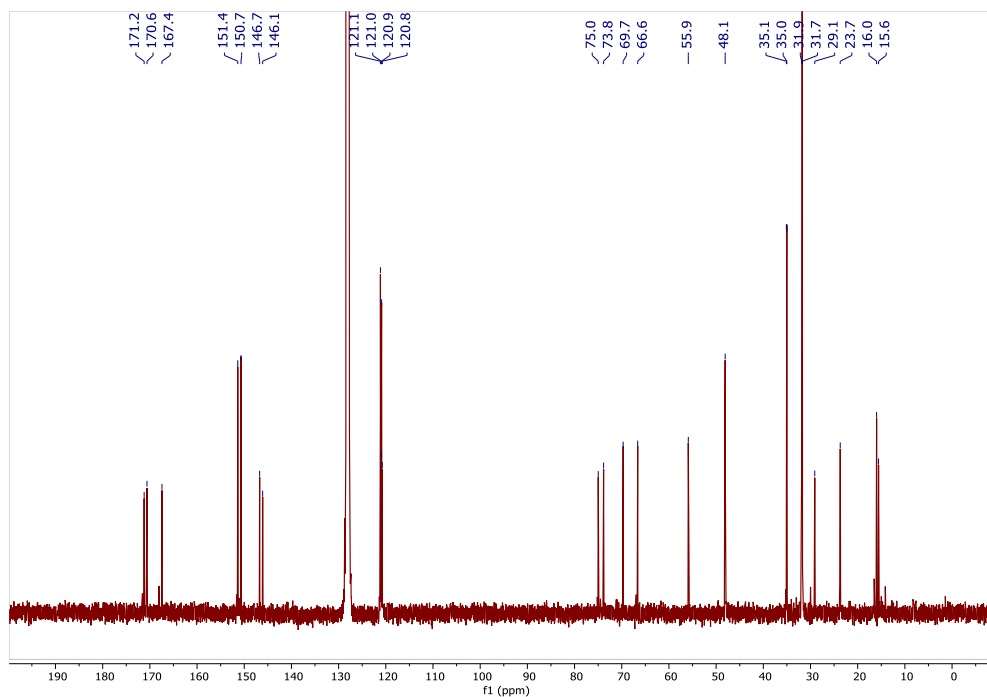


Figure S 11: ^{13}C NMR spectrum of NiC^{Et} (100 MHz, C_6D_6 , r.t.).

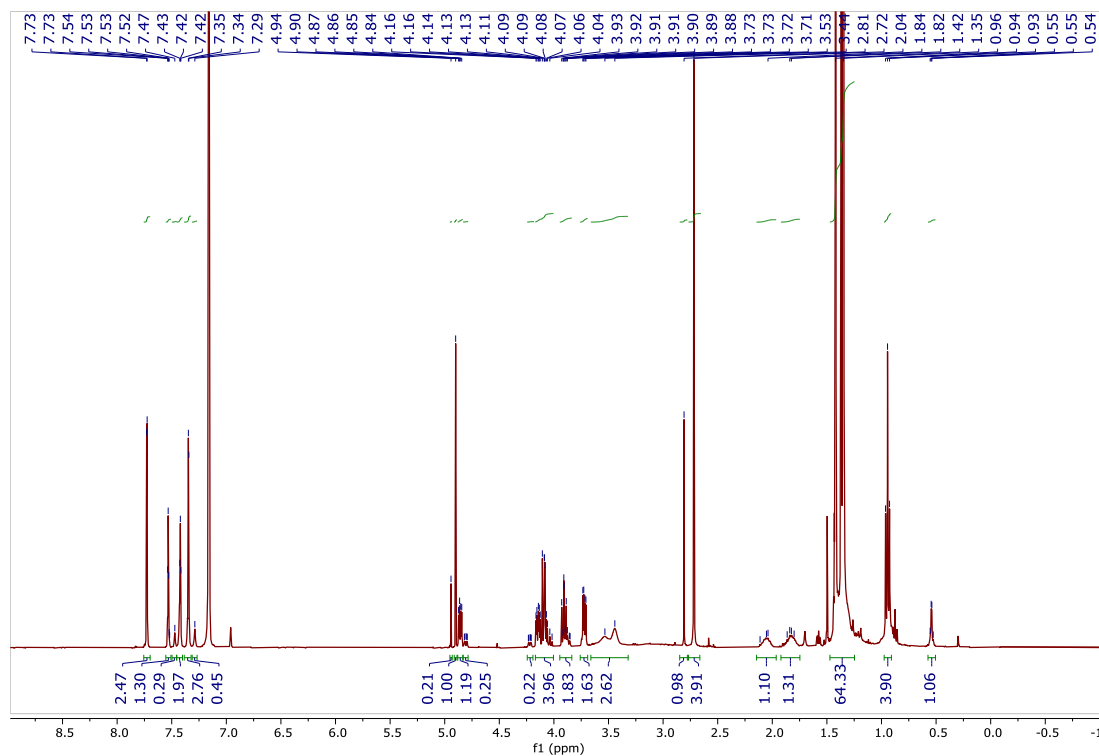


Figure S 12: ^1H NMR spectrum of NiC^{OMe} (400 MHz, C_6D_6 , r.t.).

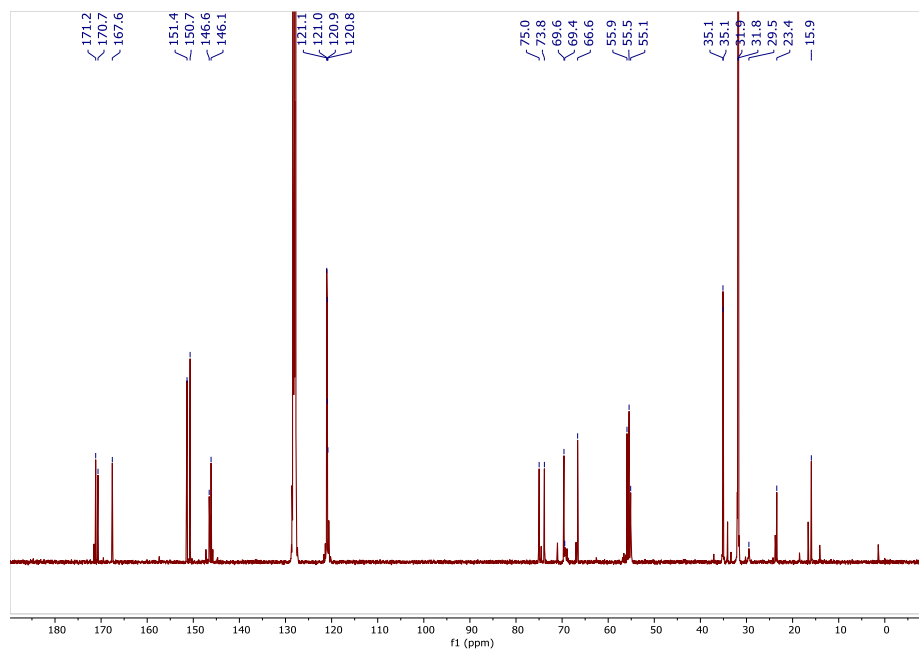


Figure S 13: ^{13}C NMR spectrum of $\text{Ni}_\text{C}^{\text{OMe}}$ (100 MHz, THF-d_8 , r.t.).

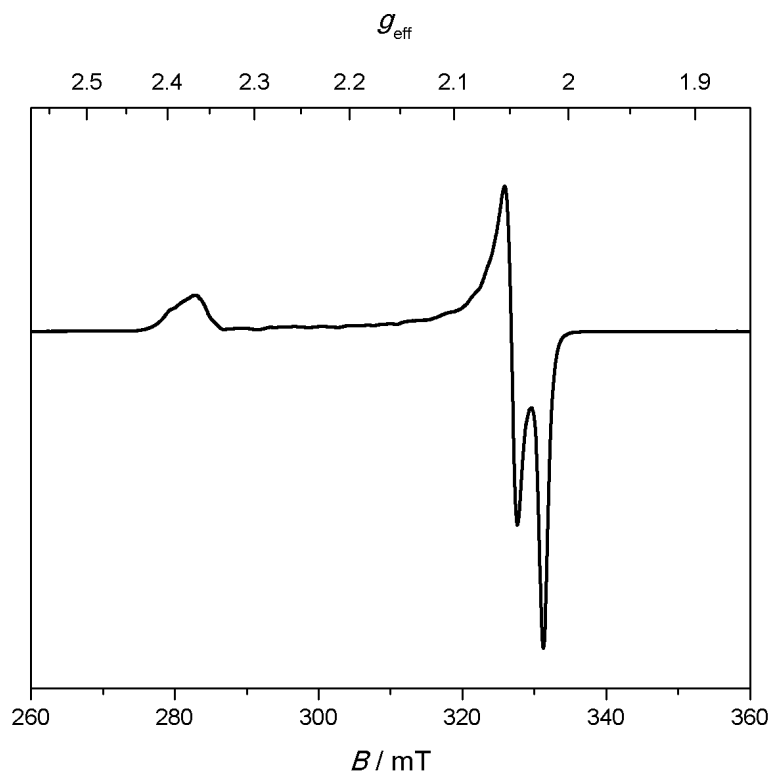
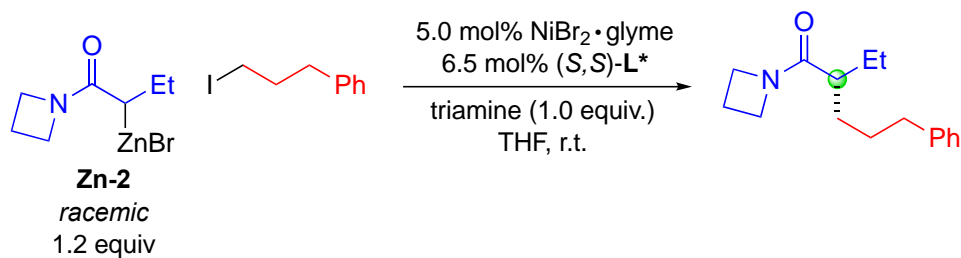


Figure S 14: X-band EPR spectrum of $\text{Ni}_\text{E}^{\text{cod}}$ in frozen toluene solution (77 K, 9.370094 GHz).

D. Monitoring a Catalyzed Reaction via UV-vis Spectroscopy



In a glovebox, NiBr₂·glyme (9.3 mg, 30 μmol) and **L*** (20.7 mg, 39.0 μmol) were added to a 4 mL vial equipped with a stir bar. THF (3.0 mL) was added, and the vial was capped and stirred at r.t. for 45 min. **Zn-2** (82 mg, 0.24 mmol, 1.2 equiv) was added to a 3 mL cuvette that contained a stir bar, and THF (2 mL) was added. The cuvette was closed with a septum cap, and then 1.0 mL of the solution of the catalyst (10 μmol, 5.0 mol% NiBr₂·glyme; 13.0 μmol, 6.5 mol% **L***) was added via syringe into the cuvette that contained the solution of nucleophile. The mixture was stirred vigorously for 3 min, leading to an orange suspension. Triamine (47 μL, 0.19 mmol, 1.0 equiv) was added via syringe, and then the electrophile (32 μL, 0.20 mmol, 1.0 equiv) was immediately added via syringe. The cuvette was immediately removed from the glovebox, and the reaction was monitored by UV-vis spectroscopy. After 20 h the reaction was quenched by the addition of ethanol (0.5 mL). The yield of the reaction was determined to be 84% (GC analysis) and the ee was determined to be 89% (SFC analysis).

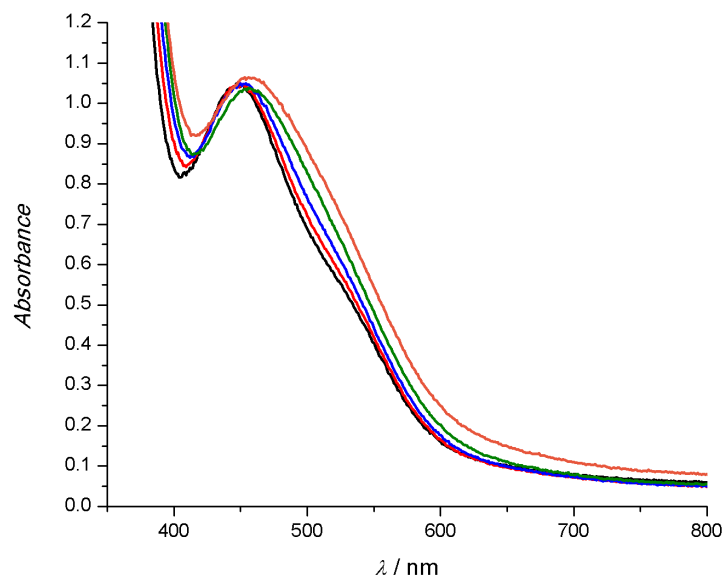


Figure S 15: UV-vis spectra (THF, r.t.) of a coupling reaction in progress, showing spectra obtained after 5 min (black), 15 min (red), 30 min (blue), 2 h (green), and 8 h (orange).

Comparison of a UV-vis spectrum obtained during a coupling reaction in progress with a spectrum obtained for isolated Ni^{Et} is consistent with Ni^{Et} being the predominant resting state during catalysis.

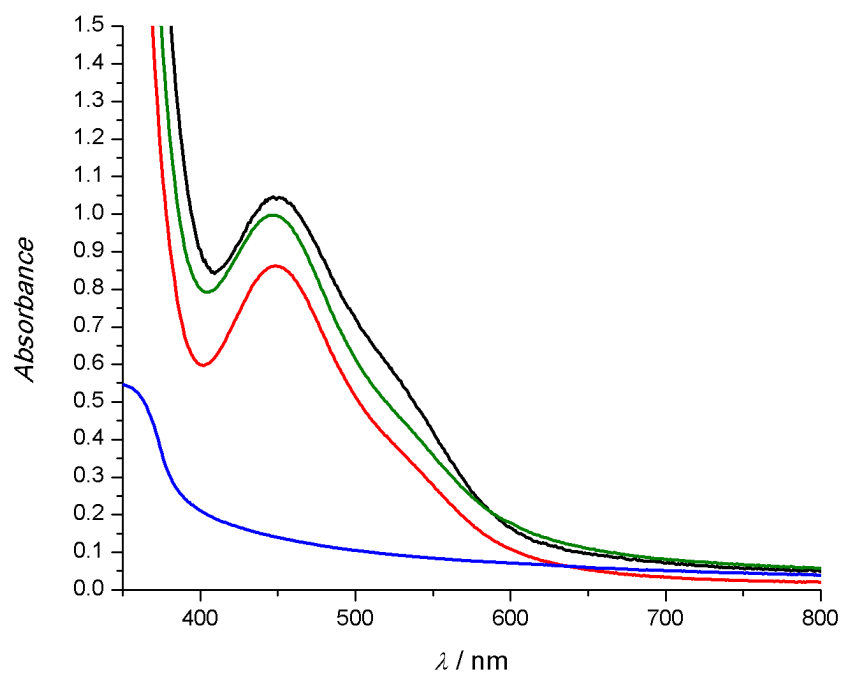


Figure S 16: UV-vis spectra (THF, r.t.) of: a coupling reaction in progress after 15 min (black), Ni_c^{Et} (red), **Zn-2** in the presence of triamine (blue), addition of the spectrum of Ni_c^{Et} to the spectrum of **Zn-2** in the presence of triamine (green). The concentration of Ni_c^{Et} , **Zn-2**, and triamine are identical to the coupling reaction.

E. Structures of $\text{Ni}_B^{\text{LiBr}}$ and Ni_B in Solution

The UV-vis spectra of isolated $\text{Ni}_B^{\text{LiBr}}$ and of Ni_B (generated from the reaction of Ni_A with **Zn-2**) show similar features. To obtain additional information about the structure of $\text{Ni}_B^{\text{LiBr}}$ and Ni_B in solution, the UV-vis spectra of $\text{Ni}_B^{\text{LiBr}}$ (1.5 mM) were recorded under several conditions. Solution-dependent structures of a related anionic Ni(II) dihalide complex have been reported. (32)

The UV-vis spectra of isolated $\text{Ni}_B^{\text{LiBr}}$ in DCM and in benzene are similar, whereas the spectrum obtained in THF shows a significantly blue-shifted absorption maxima. The spectrum obtained from a solid sample shows absorption maxima at similar positions compared to the spectra obtained in DCM or benzene (although a relatively low absorption at 530 nm is observed, compared to the solution spectra).

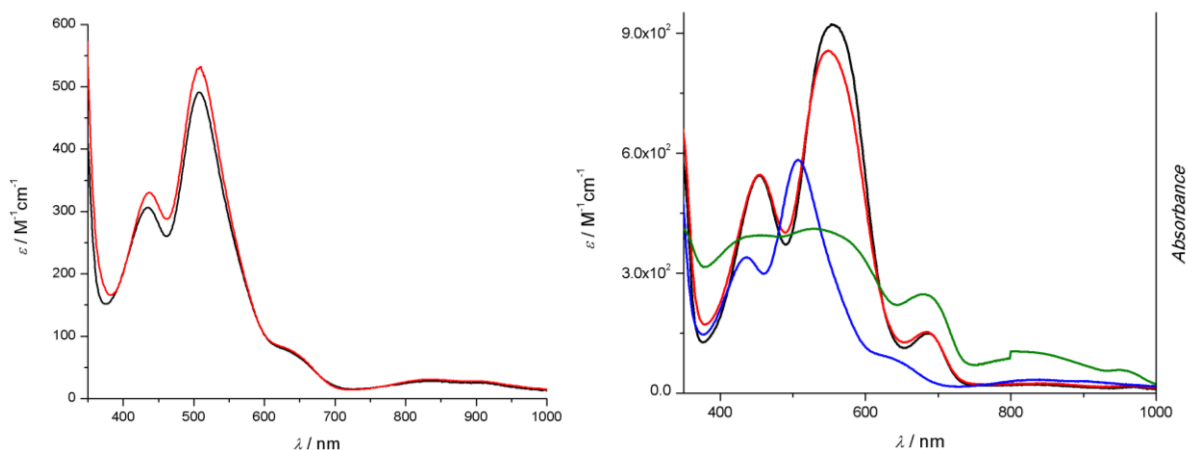


Figure S 17: (left) UV-vis spectra (THF, r.t.) of $\text{Ni}_B^{\text{LiBr}}$ (black) and $\text{Ni}_A + \text{Zn-2}$ (1 equiv) (red). (right) UV-vis spectra (r.t.) of $\text{Ni}_B^{\text{LiBr}}$ in benzene (black), DCM (red), THF (blue), and solid state (green). Solution spectra are plotted as ϵ over l , solid state spectra are plotted as A over l .

Addition of THF to a solution of $\text{Ni}_B^{\text{LiBr}}$ in DCM results in a decrease in absorbance and a blue-shift of the absorption maxima, resulting in a spectrum similar to that obtained for $\text{Ni}_B^{\text{LiBr}}$ in THF. On the other hand, addition of LiBr to $\text{Ni}_B^{\text{LiBr}}$ in THF results in a slight increase in absorbance and a red-shift of the absorption. These results are consistent with the dissociation of LiBr from $\text{Ni}_B^{\text{LiBr}}$ in THF and the formation of Ni(II) monobromide Ni_B .

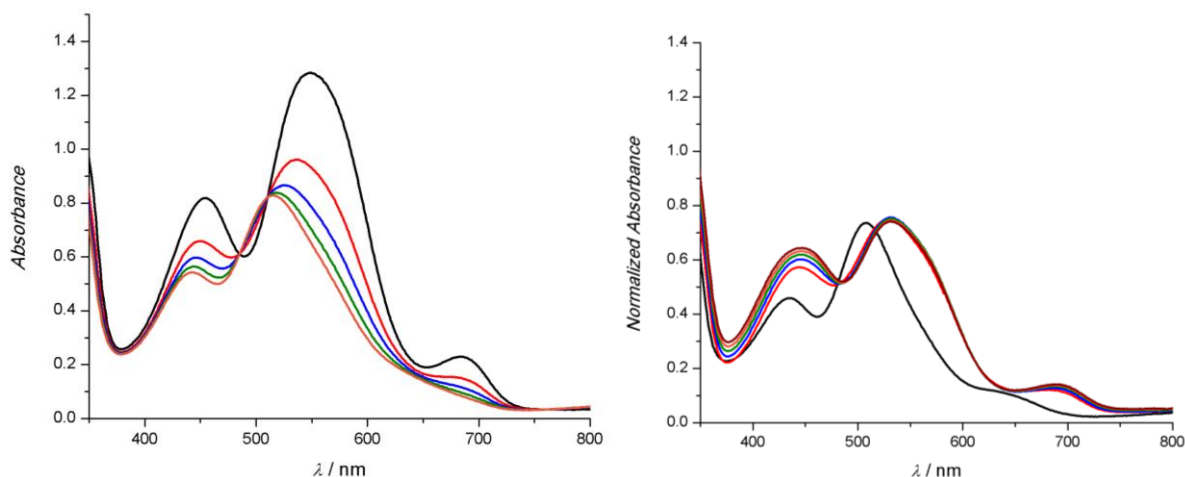


Figure S 18: (left) UV-vis spectra (DCM, r.t.) of $\text{Ni}_B^{\text{LiBr}}$ (black) in the presence of 50 equiv THF (red), 100 equiv THF (blue), 150 equiv THF (green), and 200 equiv THF (orange). (right) UV-vis spectra (THF, r.t.) of $\text{Ni}_B^{\text{LiBr}}$ (black) in the presence of 100 equiv LiBr (red), 200 equiv LiBr (blue), 300 equiv LiBr (green), 400 equiv LiBr (orange), and 500 equiv LiBr (brown). The absorbance is corrected for the difference in volume between individual measurements.

F. Addition of Zn-2 to NiBr₂·glyme/L* and to Ni_A

In a glovebox, NiBr₂·glyme (9.3 mg, 30 μmol) and chiral ligand L* (20.7 mg, 39.0 μmol) were added to a 4 mL vial equipped with a stir bar. THF (3.0 mL) was added, the vial was capped, and the reaction mixture was stirred at r.t. for 45 min. A portion of this solution of catalyst (1.0 mL; 10 μmol, 1.0 equiv NiBr₂·glyme; 13.0 μmol, 1.3 equiv L*) was transferred to a UV-vis cuvette, and then THF (2.0 mL) was added. The cuvette was capped and then removed from the glovebox, and then the solution was analyzed via UV-vis spectroscopy. Next, the sample was brought back into the glovebox and Zn-2 (3.4 mg, 9.9 μmol, 1.0 equiv) was added. The cuvette was capped and then removed from the glovebox, and then the solution was analyzed via UV-vis spectroscopy. The addition of Zn-2 was repeated twice, and then Zn-2 (71.9 mg, 0.21 mmol, 21 equiv) and triamine (47 μL, 0.20 mmol, 20 equiv) were added, with each addition being followed by UV-vis spectroscopy.

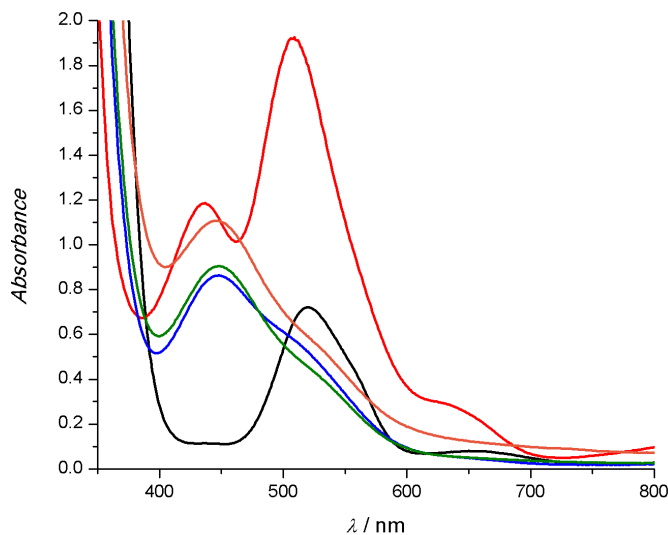


Figure S 19: UV-vis spectra (THF, r.t.) of the pre-catalyst solution in the presence of varying amounts of Zn-2 and triamine: catalyst solution (black), + 1.0 equiv Zn-2 (red), + 2.0 equiv Zn-2 (blue), + 3.0 equiv Zn-2 (green), + 24 equiv Zn-2 and 20 equiv triamine (orange).

In a glovebox, **Ni_A** (7.5 mg, 10 μ mol, 1.0 equiv) and THF (3.0 mL) were added to a UV-vis cuvette. The cuvette was capped and then removed from the glovebox, and then the solution was analyzed via UV-vis spectroscopy. The sample was brought back into the glovebox, and **Zn-2** (3.4 mg, 9.9 μ mol, 1.0 equiv) was added. The cuvette was capped and then removed from the glovebox, and then the solution was analyzed via UV-vis spectroscopy. The addition of **Zn-2** was repeated twice, and then **Zn-2** (71.9 mg, 0.21 mmol, 21 equiv) and triamine (47 μ L, 0.20 mmol, 20 equiv) were added, with each addition being followed by UV-vis spectroscopy.

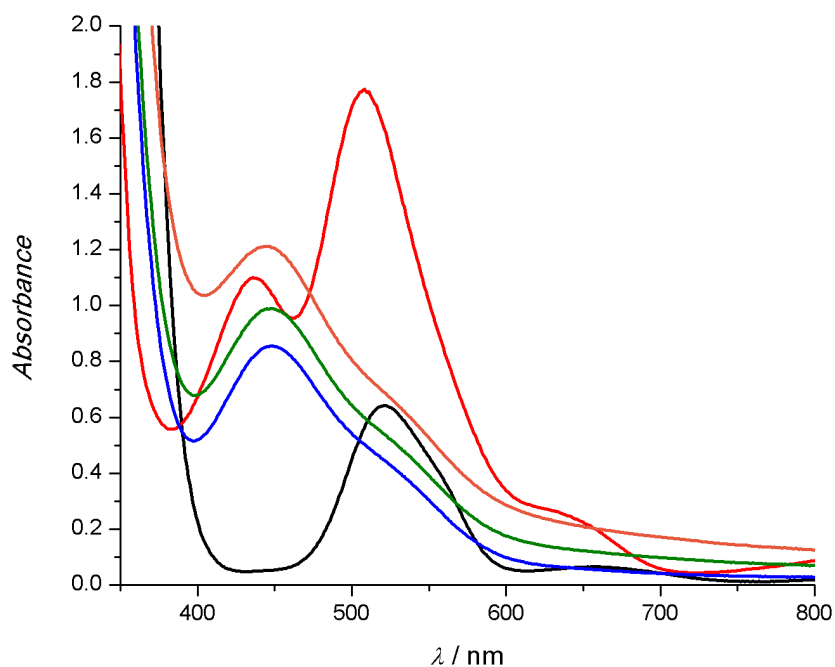
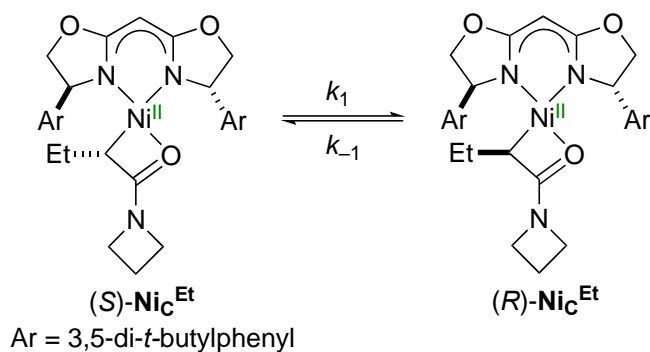


Figure S 20: UV-vis spectra (THF, r.t.) of **Ni_A** in the presence of varying amounts of **Zn-2** and triamine. **Ni_A** (black), + 1.0 equiv **Zn-2** (red), + 2.0 equiv **Zn-2** (blue), + 3.0 equiv **Zn-2** (green), + 24 equiv **Zn-2** and 20 equiv triamine (orange).

G. Rate of Epimerization of Nic

The rate of epimerization of the nickel-bound stereocenter in **Nic^{Et}** was determined via NMR spectroscopy using **Nic^{Et}** in THF-d₈ (4.7 mM).



Determination of the magnetization exchange rates was performed by integration of NOE experiments obtained with mixing times of 500 ms and 0 ms using the EXSYCALC program package by Mestrelab Research.

conditions	k_1 / s^{-1}	k_{-1} / s^{-1}
Nic^{Et}	0.033	0.163
Nic^{Et} + triamine (1.0 equiv)	0.026	0.182
Nic^{Et} + triamine (1.0 equiv) + ZnBr ₂ (1.0 equiv)	0.033	0.174

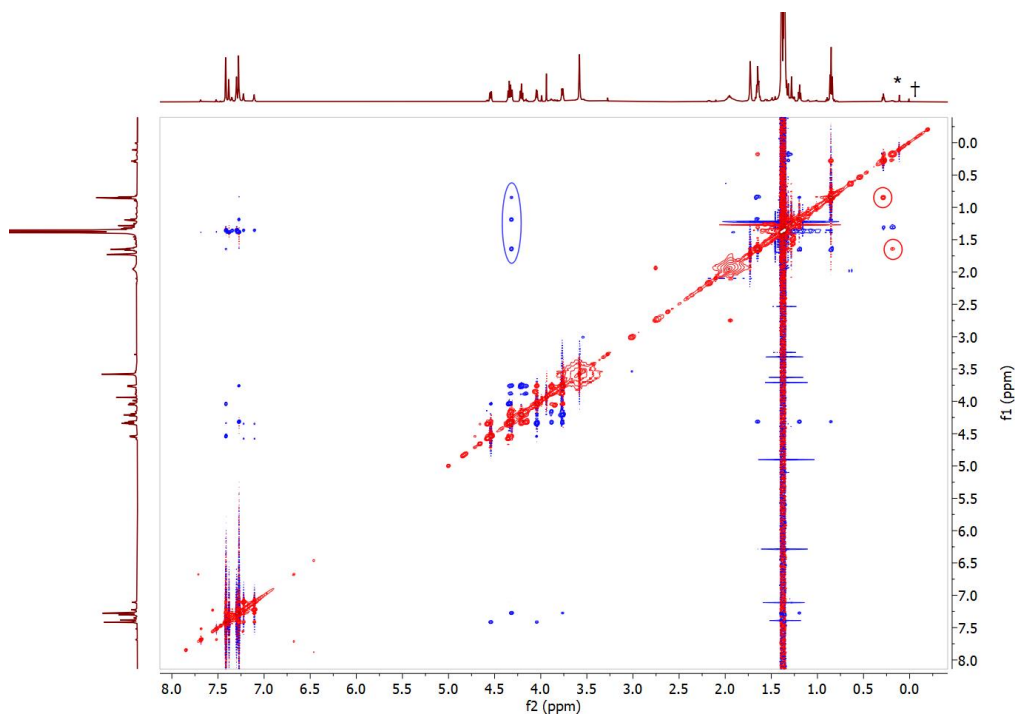


Figure S 21: NOESY spectrum (THF-d_8 , r.t.) of NiC^{Et} . *denotes grease; †denotes tetramethylsilane; blue circle highlights the interaction of the 4 position of the oxazoline with the α -nickelated alkyl chain of $(S)\text{-NiC}^{\text{Et}}$; red circles highlight chemical exchange between ethyl moieties of $(S)\text{-NiC}^{\text{Et}}$ and $(R)\text{-NiC}^{\text{Et}}$.

H. Time-Course Experiments: $\text{Ni}_B^{\text{LiBr}}$ and Ni_C^{Et} as Catalysts

Time-course experiments were performed, using **GP-9**, with the indicated nickel complexes.

All data represent the average of two experiments.

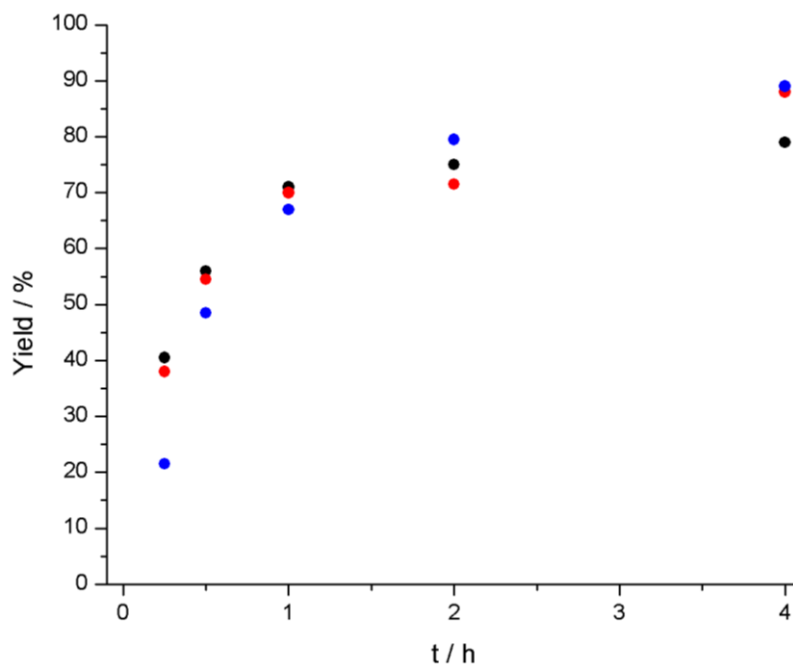


Figure S 22: Time-course experiments using various nickel catalysts. standard conditions (black), $\text{Ni}_B^{\text{LiBr}}$ (red), and Ni_C^{Et} (blue).

I. Coupling of **Zn-1** using Ni_C^{Et} as Catalyst (Fig. 4b)

In a glovebox, **Zn-1** (79 mg, 0.24 mmol, 1.2 equiv) was added to a 4 mL vial equipped with a stir bar, followed by THF (0.8 mL) and dodecane (45 μL , 0.20 mmol, 1.0 equiv). The vial was capped, and then a solution of Ni_C^{Et} (0.2 mL, 0.05 M in THF, 0.010 mmol, 5.0 mol%) was added, immediately followed by triamine (49 μL , 0.19 mmol, 1.0 equiv) and 1-iodo-3-phenylpropane (32 μL , 0.20 mmol, 1.0 equiv). Yields were determined by quenching with ethanol, followed by GC analysis, and enantiomeric excesses were determined via SFC.

J. C–C Bond Formation in Stoichiometric Reactions of Ni^{Et} (Fig. 4c)

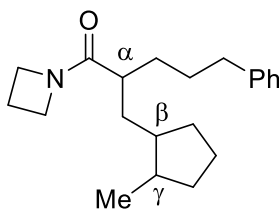
In a glovebox, a solution of Ni^{Et} (0.1 mL, 0.12 M in THF, 12 μmol , 1.0 equiv) was added to a 4 mL vial, followed by THF (0.5 mL) and a stir bar. The vial was capped with a septum cap, and then triamine (29 μL , 0.12 mmol, 10 equiv) and 1-iodo-3-phenylpropane (2.3 μL , 0.014 mmol, 1.2 equiv) were added, followed by a solution of Ni^{cod} (20 μL , 0.015 M in THF, 0.30 μmol , 0.025 equiv). Three additional portions of the same volume of Ni^{cod} (the solution of Ni^{cod} was stored at $-35\text{ }^{\circ}\text{C}$) were added after 1, 2, and 3 h of reaction time. After a total of 6 h, the reaction was quenched by the addition of ethanol, and dodecane (3.0 μL , 0.013 mmol, 1.1 equiv, internal standard) was added. The yield of the reaction was determined via GC analysis, and the enantiomeric excess was determined via SFC analysis.

A corresponding experiment was also conducted in the absence of Ni^{cod} .

All data represent the average of two experiments.

conditions	yield / %	ee / %
above	50	91
no Ni^{cod}	27	91

K. Support for the Intermediacy of an Organic Radical



1-(Azetidin-1-yl)-2-((2-methylcyclopentyl)methyl)-5-phenylpentan-1-one (mixture of diastereomers). The title compound was synthesized according to **GP-9**, with the following changes: reactions were run on a 0.20-mmol scale, a stock solution of the catalyst (0.014 M, 0.7 mL) was used, **Zn-9** (solution) was used instead of **Zn-2**, 6-iodo-1-heptene was used as the electrophile, and no internal standard was used (the product was isolated).

No acyclic coupling product was detected via NMR analysis of the unpurified reaction mixture. The product was purified by column chromatography on silica gel (20% → 60% EtOAc/hexanes), followed by preparatory TLC, which afforded a mixture of 4 diastereomers. Colorless oil.

(*R,R*)-**L***: 22 mg, 35% yield; (*S,S*)-**L***: 24 mg, 38% yield.

SFC analysis: The mixture was analyzed via SFC on a CHIRALPAK IG-3 column (20% *i*-PrOH in supercritical CO₂, 2.5 mL/min). Retention times and corresponding stereochemistry for compound obtained using (*S,S*)-**L***:

#	Retention time	Stereochemistry at C _α	Cyclopentane stereochemistry for C _β - C _γ
1	8.75	<i>R</i>	trans
2	9.34	<i>R</i>	cis
3	10.03	<i>R</i>	trans
4	10.49	<i>S</i>	trans
5	10.95	<i>R</i>	cis
6	13.42	<i>S</i>	cis + trans
7	14.18	<i>S</i>	cis

We have not been able to separate all eight stereoisomers.

(*R,R*)-**L***: 96:4 dr (C_α); (*S,S*)-**L***: 5:95 dr (C_α).

(*R,R*)-**L***: cis/trans at C_β - C_γ = 3.5:1; (*S,S*)-**L***: cis/trans at C_β - C_γ = 3.4:1.

¹H NMR (400 MHz, CDCl₃) δ 7.40 – 7.25 (m, 2H), 7.25 – 7.16 (m, 3H), 4.14 (td, *J* = 7.7, 2.1 Hz, 2H), 4.03 (ddd, *J* = 9.1, 6.0, 1.7 Hz, 2H), 2.61 (qt, *J* = 7.7, 4.7 Hz, 2H), 2.24 (dddd, *J* = 16.2, 10.7, 7.9, 4.1 Hz, 3H), 2.04 – 1.85 (m, 1H), 1.85 – 1.32 (m, 11H), 1.30 – 1.12 (m, 2H), 0.97 (d, *J* = 6.6 Hz, 0.7 H, CH₃, trans diastereomers), 0.81 – 0.76 (m, 2.3 H, CH₃, cis diastereomers).

¹³C NMR (101 MHz, CDCl₃) δ 176.13, 176.06, 142.40, 142.39, 128.47, 128.45, 128.4, 128.3, 125.8, 125.7, 50.0, 47.6, 47.5, 47.4, 45.9, 45.3, 41.3, 40.9, 40.7, 40.0, 39.8, 39.6, 37.8, 37.6, 36.6, 36.22, 36.21, 36.0, 34.6, 34.4, 33.7, 33.6, 33.44, 33.40, 33.3, 32.7, 32.5, 32.3, 31.9, 31.5, 30.0, 29.80, 29.76, 23.5, 23.4, 22.7, 22.4, 19.3, 19.0, 14.93, 14.87. Mixture of diastereomers.

FT-IR (film): 3022, 2938, 2869, 1646, 1458, 1356, 1023, 718, 598 cm^{-1} .

HRMS (ESI-MS) m/z $[\text{M}+\text{H}]^+$ calcd for $\text{C}_{21}\text{H}_{32}\text{NO}$: 314.2479, found: 314.2479.

$[\alpha]_{\text{D}}^{22} = -4.3$ from (*S,S*)-**L***.

L. X-ray Crystallography

CCDC-2150649 (**Ni**^{OMe}), CCDC-2150650 (**Ni**^{cod}), CCDC-2150652 (**Zn-2**), and 2150653 (**Ni**^{LiBr}) contain the supplementary crystallographic data for this paper. This data can be obtained free of charge via <http://www.ccdc.cam.ac.uk/products/csd/request/> (or from Cambridge Crystallographic Data Centre, 12 Union Road, Cambridge, CB2 1EZ, UK. Fax: +44-1223-336-033; e-mail: deposit@ccdc.cam.ac.uk).

Suitable single crystals for X-ray structure determination were selected from the mother liquor under an inert gas atmosphere and transferred in protective perfluoropolyether oil on a microscope slide. The selected and mounted crystals were transferred to the cold gas stream on the diffractometer. The diffraction data were obtained at 100 K on a Bruker AXS KAPPA diffractometer coupled to a PHOTON 100 CMOS detector with graphite monochromated Mo- $K\alpha$ radiation ($\lambda = 0.71073 \text{ \AA}$) or on a Bruker AXS D8 VENTURE KAPPA diffractometer coupled to a PHOTON II CPAD detector with Mo $K\alpha$ radiation ($\lambda = 0.71073 \text{ \AA}$) or Cu $K\alpha$ radiation ($\lambda = 1.54178 \text{ \AA}$) from an $I\mu\text{S}$ micro-source.

Using Apex3, the data obtained were integrated with SAINT, and a semi-empirical absorption correction from equivalents with SADABS was applied. The structure was solved and refined with the Bruker SHELX 2018 software package. All non-hydrogen atoms were refined with

anisotropic displacement parameters. All C–H hydrogen atoms were refined isotropically on calculated positions by using a riding model with their U_{iso} values constrained to 1.5 U_{eq} of their pivot atoms for terminal sp^3 carbon atoms and 1.2 times for all other carbon atoms.

Zn-2

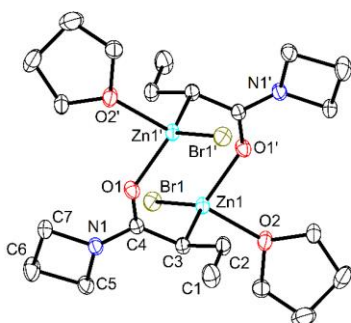


Figure S 24: Thermal ellipsoid plot of **Zn-2** with the anisotropic displacement parameters at the 50% probability level. C–H hydrogen atoms are omitted for clarity. **Zn-2** crystallizes as half a dimeric molecule in the asymmetric unit.

Table S 1: Crystal data and structure refinement for **Zn-2**.

Identification code	V22039	
Empirical formula	$\text{C}_{22}\text{H}_{40}\text{Br}_2\text{N}_2\text{O}_4\text{Zn}_2$	
Formula weight	687.12	
Temperature	100(2) K	
Wavelength	0.71073 Å	
Crystal system	monoclinic	
Space group	$P2_1/n$	
Unit cell dimensions	$a = 8.1152(15)$ Å	$a = 90^\circ$
	$b = 8.4967(12)$ Å	$b = 97.148(9)$
	$c = 20.061(5)$ Å	$g = 90^\circ$

Volume	1372.5(5) Å ³
Z	2
Density (calculated)	1.663 Mg/m ³
Absorption coefficient	4.687 mm ⁻¹
F(000)	696
Crystal size	0.150 x 0.150 x 0.300 mm ³
Theta range for data collection	2.8444 to 36.3034°
Index ranges	-13<=h<=13, -14<=k<=14, -33<=l<=33
Reflections collected	57404
Independent reflections	6670 [R(int) = 0.0369]
Completeness	99.9%
Absorption correction	Multi-scan
Max. and min. transmission	0.5400 and 0.3340
Refinement method	Full-matrix least-squares on F ²
Data / restraints / parameters	6670 / 0 / 165
Goodness-of-fit on F ²	1.054
Final R indices [I>2sigma(I)]	R1 = 0.0345, wR2 = 0.0831
R indices (all data)	R1 = 0.0449, wR2 = 0.0875
Largest diff. peak and hole	1.379 and -1.314 e·Å ⁻³

Table S 2: Bond lengths [Å] for **Zn-2**.

Br1-Zn1	2.4095(5)	Zn1-O1	1.9646(13)
Zn1-C3#1	2.0507(19)	Zn1-O2	2.1128(14)
N1-C4	1.333(2)	N1-C7	1.464(2)
N1-C5	1.471(2)	O1-C4	1.275(2)
C1-C2	1.526(3)	O2-C11	1.435(4)
O2-C8	1.454(2)	O2-C11A	1.59(2)
C2-C3	1.528(3)	C3-C4	1.459(2)

C5-C6	1.546(3)	C7-C6	1.541(3)
C8-C9	1.512(3)	C9-C10	1.524(6)
C9-C10A	1.56(2)	C10-C11	1.512(6)
C10A-C11A	1.48(3)		

Symmetry transformations used to generate equivalent atoms:

#1 -x+1, -y+1, -z+1

Table S 3: Bond angles [°] for Zn-2.

O1-Zn1-C3#1	115.84(6)	O1-Zn1-O2	88.41(6)
C3#1-Zn1-O2	105.31(7)	O1-Zn1-Br1	115.63(4)
C3#1-Zn1-Br1	122.06(5)	O2-Zn1-Br1	100.86(4)
C4-N1-C7	130.66(15)	C4-N1-C5	132.67(16)
C7-N1-C5	95.26(13)	C4-O1-Zn1	132.45(11)
C11-O2-C8	110.2(2)	C8-O2-C11A	104.9(13)
C11-O2-Zn1	120.36(19)	C8-O2-Zn1	123.12(11)
C11A-O2-Zn1	111.6(8)	C1-C2-C3	113.58(16)
C4-C3-C2	114.55(15)	C4-C3-Zn1#1	106.85(12)
C2-C3-Zn1#1	111.03(12)	O1-C4-N1	116.37(15)
O1-C4-C3	125.29(15)	N1-C4-C3	118.33(15)
N1-C5-C6	87.55(14)	N1-C7-C6	87.97(14)
C7-C6-C5	89.21(14)	O2-C8-C9	105.06(17)
C8-C9-C10	102.1(3)	C8-C9-C10A	107.5(7)
C11-C10-C9	101.7(4)	O2-C11-C10	104.6(3)
C11A-C10A-C9	103.8(16)	C10A-C11A-O2	101.0(16)

Symmetry transformations used to generate equivalent atoms:

#1 -x+1, -y+1, -z+1

Table S 4: Torsion angles [°] for **Zn-2**.

C4-O1-Zn1-Br1	-100.82(1)	C4-C3-Zn1#1-O1#1	90.74(1)
C8-O2-Zn1-Br1	-151.35(1)	C3-C4-O1-Zn1	28.85(1)
C11-O2-Zn1-Br1	59.28(1)	C3-C4-N1-C5	-4.23(1)
C1-C2-C3-C4	59.60(1)	C6-C5-N1-C7	0.04(1)
C2-C3-C4-N1	-143.68(1)	C6-C7-N1-C4	167.45(1)
C2-C3-Zn1#1-Br1#1	174.66(1)	C9-C8-O2-C11	-8.04(1)
C4-C3-Zn1#1-Br1#1	-59.78(1)	C9-C10-C11-O2	35.43(1)
N1-C4-O1-Zn1	-150.45(1)	C4-O1-Zn1-C3#1	51.63(1)
O1-C4-N1-C7	12.18(1)	C8-O2-Zn1-C3#1	80.85(1)
C6-C5-N1-C4	-167.04(1)	C11-O2-Zn1-C3#1	-68.52(1)
C5-C6-C7-N1	0.04(1)	C2-C3-C4-O1	37.04(1)
C9-C8-O2-Zn1	-160.10(1)	Zn1#1-C3-C4-N1	92.92(1)
C8-C9-C10-C11	-39.66(1)	C2-C3-Zn1#1-O2#1	60.96(1)
C10-C11-O2-C8	-17.48(1)	C4-C3-Zn1#1-O2#1	-173.49(1)
C4-O1-Zn1-O2	157.89(1)	O1-C4-N1-C5	175.12(1)
C8-O2-Zn1-O1	-35.55(1)	C3-C4-N1-C7	-167.17(1)
C11-O2-Zn1-O1	175.08(1)	N1-C5-C6-C7	-0.03(1)
C1-C2-C3-Zn1#1	-179.27(1)	C6-C7-N1-C5	-0.04(1)
Zn1#1-C3-C4-O1	-86.37(1)	O2-C8-C9-C10	29.80(1)
C2-C3-Zn1#1-O1#1	-34.82(1)	C10-C11-O2-Zn1	135.47(1)

Symmetry transformations used to generate equivalent atoms:

#1 -x+1, -y+1, -z+1

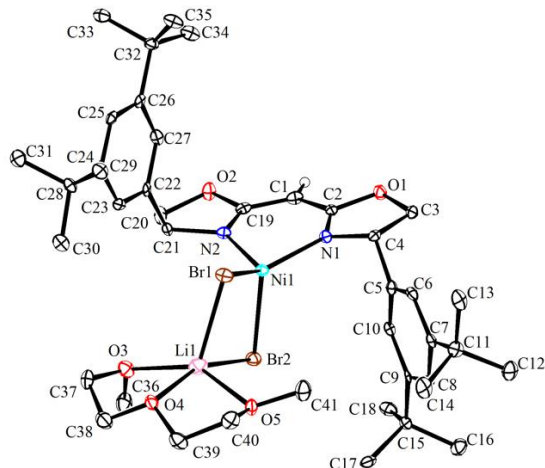
Ni_B^{LiBr}

Figure S 25: Thermal ellipsoid plot of **Ni_B^{LiBr}** with the anisotropic displacement parameters at the 50% probability level. Selected C–H hydrogen atoms are omitted for clarity.

Table S 5: Crystal data and structure refinement for **Ni_B^{LiBr}**.

Identification code	D21030	
Empirical formula	C ₄₁ H ₆₃ Br ₂ LiN ₂ NiO ₅	
Formula weight	889.40	
Temperature	101(2) K	
Wavelength	0.71073 Å	
Crystal system	triclinic	
Space group	P1	
Absolute configuration	S,S	
Unit cell dimensions	a = 8.3010(5) Å	α = 76.892(2)°
	b = 8.9001(5) Å	β = 80.722(2)°
	c = 14.9918(9) Å	γ = 87.696(2)°
Volume	1064.61(11) Å ³	
Z	1	
Density (calculated)	1.387 Mg/m ³	

Absorption coefficient	2.375 mm ⁻¹
F(000)	464
Crystal size	0.25 x 0.10x 0.01 mm ³
Theta range for data collection	2.35 to 31.46°
Index ranges	-12<=h<=12, -13<=k<=13, -21<=l<=21
Reflections collected	31056
Independent reflections	13040 [R(int) = 0.0376]
Completeness	99.2%
Absorption correction	Multi-scan
Max. and min. transmission	0.65 and 0.75
Refinement method	Full-matrix least-squares on F ²
Data / restraints / parameters	13040 / 3 / 483
Goodness-of-fit on F ²	0.920
Final R indices [I>2sigma(I)]	R1 = 0.0307, wR2 = 0.0565
R indices (all data)	R1 = 0.0396, wR2 = 0.0589
Largest diff. peak and hole	0.654 and -0.388e·Å ⁻³
Flack parameter	0.031(4)

Table S 6: Bond lengths [Å] for NiB^{LiBr}.

Br1-Ni1	2.4308(5)	Br1-Li1#2	2.645(6)
Li1-O3	2.067(6)	Li1-O4	2.077(6)
Li1-O5	2.170(6)	Li1-Br2#1	2.575(6)
Ni1-N2	1.932(2)	Ni1-N1	1.946(2)
Ni1-Br2	2.3904(4)	O1-C2	1.368(3)
O1-C3	1.448(3)	N1-C2	1.316(4)
N1-C4	1.480(4)	C1-C2	1.390(4)
C1-C15	1.394(4)	O2-C16	1.448(4)
O2-C15	1.362(4)	N2-C17	1.474(4)
N2-C15	1.308(4)	O3-C32	1.429(4)
O3-C33	1.429(4)	C4-C5	1.514(4)
C3-C4	1.535(4)	O4-C34	1.425(4)
O4-C35	1.433(4)	C5-C10	1.388(4)
C5-C6	1.391(4)	O5-C36	1.427(4)
O5-C37	1.433(4)	C6-C7	1.392(4)
C7-C11	1.540(4)	C7-C8	1.392(4)
C9-C00X	1.534(4)	C8-C9	1.389(4)
C00X-C019	1.535(4)	C9-C10	1.387(4)
C11-C13	1.526(4)	C00R-C00X	1.532(4)
C11-C12	1.541(4)	C00X-C01B	1.533(4)
C18-C19	1.375(4)	C11-C14	1.535(4)
C18-C17	1.521(4)	C18-C23	1.401(4)
C19-C20	1.402(4)	C17-C16	1.532(4)
C20-C24	1.531(4)	C20-C21	1.392(4)
C22-C28	1.537(4)	C21-C22	1.395(4)
C24-C26	1.531(4)	C22-C23	1.391(4)
C24-C25	1.537(4)	C24-C27	1.534(4)
C28-C31	1.526(4)	C28-C30	1.530(4)
C28-C29	1.539(4)	C33-C34	1.495(5)
C35-C36	1.501(4)		

Symmetry transformations used to generate equivalent atoms:

#1 x-1, y-1, z

#2 x+1, y+1, z

Table S 7: Bond angles [°] for NiB^{LiBr}.

Ni1-Br1-Li1#2	83.64(13)	O3-Li1-O4	78.6(2)
O3-Li1-O5	146.5(3)	O4-Li1-O5	78.8(2)
O3-Li1-Br2#1	99.2(2)	O4-Li1-Br2#1	113.8(3)
O5-Li1-Br2#1	112.5(2)	O3-Li1-Br1#1	97.2(2)
O4-Li1-Br1#1	156.4(3)	O5-Li1-Br1#1	93.7(2)
Br2#1-Li1-Br1#1	89.74(18)	N2-Ni1-N1	92.27(10)
N2-Ni1-Br2	115.45(8)	N1-Ni1-Br2	127.78(7)
N2-Ni1-Br1	104.09(8)	N1-Ni1-Br1	116.14(7)
Br2-Ni1-Br1	99.608(16)	C2-O1-C3	107.1(2)
C2-N1-C4	108.7(2)	C2-N1-Ni1	123.8(2)
C4-N1-Ni1	127.54(18)	C2-C1-C15	120.5(3)
Ni1-Br2-Li1#2	85.96(13)	C15-O2-C16	106.0(2)
C15-N2-C17	108.3(2)	C15-N2-Ni1	124.7(2)
C17-N2-Ni1	126.86(19)	N1-C2-O1	114.8(3)
N1-C2-C1	128.3(3)	O1-C2-C1	116.9(3)
C33-O3-C32	111.2(2)	C33-O3-Li1	110.6(2)
C32-O3-Li1	121.6(3)	O1-C3-C4	105.3(2)
N1-C4-C3	102.7(2)	O4-C35-C36	105.4(2)
C34-O4-Li1	112.0(2)	O5-C36-C35	110.4(3)
C10-C5-C6	119.9(3)	N1-C4-C5	113.6(2)
C6-C5-C4	120.2(2)	C5-C4-C3	111.9(2)
C36-O5-Li1	107.1(2)	C34-O4-C35	113.2(2)
C5-C6-C7	120.7(3)	C35-O4-Li1	113.4(2)
C6-C7-C11	122.8(3)	C10-C5-C4	119.8(2)
C9-C8-C7	123.3(3)	C36-O5-C37	112.6(2)
C10-C9-C00X	122.4(3)	C37-O5-Li1	116.1(2)
C00R-C00X-C9	112.4(2)	C6-C7-C8	117.5(3)
C9-C00X-C01B	109.3(2)	C8-C7-C11	119.6(3)
C9-C00X-C019	108.9(2)	C10-C9-C8	117.5(3)
C5-C10-C9	121.1(3)	C8-C9-C00X	120.1(2)
C13-C11-C7	112.3(2)	C00R-C00X-C01B	107.9(2)
C13-C11-C12	109.0(3)	C00R-C00X-C019	108.6(3)
C7-C11-C12	109.0(2)	C01B-C00X-C019	109.7(3)
C19-C18-C17	119.5(2)	C13-C11-C14	108.1(2)

N2-C17-C18	110.7(2)	C14-C11-C7	109.5(2)
C18-C17-C16	114.3(2)	C14-C11-C12	108.8(3)
O2-C16-C17	103.8(2)	C19-C18-C23	120.1(3)
N2-C15-O2	114.5(3)	C23-C18-C17	120.4(3)
O2-C15-C1	117.9(3)	N2-C17-C16	101.2(2)
C21-C20-C19	117.5(3)	N2-C15-C1	127.6(3)
C19-C20-C24	122.2(3)	C18-C19-C20	121.1(3)
C23-C22-C21	117.7(3)	C21-C20-C24	120.3(3)
C21-C22-C28	120.1(2)	C20-C21-C22	123.0(3)
C20-C24-C26	109.8(2)	C23-C22-C28	122.2(3)
C26-C24-C27	108.3(2)	C22-C23-C18	120.7(3)
C26-C24-C25	110.0(2)	C20-C24-C27	111.9(2)
C31-C28-C30	108.7(3)	C20-C24-C25	109.6(2)
C30-C28-C22	109.1(2)	C27-C24-C25	107.2(2)
C30-C28-C29	109.0(3)	C31-C28-C22	112.4(2)
O3-C33-C34	106.0(3)	C31-C28-C29	107.4(3)
O4-C34-C33	106.7(3)	C22-C28-C29	110.2(2)

Table S 8: Torsion angles [°] for Ni_B^{LiBr}.

C4-N1-C2-O1	4.9(3)	Ni1-N1-C2-O1	-175.54(18)
C4-N1-C2-C1	-174.5(3)	Ni1-N1-C2-C1	5.1(4)
C3-O1-C2-N1	3.4(3)	C3-O1-C2-C1	-177.1(3)
C15-C1-C2-N1	7.9(5)	C15-C1-C2-O1	-171.4(3)
C2-O1-C3-C4	-9.7(3)	C2-N1-C4-C5	-131.3(3)
Ni1-N1-C4-C5	49.1(3)	C2-N1-C4-C3	-10.3(3)
Ni1-N1-C4-C3	170.06(18)	O1-C3-C4-N1	12.0(3)
O1-C3-C4-C5	134.1(2)	N1-C4-C5-C10	44.7(4)
C3-C4-C5-C10	-70.9(3)	N1-C4-C5-C6	-139.0(3)
C3-C4-C5-C6	105.4(3)	C10-C5-C6-C7	0.4(4)
C4-C5-C6-C7	-175.9(3)	C5-C6-C7-C8	-0.8(4)
C5-C6-C7-C11	178.2(3)	C6-C7-C8-C9	0.6(4)
C11-C7-C8-C9	-178.5(3)	C7-C8-C9-C10	0.0(4)
C7-C8-C9-C00X	-179.3(3)	C10-C9-C00X-C00R	7.9(4)
C8-C9-C00X-C00R	-172.8(3)	C10-C9-C00X-C01B	127.7(3)
C8-C9-C00X-C01B	-53.0(3)	C10-C9-C00X-C019	-112.5(3)

C8-C9-C00X-C019	66.8(3)	C6-C5-C10-C9	0.2(4)
C4-C5-C10-C9	176.6(3)	C8-C9-C10-C5	-0.4(4)
C00X-C9-C10-C5	178.8(3)	C6-C7-C11-C13	-3.2(4)
C8-C7-C11-C13	175.9(3)	C6-C7-C11-C14	117.0(3)
C8-C7-C11-C14	-64.0(3)	C6-C7-C11-C12	-124.1(3)
C8-C7-C11-C12	54.9(4)	C15-N2-C17-C18	-102.3(3)
Ni1-N2-C17-C18	81.5(3)	C15-N2-C17-C16	19.1(3)
Ni1-N2-C17-C16	-157.0(2)	C19-C18-C17-N2	-110.1(3)
C23-C18-C17-N2	67.9(3)	C19-C18-C17-C16	136.5(3)
C23-C18-C17-C16	-45.4(4)	C15-O2-C16-C17	21.7(3)
N2-C17-C16-O2	-24.3(3)	C18-C17-C16-O2	94.6(3)
C17-N2-C15-O2	-6.4(4)	Ni1-N2-C15-O2	169.84(19)
C17-N2-C15-C1	173.0(3)	Ni1-N2-C15-C1	-10.7(5)
C16-O2-C15-N2	-10.4(3)	C16-O2-C15-C1	170.1(3)
C2-C1-C15-N2	-4.9(5)	C2-C1-C15-O2	174.6(3)
C23-C18-C19-C20	0.4(4)	C17-C18-C19-C20	178.4(3)
C18-C19-C20-C21	-0.4(4)	C18-C19-C20-C24	-179.1(3)
C19-C20-C21-C22	-0.2(4)	C24-C20-C21-C22	178.5(3)
C20-C21-C22-C23	0.8(4)	C20-C21-C22-C28	-179.2(3)
C21-C22-C23-C18	-0.8(4)	C28-C22-C23-C18	179.2(3)
C19-C18-C23-C22	0.3(4)	C17-C18-C23-C22	-177.8(2)
C21-C20-C24-C26	58.5(4)	C19-C20-C24-C26	-122.8(3)
C21-C20-C24-C27	178.8(3)	C19-C20-C24-C27	-2.6(4)
C21-C20-C24-C25	-62.4(4)	C19-C20-C24-C25	116.2(3)
C23-C22-C28-C31	-9.7(4)	C21-C22-C28-C31	170.2(3)
C23-C22-C28-C30	111.0(3)	C21-C22-C28-C30	-69.1(3)
C23-C22-C28-C29	-129.5(3)	C21-C22-C28-C29	50.5(4)
C32-O3-C33-C34	-175.4(3)	Li1-O3-C33-C34	46.3(3)
C35-O4-C34-C33	168.5(3)	Li1-O4-C34-C33	38.7(4)
O3-C33-C34-O4	-55.1(3)	C34-O4-C35-C36	-169.1(3)
Li1-O4-C35-C36	-40.0(3)	C37-O5-C36-C35	85.4(3)
Li1-O5-C36-C35	-43.4(3)	O4-C35-C36-O5	55.6(3)

NiC^{OMe}

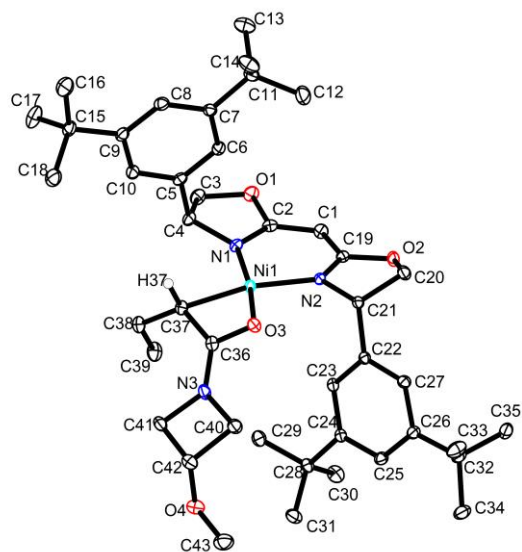


Figure S 26: Thermal ellipsoid plot of NiC^{OMe} with the anisotropic displacement parameters at the 50% probability level. Selected C–H hydrogen atoms are omitted for clarity.

Table S 9: Crystal data and structure refinement for **NiC^{OMe}**.

Identification code	V21121	
Empirical formula	C ₄₃ H ₆₃ N ₃ NiO ₄	
Formula weight	744.67	
Temperature	100(2) K	
Wavelength	0.71073 Å	
Crystal system	monoclinic	
Space group	<i>P</i> 2 ₁	
Absolute configuration	<i>S,S,S</i>	
Unit cell dimensions	a = 14.0199(5) Å	a = 90°
	b = 8.9335(4) Å	b = 93.1330(10)
	c = 16.2779(6) Å	g = 90°
Volume	2035.71(14) Å ³	
Z	2	
Density (calculated)	1.215 Mg/m ³	
Absorption coefficient	0.520 mm ⁻¹	
F(000)	804	
Crystal size	0.300 x 0.150 x 0.100 mm ³	
Theta range for data collection	1.97 to 33.14°	
Index ranges	-21 ≤ h ≤ 21, -13 ≤ k ≤ 13, -25 ≤ l ≤ 25	
Reflections collected	48506	
Independent reflections	15512 [R(int) = 0.0385]	
Completeness	100.0%	
Absorption correction	Multi-scan	
Max. and min. transmission	0.70 and 0.75	
Refinement method	Full-matrix least-squares on F ²	
Data / restraints / parameters	15512 / 1 / 474	

Goodness-of-fit on F^2	1.021
Final R indices [$I > 2\sigma(I)$]	$R_1 = 0.0335$, $wR_2 = 0.0708$
R indices (all data)	$R_1 = 0.0386$, $wR_2 = 0.0727$
Largest diff. peak and hole	0.384 and $-0.278 \text{ e} \cdot \text{\AA}^{-3}$
Flack parameter	0.017(3)

Table S 10: Bond lengths [Å] for Nic^{OMe}.

Ni1-N1	1.8731(14)	Ni1-N2	1.9021(14)
Ni1-O3	1.9128(12)	Ni1-C37	2.0013(17)
Ni1-C36	2.2162(17)	O1-C2	1.3676(19)
O1-C3	1.442(2)	O2-C19	1.367(2)
O2-C20	1.444(2)	O3-C36	1.291(2)
O4-C42	1.410(2)	O4-C43	1.424(2)
N1-C2	1.326(2)	N1-C4	1.476(2)
N2-C19	1.314(2)	N2-C21	1.476(2)
N3-C36	1.332(2)	N3-C40	1.468(2)
N3-C41	1.470(2)	C1-C2	1.381(2)
C1-C19	1.402(2)	C4-C5	1.518(2)
C3-C4	1.534(2)	C5-C10	1.386(3)
C5-C6	1.397(2)	C6-C7	1.393(2)
C7-C11	1.540(2)	C7-C8	1.399(2)
C9-C15	1.534(2)	C8-C9	1.395(3)
C11-C12	1.530(3)	C9-C10	1.403(3)
C11-C13	1.540(3)	C11-C14	1.531(3)
C15-C16	1.530(3)	C15-C18	1.536(3)
C15-C17	1.537(3)	C21-C22	1.526(2)
C20-C21	1.533(2)	C22-C27	1.390(2)
C22-C23	1.396(2)	C23-C24	1.395(2)
C24-C28	1.535(2)	C24-C25	1.401(2)
C26-C32	1.527(2)	C25-C26	1.395(2)
C28-C29	1.526(2)	C26-C27	1.404(2)
C28-C31	1.538(3)	C28-C30	1.536(3)
C32-C33	1.531(3)	C32-C35	1.536(3)
C32-C34	1.538(2)	C37-C38	1.521(2)
C36-C37	1.451(2)	C38-C39	1.524(3)
C41-C42	1.538(2)	C40-C42	1.550(3)

Table S 11: Bond angles [°] for **Nic^{OMe}**.

N1-Ni1-N2	93.58(6)	N1-Ni1-O3	171.33(6)
N2-Ni1-O3	94.27(6)	N1-Ni1-C37	100.97(7)
N2-Ni1-C37	165.17(6)	O3-Ni1-C37	71.41(6)
N1-Ni1-C36	138.64(6)	N2-Ni1-C36	125.38(6)
O3-Ni1-C36	35.49(5)	C37-Ni1-C36	39.83(6)
C2-O1-C3	106.66(13)	C19-O2-C20	104.79(13)
C36-O3-Ni1	85.19(10)	C42-O4-C43	111.47(15)
C2-N1-C4	107.56(14)	C2-N1-Ni1	125.03(12)
C4-N1-Ni1	125.38(11)	C19-N2-C21	107.45(14)
C19-N2-Ni1	125.63(11)	C21-N2-Ni1	126.48(11)
C36-N3-C40	126.36(14)	C36-N3-C41	134.23(15)
C40-N3-C41	94.44(13)	C2-C1-C19	119.04(16)
N1-C2-O1	113.95(15)	N1-C2-C1	128.83(16)
O1-C2-C1	117.12(15)	O1-C3-C4	103.89(12)
N1-C4-C3	101.48(14)	N1-C4-C5	111.90(13)
C10-C5-C4	119.84(16)	C5-C4-C3	112.58(15)
C7-C6-C5	120.90(16)	C10-C5-C6	119.39(15)
C6-C7-C11	121.44(15)	O4-C42-C41	111.36(14)
C9-C8-C7	122.50(16)	C41-C42-C40	88.58(13)
C8-C9-C15	123.27(16)	C6-C5-C4	120.74(17)
C5-C10-C9	121.61(16)	C6-C7-C8	118.19(16)
C12-C11-C13	108.77(17)	C8-C7-C11	120.35(15)
C12-C11-C7	112.17(15)	C8-C9-C10	117.40(16)
C13-C11-C7	107.72(15)	C10-C9-C15	119.33(16)
C16-C15-C18	108.69(16)	C12-C11-C14	107.83(16)
C16-C15-C17	108.23(16)	C14-C11-C13	108.97(16)
C18-C15-C17	109.17(17)	C14-C11-C7	111.32(15)
N2-C19-C1	127.23(15)	C16-C15-C9	112.48(16)
O2-C20-C21	102.97(12)	C9-C15-C18	108.98(14)
N2-C21-C22	114.26(13)	C9-C15-C17	109.25(15)
C22-C21-C20	111.95(14)	N2-C19-O2	114.48(14)
C27-C22-C23	119.50(15)	O2-C19-C1	118.28(15)
C23-C22-C21	122.40(14)	N2-C21-C20	100.90(13)
C23-C24-C25	118.35(15)	C27-C22-C21	118.09(14)

C25-C24-C28	119.82(15)	C24-C23-C22	120.86(15)
C25-C26-C27	117.76(15)	C23-C24-C28	121.79(14)
C27-C26-C32	119.07(15)	C26-C25-C24	122.20(16)
C29-C28-C24	111.64(14)	C25-C26-C32	123.15(15)
C24-C28-C30	108.48(14)	C22-C27-C26	121.32(15)
C24-C28-C31	111.29(14)	C29-C28-C30	109.18(15)
C26-C32-C33	109.75(15)	C29-C28-C31	107.41(15)
C33-C32-C35	109.29(15)	C30-C28-C31	108.79(15)
C33-C32-C34	107.71(16)	C26-C32-C35	109.02(15)
O3-C36-N3	118.48(15)	C26-C32-C34	112.20(14)
N3-C36-C37	128.17(15)	C35-C32-C34	108.83(16)
N3-C36-Ni1	144.60(13)	O3-C36-C37	112.78(15)
C36-C37-C38	121.02(15)	O3-C36-Ni1	59.32(9)
C38-C37-Ni1	129.52(12)	C37-C36-Ni1	62.08(9)
C37-C38-C39	114.44(15)	C36-C37-Ni1	78.09(10)
N3-C40-C42	88.28(13)	O4-C42-C40	115.40(16)
N3-C41-C42	88.70(13)		

Table S 12: Torsion angles [°] for **Nic^{OMe}**.

N2-Ni1-N1-C2	4.61(15)	C37-Ni1-N1-C2	-172.52(15)
C36-Ni1-N1-C2	-156.99(13)	N2-Ni1-N1-C4	-157.11(13)
C37-Ni1-N1-C4	25.77(14)	C36-Ni1-N1-C4	41.29(18)
C4-N1-C2-O1	-10.2(2)	Ni1-N1-C2-O1	-174.66(10)
C4-N1-C2-C1	166.12(17)	Ni1-N1-C2-C1	1.7(3)
C3-O1-C2-N1	-6.9(2)	C3-O1-C2-C1	176.28(15)
C19-C1-C2-N1	-7.3(3)	C19-C1-C2-O1	168.97(15)
C2-O1-C3-C4	20.04(17)	C2-N1-C4-C5	-98.75(17)
Ni1-N1-C4-C5	65.62(19)	C2-N1-C4-C3	21.52(17)
Ni1-N1-C4-C3	-174.12(12)	O1-C3-C4-N1	-24.82(16)
O1-C3-C4-C5	94.96(16)	N1-C4-C5-C10	-139.70(15)
C3-C4-C5-C10	106.75(18)	N1-C4-C5-C6	42.3(2)
C3-C4-C5-C6	-71.28(19)	C10-C5-C6-C7	-1.5(2)
C4-C5-C6-C7	176.52(15)	C5-C6-C7-C8	1.0(2)
C5-C6-C7-C11	-177.44(15)	C6-C7-C8-C9	0.1(3)
C11-C7-C8-C9	178.52(16)	C7-C8-C9-C10	-0.6(3)

C7-C8-C9-C15	178.85(15)	C6-C5-C10-C9	1.0(2)
C4-C5-C10-C9	-177.07(15)	C8-C9-C10-C5	0.0(2)
C15-C9-C10-C5	-179.41(15)	C6-C7-C11-C12	-17.5(2)
C8-C7-C11-C12	164.08(17)	C6-C7-C11-C14	-138.45(17)
C8-C7-C11-C14	43.1(2)	C6-C7-C11-C13	102.15(19)
C8-C7-C11-C13	-76.3(2)	C8-C9-C15-C16	-1.4(2)
C10-C9-C15-C16	178.03(16)	C8-C9-C15-C18	-121.98(19)
C10-C9-C15-C18	57.4(2)	C8-C9-C15-C17	118.8(2)
C10-C9-C15-C17	-61.8(2)	C21-N2-C19-O2	-3.09(19)
Ni1-N2-C19-O2	-175.93(11)	C21-N2-C19-C1	176.83(16)
Ni1-N2-C19-C1	4.0(3)	C20-O2-C19-N2	-16.93(19)
C20-O2-C19-C1	163.14(15)	C2-C1-C19-N2	4.1(3)
C2-C1-C19-O2	-175.94(15)	C19-O2-C20-C21	28.28(16)
C19-N2-C21-C22	-100.04(16)	Ni1-N2-C21-C22	72.72(18)
C19-N2-C21-C20	20.25(17)	Ni1-N2-C21-C20	-166.99(12)
O2-C20-C21-N2	-29.22(16)	O2-C20-C21-C22	92.70(15)
N2-C21-C22-C27	171.57(15)	C20-C21-C22-C27	57.7(2)
N2-C21-C22-C23	-7.3(2)	C20-C21-C22-C23	-121.21(17)
C27-C22-C23-C24	-0.2(3)	C21-C22-C23-C24	178.67(16)
C22-C23-C24-C25	-0.6(2)	C22-C23-C24-C28	-178.04(15)
C23-C24-C25-C26	0.5(3)	C28-C24-C25-C26	178.03(16)
C24-C25-C26-C27	0.3(3)	C24-C25-C26-C32	-177.96(17)
C23-C22-C27-C26	1.0(3)	C21-C22-C27-C26	-177.85(16)
C25-C26-C27-C22	-1.1(3)	C32-C26-C27-C22	177.24(16)
C23-C24-C28-C29	-16.7(2)	C25-C24-C28-C29	165.87(17)
C23-C24-C28-C30	103.63(19)	C25-C24-C28-C30	-73.8(2)
C23-C24-C28-C31	-136.71(17)	C25-C24-C28-C31	45.9(2)
C25-C26-C32-C33	-124.09(19)	C27-C26-C32-C33	57.7(2)
C25-C26-C32-C35	116.23(19)	C27-C26-C32-C35	-62.0(2)
C25-C26-C32-C34	-4.4(3)	C27-C26-C32-C34	177.36(17)
Ni1-O3-C36-N3	139.15(15)	Ni1-O3-C36-C37	-32.89(14)
C40-N3-C36-O3	13.8(3)	C41-N3-C36-O3	162.07(17)
C40-N3-C36-C37	-175.58(17)	C41-N3-C36-C37	-27.3(3)
C40-N3-C36-Ni1	90.0(2)	C41-N3-C36-Ni1	-121.7(2)
O3-C36-C37-C38	161.11(15)	N3-C36-C37-C38	-10.0(3)
Ni1-C36-C37-C38	129.20(17)	O3-C36-C37-Ni1	31.91(13)

N3-C36-C37-Ni1	-139.18(18)	C36-C37-C38-C39	-68.7(2)
Ni1-C37-C38-C39	31.9(2)	C36-N3-C40-C42	158.55(18)
C41-N3-C40-C42	0.73(14)	C36-N3-C41-C42	-155.63(19)
C40-N3-C41-C42	-0.73(14)	C43-O4-C42-C41	178.80(15)
C43-O4-C42-C40	79.82(19)	N3-C41-C42-O4	-116.12(15)
N3-C41-C42-C40	0.69(13)	N3-C40-C42-O4	112.35(16)
N3-C40-C42-C41	-0.70(13)		

Ni_E^{cod}

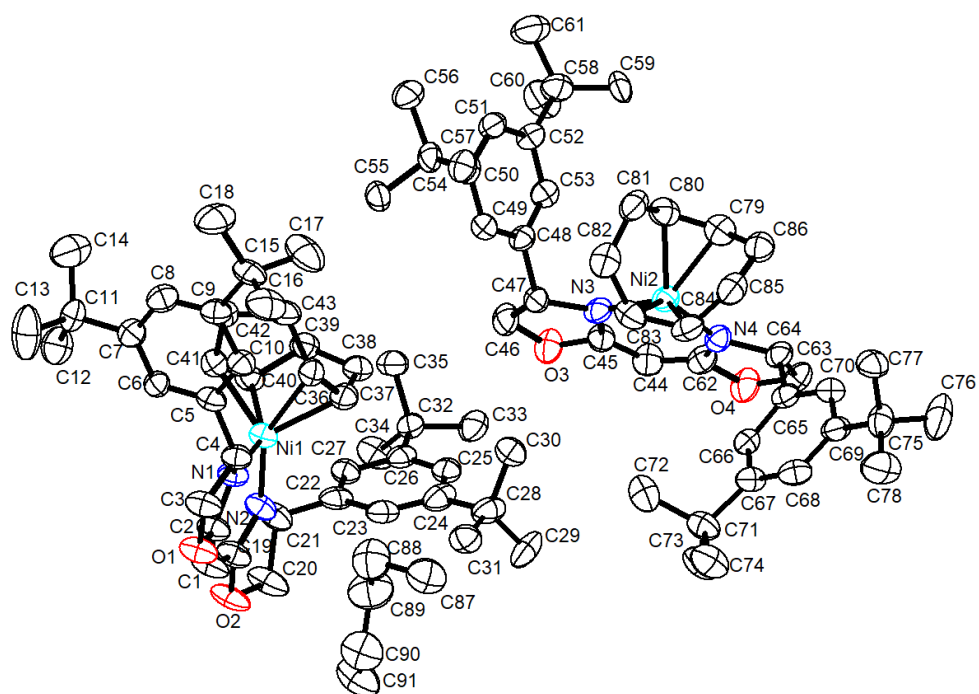


Figure S 27: Thermal ellipsoid plot of Ni_E^{cod} with the anisotropic displacement parameters at the 50% probability level. C–H hydrogen atoms are omitted for clarity.

Table S 13: Crystal data and structure refinement for NiE^{cod} .

Identification code	V21170
Empirical formula	$\text{C}_{45.50}\text{H}_{67}\text{N}_2\text{NiO}_2$
Formula weight	732.72
Temperature	100(2) K
Wavelength	1.54184 Å
Crystal system	orthorhombic
Space group	$P2_12_12_1$
Absolute configuration	S,S
Unit cell dimensions	$a = 14.4618(7)$ Å $a = 90^\circ$ $b = 18.1767(9)$ Å $b = 90^\circ$ $c = 31.1025(14)$ Å $g = 90^\circ$
Volume	$8175.8(7)$ Å ³
Z	8
Density (calculated)	1.191 Mg/m ³
Absorption coefficient	0.964 mm ⁻¹
F(000)	3184
Crystal size	0.100 x 0.150 x 0.200 mm ³
Theta range for data collection	2.82 to 66.57°
Index ranges	$-17 \leq h \leq 17$, $-21 \leq k \leq 21$, $-37 \leq l \leq 37$
Reflections collected	95602
Independent reflections	14429 [R(int) = 0.1619]
Completeness	100.0%
Absorption correction	Multi-scan
Max. and min. transmission	0.9100 and 0.8310
Refinement method	Full-matrix least-squares on F ²
Data / restraints / parameters	14429 / 31 / 1117

Goodness-of-fit on F^2	1.012
Final R indices [$I > 2\sigma(I)$]	R1 = 0.0689, wR2 = 0.1659
R indices (all data)	R1 = 0.0987, wR2 = 0.1850
Largest diff. peak and hole	0.501 and -0.506 \AA^{-3}
Flack parameter	-0.02(2)

Table S 14: Bond lengths [Å] for NiE^{cod}.

Ni1-N2	1.990(6)	Ni1-N1	1.997(6)
Ni1-C37	2.086(8)	Ni1-C36	2.123(8)
Ni1-C41	2.132(8)	Ni1-C40	2.164(7)
Ni2-N4	1.978(6)	Ni2-N3	1.983(6)
Ni2-C79	2.104(9)	Ni2-C83	2.117(8)
Ni2-C80	2.124(7)	Ni2-C84	2.154(7)
O1-C2	1.365(9)	O1-C3	1.439(9)
O2-C19	1.372(8)	O2-C20	1.457(11)
O3-C45	1.397(9)	O3-C46	1.422(9)
O4-C62	1.373(9)	O4-C63	1.432(10)
N1-C2	1.334(9)	N1-C4	1.482(8)
N2-C19	1.342(10)	N2-C21	1.476(9)
N3-C45	1.317(9)	N3-C47	1.490(9)
N4-C62	1.319(10)	N4-C64	1.483(10)
C1-C19	1.365(11)	C1-C2	1.381(10)
C3-C4	1.534(11)	C4-C5	1.510(9)
C5-C6	1.396(11)	C5-C10	1.401(10)
C6-C7	1.384(10)	C7-C8	1.406(11)
C7-C11	1.521(11)	C8-C9	1.368(11)
C9-C10	1.408(10)	C9-C15	1.524(10)
C11-C13	1.522(13)	C11-C14	1.527(13)
C11-C12	1.548(12)	C15-C16	1.516(12)
C15-C17	1.543(14)	C15-C18	1.543(11)
C20-C21	1.538(10)	C21-C22	1.512(12)
C22-C27	1.379(11)	C22-C23	1.396(11)
C23-C24	1.419(13)	C24-C25	1.376(12)
C24-C28	1.527(11)	C25-C26	1.406(11)
C26-C27	1.408(11)	C26-C32	1.518(11)
C28-C29	1.378(19)	C28-C30A	1.399(16)
C28-C31A	1.53(2)	C28-C30	1.533(18)
C28-C31	1.669(19)	C28-C29A	1.72(2)
C32-C34	1.511(11)	C32-C35	1.532(9)
C32-C33	1.532(12)	C36-C37	1.375(10)
C36-C43	1.527(10)	C37-C38	1.521(11)

C38-C39	1.524(11)	C39-C40	1.526(11)
C40-C41	1.367(11)	C41-C42	1.510(10)
C42-C43	1.538(12)	C44-C45	1.378(11)
C44-C62	1.382(12)	C46-C47	1.530(11)
C47-C48	1.507(9)	C48-C49	1.382(10)
C48-C53	1.383(11)	C49-C50	1.416(10)
C50-C51	1.387(11)	C50-C54	1.527(10)
C51-C52	1.401(11)	C52-C53	1.397(10)
C52-C58	1.518(12)	C54-C56A	1.45(5)
C54-C57	1.511(12)	C54-C55	1.511(13)
C54-C56	1.543(12)	C54-C55A	1.57(6)
C54-C57A	1.75(6)	C58-C60A	1.42(3)
C58-C59	1.482(15)	C58-C61	1.517(15)
C58-C60	1.589(16)	C58-C61A	1.59(3)
C58-C59A	1.70(3)	C63-C64	1.524(10)
C64-C65	1.507(10)	C65-C70	1.401(11)
C65-C66	1.403(11)	C66-C67	1.389(10)
C67-C68	1.394(11)	C67-C71	1.550(11)
C68-C69	1.399(12)	C69-C70	1.399(11)
C69-C75	1.52(3)	C69-C75A	1.58(4)
C71-C74	1.487(13)	C71-C73	1.515(12)
C71-C72	1.578(14)	C75-C76	1.52(3)
C75-C78	1.53(2)	C75-C77	1.54(2)
C75A-C76A	1.53(3)	C75A-C78A	1.53(2)
C75A-C77A	1.54(3)	C79-C80	1.374(12)
C79-C86	1.495(12)	C80-C81	1.521(12)
C81-C82	1.523(13)	C82-C83	1.505(11)
C83-C84	1.368(12)	C84-C85	1.509(12)
C85-C86	1.518(13)	C87A-C88A	1.55(3)
C88A-C89A	1.56(3)	C89A-C90A	1.44(3)
C90A-C91A	1.49(3)	C87-C88	1.55(2)
C88-C89	1.56(2)	C89-C90	1.43(2)
C90-C91	1.51(3)		

Table S 15: Bond angles [°] for NiE^{cod}.

N2-Ni1-N1	93.3(2)	N2-Ni1-C37	113.9(3)
N1-Ni1-C37	120.0(3)	N2-Ni1-C36	150.1(3)
N1-Ni1-C36	95.9(3)	C37-Ni1-C36	38.1(3)
N2-Ni1-C41	118.6(3)	N1-Ni1-C41	114.5(3)
C37-Ni1-C41	98.2(3)	C36-Ni1-C41	82.9(3)
N2-Ni1-C40	94.9(3)	N1-Ni1-C40	149.3(3)
C37-Ni1-C40	83.1(3)	C36-Ni1-C40	91.5(3)
C41-Ni1-C40	37.1(3)	N4-Ni2-N3	92.9(2)
N4-Ni2-C79	98.2(3)	N3-Ni2-C79	136.7(3)
N4-Ni2-C83	137.0(3)	N3-Ni2-C83	101.8(3)
C79-Ni2-C83	98.1(3)	N4-Ni2-C80	130.6(3)
N3-Ni2-C80	107.4(3)	C79-Ni2-C80	37.9(3)
C83-Ni2-C80	83.1(3)	N4-Ni2-C84	106.8(3)
N3-Ni2-C84	133.6(3)	C79-Ni2-C84	82.4(3)
C83-Ni2-C84	37.3(3)	C80-Ni2-C84	91.2(3)
C2-O1-C3	107.1(5)	C19-O2-C20	107.2(6)
C45-O3-C46	107.3(5)	C62-O4-C63	107.7(5)
C2-N1-C4	106.5(6)	C2-N1-Ni1	122.8(4)
C4-N1-Ni1	129.7(5)	C19-N2-C21	107.0(6)
C19-N2-Ni1	122.1(5)	C21-N2-Ni1	130.1(5)
C45-N3-C47	107.7(6)	C45-N3-Ni2	122.5(5)
C47-N3-Ni2	129.1(4)	C62-N4-C64	107.5(6)
C62-N4-Ni2	124.0(5)	C64-N4-Ni2	128.3(4)
C19-C1-C2	123.1(7)	N1-C2-O1	115.6(6)
N1-C2-C1	128.2(7)	O1-C2-C1	116.0(6)
O1-C3-C4	104.8(6)	N1-C4-C5	116.3(6)
N1-C4-C3	103.8(5)	C5-C4-C3	109.7(6)
C6-C5-C10	120.0(6)	C6-C5-C4	120.6(6)
C10-C5-C4	119.3(7)	C7-C6-C5	120.8(7)
C6-C7-C8	117.6(7)	C6-C7-C11	121.4(7)
C8-C7-C11	121.0(6)	C9-C8-C7	123.6(7)
C8-C9-C10	117.9(7)	C8-C9-C15	123.1(6)
C10-C9-C15	119.0(7)	C5-C10-C9	120.1(7)
C7-C11-C13	110.6(7)	C7-C11-C14	111.1(8)

C13-C11-C14	110.9(9)	C7-C11-C12	111.9(6)
C13-C11-C12	106.4(8)	C14-C11-C12	105.8(7)
C16-C15-C9	110.5(6)	C16-C15-C17	109.0(9)
C9-C15-C17	108.3(6)	C16-C15-C18	107.4(7)
C9-C15-C18	112.5(8)	C17-C15-C18	109.2(8)
N2-C19-C1	129.2(6)	N2-C19-O2	114.4(7)
C1-C19-O2	116.5(7)	O2-C20-C21	103.1(6)
N2-C21-C22	115.4(6)	N2-C21-C20	104.0(6)
C22-C21-C20	110.7(7)	C27-C22-C23	119.8(8)
C27-C22-C21	120.2(7)	C23-C22-C21	119.9(7)
C22-C23-C24	120.4(8)	C25-C24-C23	117.7(7)
C25-C24-C28	122.6(9)	C23-C24-C28	119.6(8)
C24-C25-C26	123.8(8)	C25-C26-C27	116.4(7)
C25-C26-C32	122.7(7)	C27-C26-C32	120.9(7)
C22-C27-C26	122.0(7)	C29-C28-C24	112.5(10)
C30A-C28-C24	113.8(9)	C30A-C28-C31A	117.9(13)
C24-C28-C31A	109.2(11)	C29-C28-C30	119.1(15)
C24-C28-C30	105.8(8)	C29-C28-C31	105.8(13)
C24-C28-C31	111.4(10)	C30-C28-C31	101.7(10)
C30A-C28-C29A	105.2(12)	C24-C28-C29A	107.8(9)
C31A-C28-C29A	101.6(16)	C34-C32-C26	111.0(7)
C34-C32-C35	109.3(7)	C26-C32-C35	108.9(6)
C34-C32-C33	108.4(7)	C26-C32-C33	112.0(7)
C35-C32-C33	107.2(7)	C37-C36-C43	122.4(7)
C37-C36-Ni1	69.5(4)	C43-C36-Ni1	112.4(5)
C36-C37-C38	124.5(6)	C36-C37-Ni1	72.4(5)
C38-C37-Ni1	111.0(5)	C37-C38-C39	113.5(7)
C38-C39-C40	113.5(6)	C41-C40-C39	122.6(7)
C41-C40-Ni1	70.2(4)	C39-C40-Ni1	110.9(5)
C40-C41-C42	125.3(8)	C40-C41-Ni1	72.7(4)
C42-C41-Ni1	109.9(5)	C41-C42-C43	113.2(6)
C36-C43-C42	112.9(6)	C45-C44-C62	121.1(7)
N3-C45-C44	130.4(7)	N3-C45-O3	114.6(6)
C44-C45-O3	114.9(6)	O3-C46-C47	106.0(6)
N3-C47-C48	114.5(6)	N3-C47-C46	103.7(5)
C48-C47-C46	111.5(6)	C49-C48-C53	120.2(6)

C49-C48-C47	119.2(7)	C53-C48-C47	120.5(6)
C48-C49-C50	120.4(7)	C51-C50-C49	118.2(6)
C51-C50-C54	122.0(6)	C49-C50-C54	119.7(7)
C50-C51-C52	122.0(6)	C53-C52-C51	118.1(7)
C53-C52-C58	120.9(7)	C51-C52-C58	121.0(6)
C48-C53-C52	121.0(7)	C57-C54-C55	111.1(8)
C56A-C54-C50	113.(3)	C57-C54-C50	108.9(6)
C55-C54-C50	110.0(6)	C57-C54-C56	107.4(7)
C55-C54-C56	107.6(7)	C50-C54-C56	111.8(7)
C56A-C54-C55A	118.(3)	C50-C54-C55A	114.1(18)
C56A-C54-C57A	99.(3)	C50-C54-C57A	111.7(16)
C55A-C54-C57A	97.(3)	C59-C58-C61	111.7(11)
C60A-C58-C52	118.4(15)	C59-C58-C52	110.5(8)
C61-C58-C52	113.1(9)	C59-C58-C60	109.2(11)
C61-C58-C60	105.0(10)	C52-C58-C60	107.0(8)
C60A-C58-C61A	108.7(18)	C52-C58-C61A	115.7(14)
C60A-C58-C59A	107.6(18)	C52-C58-C59A	106.3(12)
C61A-C58-C59A	97.7(18)	N4-C62-O4	114.6(7)
N4-C62-C44	128.8(7)	O4-C62-C44	116.6(6)
O4-C63-C64	104.9(6)	N4-C64-C65	111.2(6)
N4-C64-C63	103.7(6)	C65-C64-C63	114.2(5)
C70-C65-C66	118.8(6)	C70-C65-C64	120.9(7)
C66-C65-C64	120.3(7)	C67-C66-C65	121.0(7)
C66-C67-C68	119.0(7)	C66-C67-C71	119.0(7)
C68-C67-C71	121.9(7)	C67-C68-C69	121.5(7)
C70-C69-C68	118.5(7)	C70-C69-C75	122.1(11)
C68-C69-C75	119.1(11)	C70-C69-C75A	114.0(13)
C68-C69-C75A	127.2(12)	C69-C70-C65	121.1(7)
C74-C71-C73	111.0(7)	C74-C71-C67	114.7(8)
C73-C71-C67	109.6(7)	C74-C71-C72	106.1(8)
C73-C71-C72	107.7(8)	C67-C71-C72	107.4(7)
C76-C75-C69	106.0(19)	C76-C75-C78	112.(2)
C69-C75-C78	114.3(17)	C76-C75-C77	106.9(18)
C69-C75-C77	111.2(18)	C78-C75-C77	106.5(18)
C76A-C75A-C78A	108.(2)	C76A-C75A-C77A	111.(3)
C78A-C75A-C77A	108.(3)	C76A-C75A-C69	117.(3)

C78A-C75A-C69	111.(2)	C77A-C75A-C69	100.(2)
C80-C79-C86	126.0(7)	C80-C79-Ni2	71.8(5)
C86-C79-Ni2	110.7(6)	C79-C80-C81	123.9(7)
C79-C80-Ni2	70.3(5)	C81-C80-Ni2	111.8(6)
C80-C81-C82	114.1(6)	C83-C82-C81	114.0(7)
C84-C83-C82	123.6(7)	C84-C83-Ni2	72.8(5)
C82-C83-Ni2	110.5(6)	C83-C84-C85	123.2(7)
C83-C84-Ni2	69.9(5)	C85-C84-Ni2	110.8(5)
C84-C85-C86	114.2(7)	C79-C86-C85	112.8(7)
C87A-C88A-C89A	115.(3)	C90A-C89A-C88A	115.(3)
C89A-C90A-C91A	113.(2)	C87-C88-C89	110.7(15)
C90-C89-C88	116.4(17)	C89-C90-C91	113.8(19)

Table S 16: Torsion angles [°] for NiE^{cod}.

C4-N1-C2-O1	5.1(9)	Ni1-N1-C2-O1	174.9(5)
C4-N1-C2-C1	-170.6(9)	Ni1-N1-C2-C1	-0.8(13)
C3-O1-C2-N1	4.9(10)	C3-O1-C2-C1	-178.8(8)
C19-C1-C2-N1	8.6(15)	C19-C1-C2-O1	-167.1(8)
C2-O1-C3-C4	-12.2(9)	C2-N1-C4-C5	-132.7(7)
Ni1-N1-C4-C5	58.4(10)	C2-N1-C4-C3	-12.1(8)
Ni1-N1-C4-C3	179.0(5)	O1-C3-C4-N1	14.7(8)
O1-C3-C4-C5	139.7(7)	N1-C4-C5-C6	47.3(10)
C3-C4-C5-C6	-70.0(9)	N1-C4-C5-C10	-137.3(7)
C3-C4-C5-C10	105.3(8)	C10-C5-C6-C7	0.3(11)
C4-C5-C6-C7	175.6(7)	C5-C6-C7-C8	-1.9(11)
C5-C6-C7-C11	179.6(7)	C6-C7-C8-C9	2.5(12)
C11-C7-C8-C9	-178.9(7)	C7-C8-C9-C10	-1.4(12)
C7-C8-C9-C15	178.0(7)	C6-C5-C10-C9	0.8(11)
C4-C5-C10-C9	-174.5(7)	C8-C9-C10-C5	-0.3(11)
C15-C9-C10-C5	-179.7(7)	C6-C7-C11-C13	95.5(10)
C8-C7-C11-C13	-83.1(11)	C6-C7-C11-C14	-140.9(8)
C8-C7-C11-C14	40.5(10)	C6-C7-C11-C12	-22.9(11)
C8-C7-C11-C12	158.5(8)	C8-C9-C15-C16	123.3(9)
C10-C9-C15-C16	-57.3(11)	C8-C9-C15-C17	-117.4(9)
C10-C9-C15-C17	62.0(10)	C8-C9-C15-C18	3.4(12)
C10-C9-C15-C18	-177.2(8)	C21-N2-C19-C1	-178.2(9)
Ni1-N2-C19-C1	-7.6(13)	C21-N2-C19-O2	2.4(10)
Ni1-N2-C19-O2	173.0(5)	C2-C1-C19-N2	-3.8(16)
C2-C1-C19-O2	175.6(8)	C20-O2-C19-N2	11.4(10)
C20-O2-C19-C1	-168.1(8)	C19-O2-C20-C21	-19.2(10)
C19-N2-C21-C22	-135.8(7)	Ni1-N2-C21-C22	54.7(10)
C19-N2-C21-C20	-14.3(9)	Ni1-N2-C21-C20	176.1(6)
O2-C20-C21-N2	20.2(9)	O2-C20-C21-C22	144.7(7)
N2-C21-C22-C27	-139.7(6)	C20-C21-C22-C27	102.5(8)
N2-C21-C22-C23	44.4(9)	C20-C21-C22-C23	-73.4(8)
C27-C22-C23-C24	0.9(10)	C21-C22-C23-C24	176.9(6)
C22-C23-C24-C25	-0.5(10)	C22-C23-C24-C28	177.5(6)
C23-C24-C25-C26	-0.5(10)	C28-C24-C25-C26	-178.4(6)

C24-C25-C26-C27	1.0(9)	C24-C25-C26-C32	178.9(6)
C23-C22-C27-C26	-0.4(9)	C21-C22-C27-C26	-176.3(6)
C25-C26-C27-C22	-0.5(9)	C32-C26-C27-C22	-178.4(6)
C25-C24-C28-C29	-65.7(17)	C23-C24-C28-C29	116.5(16)
C25-C24-C28-C30A	113.7(12)	C23-C24-C28-C30A	-64.1(13)
C25-C24-C28-C31A	-112.2(16)	C23-C24-C28-C31A	70.0(16)
C25-C24-C28-C30	66.0(11)	C23-C24-C28-C30	-111.8(11)
C25-C24-C28-C31	175.7(8)	C23-C24-C28-C31	-2.1(11)
C25-C24-C28-C29A	-2.5(12)	C23-C24-C28-C29A	179.6(10)
C25-C26-C32-C34	136.4(7)	C27-C26-C32-C34	-45.9(8)
C25-C26-C32-C35	-103.2(8)	C27-C26-C32-C35	74.5(8)
C25-C26-C32-C33	15.1(9)	C27-C26-C32-C33	-167.2(6)
C43-C36-C37-C38	-0.3(12)	Ni1-C36-C37-C38	103.8(8)
C43-C36-C37-Ni1	-104.1(7)	C36-C37-C38-C39	-51.1(10)
Ni1-C37-C38-C39	31.5(7)	C37-C38-C39-C40	-27.9(9)
C38-C39-C40-C41	90.2(8)	C38-C39-C40-Ni1	10.9(8)
C39-C40-C41-C42	-0.2(12)	Ni1-C40-C41-C42	102.5(8)
C39-C40-C41-Ni1	-102.7(7)	C40-C41-C42-C43	-50.2(10)
Ni1-C41-C42-C43	32.3(8)	C37-C36-C43-C42	90.8(9)
Ni1-C36-C43-C42	11.6(8)	C41-C42-C43-C36	-29.2(10)
C47-N3-C45-C44	-176.2(8)	Ni2-N3-C45-C44	-4.5(12)
C47-N3-C45-O3	3.2(8)	Ni2-N3-C45-O3	174.9(5)
C62-C44-C45-N3	5.4(14)	C62-C44-C45-O3	-174.1(7)
C46-O3-C45-N3	2.2(9)	C46-O3-C45-C44	-178.3(7)
C45-O3-C46-C47	-6.4(8)	C45-N3-C47-C48	-128.5(6)
Ni2-N3-C47-C48	60.6(8)	C45-N3-C47-C46	-6.8(8)
Ni2-N3-C47-C46	-177.8(5)	O3-C46-C47-N3	7.9(8)
O3-C46-C47-C48	131.6(7)	N3-C47-C48-C49	-138.0(7)
C46-C47-C48-C49	104.7(8)	N3-C47-C48-C53	44.4(9)
C46-C47-C48-C53	-72.9(9)	C53-C48-C49-C50	-0.3(11)
C47-C48-C49-C50	-177.9(7)	C48-C49-C50-C51	-0.4(11)
C48-C49-C50-C54	-177.1(6)	C49-C50-C51-C52	1.1(11)
C54-C50-C51-C52	177.7(7)	C50-C51-C52-C53	-0.9(11)
C50-C51-C52-C58	-179.0(7)	C49-C48-C53-C52	0.5(11)
C47-C48-C53-C52	178.1(7)	C51-C52-C53-C48	0.1(11)
C58-C52-C53-C48	178.2(7)	C51-C50-C54-C56A	-55.(3)

C49-C50-C54-C56A	122.(2)	C51-C50-C54-C57	-103.3(9)
C49-C50-C54-C57	73.2(9)	C51-C50-C54-C55	134.7(8)
C49-C50-C54-C55	-48.8(9)	C51-C50-C54-C56	15.2(10)
C49-C50-C54-C56	-168.3(7)	C51-C50-C54-C55A	85.(2)
C49-C50-C54-C55A	-99.(2)	C51-C50-C54-C57A	-166.1(19)
C49-C50-C54-C57A	10.(2)	C53-C52-C58-C60A	116.2(17)
C51-C52-C58-C60A	-65.8(18)	C53-C52-C58-C59	-61.6(12)
C51-C52-C58-C59	116.4(10)	C53-C52-C58-C61	172.3(10)
C51-C52-C58-C61	-9.7(14)	C53-C52-C58-C60	57.2(11)
C51-C52-C58-C60	-124.8(10)	C53-C52-C58-C61A	-15.4(18)
C51-C52-C58-C61A	162.6(16)	C53-C52-C58-C59A	-122.7(14)
C51-C52-C58-C59A	55.3(15)	C64-N4-C62-O4	-4.3(9)
Ni2-N4-C62-O4	-179.8(5)	C64-N4-C62-C44	174.0(8)
Ni2-N4-C62-C44	-1.6(12)	C63-O4-C62-N4	-4.3(9)
C63-O4-C62-C44	177.2(7)	C45-C44-C62-N4	-1.9(14)
C45-C44-C62-O4	176.4(8)	C62-O4-C63-C64	10.6(8)
C62-N4-C64-C65	-112.7(7)	Ni2-N4-C64-C65	62.6(7)
C62-N4-C64-C63	10.4(8)	Ni2-N4-C64-C63	-174.3(5)
O4-C63-C64-N4	-12.6(7)	O4-C63-C64-C65	108.6(7)
N4-C64-C65-C70	-138.2(7)	C63-C64-C65-C70	104.9(8)
N4-C64-C65-C66	42.5(8)	C63-C64-C65-C66	-74.4(9)
C70-C65-C66-C67	3.5(10)	C64-C65-C66-C67	-177.1(6)
C65-C66-C67-C68	-2.5(10)	C65-C66-C67-C71	174.2(6)
C66-C67-C68-C69	-0.5(11)	C71-C67-C68-C69	-177.2(7)
C67-C68-C69-C70	2.4(11)	C67-C68-C69-C75	175.6(14)
C67-C68-C69-C75A	-171.2(17)	C68-C69-C70-C65	-1.4(11)
C75-C69-C70-C65	-174.4(15)	C75A-C69-C70-C65	173.1(14)
C66-C65-C70-C69	-1.5(10)	C64-C65-C70-C69	179.1(6)
C66-C67-C71-C74	-176.0(8)	C68-C67-C71-C74	0.6(11)
C66-C67-C71-C73	58.4(9)	C68-C67-C71-C73	-125.0(8)
C66-C67-C71-C72	-58.4(9)	C68-C67-C71-C72	118.3(8)
C70-C69-C75-C76	-56.(2)	C68-C69-C75-C76	131.3(14)
C70-C69-C75-C78	-179.3(15)	C68-C69-C75-C78	8.(3)
C70-C69-C75-C77	60.(3)	C68-C69-C75-C77	-112.9(16)
C70-C69-C75A-C76A	-18.(3)	C68-C69-C75A-C76A	156.(2)
C70-C69-C75A-C78A	-143.(2)	C68-C69-C75A-C78A	31.(3)

C70-C69-C75A-C77A	102.(3)	C68-C69-C75A-C77A	-84.(3)
C86-C79-C80-C81	0.7(13)	Ni2-C79-C80-C81	103.6(8)
C86-C79-C80-Ni2	-102.8(8)	C79-C80-C81-C82	-86.9(10)
Ni2-C80-C81-C82	-6.7(9)	C80-C81-C82-C83	23.4(10)
C81-C82-C83-C84	54.1(11)	C81-C82-C83-Ni2	-28.4(9)
C82-C83-C84-C85	-1.3(13)	Ni2-C83-C84-C85	102.2(7)
C82-C83-C84-Ni2	-103.5(8)	C83-C84-C85-C86	-90.8(9)
Ni2-C84-C85-C86	-11.8(8)	C80-C79-C86-C85	48.9(11)
Ni2-C79-C86-C85	-33.2(8)	C84-C85-C86-C79	29.9(9)
C87A-C88A-C89A-C90A	63.(5)	C88A-C89A-C90A-C91A	-176.(4)
C87-C88-C89-C90	70.(3)	C88-C89-C90-C91	177.(2)

2.5. References

- (1) For examples, see the following: Top Pharmaceuticals Poster. <https://njardarson.lab.arizona.edu/content/top-pharmaceuticals-poster> (accessed July 10, 2022).
- (2) Kohler, M. C.; Wengryniuk, S. E.; Coltart, D. M. Asymmetric α -Alkylation of Aldehydes, Ketones, and Carboxylic Acids. In *Stereoselective Synthesis of Drugs and Natural Products*; Andrushko, V., Andrushko, N., Eds.; John Wiley & Sons, 2014; Vol. 1, pp 183–213.
- (3) Fischer, C.; Fu, G. C. Asymmetric Nickel-Catalyzed Negishi Cross-Couplings of Secondary α -Bromo Amides with Organozinc Reagents. *J. Am. Chem. Soc.* **2005**, *127*, 4594–4595.
- (4) Wang, Z.; Yin, H.; Fu, G. C. Catalytic Enantioconvergent Coupling of Secondary and Tertiary Electrophiles with Olefins. *Nature* **2018**, *563*, 379–383.
- (5) Dugger, R. W.; Ragan, J. A.; Ripin, D. H. B. Survey of GMP Bulk Reactions Run in a Research Facility between 1985 and 2002. *Org. Process Res. Dev.* **2005**, *9*, 253–258.
- (6) Marco, J. A.; Carda, M.; Murga, J.; Falomir, E. Selected Diastereoselective Reactions: Enolate Alkylation. In *Comprehensive Chirality*; Carreira, E. M., Yamamoto, H., Eds.; Academic, 2012; Vol. 2, Chapter 2.14.
- (7) Evans, D. A. Stereoselective Alkylation Reactions of Chiral Metal Enolates. In *Asymmetric Synthesis*; Morrison, J. D., Ed.; Academic, 1984; Vol. 3, pp 1–110.

- (8) Myers, A. G.; Yang, B. H.; Chen, H.; Gleason, J. L. Use of Pseudoephedrine as a Practical Chiral Auxiliary for Asymmetric Synthesis. *J. Am. Chem. Soc.* **1994**, *116*, 9361–9362.
- (9) Heravi, M. M.; Zadsirjan, V.; Farajpour, B. Applications of Oxazolidinones as Chiral Auxiliaries in the Asymmetric Alkylation Reaction Applied to Total Synthesis. *RSC Adv.* **2016**, *6*, 30498–30551.
- (10) Wang, X.-J., et al. Asymmetric Synthesis of LFA-1 Inhibitor BIRT2584 on Metric Ton Scale. *Org. Process Res. Dev.* **2011**, *15*, 1185–1191.
- (11) Wright, T. B.; Evans, P. A. Catalytic Enantioselective Alkylation of Prochiral Enolates. *Chem. Rev.* **2021**, *121*, 9196–9242.
- (12) Vargová, D.; Némethová, I.; Plevová, K.; Šebesta, R. Asymmetric Transition-Metal Catalysis in the Formation and Functionalization of Metal Enolates. *ACS Catal.* **2019**, *9*, 3104–3143.
- (13) Remes, M.; Vesely, J. α -Alkylation of Carbonyl Compounds. In *Stereoselective Organocatalysis*; Rios Torres, R., Ed.; John Wiley & Sons, 2013; pp 267–312.
- (14) Shirakawa, S.; Moteki, S. A.; Maruoka, K. Asymmetric Phase-Transfer Catalysis. In *Modern Tools for the Synthesis of Complex Bioactive Molecules*; Cossy, J., Arseniyadis, S., Eds.; John Wiley & Sons, 2013; pp 213–242.
- (15) Oliver, S.; Evans, P. A. Transition-Metal-Catalyzed Allylic Substitution Reactions: Stereoselective Construction of α - and β -Substituted Carbonyl Compounds. *Synthesis* **2013**, *45*, 3179–3198

- (16) Lombardo, M.; Trombini, C. The Chemistry of Zinc Enolates. In *The Chemistry of Functional Groups. The Chemistry of Organozinc Compounds*; Rappoport, Z., Marek, I., Eds.; John Wiley & Sons, 2007; Chapter 18.
- (17) Hama, T.; Liu, X.; Culkin, D. A.; Hartwig, J. F. Palladium-Catalyzed α -Arylation of Esters and Amides Under More Neutral Conditions. *J. Am. Chem. Soc.* **2003**, *125*, 11176–11177.
- (18) Choi, J.; Fu, G. C. Transition Metal-Catalyzed Alkyl–Alkyl Bond Formation: Another Dimension in Cross-Coupling Chemistry. *Science* **2017**, *356*, eaaf7230.
- (19) Fu, G. C. Transition-Metal Catalysis of Nucleophilic Substitution Reactions: a Radical Alternative to S_N1 and S_N2 Processes. *ACS Cent. Sci.* **2017**, *3*, 692–700.
- (20) One of the roles of the triamine may be to accelerate/drive the transmetalation of the nucleophile from zinc to nickel. See the following: Hu, Z.; Wei, X.-J.; Handelmann, J.; Seitz, A.-K.; Rodstein, I.; Gessner, V. H.; Gooßen, L. J. Coupling of Reformatsky Reagents with Aryl Chlorides Enabled by Ylide-Functionalized Phosphine Ligands. *Angew. Chem., Int. Ed.* **2021**, *60*, 6778–6783.
- (21) Zhou, Y.; Keresztes, I.; MacMillan, S. N.; Collum, D. B. Disodium Salts of Pseudoephedrine-Derived Myers Enolates: Stereoselectivity and Mechanism of Alkylation. *J. Am. Chem. Soc.* **2019**, *141*, 16865–16876.
- (22) Algera, R. F.; Ma, Y.; Collum, D. B. Sodium Diisopropylamide in Tetrahydrofuran: Selectivities, Rates, and Mechanisms of Alkene and Diene Isomerizations and Metalations. *J. Am. Chem. Soc.* **2017**, *139*, 11544–11549.

- (23) Hoshino, J., et al. Synthesis of Optically Active Azetidine-2,4-Dicarboxylic Acid and Related Chiral Auxiliaries for Asymmetric Synthesis. *J. Chem. Soc. Perkin Trans. I* **1995**, 693–697.
- (24) Liu, C.; Achtenhagen, M.; Szostak, M. Chemoselective Ketone Synthesis by the Addition of Organometallics to *N*-Acylazetidines. *Org. Lett.* **2016**, *18*, 2375–2378.
- (25) Cordier, C. J.; Lundgren, R. J.; Fu, G. C. Enantioconvergent Cross-Couplings of Racemic Alkylmetal Reagents with Unactivated Secondary Alkyl Electrophiles: Catalytic Asymmetric Negishi α -Alkylations of *N*-Boc-Pyrrolidine. *J. Am. Chem. Soc.* **2013**, *135*, 10946–10949.
- (26) Huo, H.; Gorsline, B. J.; Fu, G. C. Catalyst-Controlled Doubly Enantioconvergent Coupling of Racemic Alkyl Nucleophiles and Electrophiles. *Science* **2020**, *367*, 559–564.
- (27) Garner, L. E., et al. Cationic Zinc Enolates as Highly Active Catalysts for Acrylate Polymerization. *J. Am. Chem. Soc.* **2006**, *128*, 14822–14823.
- (28) Greco, J. F.; McNevin, M. J.; Shoemaker, R. K.; Hagadorn, J. R. Solid- and Solution-Phase Structures of Zinc Enolates of Amides and Ketones. *Organometallics* **2008**, *27*, 1948–1953.
- (29) Hlavinka, M. L.; Hagadorn, J. R. The First Structural Characterization of α -Zincated (Reformatsky) Amides and Phosphine Oxides. *Organometallics* **2005**, *24*, 4116–4118.
- (30) Schley, N. D.; Fu, G. C. Nickel-Catalyzed Negishi Arylations of Propargylic Bromides: a Mechanistic Investigation. *J. Am. Chem. Soc.* **2014**, *136*, 16588–16593.

- (31) Yin, H.; Fu, G. C. Mechanistic Investigation of Enantioconvergent Kumada Reactions of Racemic α -Bromoketones Catalyzed by a Nickel/Bis(oxazoline) Complex. *J. Am. Chem. Soc.* **2019**, *141*, 15433–15440.
- (32) Eckert, N. A.; Bones, E. M.; Lachicotte, R. J.; Holland, P. L. Nickel Complexes of a Bulky β -Diketiminato Ligand. *Inorg. Chem.* **2003**, *42*, 1720–1725.
- (33) Luszyk, J., et al. Kinetics for the Reaction of a Secondary Alkyl Radical with Tri-*n*-butylgermanium Hydride and Calibration of a Secondary Alkyl Radical Clock Reaction. *J. Org. Chem.* **1987**, *52*, 3509–3514.
- (34) Anslyn, E. V.; Dougherty, D. A. *Modern Physical Organic Chemistry*; University Science Books, 2006; pp 155–157.
- (35) Zuo, Z.; Cong, H.; Li, W.; Choi, J.; Fu, G. C.; MacMillan, D. W. C. Enantioselective Decarboxylative Arylation of α -Amino Acids via the Merger of Photoredox and Nickel Catalysis. *J. Am. Chem. Soc.* **2016**, *138*, 1832–1835.
- (36) Gonçalves, C. R.; Lemmerer, M.; Teskey, C. J.; Adler, P.; Kaiser, D.; Maryasin, B.; González, L.; Maulide, N. Unified Approach to the Chemoselective α -Functionalization of Amides with Heteroatom Nucleophiles. *J. Am. Chem. Soc.* **2019**, *141*, 18437–18443.
- (37) Vargas-Sanchez, M.; Lakhdar, S.; Couty, F.; Evano, G. Reaction of Azetidines with Chloroformates. *Org. Lett.* **2006**, *8*, 5501–5504.

[Intentionally Redacted]

Chapter 4: Iron-Catalyzed Reductive Cross-Coupling of

Alkyl Electrophiles with Olefins

Adapted in part with permission from:

Tong, X.; Yang, Z.; Del Angel Aguillar, C. E.; Fu, G. C. Iron-Catalyzed Reductive Cross-Coupling of Alkyl Electrophiles with Olefins, *Angew. Chem. Int. Ed.* **2023**, *62*, e202306663.

© 2023 John Wiley and Sons

4.1. Introduction

Transition-metal catalysis has revolutionized the synthesis of organic molecules.¹ Whereas second-row transition metals (e.g., rhodium, ruthenium, and palladium) were exploited in many of the early breakthroughs,² recent efforts have increasingly focused on first-row metals (e.g., nickel and copper), which are often less expensive and less toxic.³ The development of catalysts based on iron is particularly attractive, due to its virtues of being by far the most abundant transition metal, as well as being minimally toxic (an essential mineral, found in hemoglobin and myoglobin) (**Figure 4.1A**).⁴

Because carbon–carbon bond construction is pivotal for organic synthesis, the development of palladium catalysts to reliably achieve couplings of organic electrophiles with organic nucleophiles (usually, aryl–aryl couplings) has been transformative, as recognized by the Nobel Prize in Chemistry in 2010.^{2c,5} More recently, nickel has emerged from the shadow of its congener and proved to be more effective than palladium for cross-couplings to form alkyl–alkyl

bonds,⁶ including enantioselective processes,⁷ thereby providing an “escape from flatland”.⁸ Although catalysis of alkyl–alkyl cross-couplings by iron would be even more attractive than nickel from the standpoints of cost and toxicity,^{3,4} progress to date has been quite limited, with most of the methods requiring Grignard reagents, which have relatively poor functional-group compatibility, as the nucleophile (**Figure 4.1B**).⁹

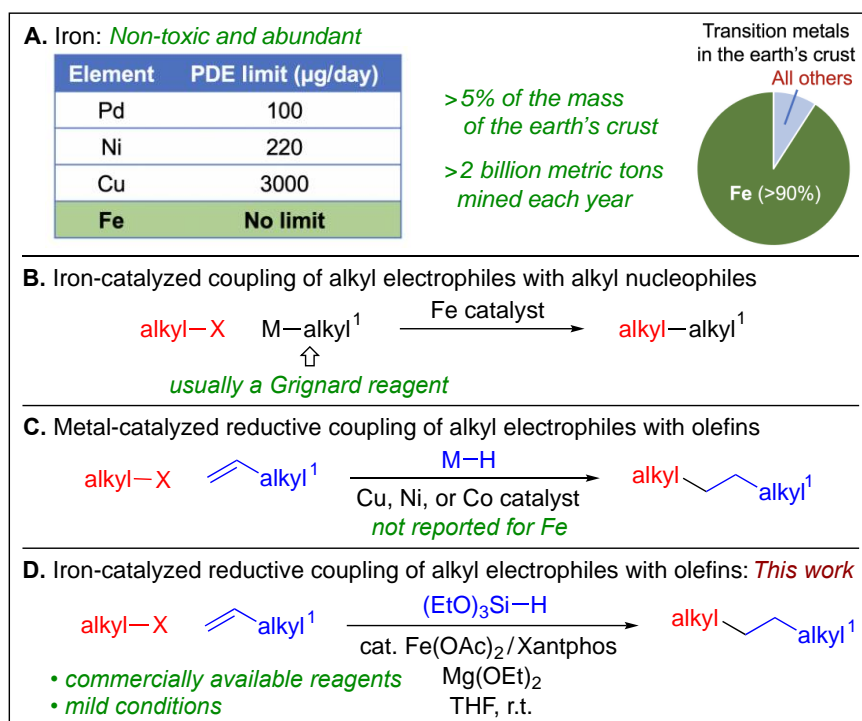


Figure 4.1. Background. (A) Iron: Minimal toxicity and abundant. (B) Iron-catalyzed coupling of alkyl electrophiles with alkyl nucleophiles. (C) Metal-catalyzed reductive coupling of alkyl electrophiles with olefins. (D) Iron-catalyzed reductive coupling of alkyl electrophiles with olefins: *This work*. PDE: permitted daily exposure.

A number of laboratories have recently reported that, for certain metal-catalyzed cross-couplings of alkyl electrophiles, the organometallic nucleophile can be replaced with an olefin in combination with a hydride reagent (**Figure 4.1C**). To our knowledge, copper,¹⁰ nickel,¹¹ and

cobalt¹²—but not iron—catalysts have been shown to be capable of achieving such alkyl–alkyl couplings.^{13,14,15}

In this report, we remedy this deficiency, describing an iron-based catalyst that couples alkyl electrophiles with olefins in the presence of a hydrosilane (**Figure 4.1D**); the method utilizes commercially available reaction components and operates under mild and convenient conditions (room temperature). Our mechanistic observations are consistent with the generation of an organic radical from the alkyl electrophile and with olefin binding to iron and insertion of the olefin into an iron–hydride intermediate being reversible.

4.2. Results and Discussion

As noted above, Grignard reagents are employed as the nucleophilic partner in most of the iron-catalyzed alkyl–alkyl cross-couplings that have been described to date.⁹ Building on these observations that an iron catalyst active for alkyl–alkyl bond formation can be accessed in the presence of a Grignard reagent, we were able to develop a first-generation method for our targeted process, the reductive cross-coupling of an alkyl electrophile with an olefin in the presence of a hydrosilane (**Figure 4.2A**, entry 1).¹⁶ Under these conditions, the Grignard reagent is necessary for the formation of the desired product (entry 2), although it does not itself serve as a nucleophilic coupling partner (<1 % yield of **A**), and KF is beneficial (entry 3).

In view of the relatively poor functional-group compatibility of Grignard reagents, we sought to develop a second-generation method that does not require a Grignard reagent. Unfortunately, replacement with milder arylmetal reagents or with reducing agents does not furnish an iron catalyst that achieves the desired coupling (**Figure 4.2A**, entries 4 and 5).

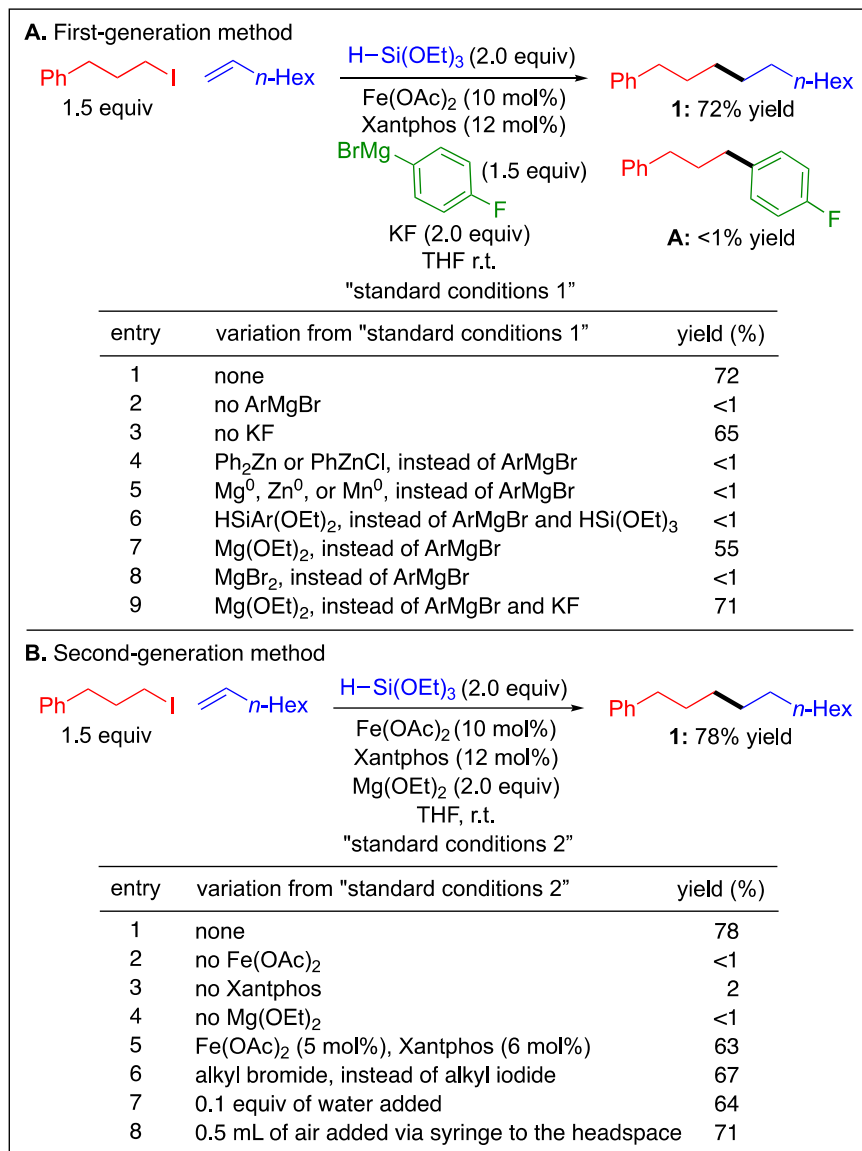


Figure 4.2. The development of iron-catalyzed reductive cross-couplings of alkyl electrophiles with olefins. (A) First-generation method. (B) Second-generation method.

We postulated that the lack of cross-coupling of the Grignard reagent with the alkyl electrophile (**Figure 4.2A**, compound **A**) might be due to a relatively rapid reaction of the Grignard reagent with HSi(OEt)₃. Indeed, when the two are mixed (ArMgBr : HSi(OEt)₃=1.00 : 1.33; Ar=4-fluorophenyl) in THF at r.t., ¹⁹F NMR spectroscopy shows that the Grignard reagent is consumed

within 5 min, with HSiAr(OEt)₂ being the predominant fluorine-containing product. Although the use of HSiAr(OEt)₂ in place of ArMgBr/HSi(OEt)₃ does not lead to the desired product (entry 6), the use of Mg(OEt)₂ in place of ArMgBr does furnish a substantial amount of alkyl–alkyl coupling (entry 7; on the other hand, MgBr₂ is not effective: entry 8). Under these conditions, omitting KF is beneficial, providing the cross-coupled product in 71 % yield (entry 9).

Our second-generation method (**Figure 4.2B**), which is comprised of commercially available components, is simpler and milder than our first-generation method (**Figure 4.2A**). The effects of several parameters on the newer method are provided in **Figure 4.2B**. Control experiments establish that virtually no cross-coupling is observed in the absence of Fe(OAc)₂,¹⁷ Xantphos, or Mg(OEt)₂ (entries 2–4), and only a small drop in yield occurs when the catalyst loading is reduced in half (entry 5) or when the corresponding alkyl bromide is used as the electrophile (entry 6). The reaction is not highly sensitive to water or to air (entries 7 and 8).

We have examined the scope of this new iron-catalyzed reductive cross-coupling of alkyl electrophiles with olefins, and we have determined that terminal olefins with widely varying steric demand (*n*-hexyl→*t*-butyl) serve as suitable reaction partners (**Figure 4.3**, entries 1–4). Moreover, a 1,1-disubstituted olefin can be coupled with reasonable efficiency (entry 5; under our standard conditions, cyclohexene and styrene are not suitable substrates: <10 % yield). The method is compatible with functional groups such as a silyl ether, an acetal, and an arylboronate ester (entries 6–8). On a gram scale, a similar yield is obtained as for a coupling conducted on a 1.0-mmol scale (entry 1).

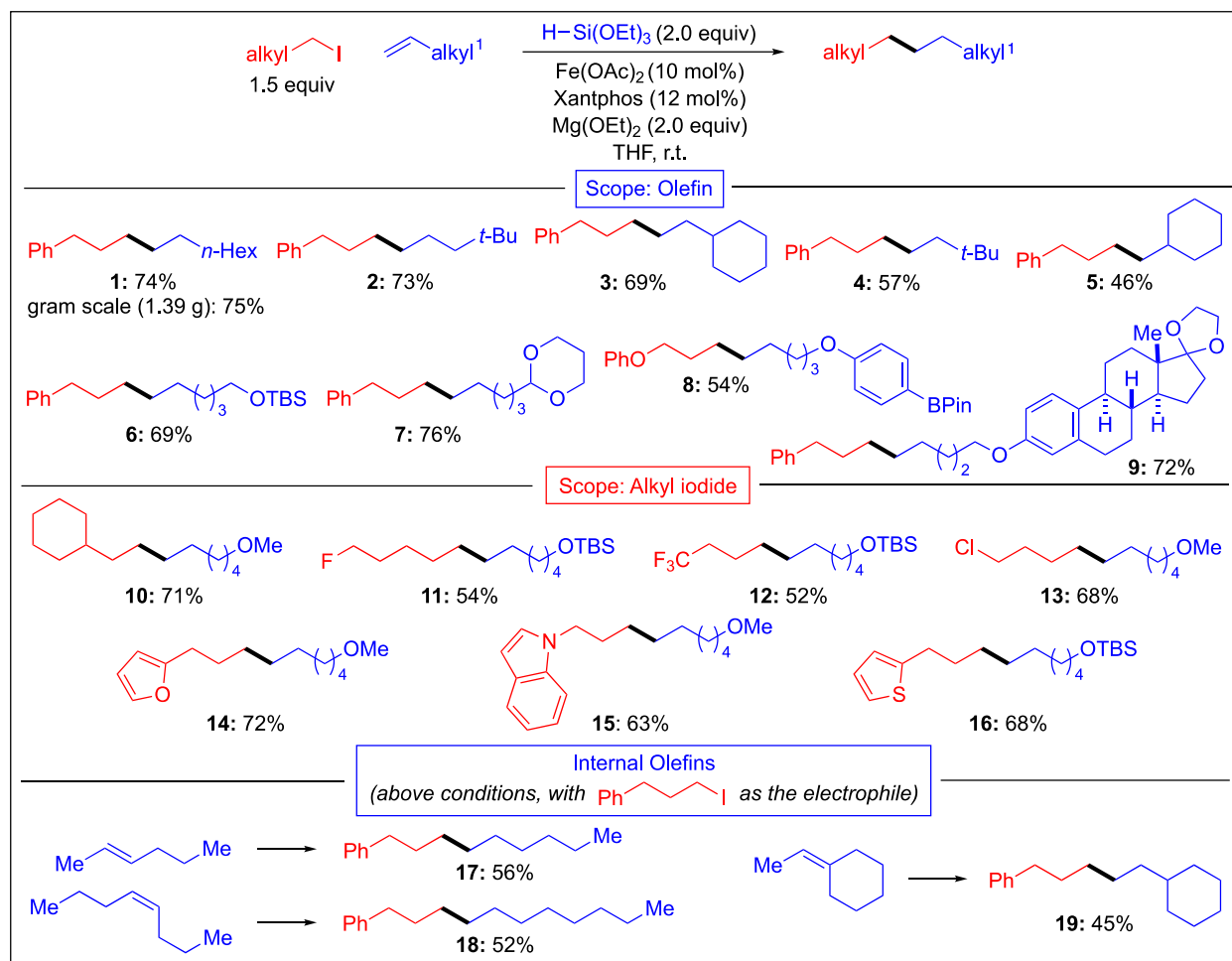


Figure 4.3. Scope of the iron-catalyzed reductive cross-coupling of alkyl electrophiles with olefins. Couplings were conducted on a 1.0-mmol scale (unless otherwise noted), and yields represent purified products.

With regard to the electrophile, the alkyl iodide can bear a variety of functional groups, including an alkyl fluoride, a trifluoromethyl group, and an alkyl chloride (**Figure 4.3**, entries 11–13), as well as an oxygen, nitrogen, or sulfur heterocycle (entries 14–16). Under our standard conditions, cyclohexyl iodide, a secondary electrophile, undergoes alkylation in <10 % yield.

The reductive coupling of an alkyl iodide with an acyclic 1,2-disubstituted olefin, such as *trans*-2-hexene or *cis*-4-octene, leads to *n*-alkylation (**Figure 4.2**, entries 17 and

18).¹⁸ Interestingly, even a trisubstituted olefin, ethylidenecyclohexane, can engage in reductive cross-coupling after chain-walking (entry 19).

We have carried out preliminary mechanistic studies of this iron-catalyzed coupling of alkyl electrophiles with olefins in the presence of a hydrosilane. In some cases, previous investigations of iron-catalyzed couplings of alkyl electrophiles with nucleophiles have implicated the intermediacy of organic radicals derived from the electrophile,^{9,19} and our observations are consistent with parallel conclusions for the current reaction. For example, if 1 (equivalent of 2,2,6,6-tetramethylpiperidin-1-yl)oxyl (TEMPO) is added to a coupling in progress, carbon-carbon bond formation essentially ceases (**Figure 4.4A**); in addition, analysis of the reaction mixture via mass spectrometry reveals the presence of a TEMPO adduct derived from the electrophile (but not from the olefin; **Figure 4.4A**).

Furthermore, a cyclization/stereochemical probe is consistent with the formation of an organic radical under the reaction conditions. Specifically, when 6-iodo-1-heptene is employed as the electrophile, cross-coupled product **B** is observed, wherein the electrophile has cyclized to generate a 3.2 : 1 (cis : trans) mixture of cyclopentane isomers, a ratio comparable to that reported for radical **I** at 25 °C²⁰ and therefore consistent with the formation of **I** under the iron-catalyzed coupling conditions (**Figure 4B**). Because **I** cyclizes with a rate constant of $\sim 1 \times 10^5 \text{ s}^{-1}$, much slower than the rate of diffusion (generally $\geq 10^8 \text{ s}^{-1}$) at 25 °C, the observation of cyclized product **B** is consistent with out-of-cage coupling of $\text{R}\cdot$ with iron.

The chain-walking that we observe in iron-catalyzed reductive couplings of internal olefins (bottom of **Figure 4.3**) is likely a result of reversible β -migratory insertion/ β -hydride elimination. To gain insight into whether such reversibility is also operative in the case of terminal olefins, as well as whether olefin binding to iron is reversible, we examined a cross-coupling in the presence

of commercially available D_2SiPh_2 (H_2SiPh_2 and $HSi(OEt)_3$ furnish comparable yields under our standard conditions) and determined that the reductively coupled product forms in 68 % yield with an ~2 : 1 ratio of monodeuteration : dideuteration (**Figure 4.4C**); furthermore, when the reaction is stopped at partial conversion, deuterated olefin is observed. Collectively, these observations are consistent with olefin complexation/dissociation and β -migratory insertion/ β -hydride elimination occurring competitively with carbon–carbon bond formation.²¹

In view of the growing potential of iron catalysis in organic synthesis, we have begun to examine the utility of $Fe(OAc)_2/Xantphos/Mg(OEt)_2$ for other olefin hydrofunctionalization processes, including with $M-H$ other than $Si-H$. We were pleased to determine that this catalyst system is also useful for reactions of $B-H$, catalyzing the regioselective hydroboration of terminal and 1,1-disubstituted olefins by HBpin (pinacolborane; **Figure 4.5**)^{22,23} under the same conditions as for the reductive cross-coupling of alkyl electrophiles with olefins (**Figure 4.3**). In the absence of $Fe(OAc)_2$, Xantphos, or $Mg(OEt)_2$, essentially no hydroboration is observed.

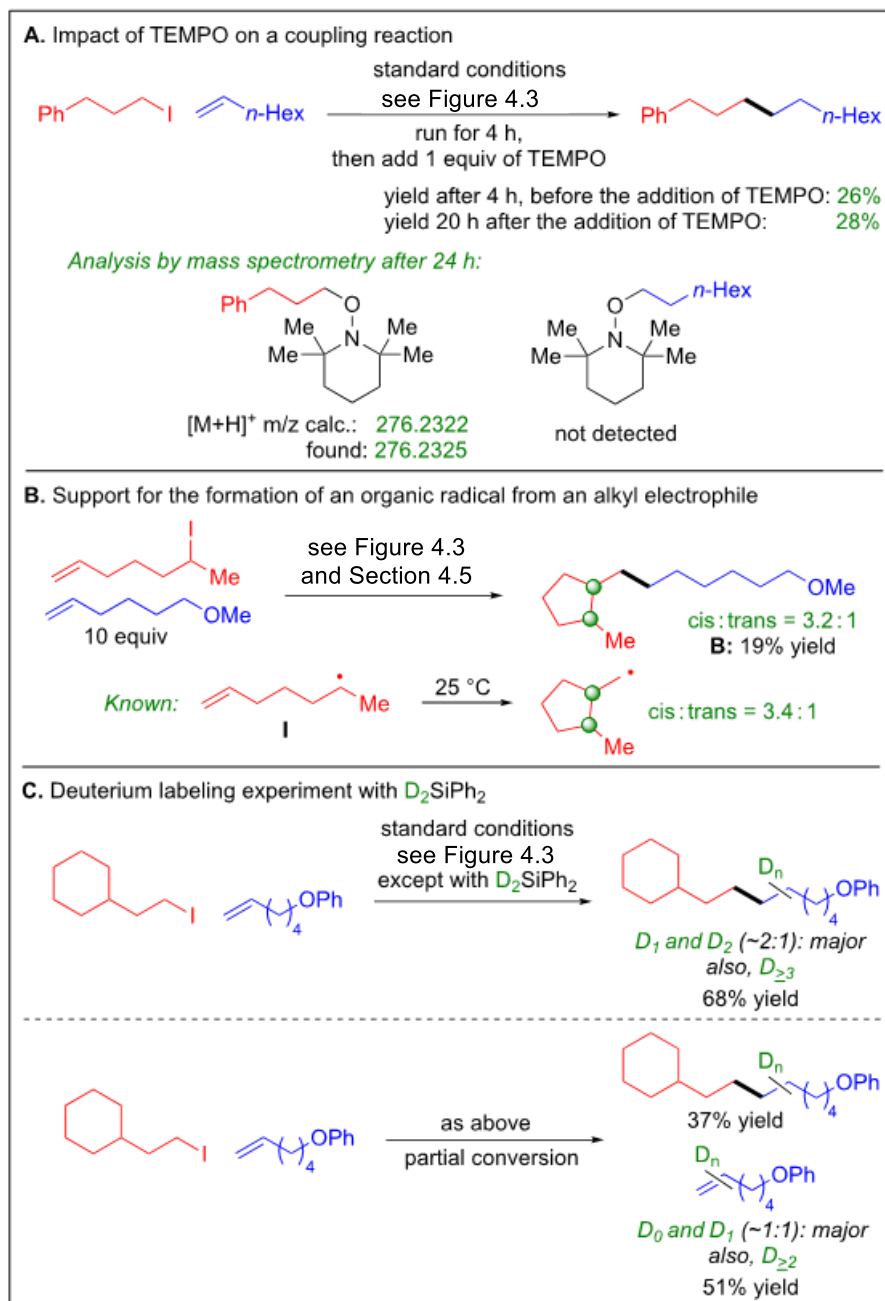


Figure 4.4. Mechanistic studies. (A) Impact of TEMPO on a coupling reaction. (B) Support for the formation of an organic radical from an alkyl electrophile. (C) Deuterium labeling experiment with D₂SiPh₂.

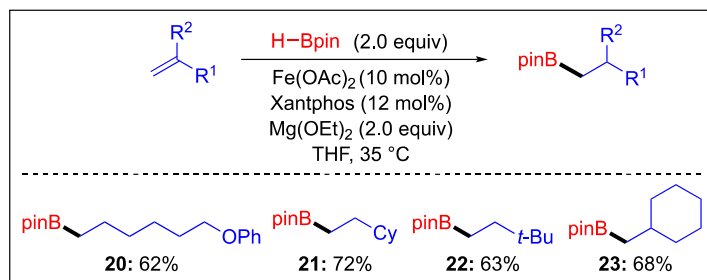


Figure 4.5. Application of $Fe(OAc)_2/Xantphos/Mg(OEt)_2$ to other hydrofunctionalization reactions of olefins: Hydroboration. Couplings were conducted on a 1.0-mmol scale, and yields represent purified products.

4.3. Conclusion

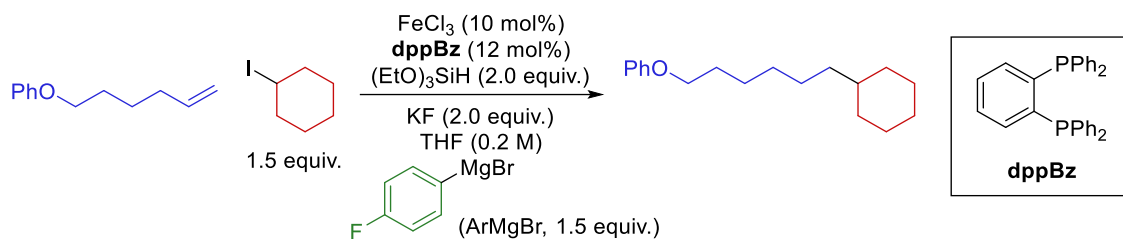
In conclusion, we have developed an iron-catalyzed method for the reductive cross-coupling of an alkyl electrophile with an olefin, in the presence of a hydrosilane, that affords an alkyl–alkyl bond under mild conditions (room temperature); this approach obviates the generation of discrete alkylmetal nucleophiles as coupling partners, permitting the use of readily accessible, easily handled olefins instead. The method employs commercially available components, and it can be applied without modification to a distinct hydrofunctionalization of olefins, specifically, hydroboration. Initial mechanistic studies are consistent with the formation of an organic radical from the alkyl electrophile, as well as with olefin complexation to iron and β -migratory insertion both being reversible. Further efforts to develop applications of earth-abundant metals as catalysts for organic synthesis are underway.

4.4. Development of a Variant for Unactivated Secondary Alkyl Electrophiles

While the current reaction is conceptually novel and takes advantage of commercially available iron catalyst, its limitations are also obvious. Most significantly, it is confined in its use of primary alkyl electrophiles. Naturally, an iron-catalyzed reductive cross-coupling of secondary electrophiles would be an attractive complementary transformation. Directly applying the current conditions (**Figure 4.3**) to unactivated secondary alkyl electrophiles, such as iodocyclohexane, does not lead to the observation of any desired cross-coupling product. Therefore, different conditions are likely required to achieve the analogous cross-coupling with broader collection of substrates.

Reevaluation of reaction conditions and screening of ligands revealed that, parallel to the initial first-generation condition applied to primary electrophiles, secondary electrophiles can be engaged in similar cross-coupling reaction with a terminal olefin in the presence of FeCl₃, **dppBz**, triethoxysilane, KF, and an aryl Grignard reagent, giving the desired product in 11% yield (**Table 4.1**, entry 1). Interestingly, under this specific set of reaction conditions, the absence of the Grignard reagent does not lead to diminished yield of the product (entry 2). Further condition optimization led to substantial improvement in the result of the reaction, giving the product in 63% yield (entry 3).

Table 4.1. Development of reaction with a secondary alkyl electrophile (iodocyclohexane).



entry	variations from conditions above	yield (%)
1	none	11
2	no ArMgBr	11
3	no ArMgBr , 50°C	63

Disappointingly, the reaction does not prove general. Specifically, when acyclic electrophiles or iodocyclopentane were used, only small amounts of cross-coupling products were obtained (**Table 4.2**, entry 1). A range of substituted structurally analogous **dppBz** ligands bearing substituted phenyl substituents were then examined. Among the ligands tested, alkyl and fluorine substitutions on the phenyl group do not improve the generality of the reaction (entries 2 – 4), but when 3,5-dimethoxyphenyl group is used (**dppBz^{OMe}**, entry 6), substantial increases in yields for all substrates were observed. Further modification to the structure of the ligand did not lead to additional improvement (entries 7 – 9). With the novel ligand **dppBz^{OMe}**, a good yield of 67% was obtained after further adjustments of reaction conditions (**Table 4.3**).

Table 4.2. Evaluation of different *dppBz* ligands.

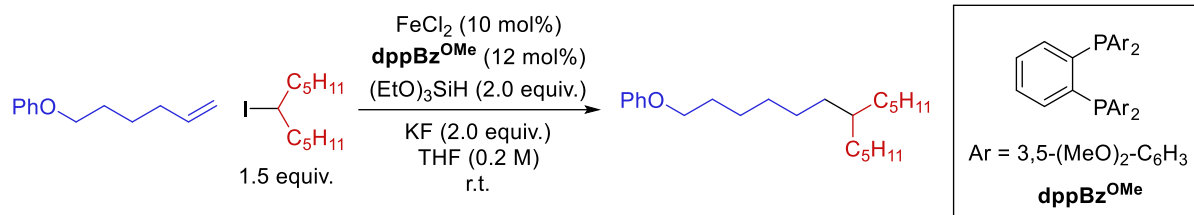
$\text{PhO-CH}_2\text{CH}_2\text{CH}_2\text{CH}_2\text{CH}=\text{CH}_2$ (1.5 equiv.) + R-I (1.5 equiv.) $\xrightarrow[\text{THF (0.2 M), r.t.}]{\text{FeCl}_3 (10 \text{ mol\%}), \text{L (12 mol\%)}, (\text{EtO})_3\text{SiH (2.0 equiv.)}, \text{KF (2.0 equiv.)}}$ $\text{PhO-CH}_2\text{CH}_2\text{CH}_2\text{CH}_2\text{CH}_2\text{CH}_2\text{R}$

L

entry	R-I				
	Ar =	P/IS ^a =			
1		0.06	0.04	0.26	0.03
2		0.12	0.09	0.83	0.09
3		0.02	0.03	0.27	0.30
4		0.08	0.06	0.12	0.04
5		0.19	0.11	0.62	0.13
6	 dppBz^{OMe}	0.50	0.44	0.84	0.42
7		0.40	0.31	0.80	0.30
8		0.35	0.25	0.85	0.33
9		0.39	0.34	0.80	0.34

^aP/IS: area of product/internal standard after integration on GC chromatogram

Table 4.3. Optimization of reaction with generic acyclic alkyl iodide.



entry	variations from conditions above	yield (%) ^a
1	none	50
2	THF/dioxane 1:4	58
3	1.0 equiv. alkyl iodide, 2.0 equiv. olefin	62
4	Mg(OEt) ₂ instead of KF	67
	1.0 equiv. alkyl iodide, 2.0 equiv. olefin	

^aYield: determined through GC analysis of the crude reaction mixture

With these highly promising results in hand, we seek to further explore these iron-catalyzed reductive cross-coupling reactions, with special attention dedicated to the comparison and contrast between the two catalytic systems reported in this chapter, as well as mechanistic investigations. These initial results in iron-catalyzed cross-coupling reactions can also serve as solid foundation for future development of iron catalysis in the Fu lab, especially asymmetric reactions.

4.5. Experimental Section

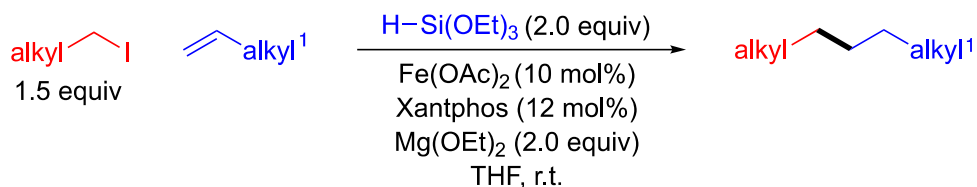
4.5.1 General Information

Unless otherwise noted, reagents received from commercial suppliers were used as received. All reactions were performed under an atmosphere of dry nitrogen. Fe(OAc)₂ was purchased from Strem; Xantphos, D₂SiPh₂, and HSi(OEt)₃ were purchased from Sigma-Aldrich; Mg(OEt)₂ and HBpin were purchased from Acros. All solvents were purified by passage through activated aluminum oxide in a solvent-purification system; THF was purified by passage through activated aluminum oxide in a solvent-purification system and stored over molecular sieves under dry nitrogen.

Glassware was oven-dried at 150 °C for a minimum of 12 h, or it was flame-dried utilizing a torch under high vacuum.

NMR spectra were collected on a Bruker 400 MHz or a Varian 500 MHz spectrometer at ambient temperature; chemical shifts (δ) are reported in ppm downfield from tetramethylsilane, using the solvent resonance as the internal standard. FT-IR measurements were carried out on a Thermo Scientific Nicolet iS5 FT-IR spectrometer equipped with an iD5 ATR accessory. LC-MS were obtained on an Agilent 6230 LC-TOF system in electrospray ionization (ESI+) mode. GC-MS analyses were carried out on an Agilent 6890N GC. Flash column chromatography was performed using silica gel (SiliaFlash[®] P60, particle size 40–63 μ m, Silicycle). Mössbauer spectra were recorded at 77 K on a spectrometer from SEE Co. (Edina, MN) operating in constant acceleration mode in a transmission geometry; the quoted isomer shifts are relative to the centroid of the spectrum of a metallic foil of α -Fe at room temperature.

4.5.2. Iron-Catalyzed Reductive Cross-Couplings and Hydroborations



General Procedure 1 (GP-1). In a nitrogen-filled glovebox, a 7-mL vial was charged with a large stir bar and a small stir bar, followed by Fe(OAc)_2 (17 mg, 0.10 mmol, 10 mol%), Xantphos (69 mg, 0.12 mmol, 12 mol%), and Mg(OEt)_2 (228 mg, 2.0 mmol, 2.0 equiv). Then, THF (5.0 mL), the olefin (1.0 mmol, 1.0 equiv), the alkyl iodide (1.5 mmol, 1.5 equiv), and HSi(OEt)_3 (0.38 mL, 2.0 mmol, 2.0 equiv; *Note:* HSi(OEt)_3 is hazardous and should be handled with care) were added. The vial was capped, wrapped with electrical tape, and removed from the glovebox. The reaction mixture was vigorously stirred at r.t. for 24 h, and then the mixture was diluted with hexanes and passed through a pad of celite on top of silica, flushing with hexanes and Et_2O . The filtrate was concentrated, and the residue was purified by column chromatography.

General Procedure 2 (GP-2). GP-1 was followed for the reaction itself. After the reaction was complete, the mixture was diluted with hexanes and passed through a pad of celite on top of silica, flushing with hexanes and Et_2O . The filtrate was concentrated, and the residue was dissolved in DCM (~10 mL). The solution was cooled to 0 °C, and H_2O_2 (30% solution in water, 0.34 mL) was added. The mixture was stirred vigorously under air for 4 h at r.t., and then it was washed with water, and the aqueous phase was extracted once with Et_2O . The organic phase was dried over Na_2SO_4 and concentrated, and the residue was purified by column chromatography.



***n*-Undecylbenzene (Figure 4.3, entries 1 and 18).** The title compound was synthesized according to **GP-1** from (3-iodopropyl)benzene and 1-octene. The product was purified by column chromatography on silica gel (100% hexanes). Colorless oil. Run 1: 169 mg, 73%. Run 2: 174 mg, 75%.

Alternatively, the title compound was synthesized according to **GP-1** from (3-iodopropyl)benzene and *cis*-4-octene. Run 1: 118 mg, 51%. Run 2: 123 mg, 53%.

^1H NMR (400 MHz, CDCl_3) δ 7.30 – 7.25 (m, 2H), 7.18 (d, $J = 7.1$ Hz, 3H), 2.67 – 2.52 (m, 2H), 1.69 – 1.56 (m, 2H), 1.39 – 1.17 (m, 16H), 0.92 – 0.81 (m, 3H).

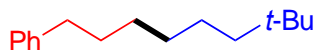
^{13}C NMR (101 MHz, CDCl_3) δ 143.0, 128.4, 128.2, 125.5, 36.0, 31.9, 31.6, 29.72, 29.68, 29.65, 29.6, 29.5, 29.4, 22.7, 14.1.

FT-IR (film): 3062, 3027, 2957, 2922, 2852, 1494, 1454, 744, 696 cm^{-1} .

MS (GC-MS) m/z $[\text{M}]^+$ calcd for $\text{C}_{17}\text{H}_{28}$: 232.22, found: 232.22, 147.11, 133.10, 92.08.

Gram-scale reaction: The reaction was scaled up to 8.0 mmol (of olefin) and set up according to **GP-1**, except that a 250-mL flask was used. 1.39 g, 75%.

Reaction with 7.5 mol% Fe: The procedure for the gram-scale reaction above was followed, using $\text{Fe}(\text{OAc})_2$ (104 mg, 0.60 mmol, 7.5 mol%), Xantphos (416 mg, 0.72 mmol, 9.0 mol%). 1.26 g, 68%.



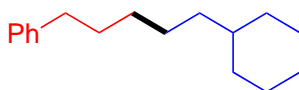
(7,7-Dimethyloctyl)benzene (Figure 4.3, entry 2). The title compound was synthesized according to **GP-1** from (3-iodopropyl)benzene and 4,4-dimethylpent-1-ene. The product was purified by column chromatography on silica gel (100% hexanes). Colorless oil. Run 1: 156 mg, 72%. Run 2: 161 mg, 74%.

^1H NMR (400 MHz, CDCl_3) δ 7.32 – 7.24 (m, 2H), 7.18 (d, $J = 7.3$ Hz, 3H), 2.67 – 2.53 (m, 2H), 1.67 – 1.57 (m, 2H), 1.42 – 1.07 (m, 8H), 0.86 (s, 9H).

^{13}C NMR (101 MHz, CDCl_3) δ 143.0, 128.4, 128.2, 125.6, 44.3, 36.0, 31.6, 30.5, 30.3 (overlapping signals), 29.4, 24.5.

FT-IR (film): 3027, 2928, 2856, 1605, 1495, 1466, 1393, 1248, 1030, 745, 696 cm^{-1} .

MS (GC-MS) m/z $[\text{M}]^+$ calcd for $\text{C}_{16}\text{H}_{26}$: 218.20, found: 218.21, 203.17, 162.14, 147.10, 133.10, 91.07.



(5-Cyclohexylpentyl)benzene (Figure 4.3, entries 3 and 19). The title compound was synthesized according to **GP-1** from (3-iodopropyl)benzene and vinylcyclohexane. The product was purified by column chromatography on silica gel (100% hexanes). Colorless oil. Run 1: 160 mg, 69%. Run 2: 156 mg, 68%.

Alternatively, the title compound was synthesized according to **GP-1** from (3-iodopropyl)benzene and ethylidenecyclohexane. Run 1: 106 mg, 46%. Run 2: 101 mg, 44%.

^1H NMR (400 MHz, CDCl_3) δ 7.29 – 7.24 (m, 2H), 7.21 – 7.06 (m, 3H), 2.60 (dd, $J = 8.8, 6.8$ Hz, 2H), 1.76 – 1.56 (m, 7H), 1.37 – 1.06 (m, 10H), 0.85 (qd, $J = 10.9, 4.4$ Hz, 2H).

^{13}C NMR (101 MHz, CDCl_3) δ 143.0, 128.4, 128.2, 125.5, 37.7, 37.5, 36.0, 33.5, 31.6, 29.7, 26.8, 26.7, 26.5.

FT-IR (film): 3026, 2919, 2850, 1495, 1448, 1030, 743, 696 cm^{-1} .

MS (GC-MS) m/z $[\text{M}]^+$ calcd for $\text{C}_{17}\text{H}_{26}$: 230.20, found: 230.22, 187.16, 147.12, 92.08.



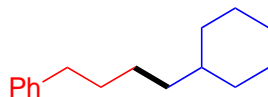
(6,6-Dimethylheptyl)benzene (Figure 4.3, entry 4). The title compound was synthesized according to **GP-1** from (3-iodopropyl)benzene and *t*-butylethylene. The product was purified by column chromatography on silica gel (100% hexanes). Colorless oil. Run 1: 115 mg, 56%. Run 2: 117 mg, 57%.

^1H NMR (400 MHz, CDCl_3) δ 7.35 – 7.26 (m, 2H), 7.18 (d, $J = 7.3$ Hz, 3H), 2.70 – 2.49 (m, 2H), 1.69 – 1.56 (m, 2H), 1.35 – 1.19 (m, 4H), 1.20 – 1.11 (m, 2H), 0.86 (s, 9H).

^{13}C NMR (101 MHz, CDCl_3) δ 143.0, 128.4, 128.2, 125.6, 44.2, 36.1, 31.6, 30.30, 30.28, 29.4, 24.4.

FT-IR (film): 3027, 2929, 2858, 1604, 1495, 1466, 1363, 1248, 743, 696 cm^{-1} .

MS (GC-MS) m/z $[\text{M}]^+$ calcd for $\text{C}_{15}\text{H}_{24}$: 204.19, found: 204.20, 189.17, 148.13, 91.07.



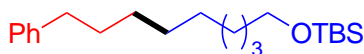
(4-Cyclohexylbutyl)benzene (Figure 4.3, entry 5). The title compound was synthesized according to **GP-1** from (3-iodopropyl)benzene and methylenecyclohexane. The product was purified by column chromatography on silica gel (100% hexanes). Colorless oil. Run 1: 97 mg, 45%. Run 2: 99 mg, 46%.

^1H NMR (400 MHz, CDCl_3) δ 7.31 – 7.25 (m, 2H), 7.18 (d, $J = 7.1$ Hz, 3H), 2.70 – 2.52 (m, 2H), 1.74 – 1.54 (m, 7H), 1.38 – 1.28 (m, 2H), 1.26 – 1.08 (m, 6H), 0.86 (tt, $J = 11.5, 6.2$ Hz, 2H).

^{13}C NMR (101 MHz, CDCl_3) δ 143.0, 128.4, 128.2, 125.5, 37.6, 37.4, 36.0, 33.5, 31.9, 26.8, 26.6, 26.5.

FT-IR (film): 2920, 2850, 1496, 1448, 1030, 744, 696, 496 cm^{-1} .

MS (GC-MS) m/z $[\text{M}]^+$ calcd for $\text{C}_{16}\text{H}_{24}$: 216.19, found: 216.21, 187.16, 173.14, 133.09, 120.09, 105.07, 92.08.



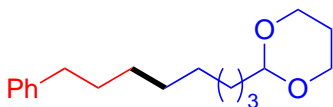
tert-Butyldimethyl((9-phenylnonyl)oxy)silane (Figure 4.3, entry 6). The title compound was synthesized according to **GP-1** from (3-iodopropyl)benzene and *tert*-butyl(hex-5-en-1-yloxy)dimethylsilane. The product was purified by column chromatography on silica gel (5 → 20% DCM in hexanes). Colorless oil. Run 1: 230 mg, 69%. Run 2: 227 mg, 68%.

^1H NMR (400 MHz, CDCl_3) δ 7.30 – 7.26 (m, 2H), 7.20 – 7.12 (m, 3H), 3.59 (t, $J = 6.6$ Hz, 2H), 2.72 – 2.49 (m, 2H), 1.69 – 1.56 (m, 2H), 1.49 (q, $J = 6.9$ Hz, 2H), 1.40 – 1.22 (m, 10H), 0.89 (s, 9H), 0.05 (s, 6H).

^{13}C NMR (101 MHz, CDCl_3) δ 143.0, 128.4, 128.2, 125.6, 63.4, 36.0, 32.9, 31.5, 29.6, 29.47, 29.45, 29.3, 26.0, 25.8, 18.4, –5.2.

FT-IR (film): 3068, 3026, 2927, 2854, 1463, 1387, 1253, 1095, 774, 745, 661 cm^{-1} .

MS (GC-MS) m/z $[\text{M}-t\text{-Bu}]^+$ calcd for $\text{C}_{17}\text{H}_{29}\text{OSi}$: 277.20, found: 277.22, 259.21, 207.04, 201.18, 165.08, 117.07, 91.07, 75.05.



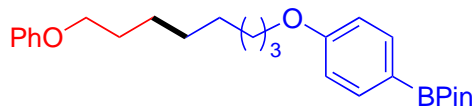
2-(8-Phenyloctyl)-1,3-dioxane (Figure 4.3, entry 7). The title compound was synthesized according to **GP-1** from (3-iodopropyl)benzene and 2-(pent-4-en-1-yl)-1,3-dioxane. The product was purified by column chromatography on silica gel (0% \rightarrow 10% DCM in hexane, followed by 0% \rightarrow 5% Et_2O + 10% DCM in hexanes). Colorless oil. Run 1: 205 mg, 74%. Run 2: 212 mg, 77%.

^1H NMR (500 MHz, CDCl_3) δ 7.39 – 7.29 (m, 2H), 7.30 – 7.11 (m, 3H), 4.55 (t, $J = 5.2$ Hz, 1H), 4.15 (ddt, $J = 10.4, 5.0, 1.4$ Hz, 2H), 3.91 – 3.72 (m, 2H), 2.78 – 2.56 (m, 2H), 2.13 (dt, $J = 13.4, 12.5, 5.0$ Hz, 1H), 1.78 – 1.59 (m, 4H), 1.49 – 1.28 (m, 11H).

^{13}C NMR (101 MHz, CDCl_3) δ 143.0, 128.4, 128.2, 125.6, 102.5, 66.9, 36.0, 35.3, 31.5, 29.49, 29.45, 29.4, 29.3, 25.9, 24.0.

FT-IR (film): 3063, 3030, 2925, 1456, 1377, 1240, 1143, 1078, 698, 474 cm^{-1} .

MS (GC-MS) m/z $[M]^+$ calcd for $\text{C}_{18}\text{H}_{28}\text{O}_2$: 276.21, found: 276.24, 200.16, 131.09, 104.07, 91.07, 87.07.



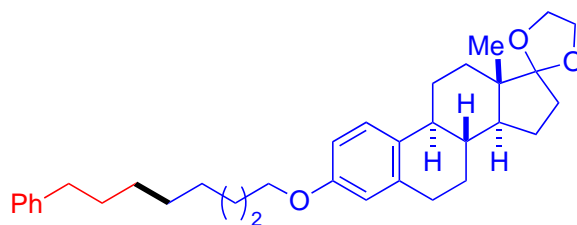
4,4,5,5-Tetramethyl-2-(4-((8-phenoxyoctyl)oxy)phenyl)-1,3,2-dioxaborolane (Figure 4.3, entry 8). The title compound was synthesized according to GP-1, scaled down to 0.5 mmol of olefin, from (3-iodopropoxy)benzene and 4,4,5,5-tetramethyl-2-(4-(pent-4-en-1-yloxy)phenyl)-1,3,2-dioxaborolane. The product was purified by column chromatography on silica gel (0% → 20% DCM in hexanes, followed by 0% → 5% EtOAc + 20% DCM in hexanes). White solid. Run 1: 111 mg, 52%. Run 2: 119 mg, 56%.

^1H NMR (400 MHz, CDCl_3) δ 7.83 – 7.55 (m, 2H), 7.38 – 7.23 (m, 2H), 7.13 – 6.75 (m, 5H), 3.97 (dt, $J = 9.8, 6.5$ Hz, 4H), 1.86 – 1.70 (m, 4H), 1.53 – 1.35 (m, 8H), 1.33 (s, 12H).

^{13}C NMR (101 MHz, CDCl_3) δ 161.7, 159.1, 136.5, 129.4, 120.5, 114.5, 113.9, 83.5, 67.8, 67.7, 29.32, 29.29, 29.2, 26.02, 25.98, 24.9 (overlapping signals).

FT-IR (film): 2976, 2928, 1604, 1395, 1359, 1318, 1275, 1077, 962, 831, 787, 736 cm^{-1} .

MS (GC-MS) m/z $[M]^+$ calcd for $\text{C}_{26}\text{H}_{37}\text{BO}_4$: 424.29, found: 424.22, 330.92, 252.99, 206.99, 190.95, 133.98, 93.98.



(8*R*,9*S*,13*S*,14*S*)-13-Methyl-3-((8-phenyloctyl)oxy)-6,7,8,9,11,12,13,14,15,16-decahydrospiro[cyclopenta[a]phenanthrene-17,2'-[1,3]dioxolane] (Figure 4.3, entry 9). The title compound was synthesized according to **GP-1** from (3-iodopropyl)benzene and (8*R*,9*S*,13*S*,14*S*)-13-methyl-3-(pent-4-en-1-yloxy)-6,7,8,9,11,12,13,14,15,16-decahydrospiro[cyclopenta[a]phenanthrene-17,2'-[1,3]dioxolane]. The product was purified by column chromatography on silica gel (0% → 10% DCM in hexanes, followed by 0% → 8% EtOAc + 10% DCM in hexanes). Colorless oil. Run 1: 365 mg, 73%. Run 2: 355 mg, 70%.

^1H NMR (400 MHz, CDCl_3) δ 7.35 – 7.26 (m, 2H), 7.22 – 7.09 (m, 4H), 6.69 (dd, $J = 8.6$, 2.7 Hz, 1H), 6.65 – 6.58 (m, 1H), 4.02 – 3.85 (m, 6H), 2.91 – 2.75 (m, 2H), 2.67 – 2.55 (m, 2H), 2.38 – 2.17 (m, 2H), 2.10 – 1.95 (m, 1H), 1.95 – 1.69 (m, 6H), 1.69 – 1.49 (m, 5H), 1.49 – 1.28 (m, 11H), 0.88 (s, 3H).

^{13}C NMR (101 MHz, CDCl_3) δ 157.0, 142.9, 138.0, 132.5, 128.4, 128.2, 126.3, 125.6, 119.5, 114.5, 112.0, 67.9, 65.3, 64.6, 49.4, 46.2, 43.7, 39.1, 36.0, 34.3, 31.5, 30.8, 29.8, 29.4, 29.34, 29.32, 29.27, 27.0, 26.2, 26.1, 22.4, 14.4.

FT-IR (film): 3027, 2929, 2856, 1608, 1497, 1454, 1308, 1255, 1161, 1104, 1067, 962, 909, 747 cm^{-1} .



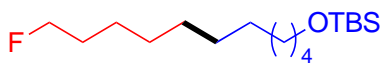
(8-Methoxyoctyl)cyclohexane (Figure 4.3, entry 10). The title compound was synthesized according to **GP-2** from (2-iodoethyl)cyclohexane and 6-methoxyhex-1-ene. The product was purified by column chromatography on silica gel (5% → 10% Et₂O in hexanes). Colorless oil. Run 1: 161 mg, 71%. Run 2: 158 mg, 70%.

¹H NMR (400 MHz, CDCl₃) δ 3.36 (t, *J* = 6.7 Hz, 2H), 3.33 (s, 3H), 1.75 – 1.50 (m, 7H), 1.39 – 1.08 (m, 16H), 0.94 – 0.76 (m, 2H).

¹³C NMR (101 MHz, CDCl₃) δ 73.0, 58.6, 37.7, 37.6, 33.5, 29.9, 29.7, 29.6, 29.5, 26.9, 26.8, 26.5, 26.1.

FT-IR (film): 2978, 2920, 2850, 1448, 1386, 1129, 948, 722 cm⁻¹.

MS (GC-MS) *m/z* [M]⁺ calcd for C₁₅H₃₀O: 226.23, found: 226.26, 194.26, 166.20, 152.18, 138.17, 124.15, 109.13, 96.14, 82.13.



***tert*-Butyl((11-fluoroundecyl)oxy)dimethylsilane (Figure 4.3, entry 11).** The title compound was synthesized according to **GP-1** from 1-fluoro-5-iodopentane and *tert*-butyl(hex-5-en-1-yloxy)dimethylsilane. The product was purified by column chromatography on silica gel (5% → 25% DCM in hexanes). Colorless oil. Run 1: 160 mg, 53%. Run 2: 164 mg, 54%.

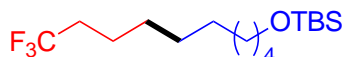
^1H NMR (400 MHz, CDCl_3) δ 4.43 (dt, $J = 47.4, 6.2$ Hz, 2H), 3.59 (t, $J = 6.6$ Hz, 2H), 1.78 – 1.60 (m, 2H), 1.50 (q, $J = 6.8$ Hz, 2H), 1.41 – 1.26 (m, 14H), 0.89 (s, 9H), 0.05 (s, 6H).

^{13}C NMR (101 MHz, CDCl_3) δ 84.3 (d, $J = 163.9$ Hz), 63.4, 32.9, 30.42 (d, $J = 19.3$ Hz), 29.6, 29.504, 29.496, 29.4, 29.3, 26.0, 25.8, 25.2 (d, $J = 5.5$ Hz), 18.4, –5.2.

^{19}F NMR (282 MHz, CDCl_3) δ 12.00 (tt, $J = 47.0, 24.6$ Hz).

FT-IR (film): 2927, 2855, 1463, 1388, 1253, 1098, 833, 773, 661 cm^{-1} .

MS (GC-MS) m/z $[\text{M}-t\text{-Bu}]^+$ calcd for $\text{C}_{13}\text{H}_{28}\text{FOSi}$: 247.19, found: 247.19, 157.13, 143.10, 133.06, 129.08, 115.07, 111.12, 107.04, 97.12.



***tert*-Butyldimethyl((10,10,10-trifluorodecyl)oxy)silane (Figure 4.3, entry 12).** The title compound was synthesized according to **GP-1** from 1,1,1-trifluoro-4-iodobutane and *tert*-butyl(hex-5-en-1-yloxy)dimethylsilane. The product was purified by column chromatography on silica gel (5% → 15% DCM in hexanes). Colorless oil. Run 1: 169 mg, 52%. Run 2: 165 mg, 51%.

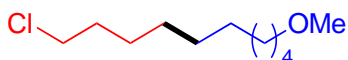
^1H NMR (400 MHz, CDCl_3) δ 3.60 (t, $J = 6.6$ Hz, 2H), 2.15 – 1.88 (m, 2H), 1.62 – 1.45 (m, 4H), 1.42 – 1.18 (m, 10H), 0.89 (s, 9H), 0.05 (s, 6H).

^{13}C NMR (101 MHz, CDCl_3) δ 127.3 (q, $J = 276.2$ Hz), 63.3, 33.7 (q, $J = 28.2$ Hz), 32.9, 29.3 (overlapping signals), 29.1, 28.8, 26.0, 25.8, 21.8 (q, $J = 2.9$ Hz), 18.4, –5.3.

^{19}F NMR (282 MHz, CDCl_3) δ -66.44 (t, $J = 11.0$ Hz)

FT-IR (film): 2929, 2857, 1471, 1387, 1254, 1140, 833, 774, 656 cm^{-1} .

MS (GC-MS) m/z $[M-t-Bu]^+$ calcd for $C_{12}H_{24}F_3OSi$: 269.15, found: 269.18, 249.19, 229.18, 175.17, 155.16, 133.12, 119.10, 113.12, 107.08.



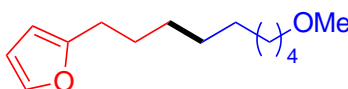
1-Chloro-10-methoxydecane (Figure 4.3, entry 13). The title compound was synthesized according to **GP-2** from 4-chloro-1-iodobutane and 6-methoxyhex-1-ene. The product was purified by column chromatography on silica gel (5% Et_2O in hexanes). Colorless oil. Run 1: 146 mg, 71%. Run 2: 134 mg, 65%.

1H NMR (400 MHz, $CDCl_3$) δ 3.53 (t, $J = 6.7$ Hz, 2H), 3.36 (t, $J = 6.6$ Hz, 2H), 3.33 (s, 3H), 1.76 (dt, $J = 14.8, 6.8$ Hz, 2H), 1.55 (dt, $J = 7.9, 6.4$ Hz, 2H), 1.42 (dq, $J = 14.1, 6.5$ Hz, 2H), 1.29 (d, $J = 2.8$ Hz, 10H).

^{13}C NMR (101 MHz, $CDCl_3$) δ 73.0, 58.6, 45.2, 32.7, 29.7, 29.47, 29.45, 29.4, 28.9, 26.9, 26.1.

FT-IR (film): 2926, 2854, 1462, 1387, 1118, 723, 652 cm^{-1} .

MS (GC-MS) m/z $[M]^+$ calcd for $C_{11}H_{23}ClO$: 206.14, found: 206.19, 205.18, 174.11, 146.08, 118.06, 104.04, 97.11, 83.10.



2-(9-Methoxynonyl)furan (Figure 4.3, entry 14). The title compound was synthesized according to **GP-1** from 2-(3-iodopropyl)furan and 6-methoxyhex-1-ene. The product was purified

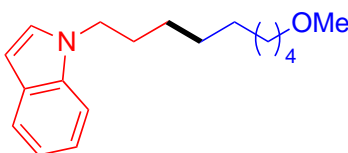
by column chromatography on silica gel (10% → 20% DCM in hexanes followed by 0% → 25% EtOAc in hexanes). Colorless oil. Run 1: 164 mg, 73%. Run 2: 160 mg, 71%.

^1H NMR (400 MHz, CDCl_3) δ 7.29 (dd, $J = 1.9, 0.9$ Hz, 1H), 6.27 (dd, $J = 3.1, 1.9$ Hz, 1H), 5.96 (dt, $J = 3.0, 0.9$ Hz, 1H), 3.36 (td, $J = 6.7, 0.8$ Hz, 2H), 3.33 (d, $J = 0.8$ Hz, 3H), 2.65 – 2.56 (m, 2H), 1.68 – 1.51 (m, 4H), 1.39 – 1.25 (m, 10H).

^{13}C NMR (101 MHz, CDCl_3) δ 156.6, 140.6, 110.0, 104.5, 73.0, 58.6, 29.7, 29.48, 29.47, 29.3, 29.2, 28.03, 27.98, 26.1.

FT-IR (film): 3120, 2926, 2854, 1596, 1507, 1458, 1387, 1118, 1006, 795 cm^{-1} .

MS (GC-MS) m/z $[\text{M}]^+$ calcd for $\text{C}_{14}\text{H}_{24}\text{O}_2$: 224.18, found: 224.19, 207.12, 163.08, 149.09, 135.08, 123.06, 107.06, 95.07, 81.06.



1-(9-Methoxynonyl)-1H-indole (Figure 4.3, entry 15). The title compound was synthesized according to **GP-1** from *N*-(3-iodopropyl)indole and 6-methoxyhex-1-ene. The product was purified by column chromatography on silica gel (10% → 30% DCM in hexanes followed by 20% → 35% Et_2O in hexanes). Colorless oil. Run 1: 172 mg, 63%. Run 2: 168 mg, 62%.

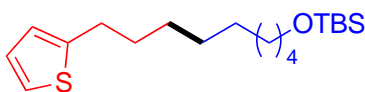
^1H NMR (400 MHz, CDCl_3) δ 7.63 (dt, $J = 7.9, 1.0$ Hz, 1H), 7.34 (dd, $J = 8.3, 1.0$ Hz, 1H), 7.20 (ddd, $J = 8.2, 6.9, 1.2$ Hz, 1H), 7.15 – 7.03 (m, 2H), 6.48 (dd, $J = 3.1, 0.8$ Hz, 1H), 4.11 (t, J

= 7.1 Hz, 2H), 3.36 (d, $J = 6.6$ Hz, 2H), 3.33 (s, 3H), 1.93 – 1.77 (m, 2H), 1.68 – 1.47 (m, 2H), 1.29 (qd, $J = 8.7, 5.5, 4.5$ Hz, 10H).

^{13}C NMR (101 MHz, CDCl_3) δ 135.9, 128.6, 127.8, 121.3, 120.9, 119.1, 109.4, 100.8, 72.9, 58.6, 46.4, 30.3, 29.6, 29.44, 29.40, 29.2, 27.0, 26.1.

FT-IR (film): 2926, 2853, 1511, 1463, 1314, 1116, 762, 736, 425 cm^{-1} .

MS (GC-MS) m/z $[\text{M}]^+$ calcd for $\text{C}_{18}\text{H}_{27}\text{NO}$: 273.21, found: 273.23, 258.21, 242.21, 228.20, 172.11, 158.09, 130.06, 117.05.



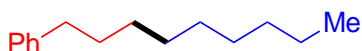
***tert*-Butyldimethyl((9-(thiophen-2-yl)nonyl)oxy)silane (Figure 4.3, entry 16).** The title compound was synthesized according to **GP-1** from 2-(3-iodopropyl)thiophene and *tert*-butyl(hex-5-en-1-yloxy)dimethylsilane. The product was purified by column chromatography on silica gel (0% → 15% DCM in hexanes). Colorless oil. Run 1: 229 mg, 67%. Run 2: 234 mg, 69%.

^1H NMR (400 MHz, CDCl_3) δ 7.10 (dd, $J = 5.1, 1.2$ Hz, 1H), 6.91 (dd, $J = 5.1, 3.4$ Hz, 1H), 6.77 (dq, $J = 3.3, 1.0$ Hz, 1H), 3.59 (t, $J = 6.6$ Hz, 2H), 2.85 – 2.75 (m, 2H), 1.72 – 1.61 (m, 2H), 1.49 (q, $J = 6.8$ Hz, 2H), 1.39 – 1.27 (m, 10H), 0.89 (s, 9H), 0.05 (s, 6H).

^{13}C NMR (101 MHz, CDCl_3) δ 145.9, 126.6, 123.9, 122.7, 63.3, 32.9, 31.8, 29.9, 29.5, 29.4, 29.3, 29.1, 26.0, 25.8, 18.4, –5.2.

FT-IR (film): 2927, 2854, 1463, 1253, 1096, 833, 773, 688 cm^{-1} .

MS (GC-MS) m/z $[M-t-Bu]^+$ calcd for $C_{15}H_{27}OSSI$: 283.16, found: 283.18, 265.17, 207.14, 171.04, 151.07, 97.03, 75.07.



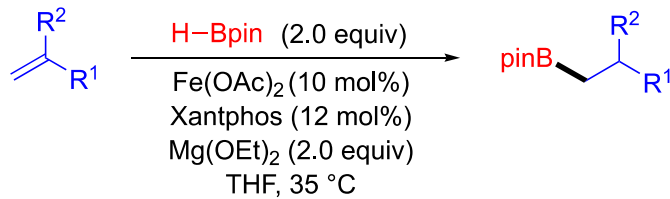
***n*-Nonylbenzene (Figure 4.3, entry 17).** The title compound was synthesized according to **GP-1** from (3-iodopropyl)benzene and *trans*-2-hexene. The product was purified by column chromatography on silica gel (100% hexanes). Colorless oil. Run 1: 114 mg, 56%. Run 2: 115 mg, 56%.

1H NMR (400 MHz, $CDCl_3$) δ 7.30 – 7.26 (m, 2H), 7.18 (d, $J = 7.2$ Hz, 3H), 2.66 – 2.56 (m, 2H), 1.66 – 1.55 (m, 2H), 1.36 – 1.21 (m, 12H), 0.92 – 0.82 (m, 3H).

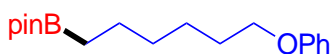
^{13}C NMR (101 MHz, $CDCl_3$) δ 143.0, 128.4, 128.2, 125.5, 36.0, 31.9, 31.6, 29.6, 29.5, 29.37, 29.35, 22.7, 14.1.

FT-IR (film): 3063, 3024, 2923, 2853, 1496, 1455, 744, 696 cm^{-1} .

MS (GC-MS) m/z $[M]^+$ calcd for $C_{15}H_{24}$: 204.19, found: 204.19, 161.13, 147.14, 133.09, 105.08, 92.08.



General Procedure 3 (GP-3). In a nitrogen-filled glovebox, a 7-mL vial was charged with a large stir bar and a small stir bar, followed by $\text{Fe}(\text{OAc})_2$ (17 mg, 0.10 mmol, 10 mol%), Xantphos (69 mg, 0.12 mmol, 12 mol%), and $\text{Mg}(\text{OEt})_2$ (228 mg, 2.0 mmol, 2.0 equiv). THF (5.0 mL) was added, and the mixture was stirred vigorously for 10 min. Then, the olefin (0.22 mL, 1.0 mmol, 1.0 equiv) and pinacolborane (0.29 mL, 2.0 mmol, 2.0 equiv) were added while the mixture was gently stirred. The vial was capped, wrapped with electrical tape, removed from the glovebox, and placed in an oil bath at 35 °C. The reaction mixture was stirred vigorously for 24 h. Next, the mixture was transferred to a 100-mL flask, diluted with Et_2O (20 mL), quenched with 0.5 mL MeOH, stirred for 30 seconds, and then passed through a pad of celite, flushing with Et_2O . The filtrate was then concentrated, and the residue was purified by column chromatography.



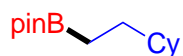
4,4,5,5-Tetramethyl-2-(6-phenoxyhexyl)-1,3,2-dioxaborolane (Figure 4.5, entry 20). The title compound was synthesized according to **GP-3** from 6-phenoxy-1-hexene. The product was purified by column chromatography on silica gel (A 1:1 DCM/ Et_2O solution was prepared, and the product was purified using 0% → 4% of this solution in hexanes.). Colorless oil. Run 1: 185 mg, 61%. Run 2: 191 mg, 63%.

^1H NMR (400 MHz, CDCl_3) δ 7.31 – 7.25 (m, 2H), 7.08 – 6.74 (m, 3H), 3.94 (t, $J = 6.6$ Hz, 2H), 1.83 – 1.71 (m, 2H), 1.51 – 1.29 (m, 6H), 1.24 (s, 12H), 0.79 (t, $J = 7.6$ Hz, 2H).

^{13}C NMR (101 MHz, CDCl_3) δ 159.1, 129.4, 120.4, 114.5, 82.9, 67.9, 32.1, 29.2, 25.8, 24.8, 23.9 (the carbon bound to boron was not observed).

FT-IR (film): 2977, 2929, 1600, 1497, 1243, 1143, 1035, 879, 752, 691 cm^{-1} .

MS (GC-MS) m/z $[\text{M}]^+$ calcd for $\text{C}_{18}\text{H}_{29}\text{BO}_3$: 304.22, found: 304.23, 281.07, 231.19, 211.19, 153.10, 119.08, 101.10, 94.05, 85.11.



2-(2-Cyclohexylethyl)-4,4,5,5-tetramethyl-1,3,2-dioxaborolane (Figure 4.5, entry 21).

The title compound was synthesized according to **GP-3** from vinylcyclohexane. The product was purified by column chromatography on silica gel (2% → 4% EtOAc in hexanes). Colorless oil.

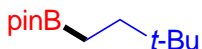
Run 1: 172 mg, 72%. Run 2: 170 mg, 71%.

^1H NMR (400 MHz, CDCl_3) δ 1.80 – 1.57 (m, 5H), 1.33 – 1.27 (m, 2H), 1.24 (s, 12H), 1.22 – 1.04 (m, 4H), 0.92 – 0.71 (m, 4H).

^{13}C NMR (101 MHz, CDCl_3) δ 82.8, 40.0, 33.0, 31.4, 26.8, 26.5, 24.8 (the carbon bound to boron was not observed).

FT-IR (film): 2977, 2922, 2851, 1450, 1374, 1318, 1232, 1146, 967, 858 cm^{-1} .

MS (GC-MS) m/z $[\text{M}]^+$ calcd for $\text{C}_{14}\text{H}_{27}\text{BO}_2$: 238.21, found: 238.21, 236.14, 223.14, 179.06, 154.06, 127.05, 84.07.



2-(3,3-Dimethylbutyl)-4,4,5,5-tetramethyl-1,3,2-dioxaborolane (Figure 4.5, entry 22).

The title compound was synthesized according to **GP-3** from *t*-butylethylene. The product was purified by column chromatography on silica gel (2% → 4% EtOAc in hexanes). Colorless oil.

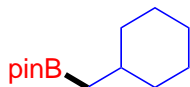
Run 1: 132 mg, 62%. Run 2: 135 mg, 64%.

^1H NMR (400 MHz, CDCl_3) δ 1.35 – 1.26 (m, 2H), 1.25 (s, 12H), 0.85 (s, 9H), 0.76 – 0.67 (m, 2H).

^{13}C NMR (101 MHz, CDCl_3) δ 82.9, 37.7, 30.8, 28.9, 24.8 (the carbon bound to boron was not observed).

FT-IR (film): 2977, 2953, 2911, 2866, 1466, 1405, 1389, 1369, 1326, 1146, 968, 682 cm^{-1} .

MS (GC-MS) m/z $[\text{M}]^+$ calcd for $\text{C}_{12}\text{H}_{25}\text{BO}_2$: 212.19, found: 212.20, 197.15, 155.10, 141.07, 127.05.



2-(Cyclohexylmethyl)-4,4,5,5-tetramethyl-1,3,2-dioxaborolane (Figure 4.5, entry 23).

The title compound was synthesized according to **GP-3** from methylenecyclohexane. The product was purified by column chromatography on silica gel (2% → 4% EtOAc in hexanes). Colorless oil. Run 1: 154 mg, 69%. Run 2: 148 mg, 66%.

^1H NMR (400 MHz, CDCl_3) δ 1.73 – 1.57 (m, 5H), 1.48 (dq, $J = 11.0, 7.4, 3.8$ Hz, 1H), 1.31 – 1.17 (m, 14H), 1.16 – 1.03 (m, 1H), 0.91 (qd, $J = 13.1, 3.8$ Hz, 2H), 0.71 (d, $J = 7.1$ Hz, 2H).

^{13}C NMR (101 MHz, CDCl_3) δ 82.8, 35.9, 34.2, 26.6, 26.3, 24.9 (the carbon bound to boron was not observed).

FT-IR (film): 2977, 2921, 2850, 1452, 1445, 1371, 1319, 1146, 1005, 972 cm^{-1} .

MS (GC-MS) m/z $[\text{M}]^+$ calcd for $\text{C}_{13}\text{H}_{25}\text{BO}_2$: 224.20, found: 224.21, 209.12, 197.06, 141.10, 127.05.

4.5.3. Observations during Reaction Development

Investigation via ^{19}F NMR spectroscopy of the reaction between ArMgBr and $\text{HSi}(\text{OEt})_3$. In a nitrogen-filled glovebox, an NMR tube was charged with THF (0.5 mL), $\text{HSi}(\text{OEt})_3$ (38 μL , 0.20 mmol, 2.0 equiv), and 4-fluorophenylmagnesium bromide (1.0 M solution in THF, 0.15 mL, 0.15 mmol, 1.5 equiv). The tube was capped, and the mixture was analyzed via ^{19}F NMR spectroscopy after 5 min at r.t.

Preparation of (4-F-C₆H₄)SiH(OEt)₂. THF (20 mL) and $\text{HSi}(\text{OEt})_3$ (4.9 mL, 25.5 mmol, 1.7 equiv) were added to a 250 mL round-bottom flask equipped with a stir bar. The mixture was cooled to -78 $^\circ\text{C}$, and then 4-fluorophenylmagnesium bromide (1.0 M solution in THF, 15 mL, 15 mmol, 1.0 equiv) was added dropwise via syringe. The mixture was allowed to warm to r.t., and then it was stirred for 1 h. Dry *n*-hexane (50 mL) was added, and the mixture was filtered. The

filtrate was concentrated and distilled under reduced pressure to give HSi(4-F-C₆H₄)(OEt)₂.
Colorless oil. 1.4 g, 44%.

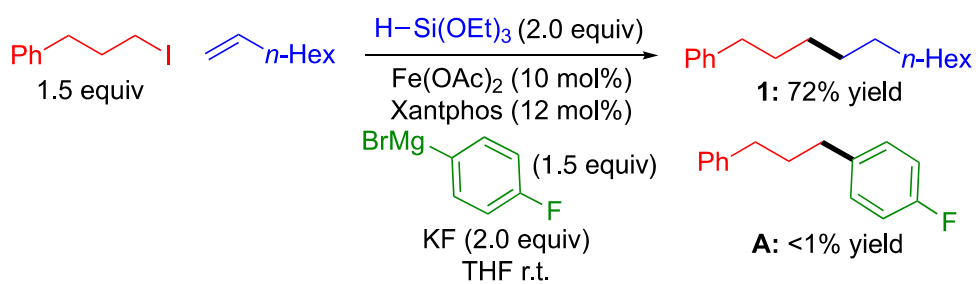
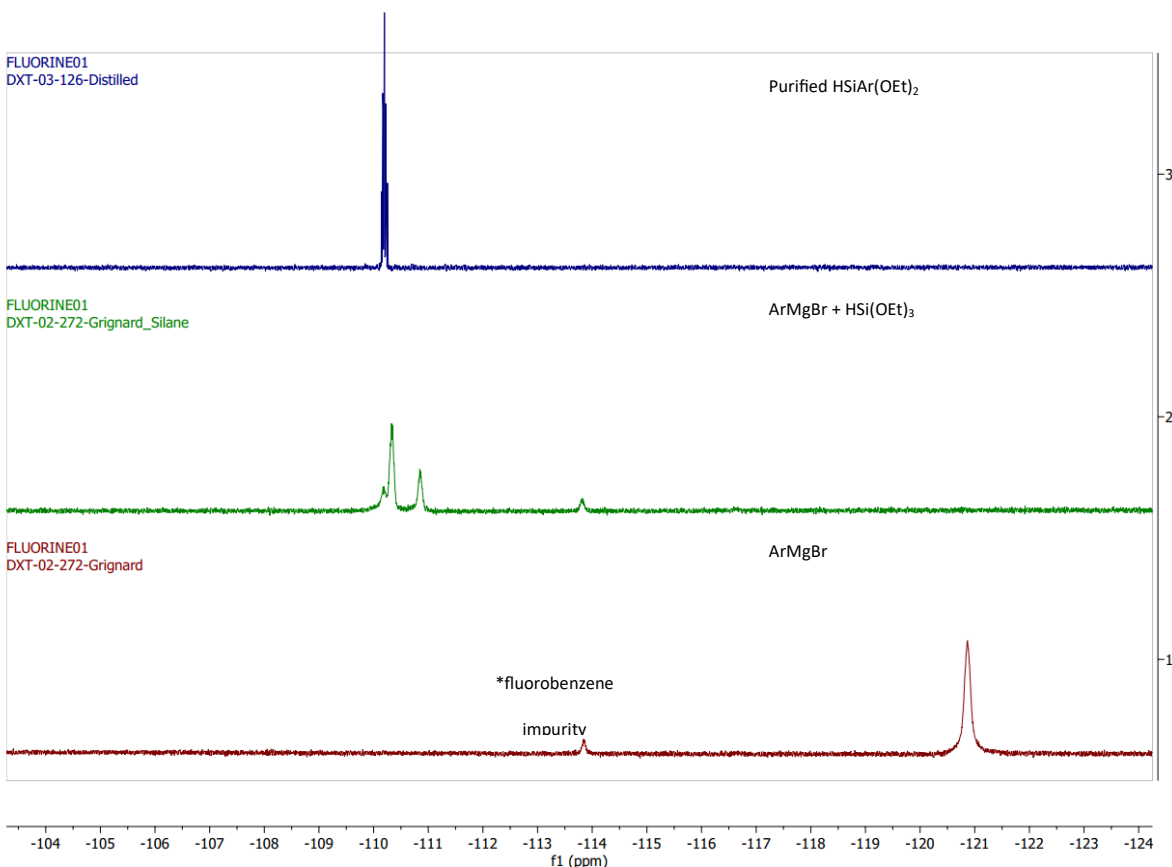
¹H NMR (400 MHz, CDCl₃) δ 7.64 – 7.51 (m, 2H), 7.08 – 6.96 (m, 2H), 4.85 (d, *J* = 0.9 Hz, 1H), 3.81 (qd, *J* = 7.0, 0.9 Hz, 4H), 1.20 (td, *J* = 7.0, 0.9 Hz, 6H).

¹³C NMR (101 MHz, CDCl₃) δ 164.7 (d, *J* = 249.8 Hz), 136.3 (d, *J* = 7.8 Hz), 115.2 (d, *J* = 19.9 Hz), 59.5, 18.3.

¹⁹F NMR (282 MHz, THF) δ –110.19 (tt, *J* = 9.4, 6.1 Hz).

FT-IR (film): 2975, 2930, 2884, 2161, 2134, 1591, 1501, 1389, 1224, 958, 823, 711, 619, 519 cm⁻¹.

MS (GC-MS) *m/z* [M]⁺ calcd for C₁₀H₁₅FO₂Si: 214.08, found: 214.10, 213.09, 199.07, 185.05, 169.06.



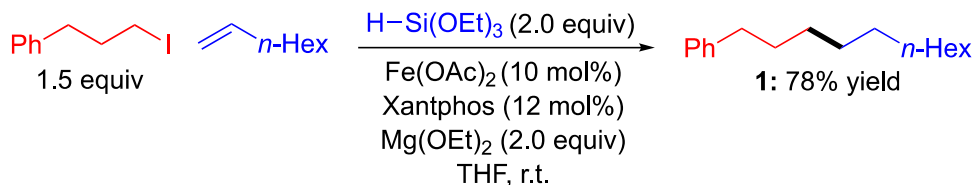
General Procedure 4 (GP-4) (Figure 4.2A). In a nitrogen-filled glovebox, a 4-mL vial was charged with a stir bar, followed by Fe(OAc)_2 (1.7 mg, 0.010 mmol, 10 mol%), Xantphos (6.9 mg, 0.012 mmol, 12 mol%), and KF (11.6 mg, 0.20 mmol, 2.0 equiv). THF (0.5 mL) was added, and the mixture was stirred for 20 min. Then, 1-octene (16 μL , 0.10 mmol, 1.0 equiv), the alkyl

iodide (24 μL , 0.15 mmol, 1.5 equiv), and $\text{HSi}(\text{OEt})_3$ (38 μL , 0.20 mmol, 2.0 equiv) were added. Finally, 4-fluorophenylmagnesium bromide (1.0 M solution in THF, 0.15 mL, 0.15 mmol, 1.5 equiv) was added. The vial was capped, wrapped with electrical tape, and removed from the glovebox. The reaction mixture was vigorously stirred for 24 h. The mixture was then diluted with hexanes, and pentadecane (28 μL , 0.10 mmol) was added as an internal standard. The mixture was passed through a pad of silica, flushing with hexanes and Et_2O . A small volume (~ 0.1 mL) of the resulting solution was diluted and analyzed via GC to determine the yield of the reaction.

For entry 8, the following procedure was followed: In a nitrogen-filled glovebox, a 4-mL vial was charged with a stir bar, $\text{HSi}(\text{OEt})_3$ (38 μL , 0.20 mmol, 2.0 equiv), and 4-fluorophenylmagnesium bromide (1.0 M solution in THF, 0.15 mL, 0.15 mmol, 1.5 equiv). This mixture was stirred for ~ 3 min. A separate 4-mL vial was charged with a stir bar, followed by $\text{Fe}(\text{OAc})_2$ (1.7 mg, 0.010 mmol, 10 mol%), Xantphos (6.9 mg, 0.012 mmol, 12 mol%), and KF (11.6 mg, 0.20 mmol, 2.0 equiv). THF (0.5 mL) was added, and then the mixture was stirred for 20 min. Next, 1-octene (16 μL , 0.10 mmol, 1.0 equiv), the alkyl iodide (24 μL , 0.15 mmol, 1.5 equiv), and the solution of Grignard reagent/silane were added. The vial was capped, wrapped with electrical tape, and removed from the glovebox. The reaction mixture was vigorously stirred for 24 h. The mixture was then diluted with hexanes, and pentadecane (28 μL , 0.10 mmol) was added as internal standard. The mixture was passed through a pad of silica, flushing with hexanes and Et_2O . A small volume (~ 0.1 mL) of the resulting solution was diluted and analyzed via GC to determine the yield of the reaction.

entry	variation from the standard conditions	yield (%)
1	none	72
2	no ArMgBr	<1
3	no KF	65
3	Ph ₂ Zn or PhZnCl, instead of ArMgBr	<1
4	LiAlH ₄ , NaBH ₄ , or L-selectride, instead of ArMgBr	<1
5	Mg ⁰ , Zn ⁰ , or Mn ⁰ , instead of ArMgBr	<1
6	MgCl ₂ or MgBr ₂ , instead of ArMgBr	<1
7	NaOMe, Na ₂ CO ₃ , K ₃ PO ₄ , NaO <i>t</i> -Bu, or LiOMe, instead of ArMgBr	<1
8	Pre-mixing ArMgBr and HSi(OEt) ₃	68
9	HSiAr(OEt) ₂ , instead of ArMgBr and HSi(OEt) ₃	<1
10	Mg(OEt) ₂ (1.5 equiv), instead of ArMgBr	55
11	Mg(OEt) ₂ (1.5 equiv), instead of ArMgBr and KF	71

4.5.4. Effect of Reaction Parameters



General Procedure 5 (GP-5) (Figure 4.2B). In a nitrogen-filled glovebox, a 4-mL vial was charged with a stir bar, followed by Fe(OAc)₂ (1.7 mg, 0.010 mmol, 10 mol%), Xantphos (6.9 mg, 0.012 mmol, 12 mol%), and Mg(OEt)₂ (22.8 mg, 0.20 mmol, 2.0 equiv). THF (0.5 mL), 1-octene (16 μ L, 0.10 mmol, 1.0 equiv), the alkyl iodide (24 μ L, 0.15 mmol, 1.5 equiv), and HSi(OEt)₃ (38 μ L, 0.20 mmol, 2.0 equiv) were added. The vial was capped, wrapped with electrical tape, and removed from the glovebox. The reaction mixture was vigorously stirred for 24 h. The mixture was then diluted with hexanes, and pentadecane (28 μ L, 0.10 mmol) was added as an internal standard. The mixture was passed through a pad of silica, flushing with hexanes and Et₂O. A small volume (~0.1 mL) of the resulting solution was diluted and analyzed via GC to determine the yield of the reaction.

entry	variation from the standard conditions	Yield (%)
1	none	78
2	no Fe(OAc) ₂	<1
3	FeCl ₂ instead of Fe(OAc) ₂	64
4	FeBr ₂ instead of Fe(OAc) ₂	72
5	Fe(acac) ₃ instead of Fe(OAc) ₂	69
6	FeF ₂ instead of Fe(OAc) ₂	1
7	no Xantphos	2
8	bipyridine, instead of Xantphos	1
9	PPh ₃ (24 mol%), instead of Xantphos	4
10	dppBz, instead of Xantphos	<1
11	no Mg(OEt) ₂	<1
12	NaOEt, instead of Mg(OEt) ₂	1
13	KF, instead of Mg(OEt) ₂	<1
14	K ₃ PO ₄ , instead of Mg(OEt) ₂	<1
15	MgBr ₂ , instead of Mg(OEt) ₂	<1
16	PMHS, instead of HSi(OEt) ₃	13
17	H ₃ SiPh, instead of HSi(OEt) ₃	51
18	HSiEt(OEt) ₂ , instead of HSi(OEt) ₃	66
19	H ₂ Ph ₂ Si, instead of HSi(OEt) ₃	70
20	MTBE, instead of THF	<1
21	toluene, instead of THF	2
22	Et ₂ O, instead of THF	<1
23	DME, instead of THF	<1
24	DMA, instead of THF	<1
25	0.1 M, instead of 0.2 M	69
26	0.4 M, instead of 0.2 M	71
27	0.7 equiv electrophile	38
28	1.2 equiv electrophile	65

29	1.8 equiv electrophile	81
30	alkyl bromide, instead of alkyl iodide	67
31	Fe(OAc) ₂ (5 mol%), Xantphos (6 mol%)	63
32	0.1 equiv of water added	72
33	0.5 equiv of water added	47
34	0.5 mL air added via syringe to the headspace	71
35	under air in a closed vial	15

4.5.5. Mechanistic Studies

Impact of TEMPO on a coupling reaction (Figure 4.4A). In a nitrogen-filled glovebox, a 4-mL vial was charged with a stir bar, followed by Fe(OAc)₂ (1.7 mg, 0.010 mmol, 10 mol%), Xantphos (6.9 mg, 0.012 mmol, 12 mol%), and Mg(OEt)₂ (22.8 mg, 0.20 mmol, 2.0 equiv). THF (0.5 mL) was added, and then pentadecane (28 μL, 0.10 mmol, internal standard), 1-octene (16 μL, 0.10 mmol, 1.0 equiv), the alkyl iodide (24 μL, 0.15 mmol, 1.5 equiv), and HSi(OEt)₃ (38 μL, 0.20 mmol, 2.0 equiv). The vial was capped and vigorously stirred for 4 h.

Next, ~20 μL of the reaction mixture was diluted with hexanes, and the resulting mixture was filtered through a syringe filter and analyzed via GC-MS, which indicated that there was a 26% yield of the cross-coupled product. TEMPO (15 mg, 1.0 equiv) was carefully added to the reaction as a solid. After stirring for 1 min, ~20 μL of the reaction mixture was analyzed via GC-MS, which indicated the presence of an electrophile/TEMPO adduct and a 26% yield of the cross-coupled product. The reaction was stirred for 20 additional hours, for a total reaction time of 24 h. At this time, an aliquot (~20 μL) of the reaction mixture was analyzed via GC-MS, which indicated the presence of an electrophile/TEMPO adduct and a 28% yield of the cross-coupled product. LC-TOF confirmed the presence of the electrophile/TEMPO adduct.

Support for the formation of an organic radical from an alkyl electrophile (Figure 4.4B). In a nitrogen-filled glovebox, a 4-mL vial was charged with a stir bar, followed by Fe(OAc)₂ (3.4 mg, 0.020 mmol, 10 mol%), Xantphos (13.9 mg, 0.024 mmol, 12 mol%), and Mg(OEt)₂ (22.8 mg, 0.20 mmol, 1.0 equiv). THF (1.0 mL) was added, and then 6-methoxyhex-1-ene (290 μL, 2.0 mmol, 10 equiv), the alkyl iodide (16 μL, 0.10 mmol, 0.50 equiv), and HSi(OEt)₃ (38 μL, 0.20 mmol, 1.0 equiv). The vial was capped and vigorously stirred in the glovebox for 7 h. Then, additional Mg(OEt)₂ (22.8 mg, 0.20 mmol, 1.0 equiv), alkyl iodide (16 μL, 0.10 mmol, 0.50 equiv), and HSi(OEt)₃ (38 μL, 0.20 mmol, 1.0 equiv.) were added. The reaction was stirred for 10 additional hours. The mixture was then diluted with hexanes, and pentadecane (56 μL, 0.20 mmol) was added as an internal standard. The mixture was passed through a pad of silica, flushing with hexanes and Et₂O.

A small volume (~0.1 mL) of the resulting solution was diluted and analyzed via GC to determine the yield of the reaction. Only two products were detected via GC, corresponding to the two diastereomers of the cyclized product. The diastereoselectivity of the reaction was determined via GC: dr = 3.2 : 1.

The mixture was concentrated and redissolved in DCM (3 mL). H₂O₂ (0.1 mL of 30% solution in water) was added, and the mixture was stirred vigorously under air for 1 h. Then, the mixture was dried over Na₂SO₄ and concentrated, and the residue was purified by column chromatography (0% → 3% Et₂O in hexanes). Colorless oil. 8.0 mg. 19% yield.

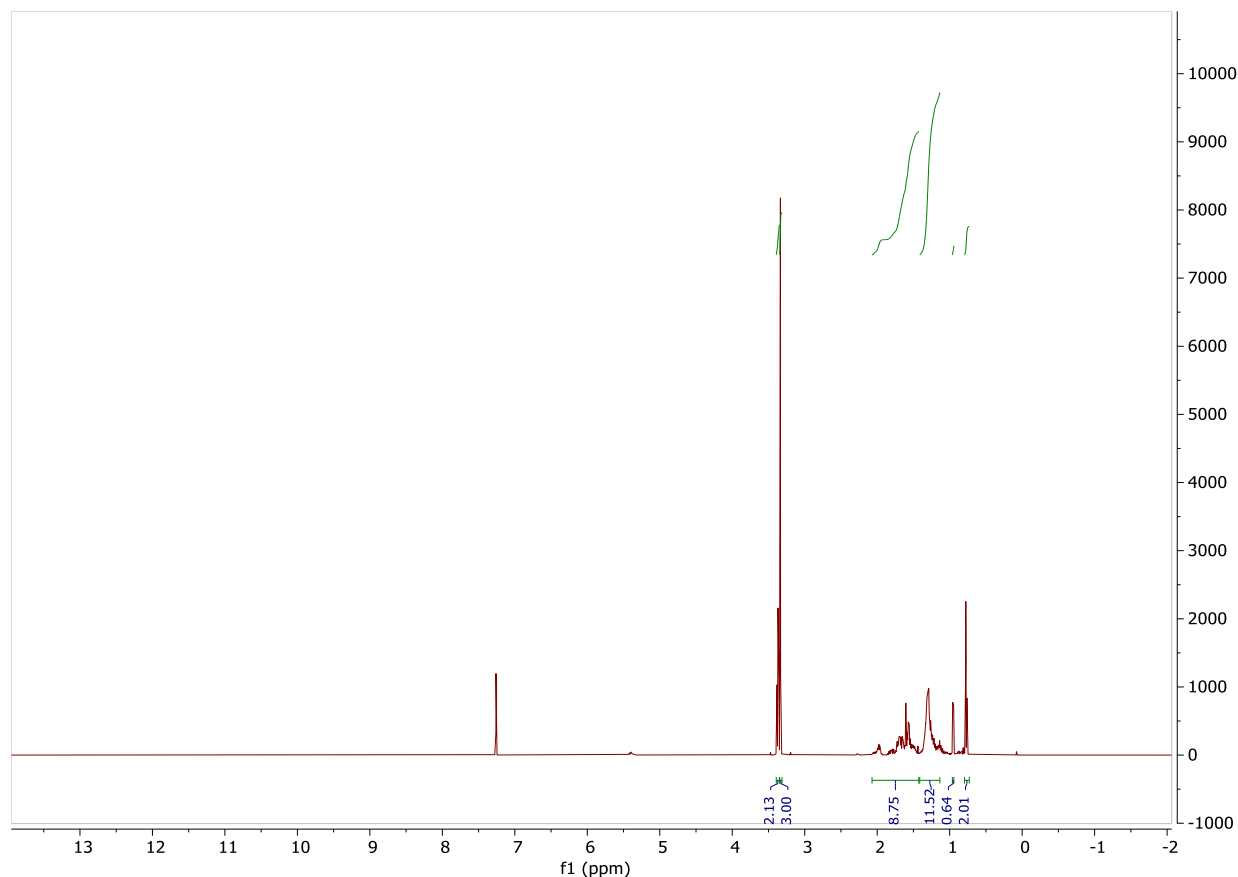
The diastereoselectivity of the reaction was determined via integration of the ¹H NMR spectrum. cis : trans = 3.2 : 1, consistent with the GC analysis.

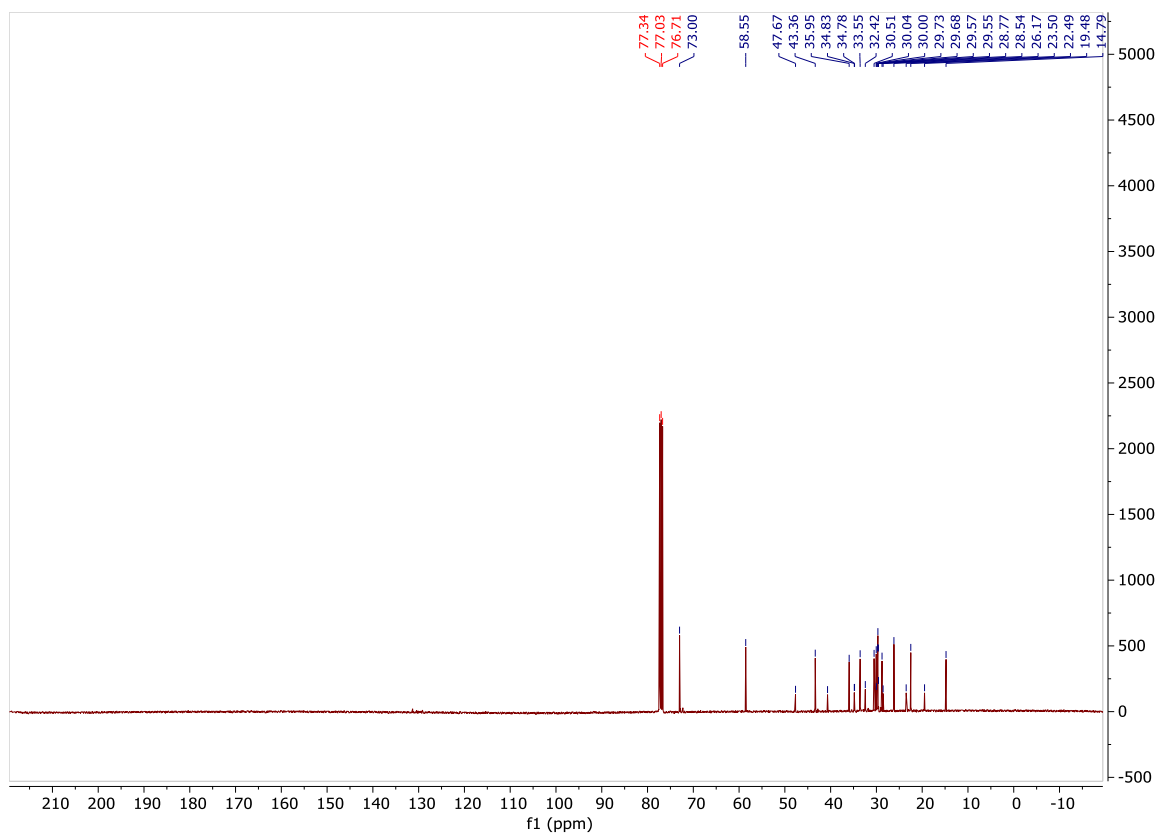
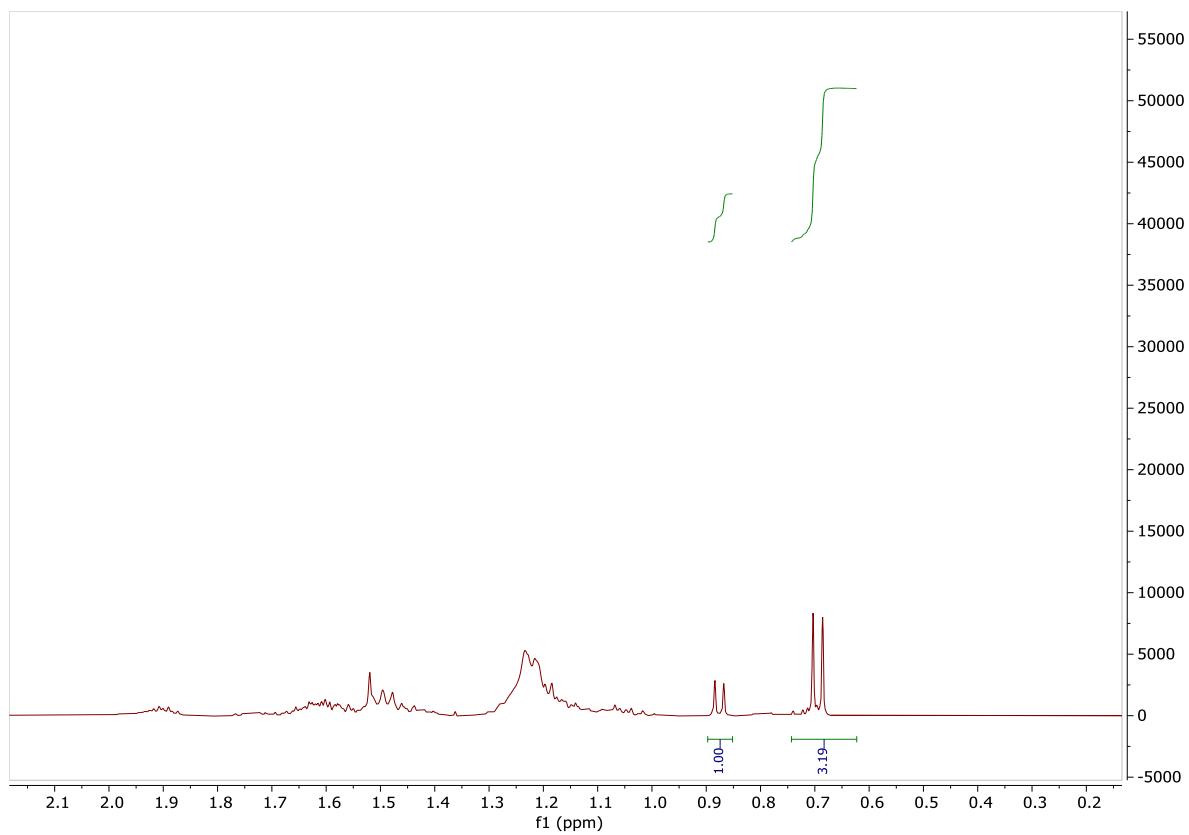
^1H NMR (500 MHz, CDCl_3) δ 3.37 (t, $J = 6.7$ Hz, 2H), 3.34 (s, 3H), 2.07 – 1.43 (m, 9H), 1.41 – 1.14 (m, 11H), 0.95 (d, $J = 6.6$ Hz, 0.6H), 0.77 (d, $J = 7.1$ Hz, 2H) (mixture of diastereomers).

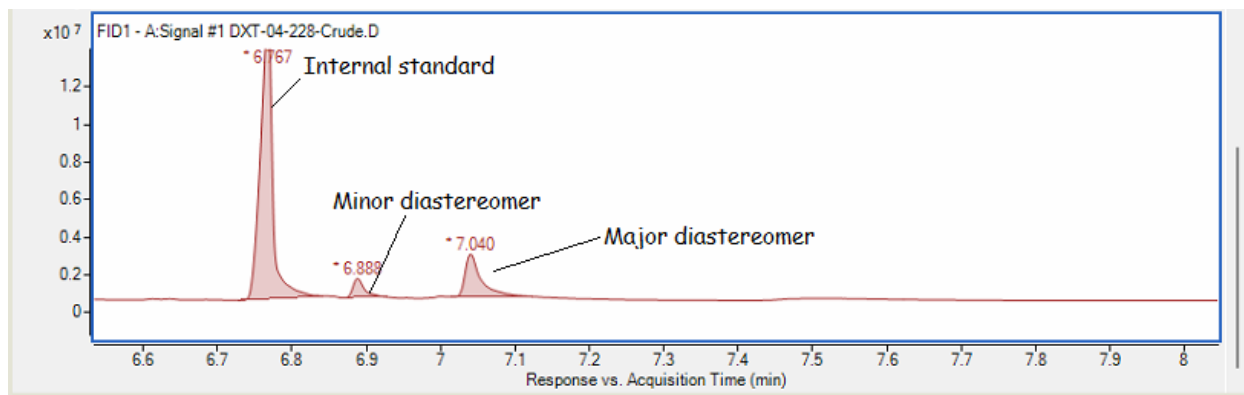
^{13}C NMR (101 MHz, CDCl_3) δ 58.6, 47.7, 43.4, 40.7, 36.0, 34.83, 34.78, 33.6, 32.4, 30.5, 30.04, 30.00, 29.73, 29.68, 29.57, 29.55, 28.8, 28.5, 26.2, 23.5, 22.5, 19.5, 14.8 (mixture of diastereomers).

FT-IR (film): 3061, 2981, 2853, 1450, 1005, 951, 731, 699 cm^{-1} .

MS (GC-MS) m/z $[\text{M}]^+$ calcd for $\text{C}_{14}\text{H}_{28}\text{O}$: 212.21, found: 212.22, 180.18, 152.14, 137.12, 124.12, 96.10, 82.09.







Peak	RT	Area	Area %	Height	Type	Satu
1	6.767	17236832.42	100	15060111.48	M	
3	7.04	3387370.15	19.65	2242959.1	M	S
2	6.888	1058419.18	6.14	995389.23	M	S

Deuterium labeling experiment with D₂SiPh₂ (top of Figure 4.4C). In a nitrogen-filled glovebox, a 4-mL vial was charged with a stir bar, followed by Fe(OAc)₂ (1.7 mg, 0.010 mmol, 10 mol%), Xantphos (6.9 mg, 0.012 mmol, 12 mol%), and Mg(OEt)₂ (22.8 mg, 0.20 mmol, 2.0 equiv). THF (0.5 mL) was added, and then 6-phenoxy-1-hexene (22 μL, 0.10 mmol, 1.0 equiv), 2-iodoethylcyclohexane (24 μL, 0.15 mmol, 1.5 equiv), and D₂SiPh₂ (36 μL, 0.20 mmol, 2.0 equiv). The vial was capped and vigorously stirred for 24 h. The mixture was then diluted with hexanes, and pentadecane (28 μL, 0.10 mmol) was added as an internal standard. The mixture was passed through a pad of silica, flushing with hexanes and Et₂O.

A small volume (~0.1 mL) of the resulting solution was diluted and analyzed via GC to determine the yield of the reaction. 68% yield.

The mixture was then concentrated and purified by preparative TLC (100% hexanes). Colorless oil. 18 mg, 63% yield.

^1H NMR (400 MHz, CDCl_3) δ 7.32 – 7.26 (m, 2H), 6.99 – 6.81 (m, 3H), 3.95 (t, $J = 6.6$ Hz, 2H), 1.78 (dt, $J = 14.7, 6.7$ Hz, 2H), 1.73 – 1.61 (m, 5H), 1.45 (td, $J = 8.9, 8.4, 4.7$ Hz, 2H), 1.37 – 1.12 (m, **12.5 H**), 0.86 (qd, $J = 10.8, 9.8, 4.5$ Hz, 2H). On the basis of the integration, an average of ~1.5 D was incorporated per molecule of product.

^2H NMR (61 MHz, CDCl_3) δ 1.31.

^{13}C NMR (101 MHz, CDCl_3) δ 159.1, 129.4, 120.5, 114.5, 67.9, 37.7, 37.6, 37.5, 33.5, 29.9, 29.8, 29.7, 29.6, 29.5, 29.43, 29.40, 29.3, 29.2, 29.0, 26.9, 26.84, 26.80, 26.5, 26.10, 26.07, 25.99 (splitting by deuterium observed, multiplets cannot be resolved and are reported as individual peaks).

Via mass spectrometry, products with 0–4 D can be observed.

MS (GC-MS) m/z $[\text{M}]^+$ calcd for $\text{C}_{20}\text{H}_{32}\text{O}$: 288.25, found: 288.27.

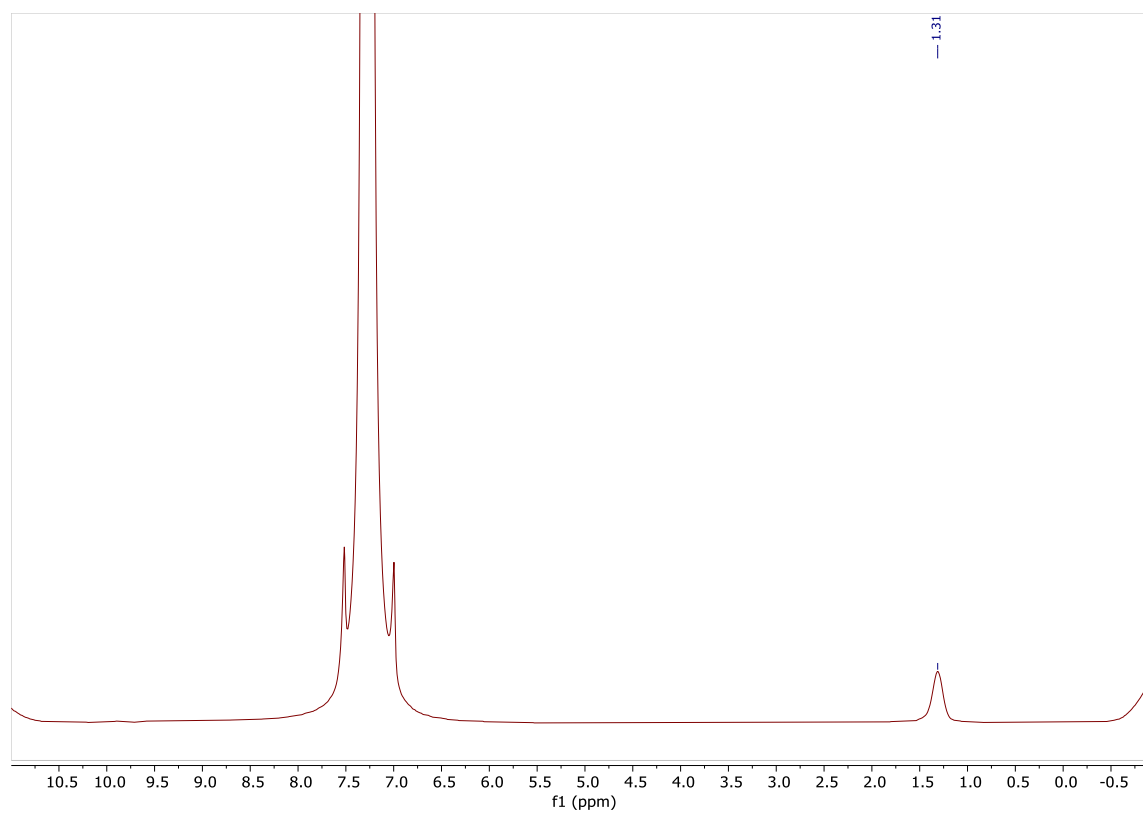
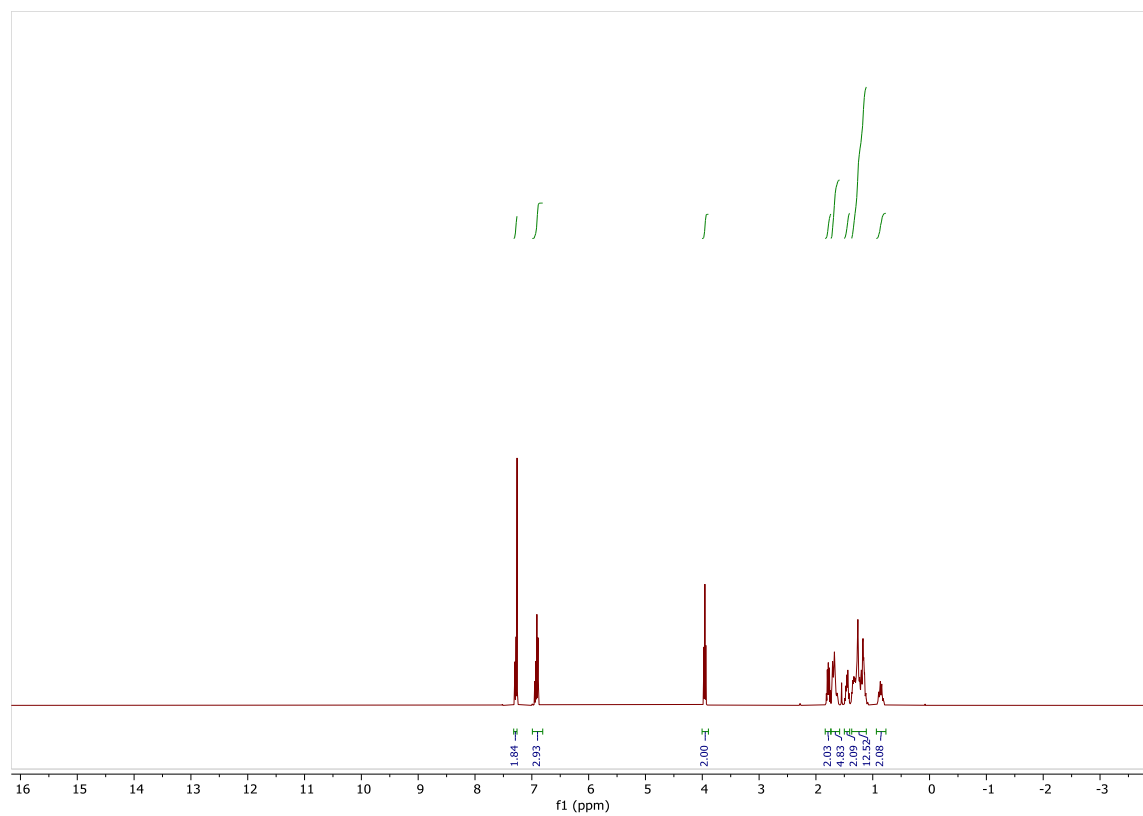
MS (GC-MS) m/z $[\text{M}]^+$ calcd for $\text{C}_{20}\text{H}_{31}\text{OD}$: 289.25, found: 289.28.

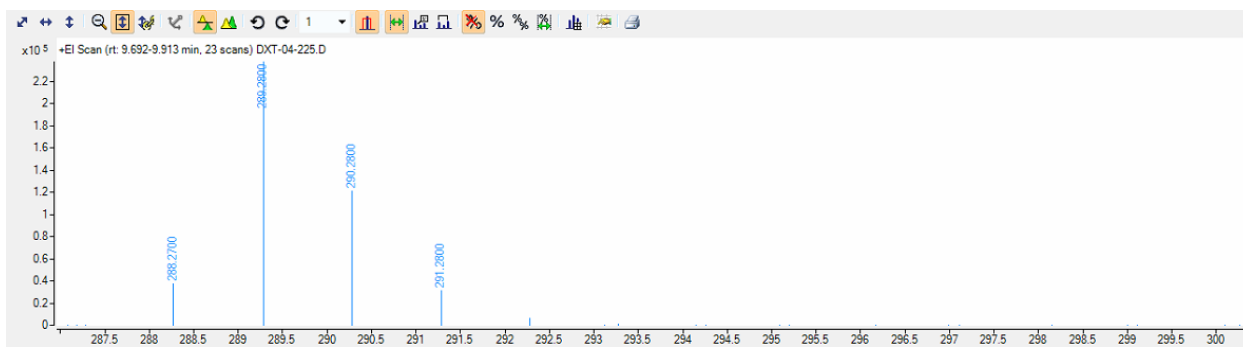
MS (GC-MS) m/z $[\text{M}]^+$ calcd for $\text{C}_{20}\text{H}_{30}\text{OD}_2$: 290.26, found: 290.28.

MS (GC-MS) m/z $[\text{M}]^+$ calcd for $\text{C}_{20}\text{H}_{29}\text{OD}_3$: 291.26, found: 291.28.

MS (GC-MS) m/z $[\text{M}]^+$ calcd for $\text{C}_{20}\text{H}_{28}\text{OD}_4$: 292.27, found: 292.28.

FT-IR (film): 2977, 2834, 1501, 1496, 741, 695 cm^{-1} .





Deuterium labeling experiment with D₂SiPh₂ (bottom of Figure 4.4C). The reaction was set up as above, but run for 7 h. The mixture was then diluted with hexanes, and pentadecane (28 μL, 0.10 mmol) was added as an internal standard. The mixture was passed through a pad of silica, flushing with hexanes and Et₂O.

A small volume (~0.1 mL) of the resulting solution was diluted and analyzed via GC to determine the yield of the reaction. 37% yield.

The remaining olefins can also be quantified via GC analysis: 51% remaining.

The mixture was then concentrated and purified by preparative TLC (100% hexanes). The various isomers of the olefin could not be separated.

¹H NMR (400 MHz, CDCl₃) δ 7.33 – 7.26 (m, 2H), 6.99 – 6.77 (m, 3H), 5.99 – 5.76 (m, 0.1H), 5.56 – 5.35 (m, 1H), 5.23 – 4.75 (m, 0.4H), 3.96 (tt, *J* = 6.5, 2.4 Hz, 2H), 2.30 – 2.20 (m, 0.7 H), 2.20 – 2.06 (m, 1H), 1.94 – 1.74 (m, 1.9H), 1.74 – 1.52 (m, 2.3H), 1.45 (d, *J* = 10.7 Hz, 0.2H), 1.39 – 1.28 (m, 0.4H), 1.32 – 1.14 (m, 0.8H) (multiple products).

²H NMR (61 MHz, CDCl₃) δ 5.88, 5.53, 5.07, 1.62, 1.33, 0.90 (multiple products).

^{13}C NMR (101 MHz, CDCl_3) δ 159.10, 159.08, 138.6, 135.8, 130.3, 129.42, 129.41, 128.1, 125.7, 124.9, 120.50, 120.49, 120.45, 114.7, 114.6, 114.53, 114.51, 114.49, 67.9, 67.6, 67.2, 67.1, 33.5, 33.3, 29.7, 29.3, 29.12, 29.06, 29.0, 28.7, 25.7, 25.4, 25.3, 23.3, 18.5, 18.0, 12.7 (multiple products).

Via mass spectrometry, products with 0–5 D can be observed.

MS (GC-MS) m/z $[\text{M}]^+$ calcd for $\text{C}_{12}\text{H}_{16}\text{O}$: 176.12, found: 176.13.

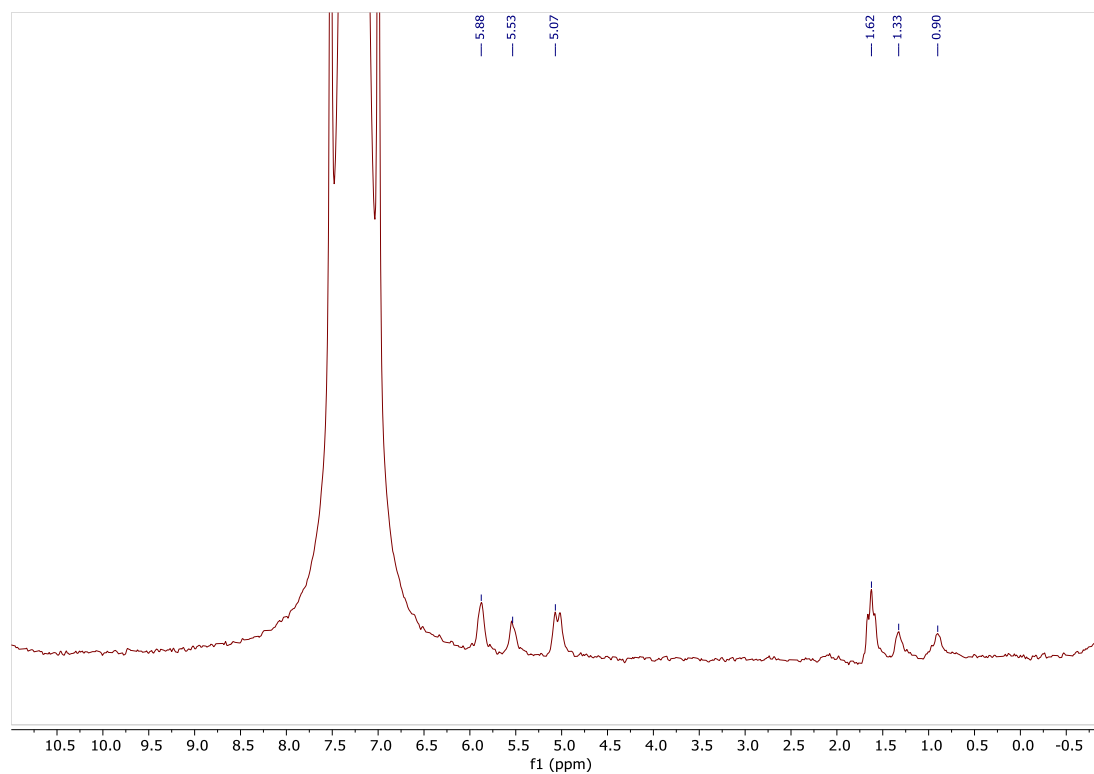
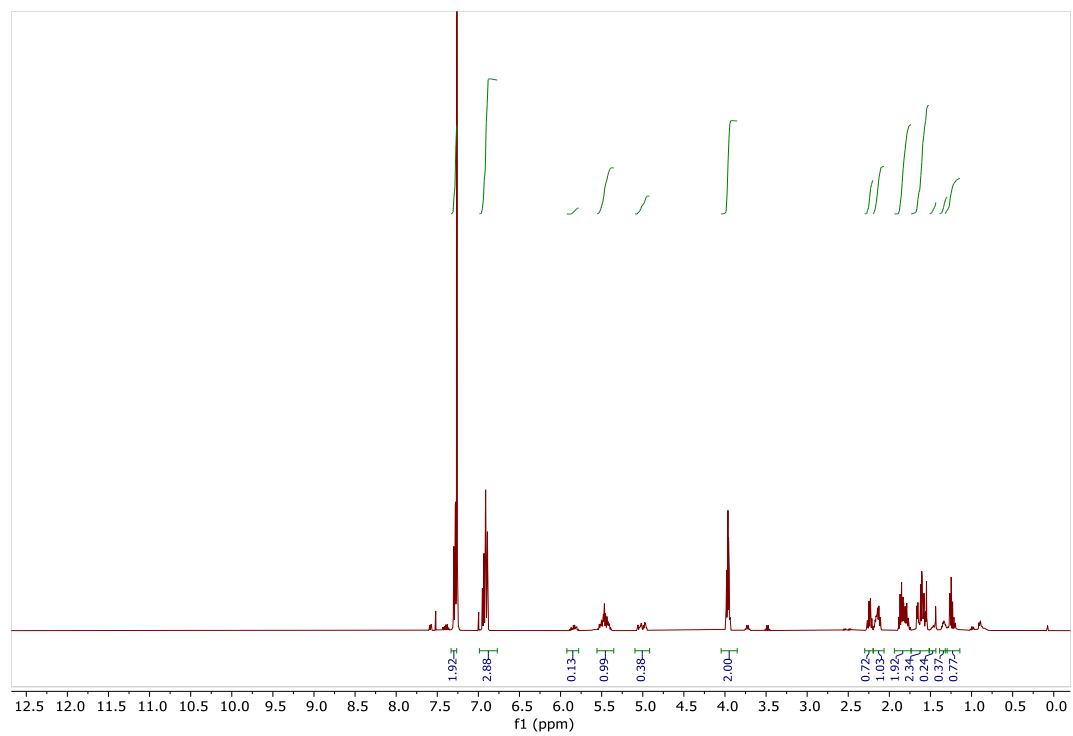
MS (GC-MS) m/z $[\text{M}]^+$ calcd for $\text{C}_{12}\text{H}_{15}\text{OD}$: 177.12, found: 177.13.

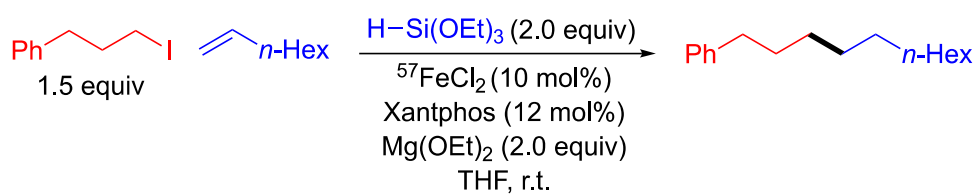
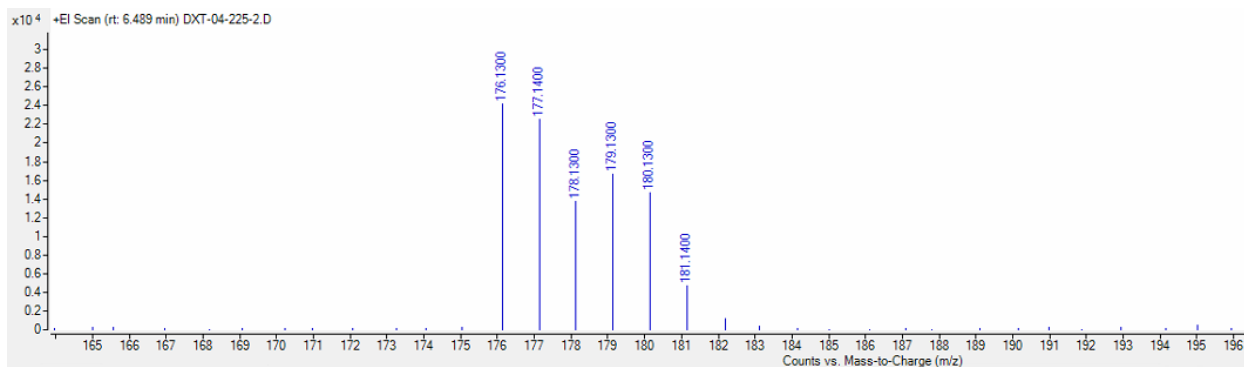
MS (GC-MS) m/z $[\text{M}]^+$ calcd for $\text{C}_{12}\text{H}_{14}\text{OD}_2$: 178.13, found: 178.14.

MS (GC-MS) m/z $[\text{M}]^+$ calcd for $\text{C}_{12}\text{H}_{13}\text{OD}_3$: 179.14, found: 179.13.

MS (GC-MS) m/z $[\text{M}]^+$ calcd for $\text{C}_{12}\text{H}_{12}\text{OD}_4$: 180.15, found: 180.13.

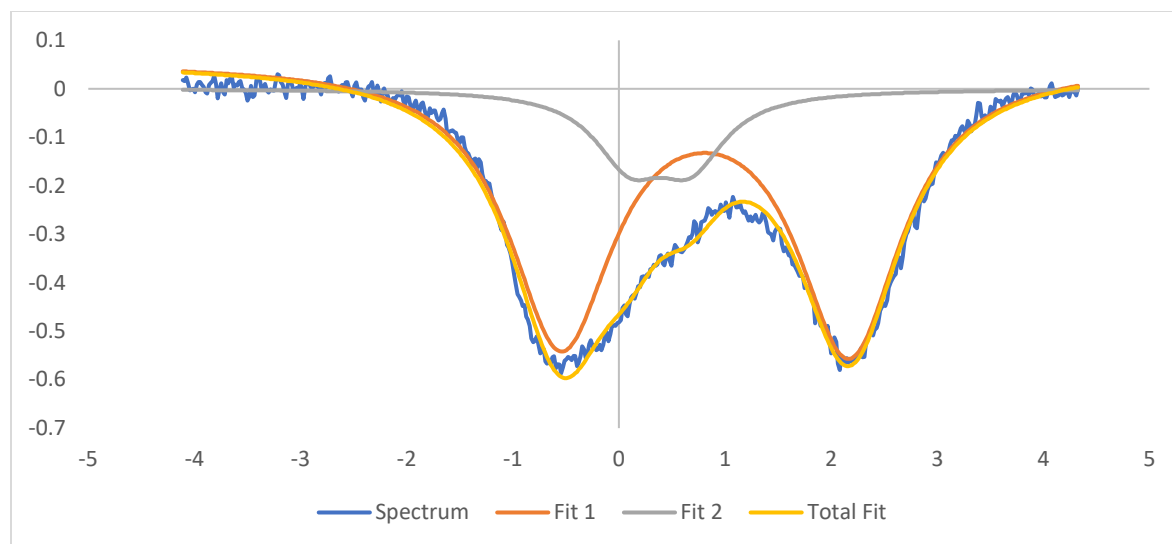
MS (GC-MS) m/z $[\text{M}]^+$ calcd for $\text{C}_{12}\text{H}_{11}\text{OD}_5$: 181.15, found: 181.14.





Mössbauer spectroscopy. GP-4 was followed and scaled to 0.2 mmol of olefin, except 10 mol% $^{57}\text{FeCl}_2$ (2.6 mg, 0.02 mmol) was used.

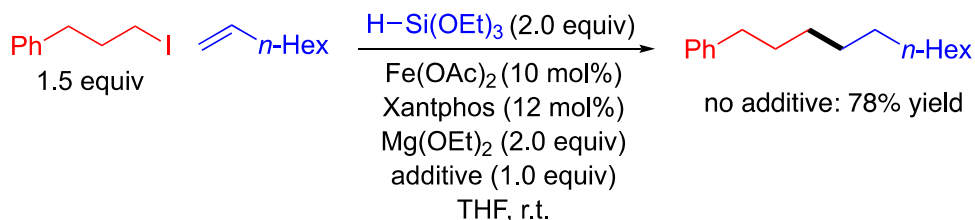
The mixture was directly freeze-quenched at 77 K in a nitrogen-filled glovebox after 4 h, and it was analyzed via Mössbauer spectroscopy while a parallel magnetic field was applied.



Fit 1: $\delta = 0.86$, $\Delta E_Q = 2.91$

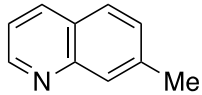
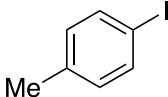
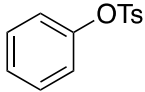
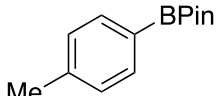
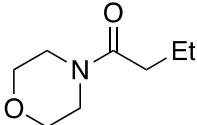
Fit 2: $\delta = 0.41$, $\Delta E_Q = 0.48$

4.5.6. Studies of Functional-Group Compatibility

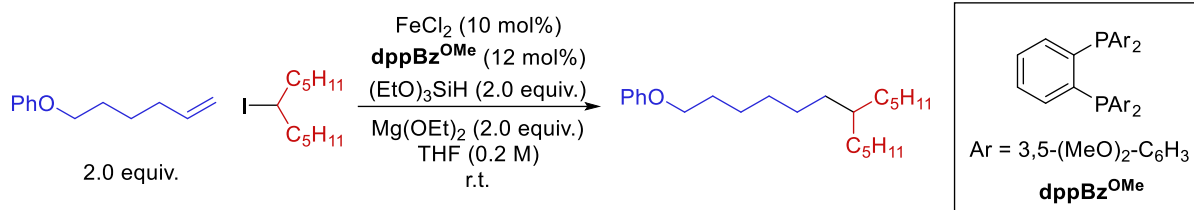


General Procedure 6 (GP-6) (Figure 4.2B). In a nitrogen-filled glovebox, a 4-mL vial was charged with a stir bar, followed by Fe(OAc)₂ (1.7 mg, 0.010 mmol, 10 mol%), Xantphos (6.9 mg, 0.012 mmol, 12 mol%), and Mg(OEt)₂ (22.8 mg, 0.20 mmol, 2.0 equiv). THF (0.5 mL), 1-octene (16 μL , 0.10 mmol, 1.0 equiv), the alkyl iodide (24 μL , 0.15 mmol, 1.5 equiv), the additive (1.0 equiv), and HSi(OEt)₃ (38 μL , 0.20 mmol, 2.0 equiv) were added. The vial was capped, wrapped with electrical tape, and removed from the glovebox. The reaction mixture was

vigorously stirred for 24 h. The mixture was then diluted with hexanes, and pentadecane (28 μ L, 0.10 mmol) was added as an internal standard. The mixture was passed through a pad of silica, flushing with hexanes and Et₂O. A small volume (~0.1 mL) of the resulting solution was diluted and analyzed via GC to determine the yield of the reaction and the percent recovery of the additive.

additive	yield of coupling product (%) (recovery of additive (%))	additive	yield of coupling product (%) (recovery of additive (%))
	85 (35)	$n\text{-C}_{12}\text{H}_{23}\text{CH}_2\text{CH}_2\text{CN}$	68 (37)
Ph(<i>n</i> -Bu)NH	82 (82)		67 (91)
	78 (>95)	PhCH ₂ CH ₂ CH ₂ OH	53 (13)
PhSPh	74 (>95)	$n\text{-C}_5\text{H}_{11}\text{C}(=\text{O})n\text{-C}_5\text{H}_{11}$	40 (17)
	73 (>95)		19 (31)
NPhBn ₂	71 (94)		

4.5.7. Reaction Development for Secondary Alkyl Electrophiles



General Procedure 7 (GP-7). In a nitrogen-filled glovebox, a 4-mL vial was charged with a stir bar, followed by FeCl₂ (1.3 mg, 0.010 mmol, 10 mol%), **dppBz**^{OMe} (8.2 mg, 0.012 mmol, 12 mol%), and Mg(OEt)₂ (22.8 mg, 0.20 mmol, 2.0 equiv.). THF (0.5 mL), olefin (34 mg, 0.20 mmol, 2.0 equiv.), the alkyl iodide (28 mg, 0.10 mmol, 1.0 equiv.), and HSi(OEt)₃ (38 μL, 0.20 mmol, 2.0 equiv.) were added. The vial was capped, wrapped with electrical tape, and removed from the glovebox. The reaction mixture was vigorously stirred for 24 h. The mixture was then diluted with hexanes, and pentadecane (28 μL, 0.10 mmol) was added as an internal standard. The mixture was passed through a pad of silica, flushing with hexanes and Et₂O. A small volume (~0.1 mL) of the resulting solution was diluted and analyzed via GC to determine the yield of the reaction.

4.6. References

- 1) For example, see: (a) *Sustainable Synthesis of Pharmaceuticals: Using Transition Metal Complexes as Catalysts*; Pereira, M. M., Calvete, M. J. F., Eds.; Royal Society of Chemistry, 2018. (b) Bates, R. *Organic Synthesis Using Transition Metals* (second edition); Wiley, 2012.
- 2) (a) The Nobel Prize in Chemistry 2001. <https://www.nobelprize.org/prizes/-chemistry/2001/-summary/> (b) The Nobel Prize in Chemistry 2005. <https://www.nobelprize.org/prizes/chemistry/2005/-summary/> (c) The Nobel Prize in Chemistry 2010. <https://www.nobelprize.org/prizes/chemistry/2010/-summary/>
- 3) For leading references, see: (a) *Catalysis with Earth-Abundant Elements*; Schneider, U., Thomas, S., Eds.; Royal Society of Chemistry, 2021. (b) *Iron Catalysis: Fundamentals and Applications*; Plietker, B., Ed.; Springer, 2011. (c) Bauer, I.; Knölker, H.-J. Iron catalysis in organic synthesis. *Chem. Rev.* **2015**, *115*, 3170–3387.
- 4) (a) Frey, P. A.; Reed, G. H. The Ubiquity of Iron. *ACS Chem. Biol.* **2012**, *7*, 1477–1481. (b) Guideline for Elemental Impurities. https://database.ich.org/sites/default/files/Q3D-R2_Guideline_Step4_2022_0308.pdf.
- 5) *Palladium-Catalyzed Coupling Reactions*; Molnar, A., Ed.; Wiley, 2013.
- 6) For example, see: (a) Kranthikumar, R. Recent Advances in C(sp³)–C(sp³) Cross-Coupling Chemistry: A Dominant Performance of Nickel Catalysts. *Organometallics* **2022**, *41*, 667–679. (b) Choi, J.; Fu, G. C. Transition Metal-Catalyzed Alkyl–Alkyl Bond Formation: Another Dimension in Cross-Coupling Chemistry. *Science* **2017**, *356*, 152 (eaaf7230).

- 7) Fu, G. C. Transition-metal Catalysis of Nucleophilic Substitution Reactions: A Radical Alternative to S_N1 and S_N2 Processes. *ACS Cent. Sci.* **2017**, *3*, 692–700.
- 8) Lovering, F.; Bikker, J.; Humblet, C. Escape from Flatland: Increasing Saturation as an Approach to Improving Clinical Success. *J. Med. Chem.* **2009**, *52*, 6752–6756.
- 9) (a) *Ni- and Fe-Based Cross-Coupling Reactions*; Correa, A., Ed.; Springer, 2016. (b) Nakamura, E.; Hatakeyama, T.; Ito, S.; Ishizuka, K.; Ilies, L.; Nakamura, M. Iron-Catalyzed Cross-Coupling Reactions. *Org. React.* **2014**, *83*, 1–209. (c) Guerinot, A.; Cossy, J. Iron-Catalyzed C–C Cross-Couplings Using Organometallics. *Top. Curr. Chem.* **2016**, *374*, 1–74. (d) Piontek, A.; Bisz, E.; Szostak, M. Iron-Catalyzed Cross-Couplings in the Synthesis of Pharmaceuticals: In Pursuit of Sustainability. *Angew. Chem. Int. Ed.* **2018**, *57*, 11116–11128. (e) Legros, J.; Figadere, B. Grignard Reagents and Iron. In *Grignard Reagents and Transition Metal Catalysts*; Cossy, J., Ed.; De Gruyter, 2016; pp 114–151.
- 10) For an early example, see: Wang, Y.-M.; Bruno, N. C.; Placeres, A. L.; Zhu, S.; Buchwald, S. L. Enantioselective Synthesis of Carbo- and Heterocycles through a CuH-Catalyzed Hydroalkylation Approach. *J. Am. Chem. Soc.* **2015**, *137*, 10524–10527.
- 11) For early examples, see: (a) Lu, X. et al. Practical Carbon–Carbon Bond Formation from Olefins through Nickel-Catalysed Reductive Olefin Hydrocarbonation. *Nat. Commun.* **2016**, *7*, 11129. (b) Wang, Z.; Yin, H.; Fu, G. C. Catalytic Enantioconvergent Coupling of Secondary and Tertiary Electrophiles with Olefins. *Nature* **2018**, *563*, 379–383.
- 12) For example, see: Li, Y.; Nie, W.; Chang, Z.; Wang, J.-W.; Lu, X.; Fu, Y. Cobalt-Catalysed Enantioselective C(sp³)–C(sp³) Coupling. *Nat. Catal.* **2021**, *4*, 901–911.

- 13) For related transition-metal-catalyzed processes wherein a carbon–carbon bond is formed via the addition of an organic radical to an alkene (not involving the transition metal), see: (a) Han, J. et al. Photoinduced Manganese-Catalysed Hydrofluorocarbofunctionalization of Alkenes. *Nat. Synth.* **2022**, *1*, 475–486. (b) Sumino, S.; Ryu, I. Hydroalkylation of Alkenes Using Alkyl Iodides and Hantzsch Ester under Palladium/Light System. *Org. Lett.* **2016**, *18*, 52–55.
- 14) For iron-catalyzed processes wherein a carbon–carbon bond is formed via the addition of an organic radical to an aryl-substituted alkene or alkyne (not involving iron), see: (a) Cheung, C. W.; Zhurkin, F. E.; Hu, X. Z-Selective Olefin Synthesis via Iron-catalyzed Reductive Coupling of Alkyl Halides with Terminal Arylalkynes. *J. Am. Chem. Soc.* **2015**, *137*, 4932–4935. (b) Pang, H.; Wang, Y.; Gallou, F.; Lipshutz, B. H. Fe-Catalyzed Reductive Couplings of Terminal (Hetero)aryl Alkenes and Alkyl Halides under Aqueous Micellar Conditions. *J. Am. Chem. Soc.* **2019**, *141*, 17117–17124.
- 15) For an iron-catalyzed three-component coupling of an alkyl halide, vinyl boronate ester, and aryl Grignard reagent, see: Liu, L.; Aguilera, M. C.; Lee, W.; Youshaw, C. R.; Neidig, M. L.; Gutierrez, O. General Method for Iron-Catalyzed Multicomponent Radical Cascades–Cross-Couplings. *Science* **2021**, *374*, 432–439.
- 16) For examples of iron/Xantphos-catalyzed cross-couplings, see: (a) Dongol, K. G.; Koh, H.; Sau, M.; Chai, C. L. L. Iron-Catalysed sp^3 – sp^3 Cross-Coupling Reactions of Unactivated Alkyl Halides with Alkyl Grignard Reagents. *Adv. Synth. Catal.* **2007**, *349*, 1015–1018. (b) Hatakeyama, T.; Hashimoto, T.; Kathriarachchi, K. K. A. D. S.; Zenmyo, T.; Seike, H.; Nakamura, M. Iron-Catalyzed Alkyl–Alkyl Suzuki–Miyaura Coupling. *Angew. Chem. Int. Ed.*

- 2012**, *51*, 8834–8837. In the case of our standard coupling partners (Figure 4.2), neither of these methods provides a significant amount of the desired coupling product ($\leq 1\%$).
- 17) For early examples of iron-catalyzed isomerization of olefins/chain-walking, see: (a) Manuel, T. A. The Iron Carbonyl-Catalyzed Isomerization of Olefins. *Trans. N. Y. Acad. Sci.* **1964**, *26*, 442–445. (b) Obligacion, J. V.; Chirik, P. J. Highly Selective Bis(imino)pyridine Iron-Catalyzed Alkene Hydroboration. *Org. Lett.* **2013**, *15*, 2680–2683.
- 18) For an early suggestion, see: Nakamura, M.; Matsuo, K.; Ito, S.; Nakamura, E. Iron-Catalyzed Cross-Coupling of Primary and Secondary Alkyl Halides with Aryl Grignard Reagents. *J. Am. Chem. Soc.* **2004**, *126*, 3686–3687.
- 19) Luszyk, J.; Maillard, B.; Deycard, S.; Lindsay, D. A.; Ingold, K. U. Kinetics for the Reaction of a Secondary Alkyl Radical with Tri-*n*-butylgermanium Hydride and Calibration of a Secondary Alkyl Radical Clock Reaction. *J. Org. Chem.* **1987**, *52*, 3509–3514.
- 20) A preliminary Mössbauer study of a coupling reaction in progress is consistent with the presence of multiple iron compounds, likely including a high-spin Fe(II) species.
- 21) For early examples of iron-catalyzed hydroborations of olefins, see: (a) Zhang, L.; Peng, D.; Leng, X.; Huang, Z. Iron-Catalyzed, Atom-Economical, Chemo- and Regioselective Alkene Hydroboration with Pinacolborane. *Angew. Chem. Int. Ed.* **2013**, *52*, 3676–3680. (b) Greenhalgh, M. D.; Thomas, S. P. Chemo-, Regio-, and Stereoselective Iron-Catalysed Hydroboration of Alkenes and Alkynes. *Chem. Commun.* **2013**, *49*, 11230–11232.

[Intentionally Redacted]